Universitat Autònoma de Barcelona

Novel methods for the detection of exosomes as biomarkers for non-communicable diseases

Arnau Pallarès Rusiñol

Universitat Autònoma de Barcelona

Novel methods for the detection of exosomes as biomarkers for non-communicable diseases

Arnau Pallarès Rusiñol

Doctoral Thesis

Doctoral studies in Chemistry

Directors:

Prof. María Isabel Pividori Gurgo

Prof. Mercè Martí Ripoll

Departament de Química

Unitat de Química Analítica

Facultat de Ciències

Setembre 2022

Memòria presentada per aspirar al Grau de Doctor per Arnau Pallarès Rusiñol

Arnau Pallarès Rusiñol

Vist i plau

Prof. María Isabel Pividori Gurgo

Catedràtica d'Universitat

Departament de Química
Universitat Autònoma de Barcelona

Prof. Mercè Martí Ripoll

Titular d'Universitat

Departament de Biologia Cel·lular,
Fisiologia i Immunologia
Universitat Autònoma de Barcelona

Bellaterra, 20 de setembre de 2022

Funding support

The present dissertation has been developed at the laboratories of the Group of Sensors and Biosensors of the Departament of Chemistry and the laboratories of Biosensing and Bioanalysis Group of *Institut de Biotecnologia i Biomedicina* from *Universitat Autònoma de Barcelona*, thanks to:

- *Ministerio de Ciencia e Innovación* (MICINN), Madrid, Spain, for the projects 'SENS4ALL. Enhancing Rapid Tests for Worldwide Diagnostics' (BIO2016-75751-R) and 'EXOSENS. The exosomes as diagnostic biomarkers in biosensors' (AEI/10.13039/501100011033).
- *Agència de Gestió d'Ajuts Universitaris i de Recerca* (AGAUR) of the *Departament de Recerca i Universitats* from *Generalitat de Catalunya*, for the projects 2014-SGR-837 and 2017-SGR-220.
- *Ministerio de* Universidades, Madrid, Spain, for the predoctoral fellowship of *Formación de Profesorado Universitario,* grant number FPU16/01579.

Grup de Sensors i Biosensors

Biosensing and Bioanalysis Group

Ministerio de Ciencia e Innovación

Ministerio de Universidades

AGAUR - Generalitat de Catalunya

Universitat Autònoma de Barcelona

When it comes to luck, you make your own.

Bruce Springsteen.

Abstract

This doctoral dissertation aims to contribute to the development of new tools for the early diagnosis and monitoring of non-communicable diseases. To achieve this goal, high throughput methodologies are available in the market, but the high cost and low accessibility difficult their implementation in primary healthcare centers in low- and middle-income countries. Thereby, the development and improvement of novel methods for low resource settings remains essential to reduce the burden of those diseases. In addition to the development of new, simpler, and less expensive instruments for diagnosis, the research of novel biomarkers in liquid biopsies is also very relevant. Among the different types of biomarkers, the study of exosomes as cell secreted vesicles, widely available in all biofluids, could provide direct information about physiological and pathological processes in the tissues. Exosomes are nano-sized extracellular vesicles which are currently under intensive study as potential diagnostic biomarkers for many health disorders. Particularly, they are emerging as a new biomarker in liquid biopsies for cancer, since it is known that they are profusely released by cancer cells containing their altered molecular fingerprint. The work thus addresses the study of rapid diagnostic tests (RDTs) for the analysis of exosomes as biomarkers of clinical interest. Specifically, it is focused on the improvement of the analytical parameters, experimental designs, and technologies of those RDTs.

All the approaches were tested and optimized with exosomes derived from cell culture supernatants from MCF-7, MDA-MB-231 and SKBR3 cell lines, as a model of breast cancer cells. The production, isolation and purification of those cultured exosomes were firstly addressed. Then, the obtained cancer-derived exosomes were physically and molecularly characterized with standard analytical methods, such as nanoparticle tracking analysis, cryogenic transmission electron microscopy and flow cytometry.

One of the main challenges dealing with exosomes in RDTs is to increase the sensitivity and improve the limits of detection of the assays. In this direction, the use of magnetic preconcentration and nucleic acid amplification techniques, as double-tagging RT-PCR, were explored for its use in this kind of samples. In this dissertation, a novel electrochemical magneto-actuated platform combining immunomagnetic separation and genosensing of double-tagged amplicons for the quantitative detection of exosomes, is reported. The approach is based on the amplification of glyceraldehyde 3-phosphate dehydrogenase (GAPDH) transcripts . The proposed RDT was tested with human serum

samples, enabling to discriminate breast cancer patients and healthy individuals and enhancing the limits of detection.

On the other hand, paper-based detection techniques, as Lateral and Vertical Flow assays, were explored to improve the simplification of the assays, able to deal with resource-limited settings. In this dissertation, the potentiality of Vertical Flow Assay (VFA) for the visual detection of exosomes is explored for the first time. This approach relies on the use of alkaline phosphatase as enzymatic reporter, producing a colorimetric signal on the surface of the paper membranes. The visual signals were quantified with an image analysis software, obtaining promising results for the characterization of protein markers on exosomes with a simple and cost-effective device.

Finally, other non-conventional approaches were explored for the detection of exosomes, focused on the detection of their intrinsic enzymatic activity. The intrinsic enzymatic activity of aldehyde dehydrogenase (ALDH) was also studied as an overexpressed biomarker in cancer disease. A novel method based on nano-flow cytometry was developed for the detection of those enzymes directly inside the exosomes. This study represents the first step towards the development of a new RDT targeting ALDH intrinsic activity of exosomes for cancer diagnostics.

Resum

En aquesta tesi doctoral es presenta el desenvolupament de noves eines per al diagnòstic precoç i el seguiment de malalties no transmissibles. Tot i que existeixen metodologies d'alt rendiment disponibles al mercat per aquest objectiu, l'alt cost i la baixa disponibilitat en entorns de baixos recursos dificulten la seva implementació en centres d'atenció primària dels països en desenvolupament. Per tant, el disseny de nous mètodes segueix sent essencial per reduir la incidència d'aquestes malalties. A més del desenvolupament de nous dispositius de diagnòstic més senzills i menys costosos, la cerca de nous biomarcadors en biòpsies líquides és molt rellevant. Entre els diferents tipus de biomarcadors, l'estudi de les vesícules secretades per les cèl·lules pot proporcionar informació rellevant sobre processos fisiològics i patològics dels teixits. Els exosomes són vesícules extracel·lulars de mida nanomètrica que s'estan estudiant intensament com a potencials biomarcadors de diagnòstic en moltes malalties, especialment, en biòpsies líquides per al càncer degut al seu alliberament augmentat per les cèl·lules canceroses amb la seva empremta molecular alterada. Aquest treball s'enfoca a l'estudi de les proves de diagnòstic ràpid (RDT, en anglès *rapid diagnostic test*) per a exosomes com a biomarcadors d'interès clínic. En concret, se centra en la millora dels paràmetres analítics, dissenys experimentals i tecnologies d'aquests RDTs.

Tots els mètodes desenvolupats s'han provat i optimitzat amb exosomes derivats de sobrenedants de cultiu cel·lular de les línies cel·lulars MCF-7, MDA-MB-231 i SKBR3, com a model de cèl·lules de càncer de mama. En primer lloc, es va abordar la producció, aïllament i purificació d'aquests exosomes cultivats. Les nanovesícules canceroses obtingudes es van caracteritzar física i molecularment amb mètodes analítics estàndard, com ara l'anàlisi de seguiment de nanopartícules, la microscòpia electrònica de transmissió criogènica i la citometria de flux.

Un dels principals reptes per analitzar els exosomes en un RDT és augmentar la sensibilitat i millorar els límits de detecció dels assajos. En aquesta direcció, es va explorar l'ús de tècniques de preconcentració magnètica i d'amplificació d'àcids nucleics, com la RT-PCR de doble marcatge, per al seu ús en aquest tipus de mostres. En aquesta tesi es desenvolupa un nova plataforma que combina la separació immunomagnètica i la detecció electroquímica d'amplicons doblement marcats per a la detecció quantitativa dels exosomes, basat en l'amplificació de les seqüències mRNA de gliceraldehid-3-fosfat deshidrogenasa (GAPDH). El mètode desenvolupat es va provar amb mostres

reals de sèrum humà i permet diferenciar pacients amb càncer de mama i individus sans, millorant notablement els límits de detecció.

D'altra banda, es van explorar RDTs basats en paper. Amb aquestes plataformes s'aconsegueix la simplificació dels assajos i la millora de les característiques per a entorns amb recursos limitats. En aquesta tesi s'explora per primera vegada la potencialitat de l'assaig de flux vertical (VFA) per a la detecció visual d'exosomes. Aquest mètode es basa en l'ús de la fosfatasa alcalina com a marcador enzimàtic, produint un senyal colorimètric a la superfície de les membranes de paper. Els senyals visuals es van poder quantificar amb un programari d'anàlisi d'imatges, obtenint resultats prometedors per a la caracterització de marcadors de proteïnes en exosomes amb un dispositiu senzill i de baix cost.

Per últim, es van explorar altres enfocaments no convencionals per a la detecció d'exosomes, centrats en la detecció de la seva activitat enzimàtica intrínseca. Es va estudiar l'activitat intrínseca de les aldehid deshidrogenases (ALDH), també com a biomarcador sobreexpressat en càncer. Es va desenvolupar un nou mètode basat en la nano-citometria de flux per a la detecció d'aquests enzims directament dins dels exosomes. Aquest estudi representa el primer pas cap al desenvolupament d'un nou RDT dirigit a l'activitat intrínseca de l'ALDH dels exosomes per al diagnòstic del càncer.

Resumen

En esta esta tesis doctoral se presenta el desarrollo de nuevas herramientas para el diagnóstico precoz y el seguimiento de enfermedades no transmisibles. Aunque existen metodologías de alto rendimiento disponibles en el mercado para conseguir este objetivo, el alto coste y la escasa disponibilidad en entornos de escasos recursos dificultan su implementación en centros de atención primaria de los países en vías de desarrollo. Por tanto, el diseño de nuevos métodos sigue siendo esencial para reducir la incidencia de estas enfermedades. Además del desarrollo de dispositivos de diagnóstico más sencillos y menos costosos, la búsqueda de nuevos biomarcadores en biopsias líquidas es muy relevante. Entre los distintos tipos de biomarcadores, el estudio de vesículas secretadas por las células puede proporcionar información relevante sobre procesos fisiológicos y patológicos de los tejidos. Los exosomas son vesículas extracelulares de tamaño nanométrico que se están estudiando intensamente como potenciales biomarcadores de diagnóstico en muchas enfermedades, especialmente, en biopsias líquidas para el cáncer, debido a su liberación aumentada por las células cancerosas con una impronta molecular alterada. Esta tesis doctoral se enfoca al estudio de las pruebas de diagnóstico rápido (RDT, del inglés *rapid diagnostic test*) para exosomas como biomarcadores de interés clínico. En concreto, se centra en la mejora de los parámetros analíticos, diseños experimentales y tecnologías de estos dispositivos.

Todos los métodos desarrollados se han probado y optimizado con exosomas derivados de sobrenadantes de cultivo celular de las líneas celulares MCF-7, MDA-MB-231 y SKBR3, como modelo de células de cáncer de mama. En primer lugar, se abordó la producción, aislamiento y purificación de estos exosomas cultivados. Las nanovesículas cancerosas obtenidas se caracterizaron física y molecularmente con métodos analíticos estándar, como el análisis de seguimiento de nanopartículas, la microscopía electrónica de transmisión criogénica y la citometría de flujo.

Uno de los principales retos para analizar los exosomas en un RDT es aumentar la sensibilidad y mejorar los límites de detección de los ensayos. En esta dirección, se exploró el uso de técnicas de preconcentración magnética y amplificación de ácidos nucleicos, como la RT-PCR de doble marcaje, para su uso en este tipo de muestras. En esta tesis se desarrolla una nueva plataforma que combina la separación inmunomagnética y la detección electroquímica de amplicones doblemente marcados para la detección cuantitativa de exosomas, basado en la amplificación de las

secuencias mRNA de la gliceraldehído-3-fosfato deshidrogenasa (GAPDH). El método desarrollado se probó con muestras reales de suero humano y permite diferenciar a pacientes con cáncer de mama e individuos sanos, mejorando notablemente los límites de detección.

Por otra parte, se exploraron RDT en papel. Con esta plataforma se consigue la simplificación analítica de los ensayos, y se mejoran sus características para entornos con recursos limitados. En esta tesis se explora por primera vez la potencialidad del ensayo de flujo vertical (VFA) para la detección visual de exosomas. Este método se basa en el uso de la fosfatasa alcalina como marcador enzimático, produciendo una señal colorimétrica en la membrana de papel. Las señales visuales pudieron cuantificarse con un software de análisis de imágenes, obteniendo resultados prometedores para la caracterización de marcadores de proteínas en exosomas con un dispositivo sencillo y de bajo coste.

Por último, se exploraron otros enfoques no convencionales para la detección de exosomas, centrados en la detección de la actividad enzimática intrínseca. Se estudió la actividad de las aldehído deshidrogenasas (ALDH), considerado también como biomarcador sobreexpresado en cáncer. Se desarrolló un nuevo método basado en la nano-citometría de flujo para la detección de estas enzimas directamente en los exosomas. Este estudio supone el primer paso hacia el desarrollo de un nuevo RDT dirigido a la actividad intrínseca de las ALDH de los exosomas para el diagnóstico del cáncer.

Table of contents

Figure index

Glossary

Ab	Antibody
ALDH	Aldehyde Dehydrogenase
ALP	Alkaline Phosphatase
BC	Breast Cancer
CD	Cluster of differentiation
cDNA	Complementary DNA
CTC	Circulating Tumor cells
DNA	Deoxyribonucleic acid
DUC	Differential ultracentrifugation
ELISA	Enzyme-linked Immunosorbent Assay
EV	Extracellular Vesicle
HRP	Horseradish Peroxidase
Ig	Immunoglobulin
IMS	Immunomagnetic separation
LFA	Lateral Flow Assay
MPs	Magnetic particles
miRNA	Micro RNA
mRNA	Messenger RNA
MW	Molecular weight
NCD	Noncommunicable disease
NTA	Nanoparticle tracking analysis
PCR	Polymerase chain reaction
RDT	Rapid Diagnostic Test
RNA	Ribonucleic Assay
RT	Reverse transcription
SEC	Size-exclusion chromatography
VFA	Vertical Flow Assay
WHO	World Health Organization

Chapter 1. Introduction

1. Introduction

1.1 Diagnostic tests and biomarkers

1.1.1 Definition

The World Health Organization (WHO) defines eight types of *in vitro* Diagnostics tests as: screening, diagnostics, aids to diagnostics, monitoring of analytes and disease progression/remission, prognostic, surveillance, and staging.[1] Regarding diagnostic tests, WHO defines it as follows:

> *"Diagnostic tests are used to determine, verify, or confirm a patient's clinical condition as a sole determinant. This type of testing also includes sole confirmatory assays (to verify results of previous testing) and sole exclusion assays (to rule out a particular condition). These tests are designed to evaluate a patient's current state."*

The need of accurate and reliable analytical information for clinical diagnosis of non-communicable diseases such as cancer, usually requires the use of long and complex procedures, which require expert personnel handling of expensive bench-top equipment in laboratory facilities. These requirements represent a major issue for clinical diagnosis in low-income countries with developing health care systems. Focusing on cancer disease, and according to 2019 WHO survey on the national capacity for the prevention and control of noncommunicable diseases[2], less than 40% of low-income countries have an early detection programme for breast cancer at the primary care level, percentage that decreases to less than 5% in the case of colon cancer. Moreover, only a 39% of low-income countries have pathology services for cancer diagnosis generally available at national level, compared with more than 95% of high-income countries.[2]

Nowadays, the standard procedure for the diagnosis of cancer disease often requires imaging techniques, such as X-ray tomography scanning or magnetic resonance imaging. Besides, the analysis of *biomarkers* obtained from biological fluids by minimally invasive procedures is gaining in importance. The WHO defines a biomarker as follows:

> *"A biomarker is any substance, structure or process that can be measured in the body or its products and influence or predict the incidence of outcome or disease".*

Biomarkers, or biological markers, can be found in any type of body fluids, such as blood, urine, saliva, as well as from tissues. Their presence or absence, and concentration in body fluids, might be related to a normal or abnormal process, disease, or condition. Examples of biomarkers include ionic, protein, or lipid-specific concentration in body fluids, gene expression patterns of specific cells, pH levels, oxygen saturation in blood, or electrical activity of the brain or heart, among many others. Their qualitative and quantitative analysis is today performed mainly in laboratory facilities by expert personnel.

The analysis of biomarkers obtained from biological fluids is currently one of the main topics in bioanalytical chemistry. The improvement of clinical diagnostic capabilities in low-resource settings remains as the first and crucial step for advancing towards a better global health. Therefore, as a response to this social challenge, the research of new rapid diagnostic tests (RDTs), as optical and electrochemical biosensors, paper-based tests, or microfluidic devices, is very relevant.

1.1.2 History of biosensors, first designs and applications

The concept of sensor was firstly proposed in the early 1920s by W. Hughes with the discovery of pH electrode[3], but it was not until 40 years later that L.C. Clark and C. Lyons developed the first biosensor, the glucometer[4]. This glucose biosensor was an evolution of Clark's oxygen electrode and is based on the integration of glucose oxidase enzyme on the membrane of that electrode. In that first design, the electrochemical signal from the oxygen electrode decreases proportionally to the glucose concentration in the solution.[4] Based on that design, Yellow Spring Instruments (Yellow Springs, OH, US) developed and commercialized the first glucose-meter in 1975.

Following the path of this first invention, the integration of bioreceptors onto electrochemical sensors has been a key element in the development of biosensors for relevant biomarkers.[5]

Another interesting milestone in the field is the invention of Clearview pregnancy test by Unipath. The particular characteristics of urine from pregnant women were known since the middle-ages in popular culture. For that reason, extensive research was done in the 60s and 70s, focusing on the human chorionic gonadotropin (hCG) hormone as pregnancy biomarker. In the late 70s, the first commercially available assays were approved by the FDA and released in the US, some of them involving tedious and long protocols. Therefore, the release of Unipath's Clearview home pregnancy test in 1988, a latex bead-based lateral flow immunoassay, is considered a major breakthrough in the RDTs research field. This test was based on the detection of hCG hormone in urine and

can predict pregnancy in a one-step protocol in a few minutes with a 99% of accuracy. This test is still today considered the paradigm of RDTs.[6,7]

1.1.3 Biosensors. Definition and classification

Among the different platforms of rapid diagnostic tests, sensors and biosensors deserve a special mention. The design and discovery of the glucose-meter, the first biosensor for clinical diagnosis, supposed a revolution in the bioanalytical field. As defined by IUPAC in its Gold Book for chemical terminology[8], a biosensor is:

> *"A device that uses specific biochemical reactions mediated by isolated enzymes, immunosystems, tissues, organelles or whole cells to detect chemical compounds usually by electrical, thermal or optical signals."*

Biosensors are integrated analytical devices capable of transforming bioanalytical information from a sample into a measurable signal. In essence, a biosensor is composed of 3 main components, depicted in Figure 1.1: i) a biorecognition element, or bioreceptor, that interacts with the analyte, ii) a transducer that transforms the biorecognition event into a measurable signal; and iii) a detector device, able to measure, amplify and process the signal coming from the transducer, and convert it into an analytical signal.

The paradigm of a biosensor is an analytical device with: i) high selectivity of the bioreceptor for the analyte of interest, without interferences from the matrix; ii) reproducibility of the signals in identical experiments, with 5 to 10% of variability is generally accepted; iii) stability of the device in front of ambient disturbances, iv) enough sensitivity for the analyte in the concentration range of interest; and v) linearity of the analytical response.[5]

Biosensors can be classified either according to the type of bioreceptor, such as antibodies, enzymes, aptamers, nucleic acids, and biomimetic materials; or according to the type of transducer, which might be electrochemical, optical, thermal-based, or mass-based. A brief overview of the different biosensors is provided in the next section.

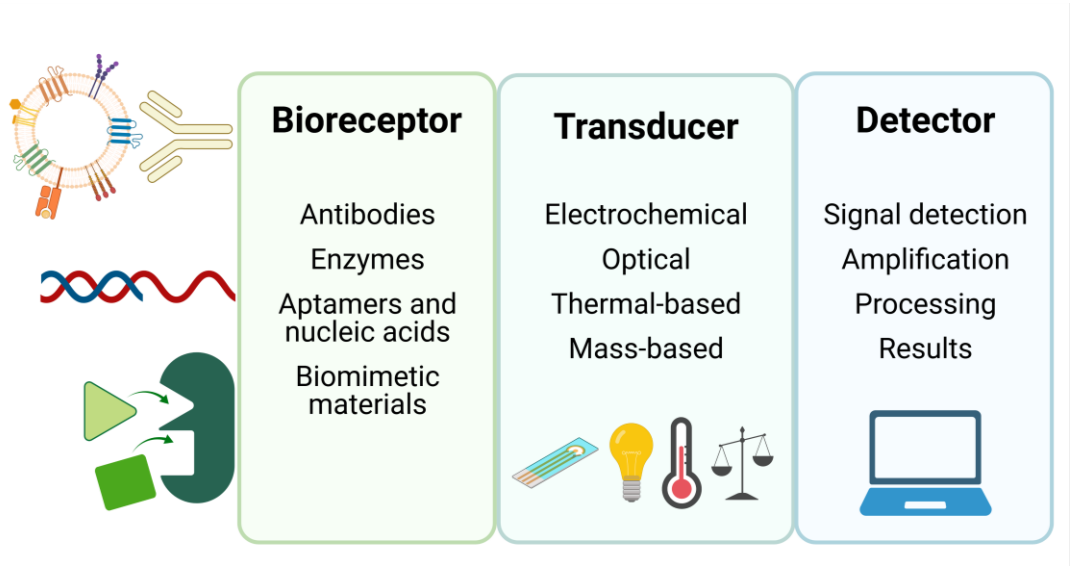

Figure 1.1. Principle of biosensors. The bioreceptor recognizes the analyte from the sample, creating a primary signal, that is converted by the transducer to a measurable signal, further detected and processed into a readable format. Created with BioRender.com.

1.1.3.1 Classification of biorecognition elements

Antibodies

Antibodies, or immunoglobulins, are proteins generated by the immune system as part of the humoral response to a foreign agent. These proteins are produced by plasmatic cells and have high specificity for a particular target, named antigen. The objective of an antibody is to identify and bind the antigen by multiple non-covalent forces, creating an antibody-antigen immunocomplex. This complex will be further detected and eliminated by phagocytic cells of the immune system. This antibody-antigen affinity reaction is based on multiple hydrogen bonds, Van der Waals forces, electrostatic and hydrophobic interactions, and is common in biological systems. The combination of all these weak interactions constitute the antibody affinity that turns to be highly specific and efficient for the antigenic determinant, or epitope (*i.e.,* region of the antigen recognized by the antibody).[9]

Immunoglobulins (Ig) are a family of proteins with five different types in humans: IgG, IgM, IgA, IgD, and IgE. Regarding bioanalytical chemistry applications, IgG antibodies are the most used, as their antigen-antibody interaction is the most specific. In general, according to how antibodies are made, there are three types of antibodies: polyclonal, monoclonal, and recombinant. Polyclonal antibodies are produced by the immune response of animal hosts injected with an antigen of interest. These antibodies are the purified anti-sera of the animals and contain a mixture of monoclonal antibodies targeting different epitopes of the antigen. On the other hand, monoclonal antibodies are

obtained from the culturing of B cells and immortalized myeloma, providing antibodies with specificity for a single epitope of the antigen.[9] Finally, recombinant antibodies are produced using artificial coding genes and phage display technology.[10]

Antibodies are the most commonly used biorecognition element in bioanalysis. From immunodetection methods, such as Enzyme-linked immunosorbent assay (ELISA), Flow cytometry, or Western blot, to paper-based lateral and vertical flow assays, and all types of biosensors. Their integration as bioreceptors is a key and fundamental element for the development of biosensors with high specificities for biological and clinical targets. Electrochemical[11], optical[12,13], and mass-based[14] biosensors have been developed integrating antibodies for multiple applications.

For example in our research group, electrochemical immunosensors with magneto-actuation have been developed targeting multiple targets of interest in bioanalytical chemistry. For example, in food safety i) foodborne bacteria as Salmonella[15] and ii) antibiotic residues[16] in milk; or in clinical diagnosis, iii) breast cancer-related exosomes from cell culture and human serum samples[17]; iv) CD4 receptor onto T lymphocytes as clinical parameter related to AIDS disease[18]; or v) for the diagnosis of celiac disease by detecting IgA anti-transglutaminase antibodies present in patient sera[19].

Enzymes

Glucose oxidase was the first biorecognition element used in a biosensor, precisely in the aforementioned design of the glucometer by Clark and Lyons[4]. The enzyme is entrapped in the surface of the working electrode, as mentioned before, and specifically reacts with the glucose in the sample. This reaction leads to an electrochemical signal that decreases proportionally to glucose concentration.[4] Other relevant examples of enzymatic biosensors include potentiometric biosensors for urea, using urease and ammonium-selective electrodes[20], or optical biosensors for cholesterol, using cholesterol oxidase and horseradish peroxidase to generate a colorimetric signal.[21]

Although the high selectivity and sensitivity of enzymes as biorecognition elements, their activity decreases over time as biologically active material degrades. Therefore, usually non-enzymatic materials, such as metallic or carbon-based nanomaterials, are used to enhance the biosensor response. For example, graphene-modified electrodes coupled with laccase enzyme were used for the detection of emerging pollutants, such as EDTA and benzoic acid.[22] More details about enzymatic biosensors have been extensively reviewed elsewhere.[23]

Aptamers and nucleic acids

Aptamers refer to single-stranded artificial DNA or RNA chains, with specific tailor-made sequences between 10 and 100 nucleotides, able to adopt a particular three-dimensional structure and selectively bind to a target (*e.g.,* peptide, protein, hormone, metabolite, among others) by non-covalent forces. Since the 90s, aptamers have been alternative bioreceptors to antibodies, with many applications especially on electrochemical biosensors. Their small size, stability (especially single-stranded DNA aptamers), versatility, and easy functionalization represent great advantages compared with antibodies. On the other hand, the design and testing of new aptamer sequences are needed for improving their binding properties and extending their application to new clinically relevant targets.[24]

Although its limitations, many proof-of-concept applications have demonstrated its potentialities, such as the detection of thrombin[25] or platelet-derived growth factor protein in blood serum[26], using aptamer-modified gold electrodes. Between different electrochemical techniques, impedance spectroscopy provides an interesting label-free transduction for aptamer-based biosensors.[27]

Biomimetic

As an alternative to biological receptors, such as antibodies or aptamers, organic chemistry has been seeking to imitate biorecognition events in nature. The reaction of cations with ionophores and crown ethers were the firsts attempts in the 60s, but it was not until the 80s and 90s that biomimetic materials gained much interest with the development of molecularly imprinted polymers (MIPs).[28]

These polymers contain selective recognition sites in their three-dimensional structure for a chemical or biochemical template of interest and can bind it through non-covalent interactions. These materials aim to mimic immune-affinity reactions between antibodies and antigens. More details about MIPs synthetic types and methods, as well as applications, have been recently reviewed.[29]

1.1.3.2 Classification of transducers

Electrochemical transduction

The preferred transducers in biosensors rely on electrochemical techniques to transform the analytical information directly into a measurable electrical signal. There are mainly three types of electrochemical measurements:

- Potentiometric: measurement of the difference in potential between a reference electrode, with a constant potential, and a working electrode.
- Conductimetric: measurement of the electrical conductivity/resistivity in the cell due to changes in ionic species or electron transfer resistance.
- Amperometric: measurement of the electrical current circulating through the cell due to redox reactions of electroactive species.

In this thesis, electrochemical measurements were done with amperometry technique using three-electrodes cells. In amperometry, the current is directly related to the reduction or oxidation of electroactive species on the surface of the working electrode, when applied a specific and fixed potential between the working and reference electrodes. The resulting current is measured between the working and counter electrodes. In the case of voltammetry, the current between working and counter electrodes is monitored during a potential scan. The type of potential changes applied to the cell determine the resulting current signal, so different types of voltammetry are defined as i) linear sweep voltammetry, ii) differential pulse voltammetry, iii) square wave voltammetry, and iv) triangular, or cyclic, voltammetry.[30,31]

In this thesis, these techniques have been used to develop an electrochemical biosensor with magnetic actuation for the measurement of double-tagged amplicons from breast cancer-related exosomes, as described Chapter 3.

Most amperometric biosensors rely on the use of enzymatic reporters, specifically oxidoreductase enzymes, to produce and amplify an electrical signal on the surface of the working electrode. Peroxidases, especially horseradish peroxidase (HRP), are the most used enzymes for electrochemical detection. These enzymes catalyze the reduction of hydrogen peroxide to water in presence of a hydrogen donor that will be oxidized. The electrochemical signal is produced by the re-reduction of the hydrogen donor on the surface of the working electrode. The presence of electron-transferring agents, named as mediators, is needed to transport the electrons from the working electrode to the enzyme. In the case of HRP enzyme, one of the most used mediators for electrochemical measurements is hydroquinone (HQ). In summary, the redox reaction of HRP with H_2O_2 and hydroquinone follows three cycles, depicted in Figure 1.2: i) the H_2O_2 from the solution is reduced by the reduced form of HRP producing water and oxidized HRP; ii) the HQ is then oxidized by the HRP producing benzoquinone and regenerates reduced HRP; and iii) the benzoquinone is reduced by the electrodes coming from the working electrode to hydroquinone, creating a reduction current in the cell.[32]

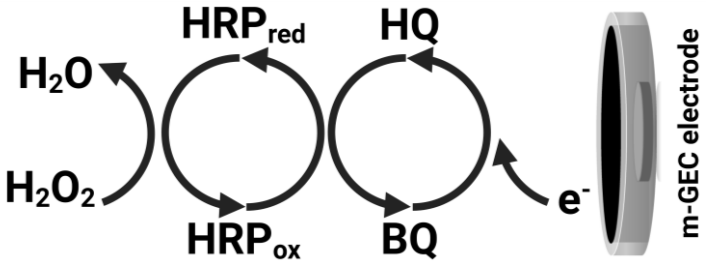

Figure 1.2. Schematic representation of the redox reaction of Horseradish peroxidase with H_2O_2 using hydroquinone as electrochemical mediator, creating a reduction current in the working electrode. Created with BioRender.com.

The current intensity recorded by the electrochemical cell is directly proportional to the concentration of mediator that reacted on the surface of the working electrode, so it can be related to the concentration of HRP enzyme. Similar reactivity applies for HRP catalyzed reactions in colorimetric assays, such as ELISA, on which the hydrogen donors are oxidized to a colored product, further quantified by spectrophotometry.

One of the main advantages of using HRP enzyme is their high turnover, which increases the electrochemical signals, therefore the sensitivity of the assays. Although, many other enzymes have been used as reporters in electrochemical measurements, such as glucose oxidase in glucometers or alkaline phosphatase (ALP). The latter is of great interest in this thesis for its presence in breast cancer-related exosomes and extracellular vesicles (EVs).[33] Further examples and information on electrochemical biosensors for clinical diagnosis can be found elsewhere.[34,35]

Optical transduction

Optical transduction relates to the measurement of changes in the wavelength of a light source when an analyte bounds to the surface of the biosensors through a specific recognition element. One of the most popular optical-transduction techniques is surface plasmon resonance (SPR) based on the interaction of light with functionalized surfaces. Those can be made of metals, carbon derivatives, silica, or polymers (*e.g.,* poly (methyl methacrylate), or PMMA). Multiple applications have been developed, from the measurement of whole microorganisms, small proteins, or even single molecules as environmental contaminants.[12,13]

Another interesting optical-transduction technique is surface-enhanced Raman spectroscopy (SERS). This technique is an improvement of Raman spectroscopy relying on the use of nanomaterials such as metallic nanoparticles for the enhancement of the Raman signals. As SERS signals are highly dependent on the distance of these enhancement tags, they can record changes on the surface of the biosensors, such as

the binding of an analyte. SERS enables *in vivo* and *in vitro* biosensing, as it is a non-destructive and minimally invasive technique. Interesting applications have been developed for the measurement of neurotransmitters, metabolites, peptides, and proteins, as well as whole microorganisms as viruses.[36,37]

Thermal-based transduction

Thermal-based biosensors involve the measurement of heat produced or absorbed during a biochemical reaction. The released or absorbed energy is proportional to the molar enthalpy and quantity of product reacted. These biosensors usually take advantage of enzymes as bioreceptors, such as oxidases and catalases. These provide exothermic biosensing reactions able to amplify the reaction rates, leading to better sensitivities. Also, flow injection analysis technique and microfluidics are used in enzyme thermistors, or thermal sensors. These sensors give a signal that is proportional to the enthalpy change, related to specific substrate concentration.[38,39]

Applications of these biosensors refer to the measurement of clinical parameters as metabolites (*e.g.,* glucose, lactate, oxalate, triglycerides, and peroxides) using its related enzymes as bioreceptors. Also, other clinically relevant parameters have been analyzed, like cholesterol or retinol. Besides environmental and industrial processes could be also monitored.[38]

Mass-based transduction

Mainly two different techniques are used as transducers in mass-based biosensors: quartz crystal microbalance, and cantilevers. Both techniques depend on the measurement of piezoelectric signal changes. Briefly, piezoelectric materials can produce voltage when are mechanically stressed. Or alternatively, a voltage given to a piezoelectric material can cause mechanical stress, *e.g.,* an oscillation when voltage is alternating. Therefore, piezoelectric materials are suitable to construct label-free biosensors only based on mass changes, recording the oscillation of the platform when applying a given voltage.[14]

Quartz crystal microbalance (QCM) is a popular platform for the construction of biosensors, using either antibodies, aptamers, or even MIPs as biorecognition elements. Particularly, high molecular weight analytes are good targets for QCM, such as proteins or microorganisms (*i.e.,* bacteria or viruses), as the oscillation changes are directly proportional to the mass of the analytes. In addition, the use of functionalized nanomaterials (*e.g.,* gold-nanoparticles) is often used to amplify the piezoelectric signals.

These functionalized nanomaterials aim to create a sandwich with the target on the surface of the biosensor [14,40]

1.1.4 Current trends and future perspectives in Rapid Diagnostic Tests

The field of Rapid Diagnostic Tests (RDTs) is continuously growing with more designs and applications in the literature and in the market each year. As a response to social needs, the development of new RDTs for communicable and non-communicable diseases is a priority in the bioanalytical field. The RDTs research is progressing in multiple directions, as looking for new methodological strategies, towards the design of integrated analytical platforms, or for the improvement of device technologies, enhancing their analytical characteristics. Remarkable advancements include: i) the use of microfluidic integrated devices[41,42], ii) the miniaturization of electrochemical biosensors using microneedle integrated electrodes for real-time monitoring[43]; iii) the use of wearable biosensors based on sweat analysis[44]; iv) the use of minimally-invasive sample collection strategies, as liquid biopsy[45,46]; and v) the development of paper-based RDTs[47,48].

Focusing on electrochemical biosensors, it is fair to say that the glucometer is still unbeaten as the gold-standard amperometric RDT for home diagnosis. Of course, many different glucometer devices are available in the market, mostly based on the same bioanalytical method but taking advantage of the last technological advances available. Nowadays, the most outstanding devices in the market might be the FreeStyle Libre 3[49] (Abbott Laboratories, Chicago, IL, US) and the Dexcom One[50] (Dexcom, San Diego, CA, US). Both are micro-needle amperometric biosensors with wireless connection, enabling real-time monitoring of glucose level in blood just using a smartphone.

Similar devices are available for the monitoring of other clinically relevant parameters at point-of-care settings. For example, CardioChek Plus[51] (PTS Diagnostics, Whitestown, IN, US) analyzer provides a full lipid panel (*i.e.,* levels of high-density and total cholesterol and triglycerides) plus glucose levels in just 90 seconds using as little as 40 µL of blood. Furthermore, the i-STAT Alinity[52] (Abbott Laboratories) blood analyzer allows the testing of several blood parameters. For example, electrolytes, blood gases, hematology, coagulation factors, or traumatic brain injury biomarkers, by using fifteen different cartridges containing the specific reagents for each measurement.

Those devices are the paradigm of an electrochemical diagnostic device, as they are fast, accurate, reliable, and cost-effective, representing the way forward for future RDTs.

Concerning paper-based RDTs, lateral flow assay (LFA) tests are the most used techniques for home diagnosis, especially for pregnancy tests and for communicable diseases, such as coronavirus disease (COVID-19). Since the first LFA, Clearview from Unipath, the use of paper as solid support for bioanalytical devices opened new possibilities for developing low-cost, equipment-free, and deliverable RDTs. The intrinsic properties of cellulose give paper-based devices some key features that makes them very attractive as bioanalytical platforms. For example, its hydrophilicity can be used as a driving force in LFA based on capillarity, its stable three-dimensional structure enables the drying of biomaterials and reagents for long-term storage, or its tunable porosity that allows it to be used as filters, among others.

Besides LFA, there are many other paper-based platforms in analytical chemistry. The simplest techniques are solid-phase assays or dipsticks, as the pH universal indicator paper patented in 1933 by Yamada. Also, paper-printed microfluidic devices have great potentialities. For example, the use of hydrophobic materials (*e.g.,* wax) deposited by inkjet printing allows to pattern the devices, integrating different reactivities in a single device.[42,53] Perhaps, one of the most interesting alternatives when dealing with hydrophobic analytes, as in the case of EVs, is Vertical Flow Assay (VFA), also named Flow-through assay.[54] In this case, the liquid flows through the paper membranes, not on top of them as in LFA. This provides some advantages that will be explored in Chapter 4 for the development of a VFA-based RDT for the rapid characterization of EVs derived from breast cancer cell lines.

Of course, the RDTs research field has experienced a revolution in the last two years due to COVID-19 pandemic. The urgent need to develop diagnostic tools for COVID-19 has concentrated efforts of all major research institutions in the field of RDTs development. Many bioanalytical research groups changed their focus to that new and widespread viral disease aiming to provide technological and scientific answers to this social need as fast as possible. The collaboration between researchers from different knowledge areas and different institutions has proven to be fundamental to provide those responses with the necessary reliability and rapidness. Besides, governments and funding agencies provided extraordinary economical resources to the research institutions, as well as to the industries and private companies for the development and mass-scale production of those new RDTs.

Between all those changes in the field, the bigger impact might be the evolution of regulatory policies for rapid diagnostic device's evaluation and approval. As an example, the US Food and Drug Administration (FDA), responsible for clinical RDTs

evaluations in the country, made significant changes in the regulatory pathway fostering to facilitate COVID-19 RDTs development. Those included a new streamlined approach for testing and evaluation of new products, aiming to facilitate its validation and approval. These FDA policy changes might suppose a new paradigm for how diagnostic tools are developed and used in primary care medicine and home diagnosis. Also, it might ease the pathway for the approval of new RDTs for other common diseases, such as hepatitis C.[55,56]

In the private sector, companies that succeeded in developing COVID-19 RDTs and diagnostic kits for point-of-care testing have seen enormous growth. As an example, Cue Health, the official provider of diagnostic kits for the U.S. N.B.A., reported a 25-fold growth in annual revenue, more than $600 million during the pandemic.[56] This could lead to an increased interest in investing on RDTs start-ups and developers aiming to create new products. This will not just generate new business opportunities and great benefits for the shareholders, but might suppose significant improvements in accessibility, affordability, and effectiveness of diagnostic tools for the benefit of global health.

In the case of Catalonia, the recently published 2021 Biocat Foundation report on life science and healthcare sector confirms that this growing interest has already started to become a reality, with exceptional growth in investments in the sector last year. Particularly, the total investment in start-ups set up a new record of €238 million last year, almost doubling the total of 2019. Besides, the number of healthcare diagnostics related start-ups that caught investors grew from just one company in 2019 to twenty companies in 2021.[57]

Finally, European institutions are also showing a renewed interest in life sciences and healthcare, providing unprecedented funding to European research programmes. The new EU ‘Horizon Europe 2021-2027 research & innovation programme’ provides a total budget of €95.5 billion, which represent a 30% budget increase compared with the previous Horizon 2020 programme. It includes €8.246 million for projects related to healthcare research.[58] Also, ‘EU4Health 2021-2027 investment programme’ provides €5.1 billion for investments in national healthcare systems and health policies from EU member states, representing a 10-fold increase from the previous programme.[59] For all of these, the future seems bright for the RDTs research field.

1.2 Exosomes

1.2.1 Definition

The definition of a consensus terminology for a scientific concept might seem as the first step to start new research. It is generally accepted that scientists know exactly the materials and analytes they are studying, so they can build up knowledge from their experimental work. However, in the field of extracellular vesicles (EVs), things are slightly different.

The nomenclature and definition of the basic concepts in the EVs research field are still under debate. The experts arise a major concern about the standardization of the terminology and methodology in this relatively new and rapidly growing research field, as can be seen in the evolution of the number of publications per year on Figure 1.3.

Although attempts have been done to reach a consensus, there is not yet a fully established rule followed by most authors. In 2013, three different definitions for exosomes were coined[60]: i) according to their endosomal biogenesis; ii) as a broad definition for cell-secreted vesicles; and iii) as a fraction of the vesicles obtained by differential centrifugation (*e.g.,* vesicles that sediment between 70,000 and 100,000 x *g*).

The International Society of Extracellular Vesicles ('ISEV') established in 2014 the basis of the harmonization in the field, proposing common criteria for the researchers to discriminate between EV and non-EV components.[61] In that statement, ISEV recognizes that *"the term 'exosomes' is considered as the most commonly used term for any kind of EV"* while advocating for its change in favor of 'extracellular vesicles'.

In 2018, ISEV released an updated version of the guidelines, named as MISEV2018.[62] It establishes a general definition of 'extracellular vesicles' as *"the generic term for particles naturally released from the cell that are delimited by a lipid bilayer and cannot replicate"*. Regarding the term 'exosomes', the MISEV2018 statement claims it as a subtype of endosomal-originated EVs but alleges that no specific biomarkers have been yet defined to classify EVs according to their origin. Therefore, it endorses authors to use either physical characteristics, biochemical composition, or conditions of cell origin to define EVs subtypes.

Certainly, the controversy was not ended with the MISEV2018 statement, as *Witwer and Théry* highlighted in 2019.[63] The popularity of 'exosomes' in terms of its usage in scientific literature has been raising equally as EV, according to the number of publications including each term in text word since 2008.

In this thesis, and following MISEV2018 recommendations to clearly define each term, the word ‘exosomes’ will be used as the generic descriptor for small EVs naturally released from the cell that are delimited by a lipidic bilayer and cannot replicate.

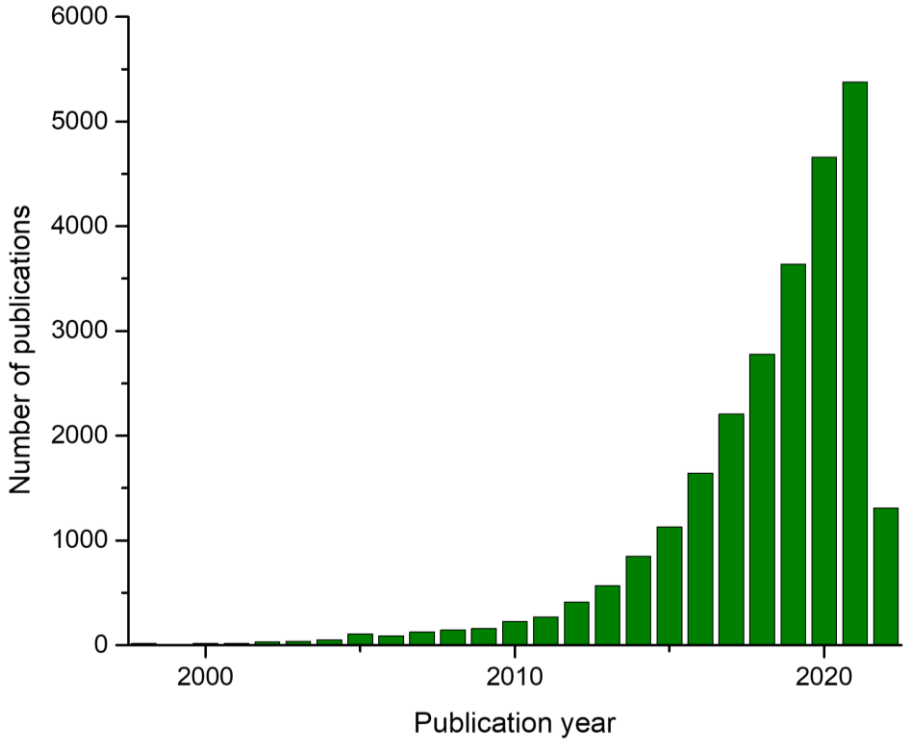

Figure 1.3. Publications related with exosomes released per year. Data from Web of knowledge core collection, keyword ‘Exosomes’, all fields. Accessed April 27th, 2022.

1.2.2 History

The confusion with ‘exosomes’ started from the very beginning. The first scientific publications that used this term[64–67] were not about extracellular vesicles. *Fox et al.*[64–66] described ‘exosomes’ as DNA fragments of external origin that are transferred into a cell and associated with the homologous chromosome segments. It was not until *Trams et al.*[68] that exfoliated membrane vesicles were proposed to be referred as exosomes. Again, in 1987, *Johnstone et al.*[69] named membrane-released vesicles as exosomes and, finally, the meaning of the term was adopted as a general rule.

Nevertheless, several previous publications showed evidence of the presence of vesicles that were released from cellular membranes. A crucial step forward was the development of electronic microscopy in the late 60s and early 70s. These techniques allow the obtention of micrographs with enough resolution to demonstrate the presence of vesicles, for example in bone matrix[70,71]. Several studies were published in the 70s and 80s, but it was not until the 2000’s that the research field experienced a continuous

expansion, as can be seen in Figure 1.3. Recently, an interesting review was published about the history of EVs from their discovery to their current state of the art and future challenges.[72]

This growing interest in exosomes research covers a broad range of topics in biotechnology and biomedicine. There are studies related with its role in intercellular communication mechanisms[73,74]; its application as biomarker for diagnosis and monitoring of cancer[75] and other diseases[76,77]; or as a drug-delivery platform for therapeutics and vaccines[78–81]; and regarding the characterization of its biochemical cargo, such as proteins[82], lipids[83], RNA[84] and microRNA[85]; among many other examples and research topics.

In the last ten years, numerous societies have been founded focusing on EV research. Besides the previously mentioned International Society of Extracellular Vesicles (ISEV) founded in 2011, there are dedicated EV societies in the US, Canada, Australia, and New Zealand and in almost every European country, including Spain's GEIVEX ('*Grupo Español de Innovación e Investigación en Vesículas Extracelulares*'). Also, there is a peer-reviewed open-access journal, Journal of Extracellular Vesicles, published by WILEY and ISEV, with an impact factor of 17.337 in 2021.

Exosomes and EVs were found to be released by all types of cells in humans and can be obtained from almost all biological fluids such as blood[86], plasma[87], serum[17], urine[88], semen[89], saliva[76], breast milk[90], or cerebrospinal fluid[82].

The potential applications of exosomes for diagnosis and therapeutics are very interesting for academics but also in biotechnology and biomedicine industry. Commercial kits are available in the market for their isolation (*e.g.,* PEG-based ExoQuick™, ExoPure™ SEC columns) and analysis (*e.g.,* Invitrogen Exosome detection reagents, MACSPlex flow cytometry kit from Miltenyi Biotec), even specialized equipment for its characterization (*e.g.,* ExoView® platform). In further sections, more examples will be presented and detailed.

1.2.3 Extracellular vesicles subtypes. Classification, biological origin, and function

The biochemical composition of all types of EVs is highly complex, as they might contain variable concentrations of many proteins, nucleic acids, lipids, and metabolites. Specific biomarkers for each group of EVs have not been clearly defined[62] and, accordingly, the classification of EVs is usually based on their size, density, and biogenesis pathway.[73,74]

Although there is not a general consensus among different authors and the biophysical properties are overlapped between the groups, the EVs are usually classified into three subtypes, as shown in Figure 1.4: exosomes (small EVs), ectosomes (medium-sized EVs), and apoptotic bodies (large EVs).[73,74,91,92]

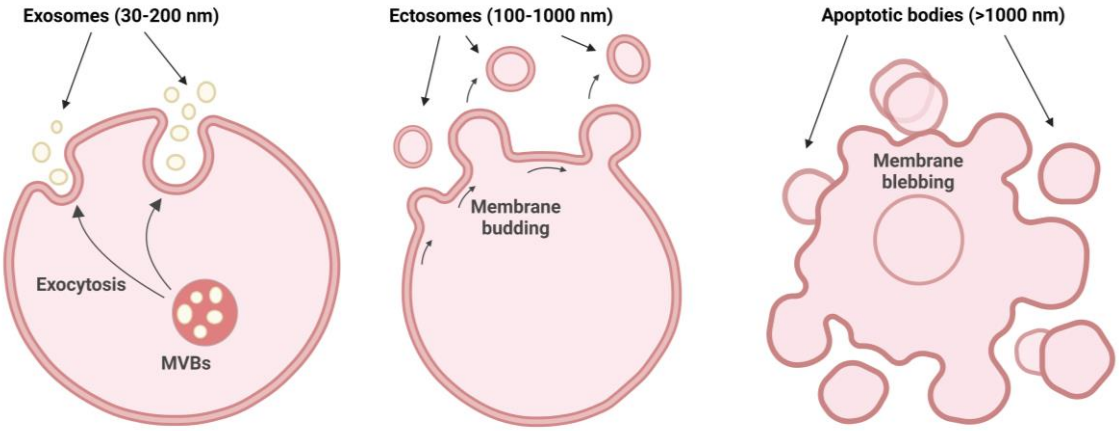

Figure 1.4. Types of extracellular vesicles, according to their biogenesis pathways: i) Exosomes come from the exocytosis process of intraluminal vesicles formed in multivesicular bodies; ii) Ectosomes, or microvesicles, come from the plasmatic membrane budding; and iii) Apoptotic bodies come from plasmatic membrane blebbing during apoptosis of the cell. Created with BioRender.com.

1.2.3.1 Exosomes

Exosomes are defined as EVs ranging from 30 to 200 nm in diameter originated from the exocytosis pathway of multivesicular bodies (MVBs), with a density range from 1.13 to 1.19 g mL^{-1} and spherical shape in solution.[73]

The biological origin of exosomes is schematized in Figure 1.5. Briefly, it can be summarized in 6 steps. (1) The internalized materials from endocytosis are (2) sorted into early endosomes, (3) which then mature into late endosomes, or multivesicular bodies. Within those MVBs, intraluminal vesicles (ILVs) are formed by the budding of the endosomal membrane during the maturation process. Besides endosomal originated cargoes, (4) cytosolic material is also internalized into ILVs. Finally, (5) the MVBs containing ILVs are transported to the plasmatic membrane and (6) its fusion releases ILVs to extracellular space, secreted as exosomes.[74,93]

However, the exact composition of the intracellular compartments from which exosomes are released is still unclear. Some studies suggest different pathways for the ILVs depending on their destination, either secretion as exosomes or degradation in lysosomes. This evidence might suggest that there might be different types of MVBs or ILVs within the MVBs, resulting in exosomes with different molecular cargo released by the same cell. It is still unknown whether the composition of the ILVs can influence their

destination, or some specific biomarkers can be indicative of their releasing pathway.[73,91,94]

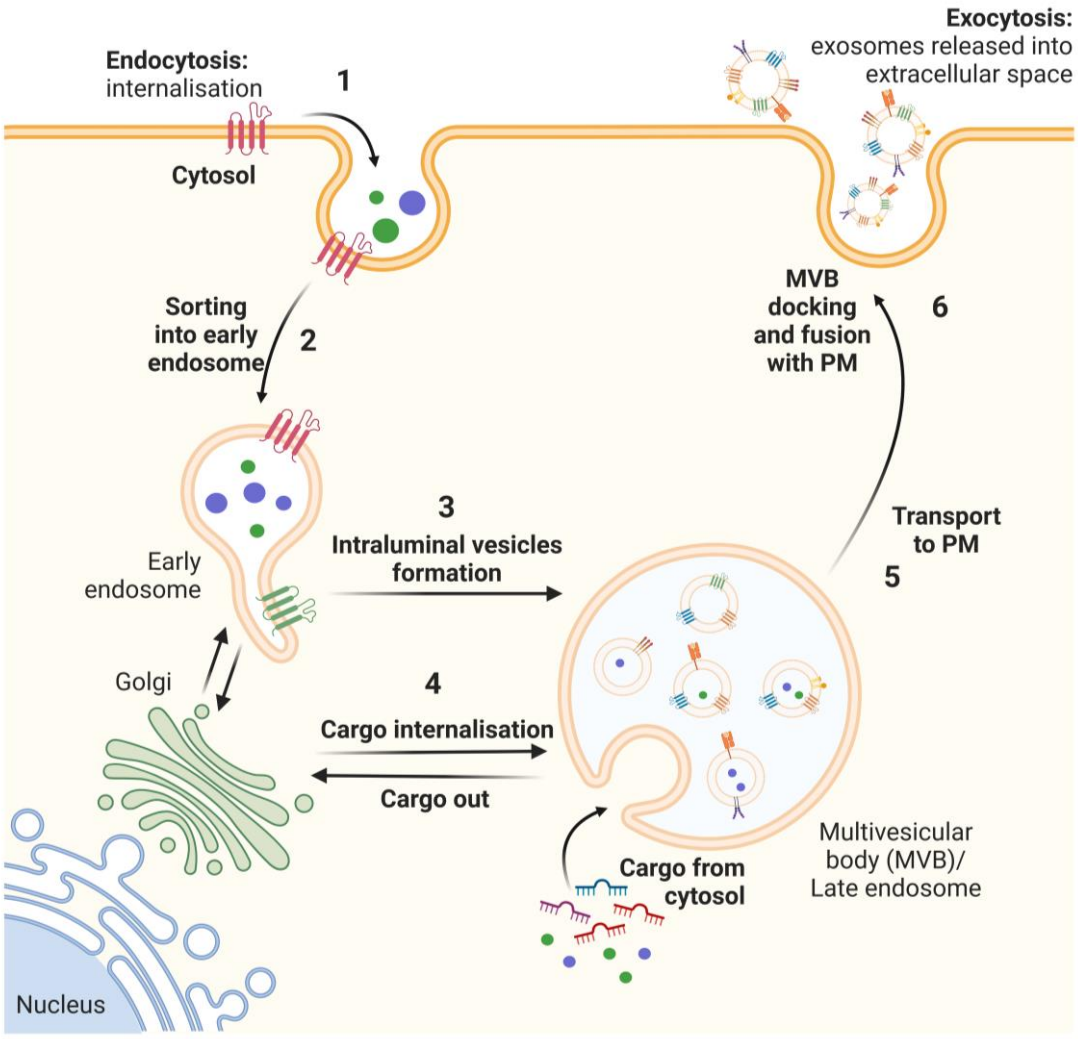

Figure 1.5. Biogenesis pathway of exosomes. Adapted from reference [73]. Created with BioRender.com.

The biological function of these small EVs has been widely studied in the last three decades. Firstly, the secretion of these ILVs as exosomes was initially believed as part of the mechanism of the cells to eliminate unnecessary proteins. However, from studies conducted in the 90s, exosomes were found to play an important role as reporters in the intercellular communication mechanism. It was firstly inferred from their relationship with the immune system and cancer disease in the 1990s. Later, it was demonstrated that the exosome mRNAs and miRNAs content remains functional and can change biological behavior when interacting with a recipient cell.[74,95]

Three mechanisms have been described for the interaction of exosomes when reaching a target cell: direct interaction, fusion with the plasma membranes, and

internalization. At first, the interaction of membrane ligands on the surface of the exosomes can bind surface receptors in the cell and generate downstream signaling. This mechanism has been described in relation to immune response and apoptotic functions. Secondly, the exosomes can fuse with the plasma membrane and release their content into the cytosol of the recipient cell. Although weak evidence, it has been observed in dendritic and tumoral cells using fluorescent reporters. At last, the main uptake mechanism is the internalization of exosomes followed by releasing of their cargo into the cytosol, using the common endocytic pathways. [73]

The study of the biogenesis, secretion, and biological functions of exosomes and EVs is beyond the focus of this thesis. To find more information about these topics, an interesting and extensive publication has been published.[96]

Regarding the biochemical content of these vesicles, proteins[82], mRNA[84], miRNA[85], enzymes[33], DNA[97], and lipids[83], were found in exosomes (Fig. 1.6). The particular biogenesis pathway gives them differential molecular composition from their parent cells, so the exhaustive characterization of these vesicles is required. Every year many studies are being published and efforts are being done to centralize and classify this massive amount of information. Particularly, Vesiclepedia[98], ExoCarta[99], exRNA Atlas[100], EV-track[101] databases compile the latest updates on the EV research field. For example, currently (February 2022) exRNA Atlas[100] contains 9,987 different RNA sequences; while Vesiclepedia[98] has 349,988 protein, 27,646 mRNA, 10,520 miRNA and 639 lipid entries.

1.2.3.2 Ectosomes

Ectosomes, also called microvesicles, are EVs ranging from 100 to 1,000 nm in diameter originating from plasmatic membrane budding, with a density range from 1.04 to 1.07 g mL^{-1} and showing an irregular shape.[73]

Although the biogenesis of ectosomes has a well-established theory, their exact formation route and the characterization of their molecular content has not been achieved yet. The lack of standardized isolation protocols for ectosomes (and the other subtypes of EVs) and the inherent heterogenicity of EVs make molecular characterization studies heavily dependent on sample collection and purification protocols.[94,102]

These conditions make it almost impossible to determine specific markers able to distinguish each subtype of EVs. Nevertheless, proteomic studies of ectosomes have determined the presence of cytosolic and plasma membrane-associated proteins, such

as tetraspanins, integrins, or matrix metalloproteinase MT1-MMP and adhesion protein P-selectin. Lipids have been also detected, such as cholesterol, sphingomyelin, and ceramide, similarly to exosomes; as well as miRNAs, mRNAs, and non-coding RNAs fragments.[94]

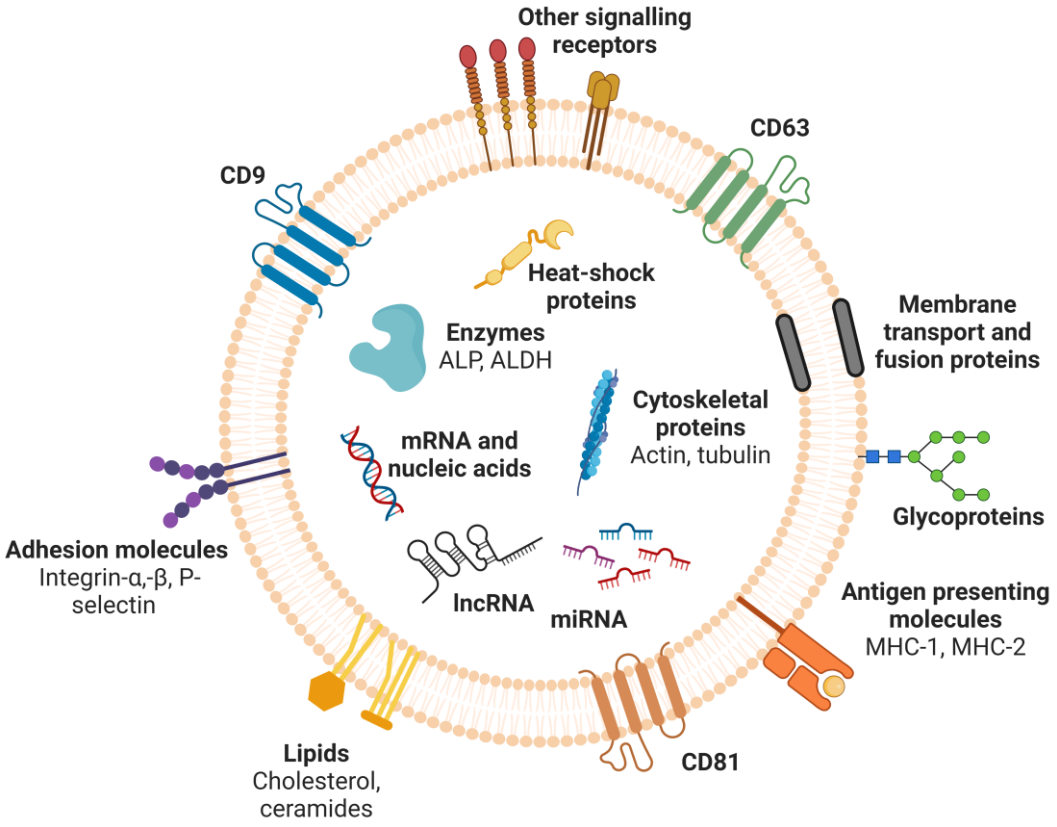

Figure 1.6. Schematic representation of an exosome. Created with BioRender.com.

Likewise exosomes, the biological function of ectosomes is related to their role in intercellular communication. It has been demonstrated that these vesicles are also able to transport functional biological material from parent cell to recipient cell, altering the functions upon its uptake and cargo delivery.[102]

1.2.3.3 Apoptotic bodies

Apoptotic bodies, or apoptotic vesicles, are large EVs (>1000 nm in diameter) originating from blebbing of the cells undergoing apoptosis, with a density range from 1.16 to 1.28 g mL^{-1} and showing variable shapes.

Apoptotic bodies do not have a particular biological function. They are formed when a part of the plasma membrane separates from the cytoskeleton in dying cells due to changes in the hydrostatic pressure. As a result, their composition is distinct from

exosomes and ectosomes, as apoptotic bodies can contain intact cellular organelles and associated proteins. Proteomic profiles from apoptotic bodies are similar to cell lysate, in contrast with other EVs.[102] Also, these vesicles have been described to contain nucleus associated proteins (*e.g.,* histones), fragments of DNA, and chromatin.[73]

1.2.4 Isolation, enrichment, and purification methods of extracellular vesicles

The low concentration of EVs in real samples and the complexity of their matrices impel the use of isolation, enrichment, and/or purification methods prior to any analysis or characterization experiment. It might be one of the most challenging tasks when dealing with EVs and exosomes, and it must be carefully considered in any experimental design. As previously mentioned, the different subtypes of EVs have overlapping biophysical properties, and physical isolation methods based on size and density, cannot separate specifically the different groups of vesicles. Moreover, the conclusions of any experiment related to EVs might be critically affected by these isolation methods.[92]

The development and standardization of isolation, enrichment, and purification protocols for EVs remain a major challenge in this research field. The next sections will review the classical physical-based isolation methods for EVs, including differential ultracentrifugation, density gradient ultracentrifugation, ultrafiltration, size-exclusion chromatography, and polymer-based precipitation, as well as other novel methods such as immunomagnetic separation, solid-phase extraction, and based on microfluidics.

1.2.4.1 Differential ultracentrifugation

Differential ultracentrifugation (DUC) remains the standard method for exosomes and EVs' isolation in most laboratories. This method was the first one described to isolate exosomes from reticulocyte tissue culture medium[69], further optimized[103] by increasing RCF centrifugation speeds up to 100,000 x *g*. Recently, an updated protocol with minor changes in centrifugation speeds and times was proposed.[104]

The main objective of this method is to eliminate different fractions of particles by successive centrifugation steps at increasing speeds. As described in Figure 1.7, four successive centrifugation steps are required to separate i) cells at 300 x *g*; ii) dead cells and large cell debris at 2,000 x *g*; iii) medium and large EVs at 10,000 x *g*; and iv) small EVs, or exosomes, at 100,000 x *g*. An interesting theoretical analysis of this isolation method was made considering commonly used instrumentation and experimental parameters.[105]

For instance, the viscosity and composition of the matrix affect the separation of exosomes using DUC. Usually, high-viscosity biological fluids (*e.g.,* blood plasma, serum, saliva, or semen) might require increased speed and length of centrifugation steps compared to exosomes obtained from less viscous matrices, as cell culture supernatants.[103] Also, in some cases, it is possible to substitute low-speed steps from DUC by filtration with 0.22 µm membranes to eliminate dead cells and large debris while keeping small EVs for further purification by DUC.[103] In other cases, a filtration step is added before the 100.000 x *g* step to reduce co-isolation of larger EVs that did not precipitate by DUC.[106]

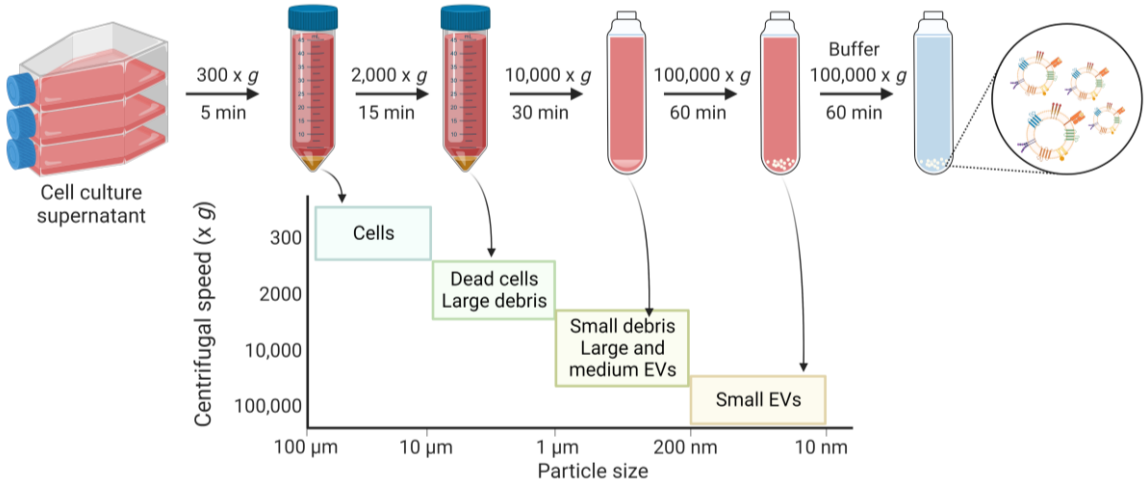

Figure 1.7. EVs isolation protocol using differential ultracentrifugation. As an example from cell culture supernatant, sequential centrifugation steps (300, 2,000, 10,000 and 100,000 x g) are applied to separate small EVs from other fractions, excluding cells, dead cells, and debris, large-sized EVs (i.e., apoptotic bodies) and medium-sized EVs (i.e., ectosomes). Created with BioRender.com.

DUC is a well-established methodology commonly used in most EVs research laboratories. It is moderately time-consuming and cost-effective compared with other methods, such as density-gradient ultracentrifugation. Little or no sample pretreatments are required, therefore DUC has less protein contamination and higher purities compared to other isolation methods.[107] On the other hand, DUC provides lower extraction yields than other techniques.[108]

Although DUC requires the use of costly, benchtop equipment that requires intensive maintenance and laboratory facilities, ultracentrifuges are vastly available in the market. Other drawbacks of DUC are the effect of high centrifugal forces (RCF up to 100,000 x *g*) on the vesicles, as mechanical damage and aggregation of individual exosomes may occur. Also, pelleted exosomes might coexist with other non-exosomal vesicles (from other non-endosomal biogenesis pathways) and precipitated protein

aggregates.[109] Considering this, DUC might be precisely considered as an 'enrichment' method, prior to a pure isolation method of exosomes.

These protein contamination issues can be minimized by combining ultracentrifugation with filtration steps, increasing the purity of the isolated exosomes, although it may reduce the yield of the method.[106]

1.2.4.2 Density gradient ultracentrifugation

Based on the same principle as DUC, density gradient ultracentrifugation[109] uses an additional density gradient matrix to improve the separation efficiency and purity. This method can separate exosomes by density from non-vesicular particles of similar sizes, such as proteins or protein/RNA aggregates, or small apoptotic bodies. Extremely pure small EVs and exosome samples can be obtained by separation from other extracellular components based on their specific density. The most common density gradient ultracentrifugation methods involve using a sucrose gradient[110] or cushion[103,111], or iodixanol gradient.[104,112,113]

Density gradient ultracentrifugation is capable of separating subcellular components, such as mitochondria, peroxisomes, and endosomes.[114,115] Also, it can isolate exosomes from high-viscosity biological samples, such as saliva.[112] In the market, there are commercial kits, such as OptiPrep™ (Abbott Laboratories), that provide centrifugation mediums for the isolation of nano-sized particles, including exosomes.[113]

Usually, these density gradient methods require longer centrifugation times (14-18h) at higher speeds (100,000-160,000 x *g*) than conventional DUC to achieve good separation and enrichment of exosomes, therefore aggregation of the vesicles and mechanical damage of the membranes may occur, as described before.[109] Besides, the high concentration of density matrix reagents (sucrose, iodixanol) can change the osmotic environment of the exosomes and negatively affect their biological activity.

Regarding highly sensitive downstream applications that require high purity samples (*e.g.,* proteomics, transcriptomics, miRNA sequencing), density gradient ultracentrifugation thus may be adequate and cost-effective.

1.2.4.3 Ultrafiltration

Ultrafiltration can separate exosomes and EVs based on their size, using size or molecular weight cut-off filtration membranes. Like any kind of filter, particles below the specific size or molecular weight cut-off of the pores can pass through the membrane while retaining larger particles. Ultrafiltration can be used to isolate exosomes from biological fluids such as urine samples[88,116] or cell culture supernatant.[117]

Compared with ultracentrifugation-based methods, ultrafiltration is simpler and faster, with lower equipment requirements, while obtaining comparable recovery yields.[118] Nevertheless, ultrafiltration units are expensive and not reusable, as often get clogged by particle aggregates during the filtration process, reducing separation yields.[119] Also, the purity of the separated exosomes might be adversely affected by large (>MWCO of the membrane) and flexible particles that can pass through the pores. Therefore, to increase the efficacy of the separation, ultrafiltration is used as an additional purification step combined with other isolation methods, such as ultracentrifugation[106,109] or size exclusion chromatography.[88,116,117,120]

In recent years, ultrafiltration has also been combined with microfluidics to develop exosome isolation platforms[121], such as ExoTIC[122], Exodisc[123], or ExoSMP[124]. Briefly, the Exosome Total Isolation Chip (ExoTIC)[122] combines five filter membranes ranging from 200 to 30 nm pore size in a modular device able to isolate EVs using a simple syringe pump to control pressure and flow rate. The Exodisc[123] is a lab-on-a-disc integrated device that uses centrifuge force to isolate EVs using two nanofilters of 600 and 20 nm, and it was recently updated to EV-Ident device (Fig. 1.8).[125] The latter devices is able not just to isolate three different exosome fractions (200, 100, and 20 nm pore size membranes) but to fluorescently label *in situ* the EVs for its protein marker expression analysis. Finally, ExoSMP platform[124] is a very simple polydimethylsiloxane (PDMS) device with two membrane filters (100 and 30 nm pore size) integrated between its microchannels, that can separate EVs in a continuous flow rate with high recovery rates and reproducibility.

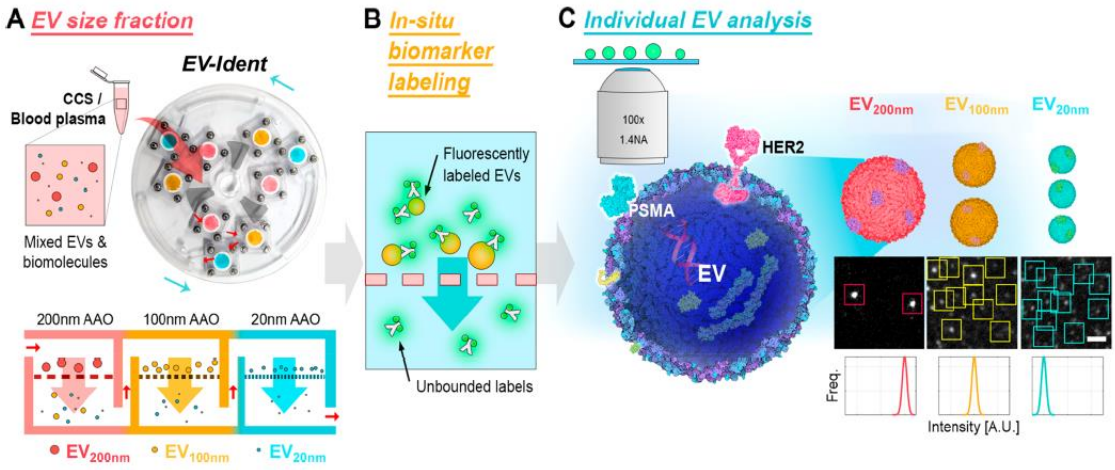

Figure 1.8. EV-Ident ultrafiltration-based EVs integrated analytical device. Reprinted with permission from reference[125]. Copyright 2022 – American Chemical Society.

In contrast with the previous microfluidic integrated platforms, that are still under development and not commercially available, there are UF units already available, such as Durapore® Membrane Filter (Merck KGaA, Darmstadt, HE, DE), Vivaspin® (Sartorius Lab Instruments GmbH & Co. KG, Goettingen, NI, DE) or exoEasyTM (Qiagen, Hilden, NW, DE).

1.2.4.4 Size-exclusion chromatography

Size-exclusion chromatography is also based on the separation of particles according to their size and passage through a physical barrier, in this case, a chromatography column. The interaction between the analyte particles and the heterosporous polymeric beads in the column relates to the separation of the particles according to their hydrodynamic radius.[119] The larger size of exosomes compared to individual proteins, protein aggregates, and other contaminants of the samples, leads to high levels of purification of exosome vesicles in complex biological samples. Moreover, the column chromatography allows the sequential elution of different EV fractions of decreasing size using a single stationary phase.[109] Sepharose-based columns are the most commonly used for EVs isolation, in specific Sepharose CL-2B (Sigma-Aldrich Inc., St. Louis, MO, US) columns allow the separation of approximately 70 nm diameter vesicles and larger.[126]

To avoid physical damage to the EVs, size-exclusion chromatography is performed under low pressures, even by gravity. This ensures the integrity of exosomes structure, although long elution times could be required. Also, the mild conditions and reagents used in this method minimally affect the biological activity of EVs, contributing to maintaining the integrity of the proteins and enzymes present in the exosomes.[127] The high purity of the preparations makes it suitable for high demanding 'omics' downstream applications, like as density gradient ultracentrifugation, but presenting several advantages regarding cost-effectiveness, lower requirements of reagents, time, and equipment. A comparison was done between EVs purified by polymer-based precipitation and size-exclusion chromatography, using mass spectrometry to characterize protein markers in the preparations.[126] This study concludes that size-exclusion chromatography is able to remove free plasma proteins, in contrast with polymer-based precipitation, and allowed the detection of several protein markers in the preparations by mass-spectroscopy proteomic analysis.

Size-exclusion chromatography is widely implemented to isolate exosomes from biological samples, such as blood plasma[118,127,128] and urine[88]. Sepharose-based columns offer good cost-benefit to obtain high purity exosomes[88,118,126–128]. In separating

exosomes from human plasma, lower recovery rates are obtained compared with polymer-based precipitation, although higher purity samples can be obtained with size-exclusion chromatography.[118]

An exhaustive protocol has been recently published[129] detailing size-exclusion chromatography column preparation, EVs separation from different biological fluids (culture media, plasma, urine, and peritoneal dialysis effluent), and their related pre-processing and characterization techniques. It also contains a washing protocol for the columns allowing its re-use up to five times. In addition, a single-step isolation protocol with sepharose-based columns has been also published for plasma samples,[120] minimizing the required time of the assay to just 20 minutes while obtaining purities and recovery rates comparable to UC, according to the authors.

To enhance the resolution, reproducibility, and comparability of size-exclusion chromatography preparations and assays, there are commercially available pre-packed sepharose columns specific for EVs isolation, for example, ExoSure (GeneCopoeia, MA, US), PURE-EVs Columns (Bio-Techne R&D Systems, Madrid, ES), or even dedicated instruments as qEV Exosome Isolation platform (Izon Science, Christchurch, CA, NZ).

1.2.4.5 Polymer-based precipitation

Polymer-based precipitation is a simple and fast method for the separation of exosomes and EVs from an aqueous solution. The principle of this method is to use a polymeric matrix that entraps water molecules in their structure, thereby forcing the less-soluble particles and components, such as exosomes and EVs, to precipitate out of the solution. Then, the precipitated particles are collected by a short, relatively low-speed (*e.g.,* 10,000 x *g*) centrifugation or filtration.[130]

The polymer-based precipitation method is widely used for exosome isolation by many researchers.[131–133] It is an efficient and mild separation method, able to preserve biological activities of exosomes derived from cell culture supernatants[132], as well as from biological samples, such as human serum, saliva[131], and urine.[134]

There are many commercial precipitation kits for exosomes, such as ExoQuick™ (System Biosciences, Mountain View, CA, US), Total Exosome Isolation kit (Invitrogen, Thermo Fisher Scientific, Waltham, MA, US), or miRCURY Exosome Isolation Kit (Qiagen, Hilden, NW, DE). These kits are user-friendly, fast, and effective to isolate exosomes of 40-180 nm in diameter, although their relatively high cost per sample. This precipitation methods require lower sample volumes than the previous methods, thus being able to deal with small volume clinical samples.[134]

As the main drawback of this technique, contaminant non-vesicular components such as lipoproteins, albumin, apolipoprotein E, and Tamm–Horsfall protein, can be coextracted with the exosomes, as well as other non-exosomal EVs, which impair their subsequent proteomic analysis [108,109,113,118,134]. Some studies reveal that lipoproteins and protein aggregates could be counted as EVs in NTA analysis, leading to an overestimation of the particle amount and highlighting the limitation of using particles per µg ratio as purity measure in human serum samples.[135]

On the other hand, the polymer-based precipitation method showed the highest exosomal RNA and miRNA extraction efficiency among EVs isolation methods[107,109,134,136], thus better results in the genomic analysis could be obtained.

1.2.4.6 Immunomagnetic separation

Immunomagnetic separation (IMS) is based on the capture and separation of the vesicles using biologically functionalized paramagnetic particles (MPs). The application of an external magnetic field to a MPs suspension can be used to separate a specific analyte bound to a solid magnetic support in a liquid matrix. In this case, functionalized MPs with biological recognition elements, mainly antibodies[137] but also aptamers[138], can react specifically with membrane receptors of the exosomes and bind to them by an affinity reaction.

The synthesis of polymer-coated paramagnetic microparticles was developed in the late 1970s by a Norwegian professor, Dr. John Ugelstad, a specialist in emulsion polymerization. The technology was licensed by Dyno Industrier in 1980, who commercialized the MPs in 1982 as Dynabeads. The company changed hands successively until 2005 when it was acquired by Invitrogen, a brand of Thermo Fisher Scientific.[139]

The composition of the MPs has basically three parts, as shown in Figure 1.9, panel A: i) a superparamagnetic core, usually made of magnetite iron oxide (Fe_3O_4), but also can be tuned with cobalt, nickel, or manganese, modifying its magnetic properties[140], ii) covered with a polymeric shell, usually made of polystyrene, silica or alumina, to protect and stabilize the core, and iii) a coating containing chemical or biochemical functionalities.

Although its relatively high cost per sample, biologically functionalized magnetic particles represent an excellent choice for their easy-of-use, stability, and versatility. Their use revolutionized the bioanalytical research field, overcoming previous limitations of isolation methods in many types of applications, besides the isolation of exosomes

and EVs. Our research group has reviewed its application for the isolation of foodborne pathogens[141] and biomarkers of infectious diseases[142]. And recently, the application of biomimetically-modified MPs for sensing and biosensing[143], summarizing interesting applications of this widely used technology in the bioanalytical field.

Regarding exosomes and EVs, the use of IMS has many advantages compared with other isolation methods. Firstly, IMS is based on an affinity reaction to capture the analytes, plus a mild magnetic field to separate them, giving this technique the ability to maintain structural integrity and biological activity in the purified analytes, exosomes in our case. As previously mentioned, classical methods of isolation, such as differential ultracentrifugation or ultrafiltration, might affect the biological activity or structure of the analytes.

There are many examples of IMS of exosomes using different types of functionalized MPs with biorecognition elements, such as antigen-specific aptamers[144,145], antibodies targeting exosomal membrane receptors[137], or lipid-based probes[146,147]. Other non-specific isolation methods for exosomes have been developed with MPs coated with TiO_2 via phospholipid interactions[148] or using molecularly imprinted polymer (MIPs) tailor-made nanocavities as recognition elements[149].

Magnetic particles can be synthesized from iron oxide powder and functionalized with relatively easy protocols and materials[150]. Nevertheless, there is a huge variety of commercially available ready-to-use MPs with different core materials, sizes, chemical, and biochemical coatings. As abovementioned, Dynabeads (Invitrogen, Thermo Fisher Scientific) was the first brand to fabricate MPs, and 30 years later, offers the largest catalogue of MPs in the market. Other companies commercialize MPs, such as PureProteome (Sigma-Aldrich, Merck KGaA), Estapor microspheres (Merck KGaA), Ademtech SA (Pessac, FR), AMS Biotechnology Ltd (Milton, OX, GB), Miltenyi Biotec (Bergisch Gladbach, NW, DE), Proteintech Group Inc. (Rosemont, IL, US), among many others.

Of particular interest for this thesis was the use of Dynabeads M-450 tosylactivated (Invitrogen, cat. no. 14013) and its covalent functionalization with proteins. These polystyrene paramagnetic particles of 4.5 µm in diameter are coated with p-tosylate groups, able to act as leaving groups in an S_N2 reaction with nucleophiles. All proteins are potential candidates to be covalently attached to MPs by the amino groups in their sequence. Particularly interesting is the coating reaction of MPs with antibodies by using the N-terminal amino groups, as detailed in Figure 1.9, panel B.

Other types of chemically active MPs contain amine, carboxy, or epoxy groups, ready to be coupled with biomolecules of interest. Also, there are biologically-modified MPs commercially available, such as those coupled with streptavidin, primary and secondary antibodies, protein A and protein G, or DNA probes as oligo(dT).[151]

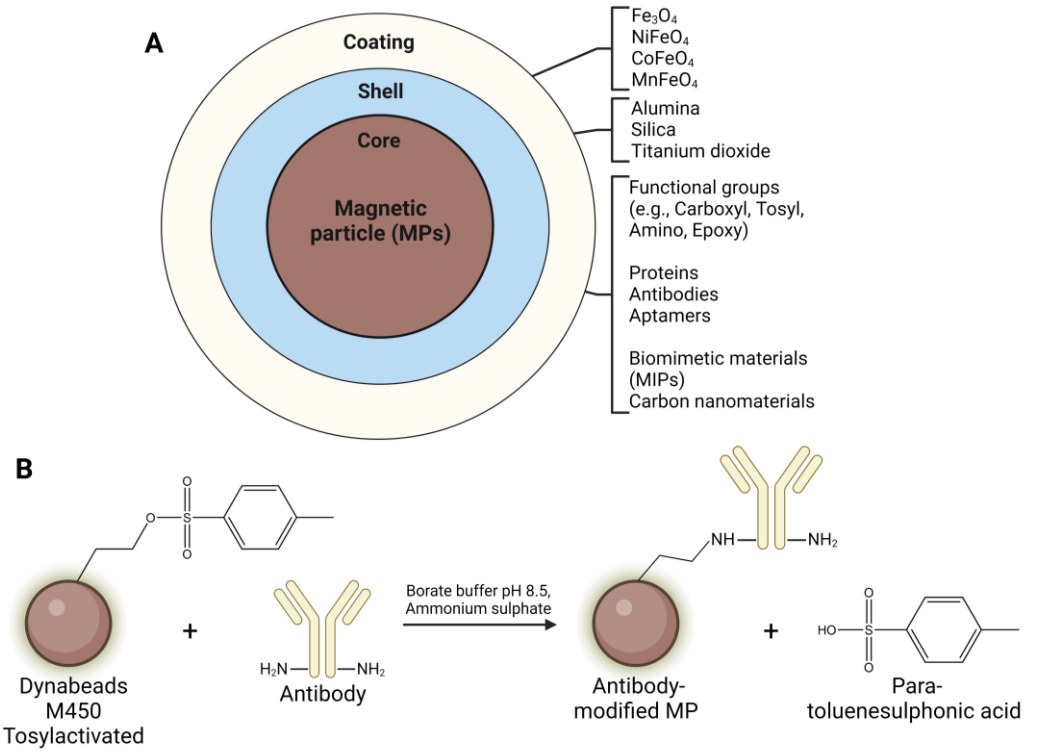

Figure 1.9. Panel A. Schematic representation of a magnetic particle, showing its three parts: a magnetic core, covered by a polymeric shell and a functional coating. Panel B. Covalent immobilization reaction of an antibody onto tosylactivated magnetic particles. Created with BioRender.com.

Our research group has developed many bioanalytical applications of magnetic separation in recent years using modified MPs.

Antibody-modified MPs are our preferred choice for the IMS of i) exosomes from breast cancer cells lines and osteoblasts, further analyzed using magneto-ELISA[137] or electrochemical detection[17,33]; ii) T lymphocytes using CD4-modified MPs in magneto-ELISA[152], or using CD3-modified MPs and quantifying the expression of GAPDH and Interferon-γ mRNA transcripts from the captured cells[153]; iii) food-borne bacteria as *Salmonella* in milk samples, analyzed using magneto-ELISA[154] or electrochemical detection[155,156]; or *Mycobacterium fortuitum* in hemodialysis water detect by magneto-ELISA[157].

Streptavidin-modified MPs (strep-MPs) have been also widely used for the capture and isolation of biotinylated proteins or tagged-DNA. For example, double-

tagged PCR amplicons from *Salmonella* and *Escherichia Coli* specific genes were isolated with strep-MPs and analyzed by electrochemical detection[158]; while biotinylated cDNA sequences of *E. coli* were captured before amplification based on Rolling Circle Amplification method and quantified by fluorescence microscopy and electrochemical detection[159]. Also for the isolation of DNA, silica-modified MPs were used in the simultaneous electrochemical detection of *Salmonella*, *Listeria,* and *E. coli* bacteria[160,161].

Finally, MPs modified with MIPs, that contain specific recognition sites in their three-dimensional structure for a specific molecule or analyte, were synthesized in our laboratories for different targets, such as i) biotin[162], the most commonly used DNA and protein tag; ii) L-thyroxine[163] hormone, considered an important biomarker for thyroid disorders; and iii) methyl parathion[150] in tuna and cat fish samples, used as a pesticide in agriculture, and bioaccumulated in fish, water and soil. These biomimetically modified MPs are a promising strategy[143] for the isolation of molecules in harsh conditions as MIPs do not suffer structural modifications or degradation in non-physiological pH, salinity, or temperature, unlike antibodies, aptamers, or most proteins.

1.2.4.7 Other methods

Solid-phase extraction

Solid-phase extraction for sample preconcentration is a widely used methodology in gas and liquid chromatography experiments. The proposed method[164] use capillary-channeled polymer (C-CP) fibers of poly (ethylene terephthalate) as a capture matrix for exosomes based on hydrophobic interactions. Briefly, the exosomes suspension was diluted using a high saline medium and transferred to C-CP fiber tips to be centrifuged for 1 minute at 300 x *g* in a 15 mL tube. The EVs and proteins in the sample were retained in the fiber, while the matrix was discarded. Next, the elution of the retained proteins was induced by 25% glycerol in PBS, and finally, the EVs were eluted with 50% glycerol in PBS. This solid-phase extraction isolation of exosomes overcomes the main drawback of size-exclusion chromatography, as reducing the time requirement down to 10 minutes per sample and reporting a good recovery rate of 75% of the vesicles initially applied to the C-CP fiber tip in various matrices (aqueous, urine and non-fat milk).[164] Recently, solid-phase extraction was combined with microfluidics to develop a new integrated chip able to separate exosomes from proteins in clinical samples, as demonstrated with undiluted human serum as a proof-of-concept.[165]

Hydrostatic filtration dialysis

Hydrostatic filtration dialysis is an additional step of DUC isolation method used to separate EVs from smaller matrix particles and proteins. The exosomes samples are purified and concentrated by dialysis prior to its centrifugation to eliminate matrix solvent and particles below molecular weight of the dialysis membrane (*e.g.,* 1,000 kDa). Then, exosomes from hydrostatic filtration dialysis concentrated sample are separated from other bigger EVs using differential centrifugation.[166] Hydrostatic filtration dialysis represents an interesting additional procedure to reduce the time per sample cost, as it can eliminate solvent (*i.e.,* reduce volume) from the initial exosomes matrices This feature can be especially interesting for processing large samples volumes, such as urine or cell-culture supernatants.[166,167]

Asymmetric flow field-flow fractionation

Asymmetric flow field-flow fractionation is a novel microfluidic isolation technique for exosomes based on their diffusion coefficient. The separation is done in a microfluidic chamber where particles are subjected to perpendicular flow profiles. The sample is driven by a laminar parabolic flow down the length of the chamber, while a perpendicular crossflow is applied to separate the particles. The larger particles are more affected by the crossflow, pushed closer to the walls where the parabolic flow is slower. Then, the smaller particles remain at the center of the chamber and elute earlier than the bigger particles. [168,169] Although this method represents a rapid and reproducible isolation method and high purities are achieved, the highly specialized equipment requirements of the technique prevent asymmetric flow field-flow fractionation from routine protocols of EV separation.

Acoustic microfluidic platforms

Other interesting microfluidic platforms for EVs isolation are based on acoustic waves as separation agents. This label and reagent-free and biocompatible method is integrated by microfluidic chips and surface acoustic wave modules to separate exosomes. In 2015, the first approach to this method was published.[170] A single-channeled device able to separate particles smaller than 190 nm from bigger ones, similarly to an ‘acoustic filtration’. By tuning the acoustic wave module frequency, the size cut-off can be adjusted. Authors propose to integrate various acoustic modules to separate different fractions according to their particle size.[170] Two years later, another acoustofluidic platform for isolating exosomes from whole blood using two separation acoustic modules was developed.[86] Briefly, the cell-removal module applies an acoustic

wave of 19.4 MHz to separate particles bigger than 1 µm in diameter (*e.g.,* red and white blood cells, and platelets). While the exosomes remain in the cell-free plasma and flow to the second module that applying 39.4 MHz can separate individual exosomes (~100 nm peak in NTA) from other bigger EVs. This device can separate the samples into 3 fractions and showed a high recovery rate and high purity for particles smaller than 140 nm in diameter.[86] While presenting many advantages such as label and reagent-free, high recovery rates, and purity, in terms of particle size, these acoustics-based microfluidic platforms are still under development and not commercially available.

1.2.5 Methods for the physical characterization of exosomes

The development of physical and molecular characterization methods for exosomes and EVs from biological samples is other major challenge in this research field. The need to assess the purity and integrity of the EVs in a sample, as well as the efficiency of its separation methods, is critical for the reliability and trustfulness of the experimental results. This characterization must be done to guarantee that findings are directly related to EVs and not any other co-isolated materials.

The physical characterization of the vesicles, which relates to the integrity of the sample, is done by different methods. Electron microscopy techniques, like Transmission and Scanning electron microscopy (TEM and SEM), provide information about the size and morphology of the vesicles with nanometric resolution, as well as atomic force microscopy (AFM). Dynamic light scattering (DLS) and nanoparticle tracking analysis (NTA) relate the Brownian motion of the particles in solution to obtain information about size distribution and particle concentration. Finally, tunable resistive pulse sensing (TRPS) is presented as an impedance-based alternative method to NTA for sizing and counting EVs.

1.2.5.1 Nanoparticle tracking analysis

Nanoparticle tracking analysis (NTA) is currently the gold-standard technique for measuring the size distribution and concentration of nanoparticles in solution.[171] NTA is based on the rate of Brownian motion of each individual particle to calculate its hydrodynamic size. Briefly, NTA uses a peristaltic pump to inject the sample solution into a flow chamber equipped with a laser light source and a CMOS camera connected to an optical microscope. The displacement of each particle is video recorded and tracked by following the scattered light, which enables the calculation of particle size distribution by using the two-dimensional Stokes-Einstein equation. Since the volume of the chamber is known the particle concentration can be calculated, in contrast with Dynamic Light Scattering method which can only calculate the size distribution. Nevertheless, scattered

light from large protein aggregates will not be distinguished from EVs by NTA, thus assuming particle concentration might not be a reliable measurement of EVs concentration.[171,172]

Figure 1.10 shows a scheme of the NTA technique (panel A) and a frame from a measurement of a sample of exosomes derived from cell culture supernatants and obtained by differential ultracentrifugation (panel B). The light points that can be observed in the screenshot are due to the scattering of perpendicular laser light produced by the particles. The light pattern produced by each particle is analyzed and resolved by NTA software, which can discriminate and quantify different exosome subpopulations in the sample. Finally, each one is fitted and quantified using Gaussian fitting. The results of the measurements obtained are size distribution histograms as depicted in panel C.

Moreover, the NTA method is considered more accurate for polydispersed suspensions than DLS, highly biased by the scattering of larger particles.[172,173] However, the NTA particle concentration range is limited, approximately between 10^7 to 10^9 particles mL^{-1} in the flow chamber, for obtaining quantitative and reliable measurements.[173–175] Therefore, proper dilution of concentrated samples (*e.g.,* exosomes purified by ultracentrifugation or polymer-based precipitation) must be applied prior to its measurement. On the other hand, NTA sensitivity might not be good enough for analyzing EVs directly from biological fluids, as its concentration can vary between 10^4 to 10^{10} exosomes mL^{-1}*,* and preconcentration and purification of samples would be required.[176] Finally, optical parameters of the CMOS (*i.e.,* complementary metal oxide semiconductor) camera and detector were found to be critical for the limit of detection of NTA-based quantification of EVs.[174]

NTA can be equipped with an integrated fluorescence module capable of analyzing a subpopulation of labeled EVs, providing specificity to the measurements.[172] High expression of the fluorescently-labelled molecules in exosomes membrane is required for good data acquisition[177] Also, lipophilic dyes have been used to stain the EVs lipidic bilayer prior to its characterization by fluorescent-NTA, allowing to separate nanovesicles from other aggregates, like proteins.[178] Fluorescent-NTA sensitivity is limited mainly because of the movement of the particles out of focus during the measurements, and photobleaching of antibody fluorochromes.[177] As an alternative method to fluorescent-NTA, with similar characteristics and objectives, nano-flow cytometry is described in §1.2.6.1.1.

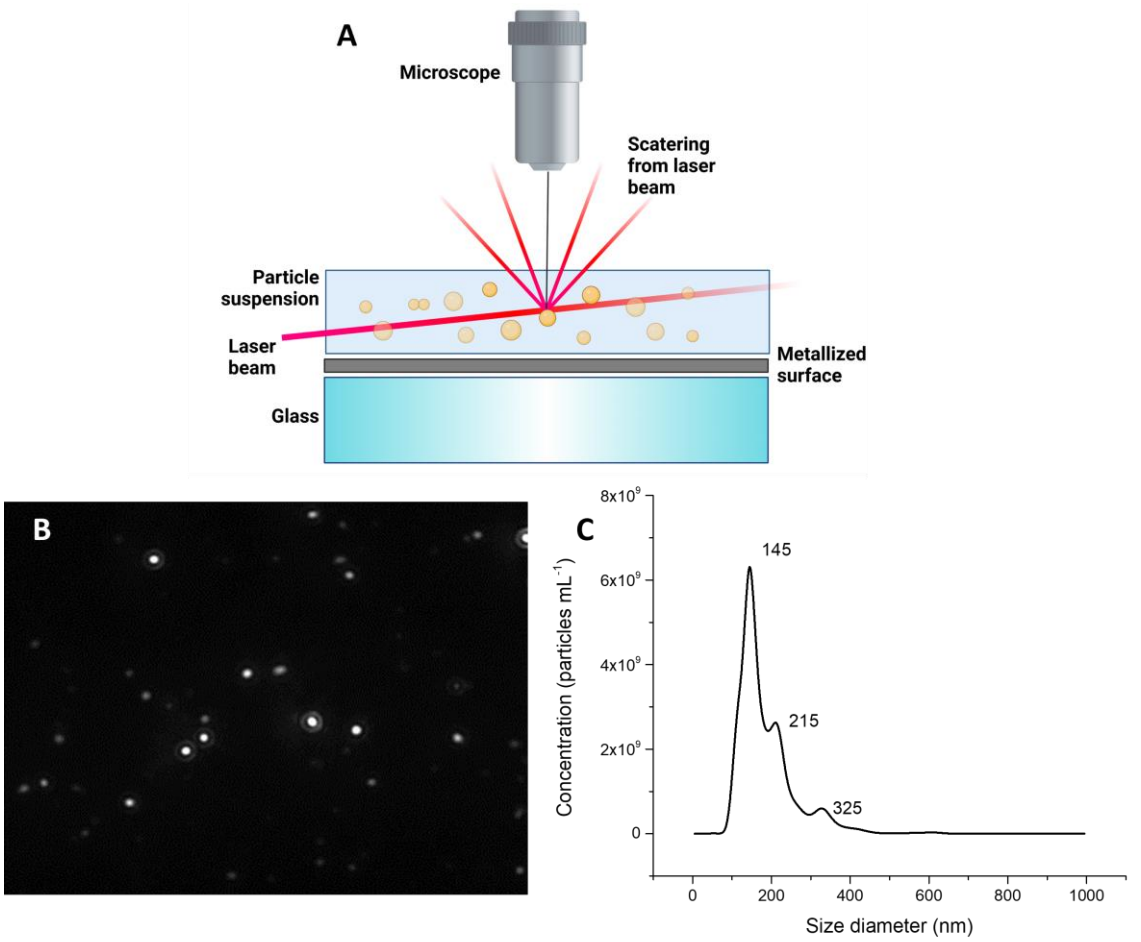

Figure 1.10. Panel A. Scheme of Nanoparticle tracking analysis instrument. Panel B and C. Screenshot and results (size distribution and concentration) of NTA measurement of MDA-MB-231 derived exosomes, diluted in sterile-filtered PBS buffer. The NTA has been performed in the ICTS "NANBIOSIS" NTA analysis service of Institut de Ciència dels Materials de Barcelona. Created with BioRender.com.

1.2.5.2 Transmission electron microscopy and Cryogenic transmission electron microscopy

Transmission electron microscopy (TEM) and specially Cryogenic TEM (Cryo-TEM) are the most popular techniques for visualizing EVs and exosomes.[179] These techniques are based on the analysis of transmitted and diffracted electron beams through a thin sample, creating a sample image with extremely high resolution, approximately 1 nm. Conventional TEM measurements require extensive sample processing, including dehydration, fixation, and metallization with heavy metals (*e.g.,* osmium tetroxide, uranyl acetate) to create 2-10 nm conductive layer. Also, TEM measurements are done under high vacuum conditions, thus TEM images usually show a deformed cup-shaped morphology of the vesicles.[118]

On the other hand, Cryo-TEM can overcome some of these drawbacks. In this case, samples are cryogenized using liquid nitrogen (*i.e.,* −196 °C) and measured at very low temperatures (*e.g.,* −182 °C maintained in liquid ethane). Consequently, sample preparation is much simpler, directly applying the sample to a carbon grid and vitrifying it, thus avoiding sample fixation, dehydration, and metallization, which might eventually distort the morphology of the EVs.[93] Figure 1.11 shows high-resolution Cryo-TEM images of exosomes derived from cell culture supernatants obtained by differential ultracentrifugation. The vesicles can be observed nearly its native state, as round structures enclosed by double bilayer membranes.[93,179] These results indicate that cup-shaped morphology reported by TEM, AFM, and SEM is an artifact, as round structures collapse due to dehydration and high vacuum.[180]

The major improvements of Cryo-TEM for the imaging of biological samples and structure elucidation of biomolecules were awarded in 2017 with the Nobel Prize in Chemistry, to Dr. Jacques Dubochet, Dr. Joachim Frank, and Dr. Richard Henderson, "*for developing cryo-electron microscopy for the high-resolution structure determination of biomolecules in solution*".

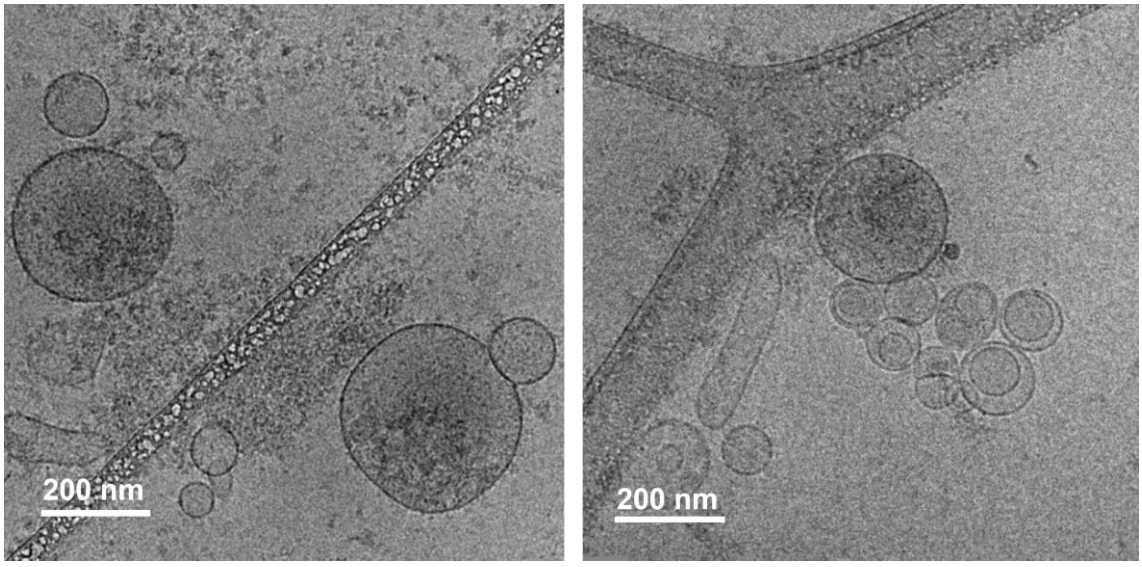

Figure 1.11. Cryo-TEM micrographs from MDA-MB-231 derived exosomes and EVs, obtained with a Jeol JEM 2011 microscope. The images were obtained in the Service of Microscopy at Universitat Autònoma de Barcelona.

1.2.5.3 Scanning electron microscopy

Scanning electron microscopy (SEM) is a well-established imaging technique that can be used to study EVs,[181] also providing information about size and morphology. SEM is based on the scattering of a focused beam of electrons when interacting with the sample. It provides information about surface topography and the composition of the

sample. As mentioned for TEM, conventional SEM requires complex and extensive sample processing, including dehydration, and high vacuum during the measurements. Thus, conventional SEM images also show vesicles with deformed cup-shaped morphology.[182] Technological advances in SEM equipment enable the development of new techniques, promising for the study biological samples. For example, Cryo-SEM is able to measure liquid nitrogen frozen samples, reducing structural damage of the vesicles[183]; and Low-Voltage SEM, that uses electron beams with lower potentials (< 1kV), can visualize EVs without metallization.[181]

1.2.5.4 Other methods

Atomic force microscopy

Atomic force microscopy (AFM) is another high-resolution imaging technique that can be used for EVs' physical characterization.[184] It is based on the interaction of a probe mounted on a cantilever with the surface of the sample. This interaction produces changes in the probe position and generates topographic images of the sample with nanometric resolution. AFM requires minimal sample preparation: the sample is adsorbed onto a holder and gently dried, without fixation or metallization needed, in contrast with conventional SEM or TEM. AFM scans can be used to analyze mixtures of different particle sizes accurately, although calculated size distribution histograms may be skewed by the deposition of the particles in the sample mica holder.[185]

Dynamic light scattering

Dynamic light scattering (DLS) is another Brownian motion-based technique for sizing EVs. [172] Similarly to NTA, DLS is based on the analysis of scattered light patterns created by the Brownian motion of particles in a solution hit by a monochromatic and polarized light beam. Equally, the temporal fluctuation rate of the light scattering patterns can be transformed to the diffusivity of the particle and determine its hydrodynamic diameter using the Stokes-Einstein equation.[185] In contrast to NTA, DLS cannot provide particle concentration, as it only measures the "bulk" scattered light pattern. Besides, as the light beam can be scattered multiple times through the sample, DLS measurements might be especially distorted by small amounts of aggregates, large particles with a high refractive index.[171,172,185] DLS allows to analyze smaller particles than NTA (particles diameters of 0.1 nm and 10 nm, respectively), although the latter had overcome the limitations of DLS and it is currently more commonly used for sizing and counting EVs.

Tunable resistive pulse sensing

Tunable resistive pulse sensing (TRPS) is an alternative technique to NTA, for sizing and counting particles in solution.[186,187] It is based on the measuring of the impedance signal, or resistive pulse, created by EVs and particles when passing through the nanopores of a non-conductive polyurethane membrane in a flow chamber when a voltage is applied.[188,189] The magnitude of the impedance signal is related to the volume of the particle, while the rate of these signals can be used to calculate particle concentration. Reference samples of particles with known size and concentration have to be used to calibrate the equipment.[188] Note that even when using a non-conductive polyurethane membrane, biological materials can interact with the membrane pores and affect the measurements.[189] As the main drawback, the smaller detectable size in TRPS is approximately 100 nm, which can lead to discrepant measurements of EVs samples when compared with other techniques such as NTA.[186,187]

1.2.6 Molecular characterization methods of exosomes

Initial studies about exosomes and EVs primarily rely on total protein concentration as the purity measurement of the samples. Although it is an important value, it can be severely affected by protein contamination during the isolation process and tends to overestimate the amount of EVs in a sample.[102] Bicinchoninic acid assay[190] and Bradford assay[191] are the standard colorimetric assays used for determining the protein concentration of EV samples. If the sample is volume-limited, an estimation of protein concentration can be done by measuring 280 nm absorbance in a Nanodrop spectrophotometer.[127]

As the EVs research field grew, more sophisticated analytical methods of protein and nucleic acid composition were used to characterize the molecular cargo of exosomes and EVs. Still, there is a need for developing protein analysis methodologies able to find specific biomarkers that can differentiate between different subpopulations of EVs. As previously mentioned, the fact that proteomic profiles of exosomes and EVs change between isolation methods used to obtain and purify the vesicles makes this challenge the most difficult in the field.[92] Therefore, the ISEV highlights in its guidelines the requirement for carefully characterizing the protein composition of EVs in publications, and suggests some general markers that should be present, or absent, in EVs.[61,62]

There are mainly two types of proteins present in EVs: i) transmembrane proteins, coming from the external plasma membrane or endosomes of EV-releasing cells, as tetraspanins CD9, CD63, and CD81; and ii) cytosolic proteins, enclosed with intracellular

material during EVs formation in the cells. For instance, other types of proteins can be found in EVs samples: iii) proteins from non-EV structures co-isolated with EVs, as lipoproteins or albumin, that can be used as purity ratio; iv) proteins from intracellular organelles other than plasma membrane and endosomes, *i.e.,* related with the nucleus, Golgi apparatus, or mitochondria; and v) secreted proteins that can associate with receptors on EV surface.[62]

As previously mentioned, efforts are being done by the scientific community to build knowledge from the extensive research in EVs molecular characterization. Initiatives such as web-based compendiums to centralize and share experimental results from protein and nucleic acids characterization are underway. Focusing on the protein cargo of EVs, Vesiclepedia[98] with 349,988 protein entries is currently the largest and most updated database. Regarding nucleic acid cargo, exRNA Atlas[100] database has 9,987 entries, carefully classified by type of EVs, biofluid of origin, RNA source, and isolation kit.

This section gives an overview of the current molecular characterization methods for EVs, focusing on the ones that had been used in this thesis, such as Flow Cytometry and Immunoassays with optical and electrochemical detection for protein analysis, and RT-PCR as an amplification method for the nucleic acid cargo.

1.2.6.1 Immunodetection methods

Most bioanalytical methods for the determination of membrane proteins in EVs rely on immune-affinity reactions with antibodies for their recognition. These methods are based on the reaction of a primary antibody with an epitope of a target protein, followed by the detection of the primary antibody through its own enzymatic or fluorescent label, or by reaction with a labelled secondary antibody. The high specificity of these methods is provided by the antigen-primary antibody biorecognition reactions.

There are several methods used to quantify proteins in EVs based on these immune-affinity reactions, and with different transductions and equipment requirements, as described in the following sections for flow cytometry, confocal microscopy, western blot, and immunoassays.

1.2.6.1.1 Flow cytometry

Flow cytometry (FC) analysis is often considered as the standard bioanalytical technique for determining the expression of proteins in biological systems or components, especially in cells. FC is a multiplexed fluorimetry analysis technique based on the measurement of laser light scattering and fluorescent signals of labelled single

particles driven by capillary flows.[192] It is a very powerful technique able to simultaneously measure multiple fluorescent signals coming from an individual vesicle or particle. Each vesicle is sequentially analyzed with different laser light beams, detected by multiple associated fluorescence detectors, each one specific for a particular wavelength. Based on these scattering and fluorescence signal patterns, vesicle populations can be analyzed, or even sorted.

FC has extensive bioanalytical applications in almost all areas of biological research, such as immunology, cellular and molecular biology, bacteriology and virology, disease diagnosis, and monitoring, among many others.[192,193]

Again, the particle size of EVs represents a challenge for this technique, with conventional FC limited to particles with diameters from 1 to 20 µm, approximately, as shown in Figure 1.12, panel A for the analysis of a cell. To overcome this size limitation, EVs can be attached onto larger particles such as latex, polystyrene, or magnetic particles, that will enlarge the analytes as well as preconcentrate the fluorescent signals of the nanovesicles.

Bead-coupled flow cytometry for EVs has been used in multiple experiments in the literature. Some interesting publications involve the preconcentration of urine-derived EVs directly onto aldehyde/sulphate latex microspheres with a diameter of 4 µm[88], as shown in Figure 1.12, panel B, or modify these latex beads with antiCD63 antibody to capture specifically CD63-positive EVs onto the beads[117], as shown in Figure 1.12, panel C. Also, streptavidin-modified polystyrene beads conjugated with biotinylated primary antibodies have been used to capture EVs and, by means of its isolation efficiency, determine the expression of protein surface markers in ovarian cancer-derived EVs.[194] Based on the same principle, the commercial kit MACSPlex Exosome kit (ref.130-108-813, Miltenyi Biotec) allows for the semi-quantitative determination of 37 EVs' surface epitopes. It is based on the specific isolation of subpopulations of EVs using 37 biologically-modified beads, plus the labelling of the EVs by a cocktail of APC-labelled (far-red fluorescent label, also named as Cyanine 5 or Cy5) anti-CD9, CD63, and CD81 antibodies.[195,196]

Towards the same goal, the preferred strategy in our research group involved the use of magnetic particles. Two different approaches were developed: i) direct covalent immobilization of EVs onto tosylactivated MPs; and ii) IMS of EVs using biologically modified magnetic particles. Then, EVs-coated MPs were further reacted with mouse monoclonal antibodies specific for proteins of interest and labelled with APC-labelled

antimouse antibodies,[197] This was applied for the molecular characterization of surface markers in EVs derived from breast cancer cell lines.[137,197]

In recent years, technological developments in flow cytometry instrumentation allow the improvement of their limits of detection, with newer instruments able to analyze particles as small as 100-200 nm, as shown in Figure 1.12, panel D. This enables the use of FC to directly detect and analyze nanovesicles, as exosomes, and determine the expression of protein markers in its membrane. The newly improved method is named as nano-flow cytometry (nanoFC), and it opens new possibilities for the molecular characterization of exosomes.

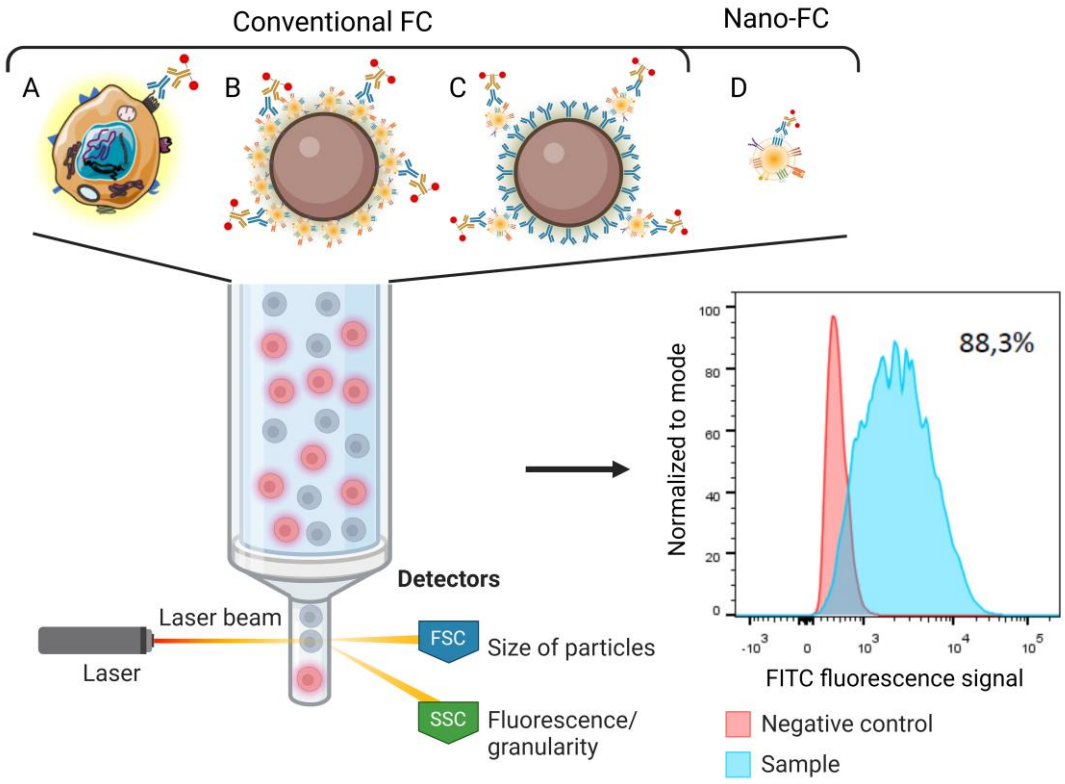

Figure 1.12. Flow cytometry methods for the characterization of cells (Panel A) and exosomes (Panels B-D). Conventional flow cytometry can measure particles from 1 µm of diameter, therefore, exosomes have been immobilized on microparticles either by covalent bonds (Panel B) or by immunoaffinity (Panel C). On the other hand, Nano flow cytometry can measure particles from 100 nm of diameter, as exosomes (Panel D). From the fluorescence intensity measurements, histograms can be plotted to determine percentages of positivity.

With these new instrumentation capabilities, different analytical strategies have been proposed by nanoFC for EVs characterization. To best of author's knowledge, the first publication[198] about characterization of EVs by nanoFC was in 2012. This study proposed the combination of a fluorescent membrane label (PKH67) with APC- and PE-labelled (red fluorescent label, named as R-Phycoerythrin) monoclonal antibodies to

quantify protein markers in single EVs. The labelled EVs were purified by sucrose gradient DGUC prior to nanoFC analysis.

Although not indispensable, as showed in 2018[199] and 2020[108], the use of membrane and cytosolic labels for EVs' general staining is commonly used to overcome one of the main issues of EVs characterization by nanoFC, the signal-to-noise discrimination. An interesting comparison was done with 4 dyes (membrane labels PKH26 and CM-Dil; nucleic acid binding SYTO RNAselect; and amine-reactive CFSE), concluding that the use of amphiphilic membrane labels (PKH26 and CM-Dil) is not suitable for EVs' nanoFC, as create 100-400 nm dye micelles which overlap the signals from EVs.[200] The study proposed amine-reactive (*i.e.,* protein-reactive) CFSE as EVs' general label in nanoFC.[200] Further studies optimized this CFSE staining strategy, also showing its suitability for combined detection of membrane protein markers with PE-labelled monoclonal antibodies.[201]

In Chapter 5, nano-flow cytometry has been used for searching the expression of a cytosolic enzyme, ALDH, inside the EVs derived from breast cancer lines.

Finally, many efforts have been done by the scientific community of EVs research field to define common guidelines for the reporting of FC studies of EVs.[202] In the proposed MIFlowCyt EV reporting framework, the authors suggest 25 components in 7 different categories that should be considered for the improvement of the quality and robustness of FC studies for EVs.[202] The main goal of this framework is to improve the ability to compare results from different laboratories and to support the validation of analytical methods and assays in this EVs research field.

As mentioned in previous sections in regards of isolation and physical characterization methods, the consistency of the experimental reported data remains as one of the major challenges for the advancement of the field. The ISEV and other scientific societies recommend the standardization of the experimental protocols and methodologies for the isolation and characterization of EVs, also in FC studies.

1.2.6.1.2 Confocal fluorescence microscopy

A complementary technique to bead-coupled FC is confocal fluorescence microscopy (CFM). This technique allows the imaging of labelled EVs attached onto functionalized particles, and quantifies its fluorescent signals, enabling the determination of membrane protein markers expression levels[197], as shown in Figure 1.13. The quantitative information obtained is comparable to FC, although CFM might be less representative as much less particles can be analyzed per sample. Due to its inherent

characteristics, CFM imaging parameters (*e.g.,* focus, field of view) must be adjusted in each sample, and beads should be imaged almost individually to be able to further process and quantify its fluorescent signals. On the other hand, bead-coupled CFM is suitable to determine the spatial distribution of labelled markers onto a particle, the homogeneity of the sample.

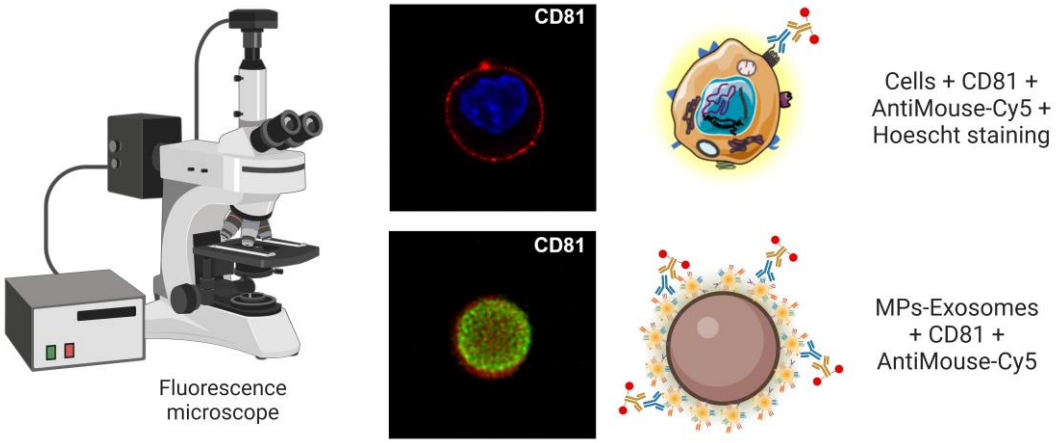

Figure 1.13. Confocal fluorescence microscopy characterization of cells and exosomes. The latter have to be immobilized on microparticles to allow its measurement within the resolution of the optical microscopes.

Besides bead-coupled strategy, high resolution CFM is also suitable for detecting labelled EVs individually[196,203] and has interesting applications for *in vivo* imaging of EVs. For example, the processes of interaction and internalization of labelled EVs by recipient cells can by followed by CFM, even obtaining 3D reconstructions of the cells.[204,205] This method enables the accurate detection and location of the EVs inside the cells, of much interest to study the different EVs uptake mechanisms, as membrane fusion or endocytosis pathways.[204–206] Another relevant paper was recently published focused on the study of dye-labelled EVs.[196] This study reveals the appearance of micelles from amphiphilic dyes with same size range as dye-labelled EVs, confirming previous results about self-aggregation.[196]

1.2.6.1.3 Western blot

Another classical bioanalytical method for the determination of protein markers in EVs is Western blot. This technique comprises the separation of proteins according to their MW by denaturing gel electrophoresis (*e.g.,* SDS-PAGE), followed by incubation with a primary antibody and revealing. Although western blot is a simple and cost-effective method, with minimum equipment requirements, its application to analyze EVs' proteins is limited due to the low concentrations of EVs' proteins in samples.

Western blot has been used in many publications as standard method for assessing the purity of EVs' preparations, usually detecting tetraspanins CD63 and CD81 proteins. Interesting examples are the analysis of EVs derived from urine and purified by size-exclusion chromatography[88], or a comparative analysis of the protein cargo of microvesicles and exosomes[207]. This last study uses EVs derived from human plasma, serum and urine samples from healthy donors and purified by sucrose gradient density gradient ultracentrifugation, was done to study the heterogeneity of their protein composition depending on the purification conditions and the kind of EVs.[207]

1.2.6.1.4 Enzyme-linked immunosorbent assay

The most common immunoassay for protein detection in all kinds of biological and clinical samples is Enzyme-linked immunosorbent assay (ELISA).

There are mainly two different assay formats, antigen-immobilized and antibody-immobilized (or sandwich) assays, either with direct or indirect detection. In brief, in i) antigen-immobilized assays, the analyte is attached onto the solid support (*i.e.,* microplate, MPs) and detected either with a directly-labelled specific primary antibody (*e.g.,* Mouse monoclonal antiCD9 HRP conjugate), or a combination of a specific primary antibody (*e.g.,* Mouse monoclonal antiCD9) and a labelled secondary antibody (*e.g.,* Antimouse HRP conjugate). On the other hand, in ii) sandwich assays, an antibody attached onto the solid support captures the analyte, which can be detected either by a directly-labelled primary antibody or using a specific primary plus a labelled secondary antibody.

Besides, there are two different analytical strategies in immunoassays: i) non-competitive, when the signal is directly proportional to the concentration of the analyte (*i.e.,* direct reaction between the analyte and the labelled antibody/ies); and ii) competitive, when the signal is inversely proportional to analyte concentration (*i.e.,* the analyte and labelled antibody/ies compete for the recognition with the solid support epitope). Figure 1.14 shows a schematic representation of the four ELISA formats previously described for the detection of exosomes.

ELISA methods usually use activated microplates as solid support for reacting with analyte or antibodies. Alternatively, in our research group, biologically-functionalized magnetic particles have been also used, leading to magneto-actuated ELISA method. Many applications have been developed, such as a phagomagnetic immunoassay for the detection of *Salmonella* in milk[154], or the quantification of surface protein in breast cancer EVs using antibody modified MPs[137].

Regarding the detection of ELISA, there are three types of optical signals that can be used: i) absorbance, using chromogenic substrates (*e.g.,* TMB for HRP enzymes; pNPP for ALP enzyme)[137]; ii) fluorescent signals of labelled antibodies (*e.g.,* fluorochromes as FITC, quantum dots antibody conjugates)[208,209]; and iii) luminescence[210]. As the analytical signal is coming from an enzymatic reporter, the reaction might be measured continuously in a kinetic assay, or at a fixed-time by stopping the reaction with a denaturing solution (usually strong acidic or basic solutions).

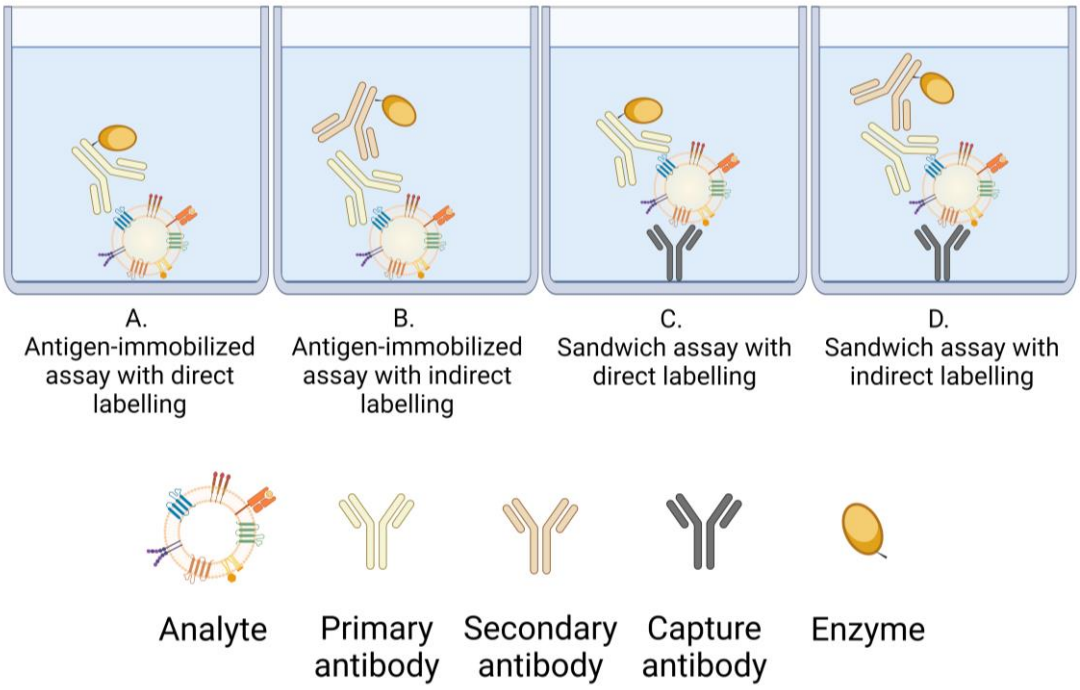

Figure 1.14. Schematic representation of the different ELISA formats for the detection of exosomes. Panel A. Antigen-immobilized ELISA with direct labelling (e.g., Mouse monoclonal antiCD9 HRP conjugate). Panel B. Antigen-immobilized ELISA with undirect labelling (e.g., Mouse monoclonal antiCD9 and antimouse HRP conjugate). Panel C. Sandwich ELISA with direct labelling. Panel D. Sandwich ELISA with indirect labelling. Created with BioRender.com.

ELISA method is one of the most widely used bioanalytical method, as its flexibility, simplicity, low cost per sample, minimum laboratory expertise and low equipment requirements represent great advantages to other techniques as FC or CFM. Commercial ELISA kits are available for almost any kind of clinical and biological sample, and specifically for the analysis of EVs, such as Human exosome ELISA kit with colorimetric and chemiluminescence detection (Bio-Techne R&D systems, Madrid, ES), ExoELISA kits, specific for CD63 marker, with colorimetric and fluorescent detection (System Biosciences, Palo Alto, CA, US), Overall Exosome ELISA kit (Abnova, Taipei, TW), or ExoQuant ELISA kits, with colorimetric and chemiluminescence detection (BioVision, Abcam, Cambridge, UK).

1.2.6.1.5 Electrochemical methods

Electrochemical readout has been widely used in biosensors for clinical applications, being amperometric glucometers their best and still unbeaten example, as previously mentioned. This type of transduction is well-known for its sensitivity, rapidity, portability, user-friendliness, and affordability. In the detection and characterization of EVs, the most used electrochemical techniques are amperometry and voltammetry.

Our research group has been fond developing electrochemical biosensors for bioanalytical applications, with many publications in the last 20 years. In particular, our group is been pioneer in the integration of magnetic particles in electrochemical biosensors, starting with the invention of magnetic graphite epoxy composite (m-GEC) electrodes.[211,212] These tailor-made electrodes incorporate a neodymium magnet which allow the capture of magnetic particles on its surface. The versatility of this biosensing approach, combining m-GEC electrodes with biologically-modified magnetic particles, has been demonstrated in a wide range of applications. For example in food safety, the detection of foodborne pathogenic bacteria, including Salmonella, Legionella and E.Coli[15,156,160,161,213–215], or of small pollutants as pesticides[16,150], antibiotics[16,216–218] and additives[219,220]. Or in the field of clinical diagnosis with relevant targets such as celiac disease[19,221], AIDS[18] or Ebola[159].

Focusing on the EVs, our group has published the characterization of protein surface markers of breast cancer cell lines derived exosomes using antibody functionalized magnetic particles and amperometric biosensors[17], showing also capabilities of working human serum samples; and recently we also developed a method for the analysis of exosomes derived from osteoblasts by detecting its intrinsic ALP enzyme activity[33].

Among the vast literature in this field, relevant examples are the multiplexed electrochemical integrated platforms iMEX[222], HiMEX[223] and iPEX[224], based on the concept developed by our research group, for the protein profiling of EVs. Based on amperometry, iMEX is an 8-electrode integrated platform that uses antiCD63 antibody-modified MPs to capture the exosomes, then reacted with monoclonal antibodies, in this case for 6 cancer-related proteins (EpCAM, CD24, CA-125, HER2, MUC18 and EGFR). Finally, an HRP reporter is used to produce the electrochemical signal.[222] This platform was updated to HiMEX, based on the same method with some improvements, as the use of a cocktail of tetraspanin-specific MPs to capture the exosomes, and a 96-electrode array for the amperometric readout.[223] This platform is an unprecedented technology that enables the high-throughput screening of cell-line derived EVs, as well

as human blood or serum samples.[223] Finally, iPEX platform was recently published, also for the molecular profiling of EVs, but using impedance spectroscopy, which do not require enzymatic labelling.[224]

Besides antibodies, aptamers have been widely used as biorecognition elements in electrochemical biosensors for exosomes.[225] There are aptasensors targeting general and specific exosomal surface proteins, being CD63 tetraspanin aptamer the most extensively used. Many different formats have been explored with CD63 aptasensors, as a competitive assay with methylene blue-modified probes, which are being displaced by CD63 positive exosomes, and measured by Square Wave Voltammetry[226]. Or using CD63 aptamer as capture probe, further labelling the exosomes with HRP reporters and measured by Differential Pulse Voltammetry[227]. Aptamers targeting cancer-related proteins have been also used to analyze exosomes, such as CEA, EpCAM, HER2, mucin-1, nucleolin, PSMA, PTK7 or AFP proteins.[225]

Perhaps, electrochemical biosensors for EVs detection and characterization are currently the most popular methods in the field, considering the rapidly growing number of publications in the last 5 years. According to recent articles, the improvement of the sensitivity through nanomaterials, and the development of miniaturized analytical systems with electrochemical detection could be considered as the main trends in the EVs bioanalytical research field.[228,229]

1.2.6.2 Nucleic acid amplification methods

The discovery that exosomes are extracellular RNA transport vesicles is triggering much interest in EVs research today.[95] Mainly composed of non-coding micro-RNA (miRNA), exosomes also contain messenger RNA (mRNA), long non-coding RNA (lncRNA), ribosomal RNA (rRNA), plus minor quantities of other types.[230] According to some studies[230–232], exosomes might contain also DNA molecules, although there is controversy in this point.[233] Although the quantity of genetic material that exosomes contain is very tiny, their analysis and characterization requires, almost unavoidably, the use of amplification methods.

As explained for the protein content, the low abundance of genetic material in the EVs is challenging for downstream applications. In fact, there is not a consensus about the genetic cargo per each individual vesicle. On the one hand, some publications suggest that subpopulations of exosomes coexist with different RNA occupancy ratios[234,235]. On the other hand, other studies suggest exosomes biological origin and loading is a highly regulated pathway.[233]

Among the different amplification methods, Polymerase Chain Reaction (PCR) is the most popular and routinely used technique. This technique, developed by Kary B. Mullis in the 80s[236], allows for the exponential amplification of a specific DNA region, fixed by a pair of forward and reverse primers that will be simultaneously extended by a DNA polymerase enzyme. The inventor was awarded with the Nobel Prize in Chemistry in 1993 "*for contributions to the developments of methods within DNA-based chemistry*".

PCR amplification is based on the use of Taq polymerase, a thermostable DNA polymerase obtained from *Thermus aquaticus* bacteria. This enzyme can synthesize double-stranded DNA copies, creating the complementary chain of a single-stranded template using deoxynucleotides (dNTPs). To bind the DNA chain and copy a specific region, the enzyme requires double-stranded DNA, so a specific pair of DNA oligomers (18-25 nucleotides) flanking the target region must be added to the reaction mixture. The enzyme will recognize this ds-DNA region, bind to it, and synthesize the complementary chain of the template from 5' to 3' direction. The PCR process has three main steps, illustrated in Figure 1.15: i) denaturation of the ds-DNA template by heat; ii) specific hybridization of the pair of primers to the ss-DNA chains from template, and iii) extension of primer by adding the complementary nucleoside, creating a new ds-DNA copy, or DNA amplicon. The experimental parameters of the PCR amplification (number of cycles, reagents and enzyme concentrations, temperature of the steps) must be carefully optimized to improve the quality of the results. Of special importance is the temperature of the annealing step, depending on the guanine-cytosine (G-C) ratio of the primers, that will determine the specific hybridization on the region of interest. Also, the number of cycles must be optimized, depending on the number of template copies available in the sample. It can vary between 25 to 40 cycles and, as PCR is an exponential amplification, per each cycle it will duplicate the number of copies synthesized according to 2^n, which *n* equals the number of cycles.

In the case RNA amplifications, as it is in exosomes, a previous step of Reverse Transcription (RT) is mandatory to transform RNA to cDNA, template of the PCR amplification. Regarding miRNA amplification, the short length of the templates makes its amplification even more challenging, as they need to be extended for its further PCR amplification and analysis. Besides the two conventional strategies, the use of stem-loop primers[237] or poly-adenylation of miRNA[238] templates, different strategies have been proposed.[239]

The PCR amplification method is well-known, fast, versatile, reliable, and widely available to any molecular biology laboratory. There are several detection techniques of

the amplified material, being agarose gel electrophoresis the standard procedure to determine the specificity of the amplification, as only one band at a specific MW should be detected. Other relevant techniques include the use of fluorescent reporters, either dyes or probes, in quantitative PCR (qPCR), or the use of modified primers, as double-tagging PCR, to label the amplimers with chemical moieties, as biotin, digoxigenin or fluorescein, among others. The latter will be discussed deeply in Chapter 3, for the development of an electrochemical biosensor with double-tagging RT-PCR amplification of mRNA from breast cancer related exosomes. Further details regarding PCR amplification method, detection techniques and applications can be found.[236,240]

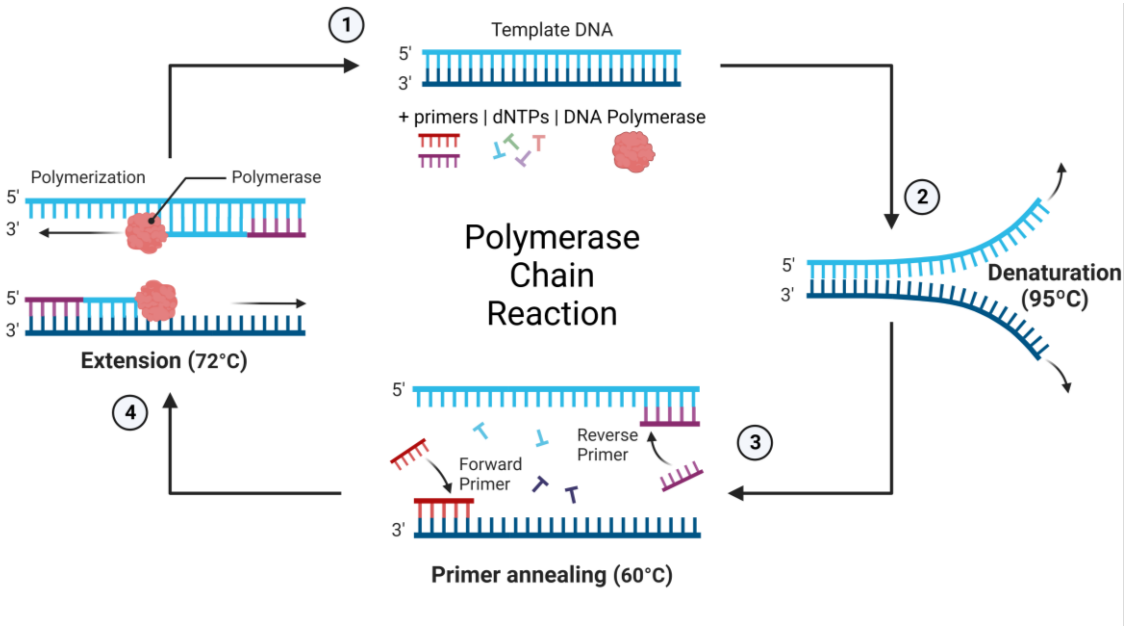

Figure 1.15. Polymerase Chain Reaction scheme. The cycle comprises four main steps: (1) initiation; (2) denaturation of template ds-DNA; (3) Primer annealing to ss-DNA; and (4) Primer extension by DNA polymerase. Created with BioRender.com.

The most frequently used method for exosomal RNA and miRNA characterization is quantitative RT-PCR. There are many publications using this technique for all kinds of samples and applications. Focusing on the characterization of cancer related exosomes, a study was published using IMS with antiCD63-modified MPs to capture exosomes from breast cancer cell lines, and analyze its miRNA cargo by qRT-PCR.[241] Another publication uses a microfluidic device to preconcentrate the exosomes from breast cancer patients and healthy individuals, followed by RT-PCR amplification of miRNA, searching for an specific biomarker of breast cancer exosomes.[242]

Other genetic amplifications have been used for the analysis of exosomal RNA, and of particular interest are isothermal amplification methods, as rolling circle amplification (RCA)[243], loop-mediated isothermal amplification (LAMP)[244] or exponential

amplification reaction (EXPAR)[245]. Regarding RCA, interesting applications have been developed also for the characterization of surface proteins on EVs, either by using specific aptamers[246] or oligo-modified antibodies[247]. The latter, named as proximity barcoding assay, is based on the recognition of surface proteins by specific oligo-modified antibodies, further amplified by RCA and detected using multiple fluorescent detection oligos to create a color barcode signal, specific for each antibody.[247] More information about the isothermal amplification methods and its applications in biosensors can be found.[248,249]

Finally, and despite the low abundance of miRNA inside the EVs, methods have been described for their analysis without genomic amplification steps. For example, an enzyme-free hybridization chain reaction (HCR) was proposed based on multiple DNA hairpin additions to create an active DNA nanowire that produces a fluorescent signal.[250] Another method described is based on a DNA three-way junction containing three fluorescent probes, that are displaced by complementary miRNA targets from EVs enabling the simultaneous detection of the targets by fluorescence.[251]

1.2.6.3 Proteomic, genomic, and lipidomic methods

Considering the highly complex and heterogeneous nature of EVs and exosomes, proteomic, genomic and lipidomic sequencing methods are of great interest for their molecular characterization. Although these methods are complex, expensive, laborious, and require trained personnel for its analysis, 'omics' methods can provide highly valuable information on the cargo of these vesicles. Its most important goal might be to find disease-specific protein and genetic biomarkers, potential targets of new RDTs.

Proteomic studies of EVs have mainly two purposes[252]: firstly, to find disease-associated proteins that could be exploited as prognostic and diagnostic biomarkers; and secondly, to investigate and understand their biological origin and function[253,254]. These profiling studies generate large amounts of data, that must be processed with bioinformatic tools to generate proteomic profiles of the samples. Thus, most of the EVs' related proteins compiled in Vesiclepedia[98], and other online compendia, are coming from proteomic studies.

In light of this interest in EVs' proteomics, even commercial devices have been developed as ExoView[255] (Nanoview Biosciences, Brighton, MA, US), able to directly analyze EVs samples, without previous purification steps, providing biophysical (sizing and concentration) and proteomic information.[196]

Concerning genomic profiling of EVs, studies reveal that the majority of RNA molecules present are miRNA (~76%)[230], targets of most exosomal RNA sequencing studies. Other types detected and quantified are ribosomal RNA (rRNA, ~9%), lncRNA (~3%), and DNA (~6%), among others.[230] Of particular interest for RDTs development are sequencing studies focusing on searching disease-specific patterns in EVs genomics, enabling to use this vesicles as diagnostic tools.[256–258] As mentioned for protein data in Vesiclepedia, most of exRNA Atlas[100] results come from genomic sequencing studies.

As mentioned in previous sections, the contamination of EVs' samples with protein aggregates from their source media is an important issue in proteomics. The high variability of proteomic results between samples and studies can be partially attributed to differences in isolation and purification of the EVs, so methodological standardization is a key factor to improve the quality of the results.[252,259] Nevertheless, in the case of genomics, some studies suggest that different isolation methods (*i.e.,* UC, DGUC, PBP) are suitable for RNA sequencing as the purity of the samples is not a critical factor, therefore it does not influence the detection of small and miRNA biomarkers.[85,260]

Finally, and as a response to the presented problematics, excellent work is being done to characterize the molecular cargo of the different fractions of EVs. Focusing on exosomes particular biochemical content, *Jeppesen et al.* reported a methodological framework to deal with the heterogeneity of extracellular vesicles, defining clear pathways for better understanding its biology.[233]. This study uses immunomagnetic separation and density gradient ultracentrifugation to improve the isolation of the different fractions of EVs, further determining its protein and genomic cargo. According to its molecular composition, the study presents a new and more precise classification of the EVs, clearing the path for future EVs discoveries. [233]

1.3 Exosomes in cancer disease

1.3.1 Non-communicable diseases and cancer incidence

The development of new diagnostic and screening tools for non-communicable diseases is considered as a key element by the World Health Organization in its related Global Action Plan.[261] The lack of affordable, available, effective and reliable RDTs for this type of diseases is particularly preeminent, compared with the technologies already available for communicable diseases, such as HIV, tuberculosis, malaria, or coronavirus disease.[262] Non-communicable diseases, such as cardiovascular diseases, cancer, respiratory diseases and diabetes are among the leading causes of death globally, accounting for more than 70% of all deaths each year. The mortality rates related with these diseases are not equal between the different countries, affecting disproportionately people in low and middle-income countries.[261] Various reasons could explain this major burden, as greater risks of exposure to harmful products or unhealthy dietary practices, however the limited access to health care systems might be the most prevalent. The low diagnostic capabilities of primary health care systems in low and middle-income countries might prevent the early detection and timely treatment of non-communicable diseases, leading to increased mortality rates.[263]

Focusing on cancer disease, it is one of the leading causes of death in high, middle, and low-income countries, and their incidence is expected to rise the next decades. According to the latest published data compiled by the Global Cancer Observatory[264], breast cancer is the most commonly diagnosed and leading cause of cancer death among women, with more than 2.2 million cases diagnosed in 2020. Data shows that approximately 1 of each 1000 women over 30 years old was diagnosed of breast cancer in the last year worldwide while among men its almost 100 times less frequent. The estimate age-standardized incidence rate of breast cancer in 2020, among females of all ages, obtained from Cancer Today database, from the Global Cancer Observatory is depicted in Figure 1.16.[265] The elevated incidence in highly developed countries (Europe, Northern America, Australia/New Zealand, and Japan) is related with higher reproductive and hormonal risks, as well as the increased detection of cases through prevention programmes, usually by mammographic screening.[264] On the other hand, the mortality rates in low and middle-income countries are higher, and rapidly rising in South America, Africa and Asia in the last 20 years. As previously mentioned, the low diagnostic capabilities increase the mortality rates as leads to late-stage presentation of the disease, reducing oncological treatment efficacy.[264]

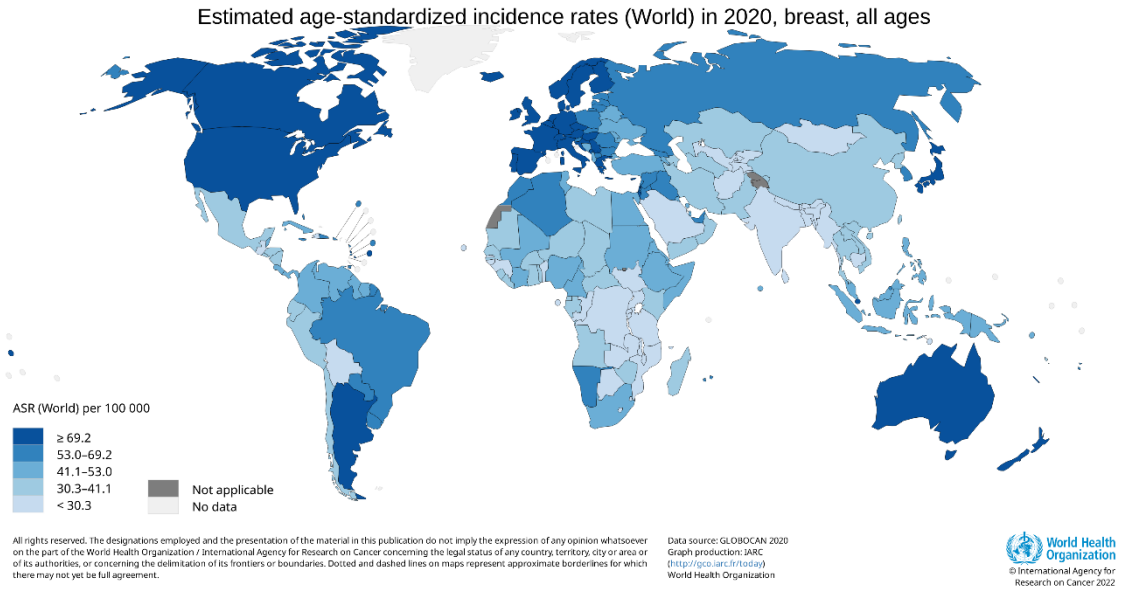

Figure 1.16. Estimated age-standardized incidence rates worldwide in 2020 of breast cancer disease in females, all ages. Obtained from Global Cancer Observatory 'Cancer Today' website.[265]

In general, cancer diseases are caused by the uncontrolled growing of abnormal cells from any type of tissue or organ, that might move beyond their tissue boundaries and get spread to other organs. This spreading process is called metastases and is the major cause of cancer related deaths. In the case of breast cancer, epithelial cells from the ducts (~80% of the cases) or from the lobules (~10%) in the glandular tissue of the breast.[261] These epithelial cells can start growing inadequately and uncontrolled, firstly, inside these ducts and lobules creating a located tumor, at metastases stage 0. If the disease progresses over time, this tumor might start invading surrounding breast tissue (stage 1 and 2), then moving to the nearby organs (stage 3), and finally, spreading to distant organs (stage 4). The advancement of the metastasis process worsens the prognostic of the patient, so an adequate and early diagnosis of the diseases and, of course, the application of the correct treatment, are key factors for improving the possibilities of recovery from cancer disease.

1.3.2 Current diagnostic and monitoring tools for cancer

1.3.2.1 Imaging techniques and biomarkers

Nowadays, the diagnosis of breast cancer is usually based on imaging techniques. X-ray mammography scanning, computed tomography scanning, magnetic resonance imaging and ultrasound imaging are the most commonly used techniques for breast tumor detection and imaging.[266] These techniques use radiation (X-ray, radio waves, ultrasounds) able to penetrate the soft tissues of the body to assess the

presence, location and morphology of a suspected tumor. They involve the use of benchtop specialized equipment, especially expensive in the case of computed tomography scanning and magnetic resonance imaging, therefore require hospital facilities and trained personnel for its use and interpretation.

The most common breast cancer prevention strategy in highly developed countries is the implementation of screening mammography programmes for the early detection of breast tumors in women of risk age groups (50-69 years). As shown by incidence and mortality rates data, thanks to screening programmes the mortality rates have significantly lowered in the last 20 years.[264] Nevertheless, it might not be feasible to implement those screening strategies in low and middle-income countries with weaker primary health care systems, as the associated equipment and personnel costs might be beyond the reach of many countries.[267]

Besides, further histological and molecular analysis through tissue biopsy of the tumor are required to assess its malignancy.[266] The molecular patterns of suspected cancer cells are important bioanalytical features that must be carefully determined. The presence of estrogen and progesterone hormone receptors and HER2 gene amplification are three key biomarkers that define the subtype of breast cancer, often classified in four categories: Luminal A or B (positive for estrogen receptor, ER, and progesterone receptor, PR), HER2 positive and Triple-negative (negative for ER, PR and HER-2).[268] The identification of the specific type of tumor is vital for the selection of the appropriate therapeutic option and clinical outcome of the patient.

1.3.2.2 Exosomes as biomarkers of cancer disease

There are mainly two targets in liquid biopsy analysis for cancer diagnosis: circulating tumor cells and exosomes.

Firstly, it is known that tumoral cells could be present in bloodstream coming from a primary tumor. These cells, named as circulating tumor cells (CTCs), are spread through the bloodstream from a primary tumor to other locations, being the cause of metastases process. Consequently, the analysis of these CTCs in liquid biopsies is very relevant, because it could provide direct information of the primary tumor cells. However, the tiny number of CTCs present in blood, in the range of ten cells per milliliter, difficult their applicability as diagnostic indicators.[269] Anyway, several methodologies have been developed for their analysis, being CellSearch system (Menarini Silicon Biosystems, Bologna, IT) the only approved by FDA.[270]

On the other hand, as mentioned in previous sections, the biological function of exosomes and EVs is related with intercellular communication mechanisms. The EVs can interact with other cells and release their molecular cargo, changing the biological behavior of the recipient cells. Hence, the analysis of the molecular content of these circulating exosomes could provide information of their parent cells, although it may not contain equally expressed levels of proteins and nucleic acids. Compared with CTCs, the targeting of exosomes as cancer diagnostic biomarkers, although representing big challenges for current technologies as previously explained, offers great advantages, such as its presence and high concentration in most biofluids (*e.g.,* ~10^9 particles mL^{-1} in blood), their molecular cargo representative of its parent cells.[271] The potential of exosomes as cancer biomarkers is well-known in the research field,[75,271,272] and several methods for the diagnosis of breast cancer have been developed using exosomes and EVs as biomarkers, as summarized in Table 1.1 focusing on the last five years relevant publications.

1.3.3 Technological challenges for low-resource settings

The REASSURED criteria establish the paradigm for the development of new RDTs, comprising all the optimal parameters that should be considered: Real time connectivity, Ease of specimen collection, Affordable, Sensitive, Specific, User-friendly, Rapid and Robust, Equipment free and Environmentally friendly, and Deliverable to end-users.[273] The research groups and developers focused on RDTs for low and middle-income countries, especially for noncommunicable diseases, should aim for the compliance of these REASSURED criteria. Of course, this paradigm presents big challenges to the researchers, which must consider innovative solutions to overcome them, as some might be beyond the scope of current technologies and designs. In the case of cancer and breast cancer disease, it is important to not just develop diagnostic tools, but also monitoring and prognostic tests, as those diseases need to be assessed and controlled usually during years.[262] The research of new RDTs based on liquid biopsies targeting exosomes and EVs must be considered as a promising point-of-care answer to this problematic.

In this PhD thesis, three of the main challenges are addressed, as i) to increase the sensitivity of the RDTs by using IMS and double-tagging RT-PCR to amplify genetic material cargo from the exosomes; ii) to simplify the designs of RDTs, developing a paper-based semiquantitative vertical flow assay for the assessment the alkaline phosphatase content of exosomes, as well as membrane protein biomarkers; and iii) to search new enzymes inside the vesicles that could be used as intrinsic enzymatic reporters in RDTs.

Table 1.1: RDTs for breast cancer diagnosis based on exosomes detection

Reference	Exosome source	Isolation technique	Detection biomarker	Signal transduction	Clinical samples
Yoshikawa, et al. 2018[274]	Plasma	DUC	miRNA-223-3p	RT-qPCR	20 healthy controls, 179 BC patients
Wu, et al. 2020[258]	Plasma	PBP	miRNA-150-5p, miRNA-576-3p, miRNA-4665-5p	RT-qPCR	20 healthy controls, 20 BC patients
Ando, et al. 2019[275]	Urine	PBP	miRNA-21, MMP1, CD63	RT-qPCR (miRNA-21), WB (MMP1, CD63)	26 healthy controls, 22 BC patients
Chen, et al. 2021[276]	Plasma	N/A	miRNA-1246	Molecular beacon-based fluorescence spectroscopy	37 healthy controls, 33 BC patients
Vinduska, et al. 2021[208]	Plasma	IMS (antiCD81-MPs)	CD340 / HER2	Quantum dots-based fluorescence spectroscopy	8 healthy controls, 8 BC patients
Liu, et al. 2018[277]	Serum	IMS (antiCD63-MPs)	GPC-1	Fluorescence spectroscopy	5 healthy controls, 5 benign breast disease patients, 12 BC patients
Moura, et al. 2020[137]	Serum	DUC + IMS (antiCD81-MPs)	CD24, CD44, CD326, CD340	ELISA + Absorbance spectroscopy	10 healthy controls, 10 BC patients
		DUC + IMS (antiCD24-MPs, antiCD340-MPs)	CD63		
Wang, et al. 2019[278]	Serum	PBP	CD82	ELISA + Chemiluminescence	80 healthy controls, 80 benign breast disease patients, 80 BC patients
Esposito, et al. 2021[279]	Serum	PBP	Ex-50 (aptamer)	ELONA + Absorbance spectroscopy	2 healthy controls, 8 benign breast disease patients, 13 BC patients
Moura, et al. 2020[17]	Serum	DUC + IMS (antiCD81-MPs)	CD24, CD44, CD326, CD340	Amperometry	10 healthy controls, 10 BC patients
		DUC + IMS (antiCD24-MPs, antiCD340-MPs)	CD63		
Cao, et al. 2020[280]	Serum	IMS (antiCD63-MPs)	PD-L1	Square wave voltammetry	6 healthy controls, 15 BC patients

An, et al. 2020[281]	Serum	PBP + IMS (CD63-aptamer)	MUC1, HER2, EpCAM, CEA (aptamers)	Differential pulse voltammetry	4 healthy controls, 4 BC patients
Kashefi-Kheyrabadi, et al. 2020[282]	Plasma	PBP	EpCAM (aptamer)	Differential pulse voltammetry	3 healthy controls, 10 BC patients
Tian, et al. 2021[283]	Plasma	N/A	PSMA (aptamer)	Thermal-based sensor	10 healthy controls, 66 BC patients
Zhao, et al. 2020[284]	Serum	DUC + UF	miRNA-375, miRNA-221, miRNA-210, miRNA-10b	Thermal-based sensor	12 healthy controls, 17 BC patients

1.4 References

(1) World Health Organization. *The Selection and Use of Essential in Vitro Diagnostics*; 2021.

(2) World Health Organization. *Assessing National Capacity for the Prevention and Control of Noncommunicable Diseases: Report of the 2019 Global Survey*; 2020.

(3) Hughes, W. S. The Potential Difference between Glass and Electrolytes in Contact with the Glass. *J. Am. Chem. Soc.* **1922**, *44* (12), 2860–2867. https://doi.org/10.1021/ja01433a021.

(4) Clark, L. C.; Lyons, C. Electrode Systems for Continuous Monitoring in Cardiovascular Surgery. *Ann. N. Y. Acad. Sci.* **1962**, *102* (1), 29–45. https://doi.org/10.1111/j.1749-6632.1962.tb13623.x.

(5) Bhalla, N.; Jolly, P.; Formisano, N.; Estrela, P. Introduction to Biosensors. *Essays Biochem.* **2016**, *60* (1), 1–8. https://doi.org/10.1042/EBC20150001.

(6) Wilven, M. Testing Times. The Birth of the Pregnancy Test. *Biomed. Sci.* **2019**, 18–22.

(7) Ben Aissa Soler, A. Rapid Diagnostic Test for the Detection of Communicable Diseases, 2020.

(8) International Union of Pure and Applied Chemistry. *The IUPAC Compendium of Chemical Terminology*; 2019. https://doi.org/10.1351/goldbook.

(9) Yu, H. W.; Halonen, M. J.; Pepper, I. L. Immunological Methods. In *Environmental Microbiology: Third Edition*; Elsevier, 2015; pp 245–269. https://doi.org/10.1016/B978-0-12-394626-3.00012-0.

(10) Alvarenga, L. M.; de Moura, J.; Billiald, P. Recombinant Antibodies: Trends for Standardized Immunological Probes and Drugs. *Curr. Dev. Biotechnol. Bioeng. Hum. Anim. Heal. Appl[1] L. M. Alvarenga, J. Moura, P. Billiald, "Recombinant Antibodies Trends Stand. Immunol. Probes Drugs," Curr. Dev. Biotechnol. Bioeng. Hum.* **2017**, 97–121. https://doi.org/10.1016/B978-0-444-63660-7.00005-X.

(11) Kim, J.; Park, M. Recent Progress in Electrochemical Immunosensors. *Biosensors* **2021**, *11* (10). https://doi.org/10.3390/bios11100360.

(12) Souto, D. E. P.; Volpe, J.; Gonçalves, C. de C.; Ramos, C. H. I.; Kubota, L. T. A Brief Review on the Strategy of Developing SPR-Based Biosensors for Application to the Diagnosis of Neglected Tropical Diseases. *Talanta* **2019**, *205* (July), 120122. https://doi.org/10.1016/j.talanta.2019.120122.

(13) Soares, M. S.; Vidal, M.; Santos, N. F.; Costa, F. M.; Marques, C.; Pereira, S. O.; Leitão, C. Immunosensing Based on Optical Fiber Technology: Recent Advances. *Biosensors* **2021**, *11* (9). https://doi.org/10.3390/bios11090305.

(14) Pohanka, M. Overview of Piezoelectric Biosensors, Immunosensors and DNA Sensors and Their Applications. *Materials (Basel).* **2018**, *11* (3). https://doi.org/10.3390/ma11030448.

(15) Liébana, S.; Lermo, A.; Campoy, S.; Cortés, M. P.; Alegret, S.; Pividori, M. I. Rapid Detection of Salmonella in Milk by Electrochemical Magneto-Immunosensing. *Biosens. Bioelectron.* **2009**, *25* (2), 510–513. https://doi.org/10.1016/j.bios.2009.07.022.

(16) Zacco, E.; Adrian, J.; Galve, R.; Marco, M. P.; Alegret, S.; Pividori, M. I. Electrochemical Magneto Immunosensing of Antibiotic Residues in Milk. *Biosens. Bioelectron.* **2007**, *22* (9–10), 2184–2191. https://doi.org/10.1016/j.bios.2006.10.014.

(17) Moura, S. L.; Martín, C. G.; Martí, M.; Pividori, M. I. Electrochemical Immunosensing of Nanovesicles as Biomarkers for Breast Cancer. *Biosens. Bioelectron.* **2020**, *150*, 111882. https://doi.org/https://doi.org/10.1016/j.bios.2019.111882.

(18) Carinelli, S.; Xufré Ballesteros, C.; Martí, M.; Alegret, S.; Pividori, M. I. Electrochemical Magneto-Actuated Biosensor for CD4 Count in AIDS Diagnosis and Monitoring. *Biosens. Bioelectron.* **2015**, *74*, 974–980. https://doi.org/10.1016/j.bios.2015.07.053.

(19) Pividori, M. I.; Lermo, A.; Bonanni, A.; Alegret, S.; del Valle, M. Electrochemical Immunosensor for the Diagnosis of Celiac Disease. *Anal. Biochem.* **2009**, *388* (2), 229–234.

https://doi.org/10.1016/j.ab.2009.02.026.

(20) Guilbault, G. G.; Montalvo, J. G. A Urea-Specific Enzyme Electrode. *J. Am. Chem. Soc.* **1969**, *91* (8), 2164–2165. https://doi.org/10.1021/ja01036a083.

(21) Lolekha, P. H.; Srisawasdi, P.; Jearanaikoon, P.; Wetprasit, N.; Sriwanthana, B.; Kroll, M. H. Performance of Four Sources of Cholesterol Oxidase for Serum Cholesterol Determination by the Enzymatic Endpoint Method. *Clin. Chim. Acta* **2004**, *339* (1–2), 135–145. https://doi.org/10.1016/j.cccn.2003.10.005.

(22) Bonet-San-emeterio, M.; Montiel, N. F.; Del Valle, M. Graphene for the Building of Electroanalytical Enzyme-Based Biosensors. Application to the Inhibitory Detection of Emerging Pollutants. *Nanomaterials* **2021**, *11* (8). https://doi.org/10.3390/nano11082094.

(23) Karunakaran, C.; Madasamy, T.; Sethy, N. K. Enzymatic Biosensors. *Biosens. Bioelectron.* **2015**, 133204. https://doi.org/10.1016/B978-0-12-803100-1.00003-7.

(24) Zhou, W.; Jimmy Huang, P. J.; Ding, J.; Liu, J. Aptamer-Based Biosensors for Biomedical Diagnostics. *Analyst*. 2014, pp 2627–2640. https://doi.org/10.1039/c4an00132j.

(25) Xiao, Y.; Lubin, A. A.; Heeger, A. J.; Plaxco, K. W. Label-Free Electronic Detection of Thrombin in Blood Serum by Using an Aptamer-Based Sensor. *Angew. Chemie - Int. Ed.* **2005**, *44* (34), 5456–5459. https://doi.org/10.1002/anie.200500989.

(26) Lai, R. Y.; Plaxco, K. W.; Heeger, A. J. Aptamer-Based Electrochemical Detection of Picomolar Platelet-Derived Growth Factor Directly in Blood Serum. *Anal. Chem.* **2007**, *79* (1), 229–233. https://doi.org/10.1021/ac061592s.

(27) Ocaña, C.; del Valle, M. Impedimetric Aptasensors Using Nanomaterials. *Nanotechnol. Biosens.* **2018**, 233–267. https://doi.org/10.1016/B978-0-12-813855-7.00008-8.

(28) Andersson, L.; Sellergren, B.; Mosbach, K. Imprinting of Amino Acid Derivatives in Macroporous Polymers. *Tetrahedron Lett.* **1984**, *25* (45), 5211–5214. https://doi.org/10.1016/S0040-4039(01)81566-5.

(29) Herrera-Chacón, A.; Cetó, X.; del Valle, M. Molecularly Imprinted Polymers - towards Electrochemical Sensors and Electronic Tongues. *Analytical and Bioanalytical Chemistry*. 2021, pp 6117–6140. https://doi.org/10.1007/s00216-021-03313-8.

(30) Bard, A. J.; Faulkner, L. R. *Electrochemical Methods: Fundamentals and Applications*, 2nd ed.; John Wiley & Sons, Inc.: New York, 2001.

(31) Skoog, D. A.; Holler, F. J.; Crouch, S. R. *Principles of Insrtumental Analysis*, 7th editio.; Cengage Learning, 2018.

(32) Chaubey, A.; Malhotra, B. D. Mediated Biosensors. *Biosens. Bioelectron.* **2002**, *17* (6–7), 441–456. https://doi.org/10.1016/S0956-5663(01)00313-X.

(33) Moura, S. L.; Pallarès-Rusiñol, A.; Sappia, L.; Martí, M.; Pividori, M. I. The Activity of Alkaline Phosphatase in Breast Cancer Exosomes Simplifies the Biosensing Design. *Biosens. Bioelectron.* **2022**, *198*, 113826. https://doi.org/10.1016/j.bios.2021.113826.

(34) Hasan, M. R.; Ahommed, M. S.; Daizy, M.; Bacchu, M. S.; Ali, M. R.; Al-Mamun, M. R.; Saad Aly, M. A.; Khan, M. Z. H.; Hossain, S. I. Recent Development in Electrochemical Biosensors for Cancer Biomarkers Detection. *Biosens. Bioelectron. X* **2021**, *8*, 100075. https://doi.org/10.1016/j.biosx.2021.100075.

(35) Kim, J. H.; Suh, Y. J.; Park, D.; Yim, H.; Kim, H.; Kim, H. J.; Yoon, D. S.; Hwang, K. S. Technological Advances in Electrochemical Biosensors for the Detection of Disease Biomarkers. *Biomed. Eng. Lett.* **2021**, *11* (4), 309–334. https://doi.org/10.1007/s13534-021-00204-w.

(36) Moore, T. J.; Moody, A. S.; Payne, T. D.; Sarabia, G. M.; Daniel, A. R.; Sharma, B. In Vitro and in Vivo Sers Biosensing for Disease Diagnosis. *Biosensors* **2018**, *8* (2). https://doi.org/10.3390/bios8020046.

(37) Ambartsumyan, O.; Gribanyov, D.; Kukushkin, V.; Kopylov, A.; Zavyalova, E. SERS-Based Biosensors for Virus Determination with Oligonucleotides as Recognition Elements. *Int. J. Mol. Sci.* **2020**, *21* (9), 1–15. https://doi.org/10.3390/ijms21093373.

(38) Ramanathan, K.; Danielsson, B. Principles and Applications of Thermal Biosensors. *Biosens. Bioelectron.* **2001**, *16* (6), 417–423. https://doi.org/10.1016/S0956-5663(01)00124-5.

(39) Zhang, Y.; Tadigadapa, S. Calorimetric Biosensors with Integrated Microfluidic Channels. *Biosens. Bioelectron.* **2004**, *19* (12), 1733–1743. https://doi.org/10.1016/j.bios.2004.01.009.

(40) Lim, H. J.; Saha, T.; Tey, B. T.; Tan, W. S.; Ooi, C. W. Quartz Crystal Microbalance-Based Biosensors as Rapid Diagnostic Devices for Infectious Diseases. *Biosens. Bioelectron.* **2020**, *168*, 112513. https://doi.org/10.1016/j.bios.2020.112513.

(41) Liao, Z.; Wang, J.; Zhang, P.; Zhang, Y.; Miao, Y.; Gao, S.; Deng, Y.; Geng, L. Recent Advances in Microfluidic Chip Integrated Electronic Biosensors for Multiplexed Detection. *Biosens. Bioelectron.* **2018**, *121*, 272–280. https://doi.org/10.1016/j.bios.2018.08.061.

(42) Loo, J. F. C.; Ho, A. H. P.; Turner, A. P. F.; Mak, W. C. Integrated Printed Microfluidic Biosensors. *Trends Biotechnol.* **2019**, *37* (10), 1104–1120. https://doi.org/10.1016/j.tibtech.2019.03.009.

(43) García-Guzmán, J. J.; Pérez-Ràfols, C.; Cuartero, M.; Crespo, G. A. Microneedle Based Electrochemical (Bio)Sensing: Towards Decentralized and Continuous Health Status Monitoring. *TrAC - Trends Anal. Chem.* **2021**, *135*, 116148. https://doi.org/10.1016/j.trac.2020.116148.

(44) Kim, J.; Campbell, A. S.; de Ávila, B. E. F.; Wang, J. Wearable Biosensors for Healthcare Monitoring. *Nat. Biotechnol.* **2019**, *37* (4), 389–406. https://doi.org/10.1038/s41587-019-0045-y.

(45) Pinzani, P.; D'Argenio, V.; Re, M. Del; Pellegrini, C.; Cucchiara, F.; Salvianti, F.; Galbiati, S. Updates on Liquid Biopsy: Current Trends and Future Perspectives for Clinical Application in Solid Tumors. *Clin. Chem. Lab. Med.* **2021**, *59* (7), 1181–1200. https://doi.org/10.1515/cclm-2020-1685.

(46) Soda, N.; Rehm, B. H. A.; Sonar, P.; Nguyen, N.-T.; Shiddiky, M. J. A. Advanced Liquid Biopsy Technologies for Circulating Biomarker Detection. *J. Mater. Chem. B* **2019**, *7* (43), 6670–6704. https://doi.org/10.1039/C9TB01490J.

(47) Jiang, N.; Tansukawat, N. D.; Gonzalez-Macia, L.; Ates, H. C.; Dincer, C.; Güder, F.; Tasoglu, S.; Yetisen, A. K. Low-Cost Optical Assays for Point-of-Care Diagnosis in Resource-Limited Settings. *ACS Sensors* **2021**, *6* (6), 2108–2124. https://doi.org/10.1021/acssensors.1c00669.

(48) Zheng, W.; Wang, K.; Xu, H.; Zheng, C.; Cao, B.; Qin, Q.; Jin, Q.; Cui, D. Strategies for the Detection of Target Analytes Using Microfluidic Paper-Based Analytical Devices. *Anal. Bioanal. Chem.* **2021**, *413* (9), 2429–2445. https://doi.org/10.1007/s00216-021-03213-x.

(49) Abbott. *Freestyle Libre 3 sensor*. https://www.freestylelibre.es/libre/productos/freestylelibre3-sensores.html#product_1 (accessed 2022-07-25).

(50) Dexcom. *Dexcom One*. https://www.dexcom.com/es-ES/dexcom-one (accessed 2022-07-25).

(51) PTS Diagnostics. *CardioChek Plus Analyzer*. https://ptsdiagnostics.com/cardiochek-plus-analyzer/ (accessed 2022-07-25).

(52) Abbott. *i-Stat Alinity*. https://www.globalpointofcare.abbott/en/product-details/apoc/istat-alinity.html (accessed 2022-07-25).

(53) Yamada, K.; Henares, T. G.; Suzuki, K.; Citterio, D. Paper-Based Inkjet-Printed Microfluidic Analytical Devices. *Angew. Chemie - Int. Ed.* **2015**, *54* (18), 5294–5310. https://doi.org/10.1002/anie.201411508.

(54) Oh, Y. K.; Joung, H. A.; Kim, S.; Kim, M. G. Vertical Flow Immunoassay (VFA) Biosensor for a Rapid One-Step Immunoassay. *Lab Chip* **2013**, *13* (5), 768–772. https://doi.org/10.1039/c2lc41016h.

(55) Gottlieb, S. FDA's Policy Changes for COVID-19 At-Home Diagnostics—Implications for Addressing Other Infectious Diseases and Future Pandemics. *JAMA Heal. Forum* **2021**, *2* (12), e215190. https://doi.org/10.1001/jamahealthforum.2021.5190.

(56) Alcorn, T. Pandemic Era Tests May Speed Hepatitis-C Detection. *The New York Times*.

February 4, 2022.

(57) Biocat. *2021 BioRegion Report*; 2021.

(58) European Comission. *Horizon Europe 2021-2027 research & innovation programme*. https://ec.europa.eu/info/research-and-innovation/funding/funding-opportunities/funding-programmes-and-open-calls/horizon-europe_en (accessed 2022-04-19).

(59) European Comission. *EU4Health 2021-2027 – a vision for a healthier European Union*. https://ec.europa.eu/health/funding/eu4health-2021-2027-vision-healthier-european-union_en (accessed 2022-04-19).

(60) Gould, S. J.; Raposo, G. As We Wait: Coping with an Imperfect Nomenclature for Extracellular Vesicles. *J. Extracell. Vesicles* **2013**, *2* (1). https://doi.org/10.3402/jev.v2i0.20389.

(61) Lötvall, J.; Hill, A. F.; Hochberg, F.; Buzás, E. I.; Vizio, D. Di; Gardiner, C.; Gho, Y. S.; Kurochkin, I. V.; Mathivanan, S.; Quesenberry, P.; Sahoo, S.; Tahara, H.; Wauben, M. H.; Witwer, K. W.; Théry, C. Minimal Experimental Requirements for Definition of Extracellular Vesicles and Their Functions: A Position Statement from the International Society for Extracellular Vesicles. *J. Extracell. Vesicles* **2014**, *3* (1). https://doi.org/10.3402/jev.v3.26913.

(62) Théry, C.; Witwer, K. W.; Aikawa, E.; et al. Minimal Information for Studies of Extracellular Vesicles 2018 (MISEV2018): A Position Statement of the International Society for Extracellular Vesicles and Update of the MISEV2014 Guidelines. *J. Extracell. Vesicles* **2018**, *7* (1). https://doi.org/10.1080/20013078.2018.1535750.

(63) Witwer, K. W.; Théry, C. Extracellular Vesicles or Exosomes? On Primacy, Precision, and Popularity Influencing a Choice of Nomenclature. *J. Extracell. Vesicles* **2019**, *8* (1). https://doi.org/10.1080/20013078.2019.1648167.

(64) Fox, A. S.; Duggleby, W. F.; Gelbart, W. M.; Yoon, S. B. *DNA-Induced Transformation in Drosophila: Evidence for Transmission without Integration.*; 1970; Vol. 67. https://doi.org/10.1073/pnas.67.4.1834.

(65) Fox, A. S.; Yoon, S. B. *DNA-Induced Transformation in Drosophila: Locus-Specificity and the Establishment of Transformed Stocks.*; 1970; Vol. 67. https://doi.org/10.1073/pnas.67.3.1608.

(66) Fox, A. S.; Yoon, S. B.; Gelbart, W. M. DNA-Induced Transformation in Drosophila: Genetic Analysis of Transformed Stocks. *Proc. Natl. Acad. Sci. U. S. A.* **1971**, *68* (2), 342–346. https://doi.org/10.1073/pnas.68.2.342.

(67) Mishra, N. C.; Tatum, E. L. *Non-Mendelian Inheritance of DNA-Induced Inositol Independence in Neurospora (Exosome/Integration/Meiosis/Transformation)*; 1973; Vol. 70.

(68) Trams, E. G.; Lauter, C. J.; Norman Salem, J.; Heine, U. Exfoliation of Membrane Ecto-Enzymes in the Form of Micro-Vesicles. *BBA - Biomembr.* **1981**, *645* (1), 63–70. https://doi.org/10.1016/0005-2736(81)90512-5.

(69) Johnstone, R. M.; Adam, M.; Hammond, J. R.; Orr, L.; Turbide, C. Vesicle Formation during Reticulocyte Maturation. Association of Plasma Membrane Activities with Released Vesicles (Exosomes). *J. Biol. Chem.* **1987**, *262* (19), 9412–9420.

(70) Anderson, H. C. Electron Microscopic Studies of Induced Cartilage Development and Calcification. *J. Cell Biol.* **1967**, *35* (1), 81–101. https://doi.org/10.1083/jcb.35.1.81.

(71) Anderson, H. C. Vesicles Associated with Calcification in the Matrix of Epiphyseal Cartilage. *J. Cell Biol.* **1969**, *41* (1), 59–72. https://doi.org/10.1083/jcb.41.1.59.

(72) Couch, Y.; Buzàs, E. I.; Vizio, D. Di; Gho, Y. S.; Harrison, P.; Hill, A. F.; Lötvall, J.; Raposo, G.; Stahl, P. D.; Théry, C.; Witwer, K. W.; Carter, D. R. F. A Brief History of Nearly EV-Erything – The Rise and Rise of Extracellular Vesicles. *J. Extracell. Vesicles* **2021**, *10* (14). https://doi.org/10.1002/jev2.12144.

(73) Gurung, S.; Perocheau, D.; Touramanidou, L.; Baruteau, J. The Exosome Journey: From Biogenesis to Uptake and Intracellular Signalling. *Cell Commun. Signal.* **2021**, *19* (1), 1–19. https://doi.org/10.1186/s12964-021-00730-1.

(74) Mathieu, M.; Martin-Jaular, L.; Lavieu, G.; Théry, C. Specificities of Secretion and Uptake of Exosomes and Other Extracellular Vesicles for Cell-to-Cell Communication. *Nat. Cell Biol.*

2019, *21* (1), 9–17. https://doi.org/10.1038/s41556-018-0250-9.

(75) Yu, W.; Hurley, J.; Roberts, D.; Chakrabortty, S. K.; Enderle, D.; Noerholm, M.; Breakefield, X. O.; Skog, J. K. Exosome-Based Liquid Biopsies in Cancer: Opportunities and Challenges. *Ann. Oncol.* **2021**, *32* (4), 466–477. https://doi.org/10.1016/j.annonc.2021.01.074.

(76) Han, P.; Bartold, P. M.; Ivanovski, S. The Emerging Role of Small Extracellular Vesicles in Saliva and Gingival Crevicular Fluid as Diagnostics for Periodontitis. *J. Periodontal Res.* **2022**, *57* (1), 219–231. https://doi.org/10.1111/jre.12950.

(77) Gao, P.; Li, X.; Du, X.; Liu, S.; Xu, Y. Diagnostic and Therapeutic Potential of Exosomes in Neurodegenerative Diseases. *Frontiers in Aging Neuroscience*. 2021, p 790863. https://doi.org/10.3389/fnagi.2021.790863.

(78) Sabanovic, B.; Piva, F.; Cecati, M.; Giulietti, M. Promising Extracellular Vesicle-Based Vaccines against Viruses, Including SARS-CoV-2. *Biology (Basel).* **2021**, *10* (2), 1–14. https://doi.org/10.3390/biology10020094.

(79) Terstappen, G. C.; Meyer, A. H.; Bell, R. D.; Zhang, W. Strategies for Delivering Therapeutics across the Blood–Brain Barrier. *Nat. Rev. Drug Discov.* **2021**, *20* (5), 362–383. https://doi.org/10.1038/s41573-021-00139-y.

(80) Herrmann, I. K.; Wood, M. J. A.; Fuhrmann, G. Extracellular Vesicles as a Next-Generation Drug Delivery Platform. *Nat. Nanotechnol.* **2021**, *16* (7), 748–759. https://doi.org/10.1038/s41565-021-00931-2.

(81) Alsaadi, N.; Srinivasan, A. J.; Seshadri, A.; Shiel, M.; Neal, M. D.; Scott, M. J. The Emerging Therapeutic Potential of Extracellular Vesicles in Trauma. *J. Leukoc. Biol.* **2022**, *111* (1), 93–111. https://doi.org/10.1002/JLB.3MIR0621-298R.

(82) Li, M.; Huang, L.; Chen, J.; Ni, F.; Zhang, Y.; Liu, F. Isolation of Exosome Nanoparticles from Human Cerebrospinal Fluid for Proteomic Analysis. *ACS Appl. Nano Mater.* **2021**, *4* (4), 3351–3359. https://doi.org/10.1021/acsanm.0c02622.

(83) Skotland, T.; Sandvig, K.; Llorente, A. Lipids in Exosomes: Current Knowledge and the Way Forward. *Prog. Lipid Res.* **2017**, *66*, 30–41. https://doi.org/10.1016/j.plipres.2017.03.001.

(84) Eldh, M.; Lötvall, J.; Malmhäll, C.; Ekström, K. Importance of RNA Isolation Methods for Analysis of Exosomal RNA: Evaluation of Different Methods. *Mol. Immunol.* **2012**, *50* (4), 278–286. https://doi.org/10.1016/j.molimm.2012.02.001.

(85) Royo, F.; Diwan, I.; Tackett, M. R.; Zuñiga, P.; Sanchez-Mosquera, P.; Loizaga-Iriarte, A.; Ugalde-Olano, A.; Lacasa, I.; Perez, A.; Unda, M.; Carracedo, A.; Falcon-Perez, J. M. Comparative MiRNA Analysis of Urine Extracellular Vesicles Isolated through Five Different Methods. *Cancers (Basel).* **2016**, *8* (12), 5–7. https://doi.org/10.3390/cancers8120112.

(86) Wu, M.; Ouyang, Y.; Wang, Z.; Zhang, R.; Huang, P.-H.; Chen, C.; Li, H.; Li, P.; Quinn, D.; Dao, M.; Suresh, S.; Sadovsky, Y.; Huang, T. J. Isolation of Exosomes from Whole Blood by Integrating Acoustics and Microfluidics. *Proc. Natl. Acad. Sci.* **2017**, *114* (40), 10584–10589. https://doi.org/10.1073/pnas.1709210114.

(87) Cumba Garcia, L. M.; Peterson, T. E.; Cepeda, M. A.; Johnson, A. J.; Parney, I. F. Isolation and Analysis of Plasma-Derived Exosomes in Patients With Glioma. *Front. Oncol.* **2019**, *9*, 651. https://doi.org/10.3389/fonc.2019.00651.

(88) Lozano-Ramos, I.; Bancu, I.; Oliveira-Tercero, A.; Armengol, M. P.; Menezes-Neto, A.; Del Portillo, H. A.; Lauzurica-Valdemoros, R.; Borràs, F. E. Size-Exclusion Chromatography-Based Enrichment of Extracellular Vesicles from Urine Samples. *J. Extracell. Vesicles* **2015**, *4* (2015), 1–11. https://doi.org/10.3402/jev.v4.27369.

(89) Mercadal, M.; Herrero, C.; López-Rodrigo, O.; Castells, M.; Fuente, A. de la; Vigués, F.; Bassas, L.; Larriba, S. Impact of Extracellular Vesicle Isolation Methods on Downstream Mirna Analysis in Semen: A Comparative Study. *Int. J. Mol. Sci.* **2020**, *21* (17), 1–18. https://doi.org/10.3390/ijms21175949.

(90) Wijenayake, S.; Eisha, S.; Tawhidi, Z.; Pitino, M. A.; Steele, M. A.; Fleming, A. S.; McGowan, P. O. Comparison of Methods for Pre-Processing, Exosome Isolation, and RNA Extraction in Unpasteurized Bovine and Human Milk. *PLoS One* **2021**, *16* (9 Septembe).

https://doi.org/10.1371/journal.pone.0257633.

(91) Théry, C.; Ostrowski, M.; Segura, E. Membrane Vesicles as Conveyors of Immune Responses. *Nat. Rev. Immunol.* **2009**, *9* (8), 581–593. https://doi.org/10.1038/NRI2567.

(92) Yáñez-Mó, M.; Siljander, P. R.-M.; Andreu, Z.; et al. Biological Properties of Extracellular Vesicles and Their Physiological Functions. *J. Extracell. vesicles* **2015**, *4*, 27066. https://doi.org/10.3402/jev.v4.27066.

(93) Van Niel, G.; D'Angelo, G.; Raposo, G. Shedding Light on the Cell Biology of Extracellular Vesicles. *Nat. Rev. Mol. Cell Biol.* **2018**, *19* (4), 213–228. https://doi.org/10.1038/nrm.2017.125.

(94) Meldolesi, J. Exosomes and Ectosomes in Intercellular Communication. *Curr. Biol.* **2018**, *28* (8), R435–R444. https://doi.org/10.1016/j.cub.2018.01.059.

(95) Valadi, H.; Ekström, K.; Bossios, A.; Sjöstrand, M.; Lee, J. J.; Lötvall, J. O. Exosome-Mediated Transfer of MRNAs and MicroRNAs Is a Novel Mechanism of Genetic Exchange between Cells. *Nat. Cell Biol.* **2007**, *9* (6), 654–659. https://doi.org/10.1038/ncb1596.

(96) Colombo, M.; Raposo, G.; Théry, C. Biogenesis, Secretion, and Intercellular Interactions of Exosomes and Other Extracellular Vesicles. *Annu. Rev. Cell Dev. Biol.* **2014**, *30* (1), 255–289. https://doi.org/10.1146/annurev-cellbio-101512-122326.

(97) Degli Esposti, C.; Iadarola, B.; Maestri, S.; Beltrami, C.; Lavezzari, D.; Morini, M.; De Marco, P.; Erminio, G.; Garaventa, A.; Zara, F.; Delledonne, M.; Ognibene, M.; Pezzolo, A. Exosomes from Plasma of Neuroblastoma Patients Contain Doublestranded Dna Reflecting the Mutational Status of Parental Tumor Cells. *Int. J. Mol. Sci.* **2021**, *22* (7). https://doi.org/10.3390/ijms22073667.

(98) Pathan, M.; Fonseka, P.; Chitti, S. V.; Kang, T.; Sanwlani, R.; Van Deun, J.; Hendrix, A.; Mathivanan, S. Vesiclepedia 2019: A Compendium of RNA, Proteins, Lipids and Metabolites in Extracellular Vesicles. *Nucleic Acids Res.* **2019**, *47* (D1), D516–D519. https://doi.org/10.1093/nar/gky1029.

(99) Keerthikumar, S.; Chisanga, D.; Ariyaratne, D.; Al Saffar, H.; Anand, S.; Zhao, K.; Samuel, M.; Pathan, M.; Jois, M.; Chilamkurti, N.; Gangoda, L.; Mathivanan, S. ExoCarta: A Web-Based Compendium of Exosomal Cargo. *J. Mol. Biol.* **2016**, *428* (4), 688–692. https://doi.org/10.1016/j.jmb.2015.09.019.

(100) Murillo, O. D.; Thistlethwaite, W.; Rozowsky, J.; et al. ExRNA Atlas Analysis Reveals Distinct Extracellular RNA Cargo Types and Their Carriers Present across Human Biofluids. *Cell* **2019**, *177* (2), 463-477.e15. https://doi.org/10.1016/j.cell.2019.02.018.

(101) Van Deun, J.; Mestdagh, P.; Agostinis, P.; et al. *EV-TRACK: Transparent Reporting and Centralizing Knowledge in Extracellular Vesicle Research*; 2017; Vol. 14. https://doi.org/10.1038/nmeth.4185.

(102) Doyle, L.; Wang, M. Overview of Extracellular Vesicles, Their Origin, Composition, Purpose, and Methods for Exosome Isolation and Analysis. *Cells* **2019**, *8* (7), 727. https://doi.org/10.3390/cells8070727.

(103) Théry, C.; Amigorena, S.; Raposo, G.; Clayton, A. Isolation and Characterization of Exosomes from Cell Culture Supernatants and Biological Fluids. *Curr. Protoc. Cell Biol.* **2006**, *30* (1), 3.22.1-3.22.29. https://doi.org/10.1002/0471143030.cb0322s30.

(104) Swatler, J.; Dudka, W.; Piwocka, K. Isolation and Characterization of Extracellular Vesicles from Cell Culture Conditioned Medium for Immunological Studies. *Curr. Protoc. Immunol.* **2020**, *129* (1), 1–26. https://doi.org/10.1002/cpim.96.

(105) Livshits, M. A.; Khomyakova, E.; Evtushenko, E. G.; Lazarev, V. N.; Kulemin, N. A.; Semina, S. E.; Generozov, E. V.; Govorun, V. M. Isolation of Exosomes by Differential Centrifugation: Theoretical Analysis of a Commonly Used Protocol. *Sci. Rep.* **2015**, *5* (1), 17319. https://doi.org/10.1038/srep17319.

(106) Zieren, R. C.; Dong, L.; Pierorazio, P. M.; Pienta, K. J.; de Reijke, T. M.; Amend, S. R. Extracellular Vesicle Isolation from Human Renal Cancer Tissue. *Med. Oncol.* **2020**, *37* (4), 1–11. https://doi.org/10.1007/s12032-020-1346-1.

(107) Tang, Y. T.; Huang, Y. Y.; Zheng, L.; Qin, S. H.; Xu, X. P.; An, T. X.; Xu, Y.; Wu, Y. S.;

Hu, X. M.; Ping, B. H.; Wang, Q. Comparison of Isolation Methods of Exosomes and Exosomal RNA from Cell Culture Medium and Serum. *Int. J. Mol. Med.* **2017**, *40* (3), 834–844. https://doi.org/10.3892/ijmm.2017.3080.

(108) Tian, Y.; Gong, M.; Hu, Y.; Liu, H.; Zhang, W.; Zhang, M.; Hu, X.; Aubert, D.; Zhu, S.; Wu, L.; Yan, X. Quality and Efficiency Assessment of Six Extracellular Vesicle Isolation Methods by Nano-Flow Cytometry. *J. Extracell. Vesicles* **2020**, *9* (1). https://doi.org/10.1080/20013078.2019.1697028.

(109) Witwer, K. W.; Buzás, E. I.; Bemis, L. T.; Bora, A.; Lässer, C.; Lötvall, J.; Nolte-'t Hoen, E. N.; Piper, M. G.; Sivaraman, S.; Skog, J.; Théry, C.; Wauben, M. H.; Hochberg, F. Standardization of Sample Collection, Isolation and Analysis Methods in Extracellular Vesicle Research. *J. Extracell. Vesicles* **2013**, *2* (1). https://doi.org/10.3402/jev.v2i0.20360.

(110) Keller, S.; Ridinger, J.; Rupp, A. K.; Janssen, J. W. G.; Altevogt, P. Body Fluid Derived Exosomes as a Novel Template for Clinical Diagnostics. *J. Transl. Med.* **2011**, *9* (1), 86. https://doi.org/10.1186/1479-5876-9-86.

(111) Lamparski, H. G.; Metha-Damani, A.; Yao, J. Y.; Patel, S.; Hsu, D. H.; Ruegg, C.; Le Pecq, J. B. Production and Characterization of Clinical Grade Exosomes Derived from Dendritic Cells. *J. Immunol. Methods* **2002**, *270* (2), 211–226. https://doi.org/10.1016/S0022-1759(02)00330-7.

(112) Iwai, K.; Minamisawa, T.; Suga, K.; Yajima, Y.; Shiba, K. Isolation of Human Salivary Extracellular Vesicles by Iodixanol Density Gradient Ultracentrifugation and Their Characterizations. *J. Extracell. Vesicles* **2016**, *5* (1). https://doi.org/10.3402/jev.v5.30829.

(113) Van Deun, J.; Mestdagh, P.; Sormunen, R.; Cocquyt, V.; Vermaelen, K.; Vandesompele, J.; Bracke, M.; De Wever, O.; Hendrix, A. The Impact of Disparate Isolation Methods for Extracellular Vesicles on Downstream RNA Profiling. *J. Extracell. Vesicles* **2014**, *3* (1). https://doi.org/10.3402/jev.v3.24858.

(114) Graham, J. M. Purification of a Crude Mitochondrial Fraction by Density-Gradient Centrifugation. *Curr. Protoc. Cell Biol.* **1999**, *4* (1), 1–22. https://doi.org/10.1002/0471143030.cb0304s04.

(115) de Araùjo, M. E. G.; Hube, L. A.; Stasyk, T. Isolation of Endocitic Organelles by Density Gradient Centrifugation. In *Methods in Molecular Biology*; 2008; pp 317–331. https://doi.org/10.1007/978-1-60327-064-9_25.

(116) Rood, I. M.; Deegens, J. K. J.; Merchant, M. L.; Tamboer, W. P. M.; Wilkey, D. W.; Wetzels, J. F. M.; Klein, J. B. Comparison of Three Methods for Isolation of Urinary Microvesicles to Identify Biomarkers of Nephrotic Syndrome. *Kidney Int.* **2010**, *78* (8), 810–816. https://doi.org/10.1038/ki.2010.262.

(117) Benedikter, B. J.; Bouwman, F. G.; Vajen, T.; Heinzmann, A. C. A.; Grauls, G.; Mariman, E. C.; Wouters, E. F. M.; Savelkoul, P. H.; Lopez-Iglesias, C.; Koenen, R. R.; Rohde, G. G. U.; Stassen, F. R. M. Ultrafiltration Combined with Size Exclusion Chromatography Efficiently Isolates Extracellular Vesicles from Cell Culture Media for Compositional and Functional Studies. *Sci. Rep.* **2017**, *7* (1), 1–13. https://doi.org/10.1038/s41598-017-15717-7.

(118) Lobb, R. J.; Becker, M.; Wen, S. W.; Wong, C. S. F. F.; Wiegmans, A. P.; Leimgruber, A.; Möller, A.; Wen Wen, S.; Wong, C. S. F. F.; Wiegmans, A. P.; Leimgruber, A.; Möller, A. Optimized Exosome Isolation Protocol for Cell Culture Supernatant and Human Plasma. *J. Extracell. Vesicles* **2015**, *4* (1), 27031. https://doi.org/10.3402/jev.v4.27031.

(119) Taylor, D. D.; Shah, S. Methods of Isolating Extracellular Vesicles Impact Down-Stream Analyses of Their Cargoes. *Methods* **2015**, *87*, 3–10. https://doi.org/10.1016/j.ymeth.2015.02.019.

(120) Böing, A. N.; van der Pol, E.; Grootemaat, A. E.; Coumans, F. A. W.; Sturk, A.; Nieuwland, R. Single-Step Isolation of Extracellular Vesicles by Size-Exclusion Chromatography. *J. Extracell. Vesicles* **2014**, *3* (1), 1–11. https://doi.org/10.3402/jev.v3.23430.

(121) Lu, J.; Pang, J.; Chen, Y.; Dong, Q.; Sheng, J.; Luo, Y.; Lu, Y.; Lin, B.; Liu, T. Application of Microfluidic Chips in Separation and Analysis of Extracellular Vesicles in Liquid Biopsy for Cancer. *Micromachines* **2019**, *10* (6), 390. https://doi.org/10.3390/mi10060390.

(122) Liu, F.; Vermesh, O.; Mani, V.; Ge, T. J.; Madsen, S. J.; Sabour, A.; Hsu, E. C.; Gowrishankar, G.; Kanada, M.; Jokerst, J. V.; Sierra, R. G.; Chang, E.; Lau, K.; Sridhar, K.; Bermudez, A.; Pitteri, S. J.; Stoyanova, T.; Sinclair, R.; Nair, V. S.; Gambhir, S. S.; Demirci, U. The Exosome Total Isolation Chip. *ACS Nano* **2017**, *11* (11), 10712–10723. https://doi.org/10.1021/acsnano.7b04878.

(123) Woo, H. K.; Sunkara, V.; Park, J.; Kim, T. H.; Han, J. R.; Kim, C. J.; Choi, H. Il; Kim, Y. K.; Cho, Y. K. Exodisc for Rapid, Size-Selective, and Efficient Isolation and Analysis of Nanoscale Extracellular Vesicles from Biological Samples. *ACS Nano* **2017**, *11* (2), 1360–1370. https://doi.org/10.1021/acsnano.6b06131.

(124) Chen, Z.; Yang, Y.; Yamaguchi, H.; Hung, M. C.; Kameoka, J. Isolation of Cancer-Derived Extracellular Vesicle Subpopulations by a Size-Selective Microfluidic Platform. *Biomicrofluidics* **2020**, *14*, 034113. https://doi.org/10.1063/5.0008438.

(125) Kim, D.; Woo, H. K.; Lee, C.; Min, Y.; Kumar, S.; Sunkara, V.; Jo, H. G.; Lee, Y. J.; Kim, J.; Ha, H. K.; Cho, Y. K. EV-Ident: Identifying Tumor-Specific Extracellular Vesicles by Size Fractionation and Single-Vesicle Analysis. *Anal. Chem.* **2020**, *92* (8), 6010–6018. https://doi.org/10.1021/acs.analchem.0c00285.

(126) de Menezes-Neto, A.; Sáez, M. J.; Lozano-Ramos, I.; Segui-Barber, J.; Martin-Jaular, L.; Ullate, J. M. E.; Fernandez-Becerra, C.; Borrás, F. E.; del Portillo, H. A. Size-Exclusion Chromatography as a Stand-Alone Methodology Identifies Novel Markers in Mass Spectrometry Analyses of Plasma-Derived Vesicles from Healthy Individuals. *J. Extracell. Vesicles* **2015**, *4* (1), 1–14. https://doi.org/10.3402/jev.v4.27378.

(127) Gámez-Valero, A.; Monguió-Tortajada, M.; Carreras-Planella, L.; Franquesa, M.; Beyer, K.; Borràs, F. E. Size-Exclusion Chromatography-Based Isolation Minimally Alters Extracellular Vesicles' Characteristics Compared to Precipitating Agents. *Sci. Rep.* **2016**, *6* (June), 1–9. https://doi.org/10.1038/srep33641.

(128) Taylor, D. D.; Gerçel-Taylor, C. Tumour-Derived Exosomes and Their Role in Cancer-Associated T-Cell Signalling Defects. *Br. J. Cancer* **2005**, *92* (2), 305–311. https://doi.org/10.1038/sj.bjc.6602316.

(129) Monguió-Tortajada, M.; Morón-Font, M.; Gámez-Valero, A.; Carreras-Planella, L.; Borràs, F. E.; Franquesa, M. Extracellular-Vesicle Isolation from Different Biological Fluids by Size-Exclusion Chromatography. *Curr. Protoc. Stem Cell Biol.* **2019**, *49* (1), 1–24. https://doi.org/10.1002/cpsc.82.

(130) Lewis, G. D.; Metcalf, T. G. Polyethylene Glycol Precipitation for Recovery of Pathogenic Viruses, Including Hepatitis A Virus and Human Rotavirus, from Oyster, Water, and Sediment Samples. *Appl. Environ. Microbiol.* **1988**, *54* (8), 1983–1988. https://doi.org/10.1128/aem.54.8.1983-1988.1988.

(131) Deregibus, M. C.; Figliolini, F.; D'Antico, S.; Manzini, P. M.; Pasquino, C.; De Lena, M.; Tetta, C.; Brizzi, M. F.; Camussi, G. Charge-Based Precipitation of Extracellular Vesicles. *Int. J. Mol. Med.* **2016**, *38* (5), 1359–1366. https://doi.org/10.3892/ijmm.2016.2759.

(132) Niu, Z.; Pang, R. T. K.; Liu, W.; Li, Q.; Cheng, R.; Yeung, W. S. B. Polymer-Based Precipitation Preserves Biological Activities of Extracellular Vesicles from an Endometrial Cell Line. *PLoS One* **2017**, *12* (10), 1–21. https://doi.org/10.1371/journal.pone.0186534.

(133) Rider, M. A.; Hurwitz, S. N.; Meckes, D. G. ExtraPEG: A Polyethylene Glycol-Based Method for Enrichment of Extracellular Vesicles. *Sci. Rep.* **2016**, *6* (October 2015), 1–14. https://doi.org/10.1038/srep23978.

(134) Alvarez, M. L.; Khosroheidari, M.; Kanchi Ravi, R.; Distefano, J. K. Comparison of Protein, MicroRNA, and MRNA Yields Using Different Methods of Urinary Exosome Isolation for the Discovery of Kidney Disease Biomarkers. *Kidney Int.* **2012**, *82* (9), 1024–1032. https://doi.org/10.1038/ki.2012.256.

(135) Brennan, K.; Martin, K.; FitzGerald, S. P.; O'Sullivan, J.; Wu, Y.; Blanco, A.; Richardson, C.; Mc Gee, M. M. A Comparison of Methods for the Isolation and Separation of Extracellular Vesicles from Protein and Lipid Particles in Human Serum. *Sci. Rep.* **2020**, *10* (1), 1039. https://doi.org/10.1038/s41598-020-57497-7.

(136) Taylor, D. D.; Zacharias, W.; Gercel-taylor, C. Serum/Plasma Proteomics: Methods and Protocols. In *Methods in Molecular Biology*; 2011; Vol. 728, pp 235–246. https://doi.org/10.1007/978-1-61779-068-3.

(137) Moura, S. L.; Martín, C. G.; Martí, M.; Pividori, M. I. Multiplex Detection and Characterization of Breast Cancer Exosomes by Magneto-Actuated Immunoassay. *Talanta* **2020**, *211*, 120657. https://doi.org/https://doi.org/10.1016/j.talanta.2019.120657.

(138) Yu, X.; He, L.; Pentok, M.; Yang, H.; Yang, Y.; Li, Z.; He, N.; Deng, Y.; Li, S.; Liu, T.; Chen, X.; Luo, H. An Aptamer-Based New Method for Competitive Fluorescence Detection of Exosomes. *Nanoscale* **2019**, *11* (33), 15589–15595. https://doi.org/10.1039/c9nr04050a.

(139) Thermo Fisher Scientific. *The history of Dynabeads*. https://www.thermofisher.com/es/es/home/brands/product-brand/dynal/the-history-of-dynabeads.html (accessed 2022-04-27).

(140) Lasheras, X.; Insausti, M.; Gil De Muro, I.; Garaio, E.; Plazaola, F.; Moros, M.; De Matteis, L.; M. De La Fuente, J.; Lezama, L. Chemical Synthesis and Magnetic Properties of Monodisperse Nickel Ferrite Nanoparticles for Biomedical Applications. *J. Phys. Chem. C* **2016**, *120* (6), 3492–3500. https://doi.org/10.1021/acs.jpcc.5b10216.

(141) Brandão, D.; Liébana, S.; Pividori, M. I. Multiplexed Detection of Foodborne Pathogens Based on Magnetic Particles. *N. Biotechnol.* **2015**, *32* (5), 511–520. https://doi.org/10.1016/j.nbt.2015.03.011.

(142) Carinelli, S.; Martí, M.; Alegret, S.; Pividori, M. I. Biomarker Detection of Global Infectious Diseases Based on Magnetic Particles. *N. Biotechnol.* **2015**, *32* (5), 521–532. https://doi.org/10.1016/j.nbt.2015.04.002.

(143) Marfà, J.; Pupin, R. R.; Sotomayor, M.; Pividori, M. I. Magnetic-Molecularly Imprinted Polymers in Electrochemical Sensors and Biosensors. *Anal. Bioanal. Chem.* **2021**, *413* (24), 6141–6157. https://doi.org/10.1007/s00216-021-03461-x.

(144) Dong, H.; Chen, H.; Jiang, J.; Zhang, H.; Cai, C.; Shen, Q. Highly Sensitive Electrochemical Detection of Tumor Exosomes Based on Aptamer Recognition-Induced Multi-DNA Release and Cyclic Enzymatic Amplification. *Anal. Chem.* **2018**, *90* (7), 4507–4513. https://doi.org/10.1021/acs.analchem.7b04863.

(145) Cheng, S.; Kong, Q.; Hu, X.; Zhang, C.; Xian, Y. An Ultrasensitive Strand Displacement Signal Amplification-Assisted Synchronous Fluorescence Assay for Surface Proteins of Small Extracellular Vesicle Analysis and Cancer Identification. *Anal. Chem.* **2022**, *94* (2), 1085–1091. https://doi.org/10.1021/acs.analchem.1c04122.

(146) Wan, Y.; Cheng, G.; Liu, X.; Hao, S. J.; Nisic, M.; Zhu, C. D.; Xia, Y. Q.; Li, W. Q.; Wang, Z. G.; Zhang, W. L.; Rice, S. J.; Sebastian, A.; Albert, I.; Belani, C. P.; Zheng, S. Y. Rapid Magnetic Isolation of Extracellular Vesicles via Lipid-Based Nanoprobes. *Nat. Biomed. Eng.* **2017**, *1* (4), 1–11. https://doi.org/10.1038/s41551-017-0058.

(147) Xu, H.; Liao, C.; Zuo, P.; Liu, Z.; Ye, B. C. Magnetic-Based Microfluidic Device for On-Chip Isolation and Detection of Tumor-Derived Exosomes. *Anal. Chem.* **2018**, *90* (22), 13451–13458. https://doi.org/10.1021/acs.analchem.8b03272.

(148) Gao, F.; Jiao, F.; Xia, C.; Zhao, Y.; Ying, W.; Xie, Y.; Guan, X.; Tao, M.; Zhang, Y.; Qin, W.; Qian, X. A Novel Strategy for Facile Serum Exosome Isolation Based on Specific Interactions between Phospholipid Bilayers and TiO2. *Chem. Sci.* **2019**, *10* (6), 1579–1588. https://doi.org/10.1039/c8sc04197k.

(149) Yang, J.; Pan, B.; Zeng, F.; He, B.; Gao, Y.; Liu, X.; Song, Y. Magnetic Colloid Antibodies Accelerate Small Extracellular Vesicles Isolation for Point-of-Care Diagnostics. *Nano Lett.* **2021**, *21* (5), 2001–2009. https://doi.org/10.1021/acs.nanolett.0c04476.

(150) Hassan, A. H. A.; Moura, S. L.; Ali, F. H. M.; Moselhy, W. A.; Taboada Sotomayor, M. del P.; Pividori, M. I. Electrochemical Sensing of Methyl Parathion on Magnetic Molecularly Imprinted Polymer. *Biosens. Bioelectron.* **2018**, *118*, 181–187. https://doi.org/10.1016/j.bios.2018.06.052.

(151) Thermo Fisher Scientific. *Dynabeads products selection guide*. https://www.thermofisher.com/es/es/home/brands/product-brand/dynal/dynabeads-magnetic-separation-products-selection-guide.html (accessed 2022-04-27).

(152) Carinelli, S.; Xufré, C.; Alegret, S.; Martí, M.; Pividori, M. I. CD4 Quantification Based on Magneto ELISA for AIDS Diagnosis in Low Resource Settings. *Talanta* **2016**, *160*, 36–45. https://doi.org/10.1016/j.talanta.2016.06.055.

(153) Carinelli, S.; Xufré, C.; Martí, M.; Pividori, M. I. Interferon Gamma Transcript Detection on T Cells Based on Magnetic Actuation and Multiplex Double-Tagging Electrochemical Genosensing. *Biosens. Bioelectron.* **2018**, *117*, 183–190. https://doi.org/10.1016/j.bios.2018.05.030.

(154) Laube, T.; Cortés, P.; Llagostera, M.; Alegret, S.; Pividori, M. I. Phagomagnetic Immunoassay for the Rapid Detection of Salmonella. *Appl. Microbiol. Biotechnol.* **2014**, *98* (4), 1795–1805. https://doi.org/10.1007/s00253-013-5434-4.

(155) Brandão, D.; Liébana, S.; Campoy, S.; Alegret, S.; Pividori, M. I. Immunomagnetic Separation of Salmonella with Tailored Magnetic Micro and Nanocarriers. A Comparative Study. *Talanta* **2015**, *143*, 198–204. https://doi.org/10.1016/j.talanta.2015.05.035.

(156) Liébana, S.; Spricigo, D. A.; Cortés, M. P.; Barbé, J.; Llagostera, M.; Alegret, S.; Pividori, M. I. Phagomagnetic Separation and Electrochemical Magneto-Genosensing of Pathogenic Bacteria. *Anal. Chem.* **2013**, *85* (6), 3079–3086. https://doi.org/10.1021/ac3024944.

(157) Brugnera, M. F.; Bundalian, R.; Laube, T.; Julián, E.; Luquin, M.; Zanoni, M. V. B.; Pividori, M. I. Magneto-Actuated Immunoassay for the Detection of Mycobacterium Fortuitum in Hemodialysis Water. *Talanta* **2016**, *153*, 38–44. https://doi.org/10.1016/j.talanta.2016.02.041.

(158) Ben Aissa, A.; Jara, J. J.; Sebastián, R. M.; Vallribera, A.; Campoy, S.; Pividori, M. I. Comparing Nucleic Acid Lateral Flow and Electrochemical Genosensing for the Simultaneous Detection of Foodborne Pathogens. *Biosens. Bioelectron.* **2017**, *88*, 265–272. https://doi.org/10.1016/j.bios.2016.08.046.

(159) Carinelli, S.; Kühnemund, M.; Nilsson, M.; Pividori, M. I. Yoctomole Electrochemical Genosensing of Ebola Virus CDNA by Rolling Circle and Circle to Circle Amplification. *Biosens. Bioelectron.* **2017**, *93*, 65–71. https://doi.org/10.1016/j.bios.2016.09.099.

(160) Liébana, S.; Brandão, D.; Cortés, P.; Campoy, S.; Alegret, S.; Pividori, M. I. Electrochemical Genosensing of Salmonella, Listeria and Escherichia Coli on Silica Magnetic Particles. *Anal. Chim. Acta* **2016**, *904*, 1–9. https://doi.org/10.1016/j.aca.2015.09.044.

(161) Brandão, D.; Liébana, S.; Campoy, S.; Cortés, M. P.; Alegret, S.; Pividori, M. I. Simultaneous Electrochemical Magneto Genosensing of Foodborne Bacteria Based on Triple-Tagging Multiplex Amplification. *Biosens. Bioelectron.* **2015**, *74*, 652–659. https://doi.org/10.1016/j.bios.2015.07.008.

(162) Ben Aissa, A.; Herrera-Chacon, A.; Pupin, R. R.; Sotomayor, M. D. P. T.; Pividori, M. I. Magnetic Molecularly Imprinted Polymer for the Isolation and Detection of Biotin and Biotinylated Biomolecules. *Biosens. Bioelectron.* **2017**, *88*, 101–108. https://doi.org/10.1016/j.bios.2016.07.096.

(163) Moura, S. L.; Fajardo, L. M.; Cunha, L. dos A.; Sotomayor, M. D. P. T.; Machado, F. B. C.; Ferrão, L. F. A.; Pividori, M. I. Theoretical and Experimental Study for the Biomimetic Recognition of Levothyroxine Hormone on Magnetic Molecularly Imprinted Polymer. *Biosens. Bioelectron.* **2018**, *107*, 203–210. https://doi.org/10.1016/j.bios.2018.01.028.

(164) Jackson, K. K.; Powell, R. R.; Bruce, T. F.; Marcus, R. K. Solid-Phase Extraction of Exosomes from Diverse Matrices via a Polyester Capillary-Channeled Polymer (C-CP) Fiber Stationary Phase in a Spin-down Tip Format. *Anal. Bioanal. Chem.* **2020**, *412* (19), 4713–4724. https://doi.org/10.1007/s00216-020-02728-z.

(165) Leong, S. Y.; Ong, H. B.; Tay, H. M.; Kong, F.; Upadya, M.; Gong, L.; Dao, M.; Dalan, R.; Hou, H. W. Microfluidic Size Exclusion Chromatography (MSEC) for Extracellular Vesicles and Plasma Protein Separation. *Small* **2022**, *18* (6), 2104470. https://doi.org/10.1002/smll.202104470.

(166) Musante, L.; Tataruch, D.; Gu, D.; Benito-Martin, A.; Calzaferri, G.; Aherne, S.; Holthofer, H. A Simplified Method to Recover Urinary Vesicles for Clinical Applications, and Sample Banking. *Sci. Rep.* **2014**, *4*. https://doi.org/10.1038/srep07532.

(167) Musante, L.; Tataruch-Weinert, D.; Kerjaschki, D.; Henry, M.; Meleady, P.; Holthofer, H.

Residual Urinary Extracellular Vesicles in Ultracentrifugation Supernatants after Hydrostatic Filtration Dialysis Enrichment. *J. Extracell. Vesicles* **2017**, *6* (1). https://doi.org/10.1080/20013078.2016.1267896.

(168) Sitar, S.; Kejžar, A.; Pahovnik, D.; Kogej, K.; Tušek-Žnidarič, M.; Lenassi, M.; Žagar, E. Size Characterization and Quantification of Exosomes by Asymmetrical-Flow Field-Flow Fractionation. *Anal. Chem.* **2015**, *87* (18), 9225–9233. https://doi.org/10.1021/acs.analchem.5b01636.

(169) Wu, B.; Chen, X.; Wang, J.; Qing, X.; Wang, Z.; Ding, X.; Xie, Z.; Niu, L.; Guo, X.; Cai, T.; Guo, X.; Yang, F. Separation and Characterization of Extracellular Vesicles from Human Plasma by Asymmetrical Flow Field-Flow Fractionation. *Anal. Chim. Acta* **2020**, *1127*, 234–245. https://doi.org/10.1016/j.aca.2020.06.071.

(170) Lee, K.; Shao, H.; Weissleder, R.; Lee, H. Acoustic Purification of Extracellular Microvesicles. *ACS Nano* **2015**, *9* (3), 2321–2327. https://doi.org/10.1021/nn506538f.

(171) Gardiner, C.; Ferreira, Y. J.; Dragovic, R. A.; Redman, C. W. G.; Sargent, I. L. Extracellular Vesicle Sizing and Enumeration by Nanoparticle Tracking Analysis. *J. Extracell. Vesicles* **2013**, *2* (1), 1–11. https://doi.org/10.3402/jev.v2i0.19671.

(172) Gercel-Taylor, C.; Atay, S.; Tullis, R. H.; Kesimer, M.; Taylor, D. D. Nanoparticle Analysis of Circulating Cell-Derived Vesicles in Ovarian Cancer Patients. *Anal. Biochem.* **2012**, *428* (1), 44–53. https://doi.org/10.1016/j.ab.2012.06.004.

(173) Filipe, V.; Hawe, A.; Jiskoot, W. Critical Evaluation of Nanoparticle Tracking Analysis (NTA) by NanoSight for the Measurement of Nanoparticles and Protein Aggregates. *Pharm. Res.* **2010**, *27* (5), 796–810. https://doi.org/10.1007/s11095-010-0073-2.

(174) Maas, S. L. N.; De Vrij, J.; Van Der Vlist, E. J.; Geragousian, B.; Van Bloois, L.; Mastrobattista, E.; Schiffelers, R. M.; Wauben, M. H. M.; Broekman, M. L. D.; Nolte-'T Hoen, E. N. M. Possibilities and Limitations of Current Technologies for Quantification of Biological Extracellular Vesicles and Synthetic Mimics. *J. Control. Release* **2015**, *200*, 87–96. https://doi.org/10.1016/j.jconrel.2014.12.041.

(175) Dragovic, R. A.; Gardiner, C.; Brooks, A. S.; Tannetta, D. S.; Ferguson, D. J. P.; Hole, P.; Carr, B.; Redman, C. W. G.; Harris, A. L.; Dobson, P. J.; Harrison, P.; Sargent, I. L. Sizing and Phenotyping of Cellular Vesicles Using Nanoparticle Tracking Analysis. *Nanomedicine Nanotechnology, Biol. Med.* **2011**, *7* (6), 780–788. https://doi.org/10.1016/j.nano.2011.04.003.

(176) Zhang, P.; He, M.; Zeng, Y. Ultrasensitive Microfluidic Analysis of Circulating Exosomes Using a Nanostructured Graphene Oxide/Polydopamine Coating. *Lab Chip* **2016**, *16* (16), 3033–3042. https://doi.org/10.1039/c6lc00279j.

(177) Szatanek, R.; Baj-Krzyworzeka, M.; Zimoch, J.; Lekka, M.; Siedlar, M.; Baran, J. The Methods of Choice for Extracellular Vesicles (EVs) Characterization. *Int. J. Mol. Sci.* **2017**, *18* (6), 1153. https://doi.org/10.3390/ijms18061153.

(178) Midekessa, G.; Godakumara, K.; Dissanayake, K.; Hasan, M. M.; Reshi, Q. U. A.; Rinken, T.; Fazeli, A. Characterization of Extracellular Vesicles Labelled with a Lipophilic Dye Using Fluorescence Nanoparticle Tracking Analysis. *Membranes (Basel).* **2021**, *11* (10). https://doi.org/10.3390/membranes11100779.

(179) Choi, H.; Mun, J. Y. Structural Analysis of Exosomes Using Different Types of Electron Microscopy. *Appl. Microsc.* **2017**, *47* (3), 171–175. https://doi.org/10.9729/am.2017.47.3.171.

(180) Lee, Y.; El Andaloussi, S.; Wood, M. J. A. Exosomes and Microvesicles: Extracellular Vesicles for Genetic Information Transfer and Gene Therapy. *Hum. Mol. Genet.* **2012**, *21* (R1), 125–134. https://doi.org/10.1093/hmg/dds317.

(181) Kondratov, K. A.; Petrova, T. A.; Mikhailovskii, V. Y.; Ivanova, A. N.; Kostareva, A. A.; Fedorov, A. V. A Study of Extracellular Vesicles Isolated from Blood Plasma Conducted by Low-Voltage Scanning Electron Microscopy. *Cell tissue biol.* **2017**, *11* (3), 181–190. https://doi.org/10.1134/S1990519X17030051.

(182) Shao, H.; Chung, J.; Balaj, L.; Charest, A.; Bigner, D. D.; Carter, B. S.; Hochberg, F. H.; Breakefield, X. O.; Weissleder, R.; Lee, H. Protein Typing of Circulating Microvesicles Allows Real-Time Monitoring of Glioblastoma Therapy. *Nat. Med.* **2012**, *18* (12), 1835–1840.

https://doi.org/10.1038/nm.2994.

(183) Enderle, D.; Spiel, A.; Coticchia, C. M.; Berghoff, E.; Mueller, R.; Schlumpberger, M.; Sprenger-Haussels, M.; Shaffer, J. M.; Lader, E.; Skog, J.; Noerholm, M. Characterization of RNA from Exosomes and Other Extracellular Vesicles Isolated by a Novel Spin Column-Based Method. *PLoS One* **2015**, *10* (8), 1–19. https://doi.org/10.1371/journal.pone.0136133.

(184) Sharma, S.; Rasool, H. I.; Palanisamy, V.; Mathisen, C.; Schmidt, M.; Wong, D. T.; Gimzewski, J. K. Structural-Mechanical Characterization of Nanoparticle Exosomes in Human Saliva, Using Correlative AFM, FESEM, and Force Spectroscopy. *ACS Nano* **2010**, *4* (4), 1921–1926. https://doi.org/10.1021/nn901824n.

(185) Hoo, C. M.; Starostin, N.; West, P.; Mecartney, M. L. A Comparison of Atomic Force Microscopy (AFM) and Dynamic Light Scattering (DLS) Methods to Characterize Nanoparticle Size Distributions. *J. Nanoparticle Res.* **2008**, *10* (SUPPL. 1), 89–96. https://doi.org/10.1007/s11051-008-9435-7.

(186) Akers, J. C.; Ramakrishnan, V.; Nolan, J. P.; Duggan, E.; Fu, C. C.; Hochberg, F. H.; Chen, C. C.; Carter, B. S. Comparative Analysis of Technologies for Quantifying Extracellular Vesicles (EVs) in Clinical Cerebrospinal Fluids (CSF). *PLoS One* **2016**, *11* (2), 1–11. https://doi.org/10.1371/journal.pone.0149866.

(187) Shao, H.; Im, H.; Castro, C. M.; Breakefield, X.; Weissleder, R.; Lee, H. New Technologies for Analysis of Extracellular Vesicles. *Chem. Rev.* **2018**, *118* (4), 1917–1950. https://doi.org/10.1021/acs.chemrev.7b00534.

(188) Maas, S. L. N.; Vrij, J. De; Broekman, M. L. D. Quantification and Size-Profiling of Extracellular Vesicles Using Tunable Resistive Pulse Sensing. *J. Vis. Exp.* **2014**, No. 92, 1–7. https://doi.org/10.3791/51623.

(189) Roberts, G. S.; Kozak, D.; Anderson, W.; Broom, M. F.; Vogel, R.; Trau, M. Tunable Nano/Micropores for Particle Detection and Discrimination: Scanning Ion Occlusion Spectroscopy. *Small* **2010**, *6* (23), 2653–2658. https://doi.org/10.1002/smll.201001129.

(190) Smith, P. K.; Krohn, R. I.; Hermanson, G. T.; Mallia, A. K.; Gartner, F. H.; Provenzano, M. D.; Fujimoto, E. K.; Goeke, N. M.; Olson, B. J.; Klenk, D. C. Measurement of Protein Using Bicinchoninic Acid. *Anal. Biochem.* **1985**, *150* (1), 76–85. https://doi.org/10.1016/0003-2697(85)90442-7.

(191) Bradford, M. M. A Rapid and Sensitive Method for the Quantitation of Microgram Quantities of Protein Utilizing the Principle of Protein-Dye Binding. *Anal. Biochem.* **1976**, *72* (1–2), 248–254. https://doi.org/10.1016/0003-2697(76)90527-3.

(192) McKinnon, K. M. Flow Cytometry: An Overview. *Curr. Protoc. Immunol.* **2018**, *2018*, 5.1.1-5.1.11. https://doi.org/10.1002/cpim.40.

(193) Adan, A.; Alizada, G.; Kiraz, Y.; Baran, Y.; Nalbant, A. Flow Cytometry: Basic Principles and Applications. *Crit. Rev. Biotechnol.* **2017**, *37* (2), 163–176. https://doi.org/10.3109/07388551.2015.1128876.

(194) Zaborowski, M. P.; Lee, K.; Na, Y. J.; Sammarco, A.; Zhang, X.; Iwanicki, M.; Cheah, P. S.; Lin, H. Y.; Zinter, M.; Chou, C. Y.; Fulci, G.; Tannous, B. A.; Lai, C. P. K.; Birrer, M. J.; Weissleder, R.; Lee, H.; Breakefield, X. O. Methods for Systematic Identification of Membrane Proteins for Specific Capture of Cancer-Derived Extracellular Vesicles. *Cell Rep.* **2019**, *27* (1), 255-268.e6. https://doi.org/10.1016/j.celrep.2019.03.003.

(195) Milteny Biotec. *MACSPlex Exosome kit*. https://www.miltenyibiotec.com/ES-en/products/macsplex-exosome-kit-human.html#for-up-to-96-tests (accessed 2022-04-12).

(196) Melling, G. E.; Conlon, R.; Pantazi, P.; Dellar, E. R.; Samuel, P.; Baena-Lopez, L. A.; Simpson, J. C.; Carter, D. R. F. Confocal Microscopy Analysis Reveals That Only a Small Proportion of Extracellular Vesicles Are Successfully Labelled with Commonly Utilised Staining Methods. *Sci. Rep.* **2022**, *12* (1). https://doi.org/10.1038/s41598-021-04225-4.

(197) Moura, S. L.; Martì, M.; Pividori, M. I. Matrix Effect in the Isolation of Breast Cancer-Derived Nanovesicles by Immunomagnetic Separation and Electrochemical Immunosensing— A Comparative Study. *Sensors (Switzerland)* **2020**, *20* (4), 965. https://doi.org/10.3390/s20040965.

(198) Hoen, E. N. M. N. t.; van der Vlist, E. J.; Aalberts, M.; Mertens, H. C. H.; Bosch, B. J.; Bartelink, W.; Mastrobattista, E.; van Gaal, E. V. B.; Stoorvogel, W.; Arkesteijn, G. J. A.; Wauben, M. H. M. Quantitative and Qualitative Flow Cytometric Analysis of Nanosized Cell-Derived Membrane Vesicles. *Nanomedicine Nanotechnology, Biol. Med.* **2012**, *8* (5), 712–720. https://doi.org/10.1016/j.nano.2011.09.006.

(199) Tian, Y.; Ma, L.; Gong, M.; Su, G.; Zhu, S.; Zhang, W.; Wang, S.; Li, Z.; Chen, C.; Li, L.; Wu, L.; Yan, X. Protein Profiling and Sizing of Extracellular Vesicles from Colorectal Cancer Patients via Flow Cytometry. *ACS Nano* **2018**, *12* (1), 671–680. https://doi.org/10.1021/acsnano.7b07782.

(200) Morales-Kastresana, A.; Telford, B.; Musich, T. A.; McKinnon, K.; Clayborne, C.; Braig, Z.; Rosner, A.; Demberg, T.; Watson, D. C.; Karpova, T. S.; Freeman, G. J.; Dekruyff, R. H.; Pavlakis, G. N.; Terabe, M.; Robert-Guroff, M.; Berzofsky, J. A.; Jones, J. C. Labeling Extracellular Vesicles for Nanoscale Flow Cytometry. *Sci. Rep.* **2017**, *7* (1). https://doi.org/10.1038/s41598-017-01731-2.

(201) Ender, F.; Zamzow, P.; von Bubnoff, N.; Gieseler, F. Detection and Quantification of Extracellular Vesicles via FACS: Membrane Labeling Matters! *Int. J. Mol. Sci.* **2020**, *21* (1). https://doi.org/10.3390/ijms21010291.

(202) Welsh, J. A.; Van Der Pol, E.; Arkesteijn, G. J. A.; Bremer, M.; Brisson, A.; Coumans, F.; Dignat-George, F.; Duggan, E.; Ghiran, I.; Giebel, B.; Görgens, A.; Hendrix, A.; Lacroix, R.; Lannigan, J.; Libregts, S. F. W. M.; Lozano-Andrés, E.; Morales-Kastresana, A.; Robert, S.; De Rond, L.; Tertel, T.; Tigges, J.; De Wever, O.; Yan, X.; Nieuwland, R.; Wauben, M. H. M.; Nolan, J. P.; Jones, J. C. MIFlowCyt-EV: A Framework for Standardized Reporting of Extracellular Vesicle Flow Cytometry Experiments. *J. Extracell. Vesicles* **2020**, *9* (1). https://doi.org/10.1080/20013078.2020.1713526.

(203) Hisada, Y.; Auriemma, A. C.; Alexander, W.; Ay, C.; Mackman, N. Detection of Tissue Factor-Positive Extracellular Vesicles by Laser Scanning Confocal Microscopy. *Thromb. Res.* **2017**, *150*, 65–72. https://doi.org/10.1016/j.thromres.2016.12.021.

(204) Durak-Kozica, M.; Baster, Z.; Kubat, K.; Stępień, E. 3D Visualization of Extracellular Vesicle Uptake by Endothelial Cells. *Cell. Mol. Biol. Lett.* **2018**, *23* (1), 1–9. https://doi.org/10.1186/s11658-018-0123-z.

(205) Arasu, U. T.; Härkönen, K.; Koistinen, A.; Rilla, K. Correlative Light and Electron Microscopy Is a Powerful Tool to Study Interactions of Extracellular Vesicles with Recipient Cells. *Exp. Cell Res.* **2019**, *376* (2), 149–158. https://doi.org/10.1016/j.yexcr.2019.02.004.

(206) He, F.; Ye, Z. Y.; Zhao, L. D.; Yin, B. C.; Ye, B. C. Probing Exosome Internalization Pathways through Confocal Microscopy Imaging. *Chem. Commun.* **2019**, *55* (93), 14015–14018. https://doi.org/10.1039/c9cc07491k.

(207) Santucci, L.; Bruschi, M.; Zotto, G. Del; Antonini, F.; Ghiggeri, G. M.; Panfoli, I.; Candiano, G. Biological Surface Properties in Extracellular Vesicles and Their Effect on Cargo Proteins. *Sci. Rep.* **2019**, *9* (1). https://doi.org/10.1038/s41598-019-47598-3.

(208) Vinduska, V.; Gallops, C. E.; O'connor, R.; Wang, Y.; Huang, X. Exosomal Surface Protein Detection with Quantum Dots and Immunomagnetic Capture for Cancer Detection. *Nanomaterials* **2021**, *11* (7). https://doi.org/10.3390/nano11071853.

(209) Xia, Y.; Chen, T.; Chen, G.; Weng, Y.; Zeng, L.; Liao, Y.; Chen, W.; Lan, J.; Zhang, J.; Chen, J. A Nature-Inspired Colorimetric and Fluorescent Dual-Modal Biosensor for Exosomes Detection. *Talanta* **2020**, *214*, 120851. https://doi.org/10.1016/j.talanta.2020.120851.

(210) Roda, A.; Mirasoli, M.; Michelini, E.; Di Fusco, M.; Zangheri, M.; Cevenini, L.; Roda, B.; Simoni, P. Progress in Chemical Luminescence-Based Biosensors: A Critical Review. *Biosens. Bioelectron.* **2016**, *76*, 164–179. https://doi.org/10.1016/J.BIOS.2015.06.017.

(211) Zacco, E.; Pividori, M. I.; Alegret, S.; Galve, R.; Marco, M. P. Electrochemical Magnetoimmunosensing Strategy for the Detection of Pesticides Residues. *Anal. Chem.* **2006**, *78* (6), 1780–1788. https://doi.org/10.1021/ac0512610.

(212) Pividori, M. I.; Alegret, S. Electrochemical Genosensing Based on Rigid Carbon Composites. A Review. *Anal. Lett.* **2005**, *38* (15), 2541–2565.

https://doi.org/10.1080/00032710500369745.

(213) Liébana, S.; Lermo, A.; Campoy, S.; Barbé, J.; Alegret, S.; Pividori, M. I. Magneto Immunoseparation of Pathogenic Bacteria and Electrochemical Magneto Genosensing of the Double-Tagged Amplicon. *Anal. Chem.* **2009**, *81* (14), 5812–5820. https://doi.org/10.1021/ac9007539.

(214) Lermo, A.; Campoy, S.; Barbé, J.; Hernández, S.; Alegret, S.; Pividori, M. I. In Situ DNA Amplification with Magnetic Primers for the Electrochemical Detection of Food Pathogens. *Biosens. Bioelectron.* **2007**, *22* (9–10), 2010–2017. https://doi.org/10.1016/j.bios.2006.08.048.

(215) Lermo, A.; Zacco, E.; Barak, J.; Delwiche, M.; Campoy, S.; Barbé, J.; Alegret, S.; Pividori, M. I. Towards Q-PCR of Pathogenic Bacteria with Improved Electrochemical Double-Tagged Genosensing Detection. *Biosens. Bioelectron.* **2008**, *23* (12), 1805–1811. https://doi.org/10.1016/j.bios.2008.02.020.

(216) Muriano, A.; Pinacho, D. G.; Chabottaux, V.; Diserens, J. M.; Granier, B.; Stead, S.; Sanchez Baeza, F.; Pividori, M. I.; Marco, M. P. A Portable Electrochemical Magnetoimmunosensor for Detection of Sulfonamide Antimicrobials in Honey Rapid Detection in Food and Feed. *Anal. Bioanal. Chem.* **2013**, *405* (24), 7885–7895. https://doi.org/10.1007/s00216-013-7219-0.

(217) Pinacho, D. G.; Sánchez-Baeza, F.; Pividori, M. I.; Marco, M. P. Electrochemical Detection of Fluoroquinolone Antibiotics in Milk Using a Magneto Immunosensor. *Sensors (Switzerland)* **2014**, *14* (9), 15965–15980. https://doi.org/10.3390/s140915965.

(218) Valera, E.; Muriano, A.; Pividori, I.; Sánchez-Baeza, F.; Marco, M. P. Development of a Coulombimetric Immunosensor Based on Specific Antibodies Labeled with CdS Nanoparticles for Sulfonamide Antibiotic Residues Analysis and Its Application to Honey Samples. *Biosens. Bioelectron.* **2013**, *43* (1), 211–217. https://doi.org/10.1016/J.BIOS.2012.12.017.

(219) Lermo, A.; Fabiano, S.; Hernández, S.; Galve, R.; Marco, M. P.; Alegret, S.; Pividori, M. I. Immunoassay for Folic Acid Detection in Vitamin-Fortified Milk Based on Electrochemical Magneto Sensors. *Biosens. Bioelectron.* **2009**, *24* (7), 2057–2063. https://doi.org/10.1016/j.bios.2008.10.020.

(220) Kergaravat, S. V.; Gómez, G. A.; Fabiano, S. N.; Laube Chávez, T. I.; Pividori, M. I.; Hernández, S. R. Biotin Determination in Food Supplements by an Electrochemical Magneto Biosensor. *Talanta* **2012**, *97*, 484–490. https://doi.org/10.1016/j.talanta.2012.05.003.

(221) Kergaravat, S. V.; Beltramino, L.; Garnero, N.; Trotta, L.; Wagener, M.; Isabel Pividori, M.; Hernandez, S. R. Electrochemical Magneto Immunosensor for the Detection of Anti-TG2 Antibody in Celiac Disease. *Biosens. Bioelectron.* **2013**, *48*, 203–209. https://doi.org/10.1016/j.bios.2013.04.012.

(222) Jeong, S.; Park, J.; Pathania, D.; Castro, C. M.; Weissleder, R.; Lee, H. Integrated Magneto-Electrochemical Sensor for Exosome Analysis. *ACS Nano* **2016**, *10* (2), 1802–1809. https://doi.org/10.1021/acsnano.5b07584.

(223) Park, J.; Park, J. S.; Huang, C. H.; Jo, A.; Cook, K.; Wang, R.; Lin, H. Y.; Van Deun, J.; Li, H.; Min, J.; Wang, L.; Yoon, G.; Carter, B. S.; Balaj, L.; Choi, G. S.; Castro, C. M.; Weissleder, R.; Lee, H. An Integrated Magneto-Electrochemical Device for the Rapid Profiling of Tumour Extracellular Vesicles from Blood Plasma. *Nat. Biomed. Eng.* **2021**, *5* (7), 678–689. https://doi.org/10.1038/s41551-021-00752-7.

(224) Kilic, T.; Cho, Y. K.; Jeong, N.; Shin, I. S.; Carter, B. S.; Balaj, L.; Weissleder, R.; Lee, H. Multielectrode Spectroscopy Enables Rapid and Sensitive Molecular Profiling of Extracellular Vesicles. *ACS Cent. Sci.* **2022**, *8* (1), 110–117. https://doi.org/10.1021/acscentsci.1c01193.

(225) Zhu, C.; Li, L.; Wang, Z.; Irfan, M.; Qu, F. Recent Advances of Aptasensors for Exosomes Detection. *Biosensors and Bioelectronics*. Elsevier July 15, 2020, p 112213. https://doi.org/10.1016/j.bios.2020.112213.

(226) Zhou, Q.; Rahimian, A.; Son, K.; Shin, D. S.; Patel, T.; Revzin, A. Development of an Aptasensor for Electrochemical Detection of Exosomes. *Methods* **2016**, *97*, 88–93. https://doi.org/10.1016/j.ymeth.2015.10.012.

(227) An, Y.; Jin, T.; Zhu, Y.; Zhang, F.; He, P. An Ultrasensitive Electrochemical Aptasensor

for the Determination of Tumor Exosomes Based on Click Chemistry. *Biosens. Bioelectron.* **2019**, *142*, 111503. https://doi.org/10.1016/J.BIOS.2019.111503.

(228) Xu, L.; Shoaie, N.; Jahanpeyma, F.; Zhao, J.; Azimzadeh, M.; Al−Jamal, K. T. Optical, Electrochemical and Electrical (Nano)Biosensors for Detection of Exosomes: A Comprehensive Overview. *Biosens. Bioelectron.* **2020**, *161*, 112222. https://doi.org/10.1016/j.bios.2020.112222.

(229) Cheng, N.; Du, D.; Wang, X.; Liu, D.; Xu, W.; Luo, Y.; Lin, Y. Recent Advances in Biosensors for Detecting Cancer-Derived Exosomes. *Trends Biotechnol.* **2019**, *37* (11), 1236–1254. https://doi.org/10.1016/j.tibtech.2019.04.008.

(230) Huang, X.; Yuan, T.; Tschannen, M.; Sun, Z.; Jacob, H.; Du, M.; Liang, M.; Dittmar, R. L.; Liu, Y.; Liang, M.; Kohli, M.; Thibodeau, S. N.; Boardman, L.; Wang, L. Characterization of Human Plasma-Derived Exosomal RNAs by Deep Sequencing. *BMC Genomics* **2013**, *14* (1), 319. https://doi.org/10.1186/1471-2164-14-319.

(231) Wang, L.; Li, Y.; Guan, X.; Zhao, J.; Shen, L.; Liu, J. Exosomal Double-Stranded DNA as a Biomarker for the Diagnosis and Preoperative Assessment of Pheochromocytoma and Paraganglioma. *Mol. Cancer* **2018**, *17* (1), 1–6. https://doi.org/10.1186/s12943-018-0876-z.

(232) Fernando, M. R.; Jiang, C.; Krzyzanowski, G. D.; Ryan, W. L. New Evidence That a Large Proportion of Human Blood Plasma Cell-Free DNA Is Localized in Exosomes. *PLoS One* **2017**, *12* (8), 1–15. https://doi.org/10.1371/journal.pone.0183915.

(233) Jeppesen, D. K.; Fenix, A. M.; Franklin, J. L.; Higginbotham, J. N.; Zhang, Q.; Zimmerman, L. J.; Liebler, D. C.; Ping, J.; Liu, Q.; Evans, R.; Fissell, W. H.; Patton, J. G.; Rome, L. H.; Burnette, D. T.; Coffey, R. J. Reassessment of Exosome Composition. *Cell* **2019**, *177* (2), 428-445.e18. https://doi.org/10.1016/j.cell.2019.02.029.

(234) Chevillet, J. R.; Kang, Q.; Ruf, I. K.; Briggs, H. A.; Vojtech, L. N.; Hughes, S. M.; Cheng, H. H.; Arroyo, J. D.; Meredith, E. K.; Gallichotte, E. N.; Pogosova-Agadjanyan, E. L.; Morrissey, C.; Stirewalt, D. L.; Hladik, F.; Yu, E. Y.; Higano, C. S.; Tewari, M. Quantitative and Stoichiometric Analysis of the MicroRNA Content of Exosomes. *Proc. Natl. Acad. Sci. U. S. A.* **2014**, *111* (41), 14888–14893. https://doi.org/10.1073/pnas.1408301111.

(235) Li, M.; Zeringer, E.; Barta, T.; Schageman, J.; Cheng, A.; Vlassov, A. V. Analysis of the RNA Content of the Exosomes Derived from Blood Serum and Urine and Its Potential as Biomarkers. *Philos. Trans. R. Soc. B Biol. Sci.* **2014**, *369* (1652). https://doi.org/10.1098/rstb.2013.0502.

(236) Mullis, K. B.; Faloona, F. A. Specific Synthesis of DNA in Vitro via a Polymerase-Catalyzed Chain Reaction. *Methods Enzymol.* **1987**, *155*, 335–350.

(237) Chen, C.; Ridzon, D. A.; Broomer, A. J.; Zhou, Z.; Lee, D. H.; Nguyen, J. T.; Barbisin, M.; Xu, N. L.; Mahuvakar, V. R.; Andersen, M. R.; Lao, K. Q.; Livak, K. J.; Guegler, K. J. Real-Time Quantification of MicroRNAs by Stem-Loop RT-PCR. *Nucleic Acids Res.* **2005**, *33* (20), e179–e179. https://doi.org/10.1093/nar/gni178.

(238) Balcells, I.; Cirera, S.; Busk, P. K. Specific and Sensitive Quantitative RT-PCR of MiRNAs with DNA Primers. *BMC Biotechnol.* **2011**, *11* (1), 70. https://doi.org/10.1186/1472-6750-11-70.

(239) Shen, Y.; Tian, F.; Chen, Z.; Li, R.; Ge, Q.; Lu, Z. Amplification-Based Method for MicroRNA Detection. *Biosensors and Bioelectronics*. 2015, pp 322–331. https://doi.org/10.1016/j.bios.2015.04.057.

(240) Metzker, M. L.; Caskey, C. T. Polymerase Chain Reaction (PCR). In *Encyclopedia of Life Sciences*; John Wiley & Sons, Ltd, 2009; pp 1051–1052. https://doi.org/10.1002/9780470015902.a0000998.pub2.

(241) Hannafon, B. N.; Trigoso, Y. D.; Calloway, C. L.; Zhao, Y. D.; Lum, D. H.; Welm, A. L.; Zhao, Z. J.; Blick, K. E.; Dooley, W. C.; Ding, W. Q. Plasma Exosome MicroRNAs Are Indicative of Breast Cancer. *Breast Cancer Res.* **2016**, *18* (1), 90. https://doi.org/10.1186/s13058-016-0753-x.

(242) Chen, W.; Cao, R.; Su, W.; Zhang, X.; Xu, Y.; Wang, P.; Gan, Z.; Xie, Y.; Li, H.; Qin, J. Simple and Fast Isolation of Circulating Exosomes with a Chitosan Modified Shuttle Flow Microchip for Breast Cancer Diagnosis. *Lab Chip* **2021**, *21* (9), 1759–1770. https://doi.org/10.1039/d0lc01311k.

(243) Wang, Z.; Zong, S.; Liu, Y.; Qian, Z.; Zhu, K.; Yang, Z.; Wang, Z.; Cui, Y. Simultaneous Detection of Multiple Exosomal MicroRNAs for Exosome Screening Based on Rolling Circle Amplification. *Nanotechnology* **2021**, *32* (8), 085504. https://doi.org/10.1088/1361-6528/abc7d4.

(244) Lin, Q.; Huang, Z.; Ye, X.; Yang, B.; Fang, X.; Liu, B.; Chen, H.; Kong, J. Lab in a Tube: Isolation, Extraction, and Isothermal Amplification Detection of Exosomal Long Noncoding RNA of Gastric Cancer. *Talanta* **2021**, *225*. https://doi.org/10.1016/j.talanta.2021.122090.

(245) Qian, J.; Zhang, Q.; Liu, M.; Wang, Y.; Lu, M. A Portable System for Isothermal Amplification and Detection of Exosomal MicroRNAs. *Biosens. Bioelectron.* **2022**, *196*, 956–5663. https://doi.org/10.1016/j.bios.2021.113707.

(246) Zhang, J.; Shi, J.; Zhang, H.; Zhu, Y.; Liu, W.; Zhang, K.; Zhang, Z. Localized Fluorescent Imaging of Multiple Proteins on Individual Extracellular Vesicles Using Rolling Circle Amplification for Cancer Diagnosis. *J. Extracell. Vesicles* **2020**, *10* (1). https://doi.org/10.1002/jev2.12025.

(247) Wu, D.; Yan, J.; Shen, X.; Sun, Y.; Thulin, M.; Cai, Y.; Wik, L.; Shen, Q.; Oelrich, J.; Qian, X.; Dubois, K. L.; Ronquist, K. G.; Nilsson, M.; Landegren, U.; Kamali-Moghaddam, M. Profiling Surface Proteins on Individual Exosomes Using a Proximity Barcoding Assay. *Nat. Commun.* **2019**, *10* (1), 1–10. https://doi.org/10.1038/s41467-019-11486-1.

(248) Qi, H.; Yue, S.; Bi, S.; Ding, C.; Song, W. Isothermal Exponential Amplification Techniques: From Basic Principles to Applications in Electrochemical Biosensors. *Biosens. Bioelectron.* **2018**, *110*, 207–217. https://doi.org/10.1016/J.BIOS.2018.03.065.

(249) Glökler, J.; Lim, T. S.; Ida, J.; Frohme, M. Isothermal Amplifications–a Comprehensive Review on Current Methods. *Critical Reviews in Biochemistry and Molecular Biology*. 2021, pp 543–586. https://doi.org/10.1080/10409238.2021.1937927.

(250) He, D.; Hai, L.; Wang, H.; Wu, R.; Li, H. W. Enzyme-Free Quantification of Exosomal MicroRNA by the Target-Triggered Assembly of the Polymer DNAzyme Nanostructure. *Analyst* **2018**, *143* (4), 813–816. https://doi.org/10.1039/c7an01691c.

(251) Wang, H.; He, D.; Wan, K.; Sheng, X.; Cheng, H.; Huang, J.; Zhou, X.; He, X.; Wang, K. In Situ Multiplex Detection of Serum Exosomal MicroRNAs Using an All-in-One Biosensor for Breast Cancer Diagnosis. *Analyst* **2020**, *145* (9), 3289–3296. https://doi.org/10.1039/d0an00393j.

(252) Kreimer, S.; Belov, A. M.; Ghiran, I.; Murthy, S. K.; Frank, D. A.; Ivanov, A. R. Mass-Spectrometry-Based Molecular Characterization of Extracellular Vesicles: Lipidomics and Proteomics. *J. Proteome Res.* **2015**, *14* (6), 2367–2384. https://doi.org/10.1021/pr501279t.

(253) Kowal, J.; Arras, G.; Colombo, M.; Jouve, M.; Morath, J. P.; Primdal-Bengtson, B.; Dingli, F.; Loew, D.; Tkach, M.; Théry, C. Proteomic Comparison Defines Novel Markers to Characterize Heterogeneous Populations of Extracellular Vesicle Subtypes. *Proc. Natl. Acad. Sci. U. S. A.* **2016**, *113* (8), E968–E977. https://doi.org/10.1073/pnas.1521230113.

(254) Larssen, P.; Wik, L.; Czarnewski, P.; Eldh, M.; Lof, L.; Goran Ronquist, K.; Dubois, L.; Freyhult, E.; Gallant, C. J.; Oelrich, J.; Larsson, A.; Ronquist, G.; Villablanca, E. J.; Landegren, U.; Gabrielsson, S.; Kamali-Moghaddam, M. Tracing Cellular Origin of Human Exosomes Using Multiplex Proximity Extension Assays. *Mol. Cell. Proteomics* **2017**, *16* (3), 502–511. https://doi.org/10.1074/mcp.M116.064725.

(255) Nanoview Biosciences. *Exoview R200 Automated exosome measurement*. https://www.nanoviewbio.com/products/exosome-detection/exoview-r200-automated-exosome-measurement (accessed 2022-04-12).

(256) Smolarz, M.; Widlak, P. Serum Exosomes and Their MiRNA Load — A Potential Biomarker of Lung Cancer. *Cancers (Basel).* **2021**, *13* (6), 1–20. https://doi.org/10.3390/cancers13061373.

(257) Yi, Y.; Wu, M.; Zeng, H.; Hu, W.; Zhao, C.; Xiong, M.; Lv, W.; Deng, P.; Zhang, Q.; Wu, Y. Tumor-Derived Exosomal Non-Coding RNAs: The Emerging Mechanisms and Potential Clinical Applications in Breast Cancer. *Front. Oncol.* **2021**, *11*, 1. https://doi.org/10.3389/fonc.2021.738945.

(258) Wu, H.; Wang, Q.; Zhong, H.; Li, L.; Zhang, Q.; Huang, Q.; Yu, Z. Differentially Expressed MicroRNAs in Exosomes of Patients with Breast Cancer Revealed by Next-Generation Sequencing. *Oncol. Rep.* **2020**, *43* (1), 240–250. https://doi.org/10.3892/or.2019.7401.

(259) Subedi, P.; Schneider, M.; Philipp, J.; Azimzadeh, O.; Metzger, F.; Moertl, S.; Atkinson, M. J.; Tapio, S. Comparison of Methods to Isolate Proteins from Extracellular Vesicles for Mass Spectrometry-Based Proteomic Analyses. *Anal. Biochem.* **2019**, *584* (August), 113390. https://doi.org/10.1016/j.ab.2019.113390.

(260) Quek, C.; Bellingham, S. A.; Jung, C. H.; Scicluna, B. J.; Shambrook, M. C.; Sharples, R. A.; Cheng, L.; Hill, A. F. Defining the Purity of Exosomes Required for Diagnostic Profiling of Small RNA Suitable for Biomarker Discovery. *RNA Biol.* **2017**, *14* (2), 245–258. https://doi.org/10.1080/15476286.2016.1270005.

(261) World Health Organization. *Global Action Plan for the Prevention and Control of NCDs 2013-2020*; 2013.

(262) Bernabé-Ortiz, A.; Zafra-Tanaka, J. H.; Moscoso-Porras, M.; Sampath, R.; Vetter, B.; Miranda, J. J.; Beran, D. Diagnostics and Monitoring Tools for Noncommunicable Diseases: A Missing Component in the Global Response. *Global. Health* **2021**, *17* (1), 6–10. https://doi.org/10.1186/s12992-021-00676-6.

(263) World Health Organization. *WHO Fact Sheet. Noncommunicable diseases*. https://www.who.int/news-room/fact-sheets/detail/noncommunicable-diseases (accessed 2022-04-21).

(264) Sung, H.; Ferlay, J.; Siegel, R. L.; Laversanne, M.; Soerjomataram, I.; Jemal, A.; Bray, F. Global Cancer Statistics 2020: GLOBOCAN Estimates of Incidence and Mortality Worldwide for 36 Cancers in 185 Countries. *CA. Cancer J. Clin.* **2021**, *71* (3), 209–249. https://doi.org/10.3322/caac.21660.

(265) Ferlay, J.; Ervik, M.; Lam, F.; Colombet, M.; Mery, L.; Piñeros, M.; Znaor, A.; Soerjomataram, I.; Bray, F. *Global Cancer Observatory: Cancer Today*. https://gco.iarc.fr/today (accessed 2022-04-21).

(266) Delorme, S.; Baumann, M. Oncology Imaging. In *Encyclopedia of Cancer*; Academic Press, 2018; pp 98–118. https://doi.org/10.1016/B978-0-12-801238-3.65427-2.

(267) Birnbaum, J. K.; Duggan, C.; Anderson, B. O.; Etzioni, R. Early Detection and Treatment Strategies for Breast Cancer in Low-Income and Upper Middle-Income Countries: A Modelling Study. *Lancet Glob. Heal.* **2018**, *6* (8), e885–e893. https://doi.org/10.1016/S2214-109X(18)30257-2.

(268) Yersal, O.; Barutca, S. Biological Subtypes of Breast Cancer: Prognostic and Therapeutic Implications. *World J. Clin. Oncol.* **2014**, *5* (3), 412–424. https://doi.org/10.5306/wjco.v5.i3.412.

(269) Racila, E.; Euhus, D.; Weiss, A. J.; Rao, C.; McConnell, J.; Terstappen, L. W. M. M.; Uhr, J. W. Detection and Characterization of Carcinoma Cells in the Blood. *Proc. Natl. Acad. Sci. U. S. A.* **1998**, *95* (8), 4589–4594. https://doi.org/10.1073/pnas.95.8.4589.

(270) Poudineh, M.; Sargent, E. H.; Pantel, K.; Kelley, S. O. Profiling Circulating Tumour Cells and Other Biomarkers of Invasive Cancers. *Nature Biomedical Engineering*. Nature Publishing Group February 6, 2018, pp 72–84. https://doi.org/10.1038/s41551-018-0190-5.

(271) Yu, D.; Li, Y.; Wang, M.; Gu, J.; Xu, W.; Cai, H.; Fang, X.; Zhang, X. Exosomes as a New Frontier of Cancer Liquid Biopsy. *Mol. Cancer* **2022**, *21* (1), 1–33. https://doi.org/10.1186/s12943-022-01509-9.

(272) Weng, J.; Xiang, X.; Ding, L.; Li, A.; Wong, -Ann; Zeng, Q.; Sethi, G.; Wang, L.; Lee, S. C.; Goh, B. C. Extracellular Vesicles, the Cornerstone of next-Generation Cancer Diagnosis? *Semin. Cancer Biol.* **2021**, *74*, 105–120. https://doi.org/10.1016/j.semcancer.2021.05.011.

(273) Land, K. J.; Boeras, D. I.; Chen, X. S.; Ramsay, A. R.; Peeling, R. W. REASSURED Diagnostics to Inform Disease Control Strategies, Strengthen Health Systems and Improve Patient Outcomes. *Nat. Microbiol.* **2019**, *4* (1), 46–54. https://doi.org/10.1038/S41564-018-0295-3.

(274) Yoshikawa, M.; Iinuma, H.; Umemoto, Y.; Yanagisawa, T.; Matsumoto, A.; Jinno, H. Exosome-Encapsulated MicroRNA-223-3p as a Minimally Invasive Biomarker for the Early Detection of Invasive Breast Cancer. *Oncol. Lett.* **2018**, *15* (6), 9584–9592. https://doi.org/10.3892/ol.2018.8457.

(275) Ando, W.; Kikuchi, K.; Uematsu, T.; Yokomori, H.; Takaki, T.; Sogabe, M.; Kohgo, Y.; Otori, K.; Ishikawa, S.; Okazaki, I. Novel Breast Cancer Screening: Combined Expression of MiR-21 and MMP-1 in Urinary Exosomes Detects 95% of Breast Cancer without Metastasis. *Sci. Rep.* **2019**, *9* (1), 13595. https://doi.org/10.1038/s41598-019-50084-5.

(276) Chen, Y.; Zhai, L. Y.; Zhang, L. M.; Ma, X. S.; Liu, Z.; Li, M. M.; Chen, J. X.; Duan, W. J. Breast Cancer Plasma Biopsy by: In Situ Determination of Exosomal MicroRNA-1246 with a Molecular Beacon. *Analyst* **2021**, *146* (7), 2264–2276. https://doi.org/10.1039/d0an02224a.

(277) Liu, C.; Xu, X.; Li, B.; Situ, B.; Pan, W.; Hu, Y.; An, T.; Yao, S.; Zheng, L. Single-Exosome-Counting Immunoassays for Cancer Diagnostics. *Nano Lett.* **2018**, *18* (7), 4226–4232. https://doi.org/10.1021/acs.nanolett.8b01184.

(278) Wang, X.; Zhong, W.; Bu, J.; Li, Y.; Li, R.; Nie, R.; Xiao, C.; Ma, K.; Huang, X.; Li, Y. Exosomal Protein CD82 as a Diagnostic Biomarker for Precision Medicine for Breast Cancer. *Mol. Carcinog.* **2019**, *58* (5), 674–685. https://doi.org/10.1002/mc.22960.

(279) Esposito, C. L.; Quintavalle, C.; Ingenito, F.; Rotoli, D.; Roscigno, G.; Nuzzo, S.; Thomas, R.; Catuogno, S.; de Franciscis, V.; Condorelli, G. Identification of a Novel RNA Aptamer That Selectively Targets Breast Cancer Exosomes. *Mol. Ther. - Nucleic Acids* **2021**, *23*, 982–994. https://doi.org/10.1016/j.omtn.2021.01.012.

(280) Cao, Y.; Wang, Y.; Yu, X.; Jiang, X.; Li, G.; Zhao, J. Identification of Programmed Death Ligand-1 Positive Exosomes in Breast Cancer Based on DNA Amplification-Responsive Metal-Organic Frameworks. *Biosens. Bioelectron.* **2020**, *166*, 112452. https://doi.org/10.1016/j.bios.2020.112452.

(281) An, Y.; Li, R.; Zhang, F.; He, P. Magneto-Mediated Electrochemical Sensor for Simultaneous Analysis of Breast Cancer Exosomal Proteins. *Anal. Chem.* **2020**, *92* (7), 5404–5410. https://doi.org/10.1021/acs.analchem.0c00106.

(282) Kashefi-Kheyrabadi, L.; Kim, J.; Chakravarty, S.; Park, S.; Gwak, H.; Kim, S. Il; Mohammadniaei, M.; Lee, M. H.; Hyun, K. A.; Jung, H. Il. Detachable Microfluidic Device Implemented with Electrochemical Aptasensor (DeMEA) for Sequential Analysis of Cancerous Exosomes. *Biosens. Bioelectron.* **2020**, *169*. https://doi.org/10.1016/j.bios.2020.112622.

(283) Tian, F.; Zhang, S.; Liu, C.; Han, Z.; Liu, Y.; Deng, J.; Li, Y.; Wu, X.; Cai, L.; Qin, L.; Chen, Q.; Yuan, Y.; Liu, Y.; Cong, Y.; Ding, B.; Jiang, Z.; Sun, J. Protein Analysis of Extracellular Vesicles to Monitor and Predict Therapeutic Response in Metastatic Breast Cancer. *Nat. Commun.* **2021**, *12* (1). https://doi.org/10.1038/s41467-021-22913-7.

(284) Zhao, J.; Liu, C.; Li, Y.; Ma, Y.; Deng, J.; Li, L.; Sun, J. Thermophoretic Detection of Exosomal MicroRNAs by Nanoflares. *J. Am. Chem. Soc.* **2020**, *142* (11), 4996–5001. https://doi.org/10.1021/jacs.9b13960.

Chapter 2. Objectives

2. Objectives

The development of new tools for the early diagnosis and monitoring is essential to reduce the burden of non-communicable diseases. Although high throughput methodologies are available in the market, the high cost and low accessibility difficult their implementation in primary health care centers in low- and middle-income countries. Thereby, the development and improvement of methods for low resource settings remains as central topic in bioanalytical chemistry research. In addition to the development of new, simpler, and less expensive instruments for diagnosis, the research of novel biomarkers in liquid biopsies is also very relevant. Among the different types of biomarkers, the study of exosomes as cell secreted vesicles, widely available in all biofluids, could provide direct information about physiological and pathological processes in the tissues. Therefore, exosomes have an enormous potentiality as diagnostic biomarkers. In this doctoral dissertation, the main objective is the design of bioanalytical methods for the qualitative and quantitative analysis of novel biomarkers based on the exosomes, focusing on breast cancer as model application.

Consequently, the **general objectives** of this dissertation were proposed as follows:

- To obtain breast cancer cells and derived exosomes from MCF7, SKBR3 and MDA-MB-231 cell lines, as model analytes for breast cancer diseases.
- To characterize the size distribution and morphology of exosomes by nanoparticle tracking analysis (NTA) and cryogenic transmission electron microscopy (Cryo-TEM).
- To characterize the surface protein markers of exosomes by flow cytometry and confocal microscopy as standard cell-oriented characterization methods.
- To stablish novel strategies for the isolation and preconcentration of exosomes based on solid phase separation and magnetic actuation with biologically-modified magnetic particles.
- To design and test diagnostic platforms for the rapid detection and quantification of exosomes.
- To stablish and test analytical strategies to improve the analytical performances of RDTs for exosomes, focusing on the increase of their analytical signals and the improvement of LODs.
- To conceptualize novel routes for the analytical simplification in the detection of exosomes in RDTs.

Chapter 3 addresses the development of novel bioanalytical strategies to increase the signal and the sensitivity for the detection of the exosomes, being the specific objectives as follows:

- To develop a biosensing approach for the detection and quantification of exosomes combining immunomagnetic separation (IMS) and double-tagging polymerase chain reaction (PCR).
    - ⇒ To design and test the IMS of MCF7 breast cancer cells and exosomes based on general and specific surface protein markers.
    - ⇒ To design and test the mRNA extraction of the cells and exosomes using oligo-modified magnetic particles.
    - ⇒ To optimize the experimental parameters of the double-tagging RT-PCR targeting GAPDH transcripts of MCF7 cells and exosomes.
    - ⇒ To assess the sensitivity and limit of detection of the proposed methodology with MCF7 cells and exosomes.
- To evaluate the analytical performance of the methods by analyzing human serum from breast cancer patients and healthy individuals.

Chapter 4 is focused on the conceptualization of novel routes for the analytical simplification for the detection of exosomes, being the specific objectives as follows:

- To design a novel a paper-based platform based on Vertical Flow Assay (VFA) for the analysis of exosomes relying on alkaline phosphatase (ALP) for the visual detection of exosomes.
    a. To design and construct a suitable VFA cartridge.
    b. To optimize the membranes and materials for the VFA.
    c. To test and optimize the blocking of the VFA nitrocellulose membrane.
- To develop an ELISA-like VFA-based immunoassay for the semi-quantitative determination of surface protein markers of exosomes derived from SKBR3 and MDA-MB-231 breast cancer cell lines.

Finally, **Chapter 5**, addresses the rational study of novel enzymatic biomarkers for the detection of the exosomes, being the specific objectives as follows:

- To investigate the presence and activity of aldehyde dehydrogenase (ALDH) enzymes in SKBR3, MDA-MB-231 and MCF7 breast cancer cells and exosomes as cancer related biomarkers.
    a. To evaluate the presence and activity of ALDH enzymes in breast cancer cells by flow cytometry and fluorometric assays.
    b. To design and optimize the detection of exosomes by nano-flow cytometry.
    c. To develop a fluorescence-based assay for the assessment of ALDH activity in exosomes using nano-flow cytometry.
- To evaluate the use of the intrinsic ALDH activity for the development of a new bioanalytical strategy based on fluorescence readout for the detection of exosomes

Chapter 3. Electrochemical genosensing of overexpressed GAPDH transcripts in breast cancer CTCs and exosomes

3. Electrochemical genosensing of overexpressed GAPDH transcripts in breast cancer CTCs and exosomes

3.1 Abstract

A rapid and sensitive method for the detection of breast cancer exosomes is reported. In this approach, the exosomes are preconcentrated from serum by immunomagnetic separation (IMS) based on CD326 expression as specific epithelial cancer-related biomarker and analyzed by the content of GAPDH transcripts. GAPDH is a key glycolytic enzyme and responsible for the dysregulation of glycolysis in cancer. Following the lysis of the captured exosomes, the released GAPDH transcripts are amplified by RT-PCR with a double-tagging set of primers on poly(dT) modified-MPs, to increase the sensitivity. The double-tagged amplicon is then quantified by electrochemical genosensing. The IMS/double-tagging RT-PCR/electrochemical genosensing approach is firstly demonstrated for the sensitive detection of exosomes derived from MCF7 breast cancer cells and compared with CTCs in terms of the analytical performance, showing a LOD of 4 x 10^2 exosomes μL^{-1}. The genosensor was applied to human samples by immunocapturing the exosomes directly from serum from breast cancer patients, showed a higher electrochemical signal (6.7-fold, $p < 0.05$), when compared with healthy controls, suggesting an overexpression of GAPDH on serum-derived exosomes from breast cancer patients. The detection of GAPDH transcripts is performed from only 1.0 mL of human serum using specific magnetic particles, improving the analytical simplification, and avoiding centrifugation steps, demonstrating to be a promising strategy for minimal invasive liquid biopsy.

Keywords: Exosomes, CTCs, GAPDH transcripts, EpCAM, Breast cancer, Electrochemical genosensor, immunomagnetic separation.

3.2 Introduction

Breast cancer is a highly lethal malignancy and most commonly diagnosed cancer among women, with an estimated over 2 million new cases in 2020[1]. Most of the currently available technologies for breast cancer diagnosis are based on imaging

techniques[2], such as X-ray imaging, positron-emission tomography, magnetic resonance imaging and multislice computed tomography, among many others. Although these techniques allow the precise location and sizing of the tumours, its high costs of acquisition and maintenance of the necessary equipment prevent medical centres on low-resource settings of being able to early diagnose.

At this point, the use of biomarkers related with breast cancer in liquid biopsies, that can simplify the equipment requirements and operational costs, while maintaining its high sensitivity, specificity, and accuracy, is very important for early identification of individuals with putative disease. In high-income countries, breast cancer are detected at stages I and II in 70% of women compared to 20-50% in low- and medium-income countries. Moreover, the time delay that exists between diagnosis and treatment is about 4 to 6 weeks in high-income countries but it can be 3 to 8 months in countries with low resources.[3]

The routine clinical diagnosis in liquid biopsies is based on ELISA methodologies for the quantitative analysis of biomarkers[4], existing many commercial kits targeting breast cancer related biomarkers (e.g. BRCA1 ELISA kit, from MBS; CA15-3 ELISA kit, from Abcam; or BCAR ELISA kit, from Biogen). Besides, other techniques aim for the detection of circulating tumour cells (CTCs)[5], considered one of the most significative breast cancer related biomarkers. CellSearch™ [6,7] is the first and the only CTCs-based assay commercially available approved by the US Food and Drug Administration (FDA). CellSearch™ enriches CTCs using magnetic particles containing antibodies against Epithelial Cell Adhesion Molecule (EpCAM) (also known as CD326). EpCAM is a cell-surface glycoprotein that is known to be highly expressed in epithelial carcinomas, including breast cancer and prostate[8]. However, the clinical use of CTCs is limited by their scarcity in the peripheral blood (1 CTC / $10^{5–6}$ blood cells)[9].

Exosomes[10] are nano-sized (30-200 nm in diameter) extracellular vesicles that received highlighted attention as new biomarkers for the detection of cancer in early-stages, since their relation with intercellular communication mechanisms and increased in cancer cells[11]. Exosomes have their biogenesis arise from intraluminal vesicles (ILVs) formed in the endosomal membrane during maturation of multivesicular endosomes (MVEs)[12], which turns into an intercellular shuttle-like vesicles with molecular cargo as mRNA, microRNA, DNA, lipids and proteins[13]. Most cell types, including normal and tumour cells release exosomes in many different biological fluids as blood, plasma, serum, or urine, among others[13]. It is known that a single cell is able to release many exosomes per hour into the extracellular space[14], at increased rate by tumor cells. The

high number of exosomes that can be release by a single tumor cell reveals the strong potential application of exosomes as an alternative biomarker for early diagnostics, overcoming the most challenging limitation that present CTCs assays: their very low concentration in blood. Exosomes can potentially be used to detect the presence of tumour cells and deposits in the early stage of growth with a simple and minimally invasive procedure as a liquid biopsy.

In this work, it is proposed an electrochemical genosensor for the detection glyceraldehyde-3-phosphate dehydrogenase (GAPDH) gene transcripts in breast cancer cells and exosomes derived human serum from healthy donors and breast cancer patients. The approach is based on immunomagnetic separation of the exosomes using CD326 cancer-related biomarker, followed by amplification by double-tagging reverse transcription PCR of the GAPDH transcripts on poly(dT)-MPs, and electrochemical genosensing using streptavidin-MPs as a support. This approach is firstly optimized and tested with breast cancer cell line MCF7 cells and exosomes.

The electrochemical genosensing approach allows the quantitative measurement of transcripts with high sensitivity, robustness and simplicity. It has been widely used in our group[15], especially for the detection of DNA amplicons from double-tagging PCR[16,17] and quadruple-tagging multiplex PCR[18,19] . To the best of the authors' knowledge, this is the first study on expression of GAPDH gene in MCF7 breast cancer cell line and from serum-derived exosomes from breast cancer patients. Here, the double-tagging PCR and electrochemical genosensing of the GAPDH transcript is performed from only 1.0 mL of human serum without ultracentrifugation steps, using CD326 modified magnetic particles to specifically capture breast cancer related, improving the analytical simplification and specificity. Finally, although further clinical validation should be performed with a higher number of samples, the significative increase of the GAPDH transcript content in exosomes from patients compared to healthy individuals envisages its role as a putative biomarker for breast cancer diagnostics.

3.3 Experimental

3.3.1 Instrumentation

Nanoparticle tracking analysis (NTA) was performed using the NanoSight LM10-HS system (NanoSight Ltd, Malvern, GB). The cryogenic transmission electron microscopy (TEM) images were collected by a Jeol JEM 2011 (JEOL USA Inc., MA, US) microscope. Flow cytometry was performed using BD FACSCANTO II (BD Biosciences,

NJ, US) equipment. Mean Fluorescence Intensity (MFI) and beads count data were obtained by FlowJo analysis software (FlowJo LLC, BD Biosciences) of every sample-reading file. The confocal images were collected on the microscope Leica, TCS SP5 (Leica Microsystems, DE). SimpliAmp Thermal Cycler (Applied Biosystems, US) was used for the double-tagging RT-PCR amplification. All electrochemical experiments were performed using an Autolab PGSTAT10 (Metrohm AG, CH) potentiostat/galvanostat electrochemical analyzer. A magneto-actuated graphite-epoxy composite (m-GEC) electrode as working electrode (geometric area = 0.5 cm^2), $Ag/AgCl/KCl_{(sat.)}$ as reference electrode, a disc platinum counter electrode (geometric area = 3.0 cm^2) and a standard 500-µL one compartment three-electrode cell was used in all experiments.

3.3.2 Chemicals and biochemicals

Tosylactivated magnetic particles (MPs) (Dynabeads M450 Tosylactivated, ref. 14013), MPs modified with EpCAM antibody (antiCD326-MPs, Dynabeads Epithelial Enrich, ref. 16102), MPs modified with poly(dT) (polydT-MPs, Dynabeads Oligo(dT)25, ref. 61002), MPs modified with streptavidin (strep-MPs, Dynabeads MyOne Streptavidin T1, ref. 65601), mouse monoclonal antibody antiCD81 (ref. 10630D), and BCA protein assay kit (ref. 23225) were purchased from Thermo Fisher Scientific (MA, US). Mouse monoclonal antibody antiCD326, or EpCAM (ref. ab7504) and a goat anti-mouse IgG H&L (Cy5®) (antimouse-Cy5, ref. ab97037) were purchased from Abcam (Cambridge, GB). Antidigoxigenin-horseradish peroxidase Fab fragments (antiDIG-HRP, ref. 11207733910) was purchased from Roche Diagnostics (Basel, CH).

The primers for the double-tagging PCR were selected for the specific amplification of GAPDH (glyceraldehyde 3-phosphate dehydrogenase) and were purchased from Sigma-Aldrich (Merck KGaA, DE). The sequence for the digoxigenin-modified forward primer (DIG-Fw) was 5'-[DIG] CTTCTTTTGCGTCGCCAG; while the sequence for the biotin-modified reverse primer (BIO-Rev) was 5'-[BIO] AGCCCCSGCCTTCTCCA. All solutions, described in §3.6.1 (Supp. Data), were prepared with Ultrapure water (Millipore® System, resistivity 18.2 MΩ cm) and solutions used in RNA preparation were RNase-free by treatment with 0.1% DEPC.

3.3.3 Cell culturing, exosome isolation and purification from MCF7 cell line

The exosomes were obtained from MCF7 cell line (ATCC, ref. HTB-22), and the culture conditions are detailed in §3.6.2 (Supp. Data). The MCF7 cells were used as a model of breast cancer. The exosomes were purified from culture supernatant by differential ultracentrifugation according to *Théry et al.*[20] with minor changes. Exosomes

were resuspended in Tris 1x buffer (pH 7.4, 0.22 µm sterile-filtered) and stored at -80°C. All the experimental data are provided in §3.6.2 (Supp. Data).

3.3.4 Characterization of the exosomes derived from MCF7 breast cancer cell line

The size distribution and concentration of exosomes were measured by nanoparticle tracking analysis (NTA). The morphology was analyzed by the cryogenic transmission electron microscopy (Cryo-TEM). And the total protein concentration of exosomes samples was estimated by BCA protein assay kit (Pierce BCA protein assay kit, ref. 23227, Thermo Fisher Scientific).

To set up the technical approach, the expression study of CD81, a tetraspanin general marker for exosomes, and CD326, a cancer-related epithelial receptor, on the MCF7 cell line and their derived exosomes was carried out by flow cytometry. In the case of the cells, the indirect labeling was performed by incubation of specific antibodies antiCD81 and antiCD326, followed by labeling with antimouse-Cy5 antibody (a far-red-fluorescent dye, excitation 647 nm, emission 665 nm). The labeled cells were resuspended in Tris 1x buffer solution containing 0.5 % BSA solution.

In order to compare the expression on the exosomes, the same procedure of labeling was performed, but in this case, the exosomes were firstly immobilized on the surface of MPs due to their size and resolution of the technique. To achieve that, exosomes were covalently immobilized on tosylactivated MPs, as detailed in the §3.6.3 and Figure 3.5, panel A (Supp. Data). Then, the indirect labeling was performed firstly incubating with antiCD81 or antiCD326, followed by incubation with antimouse-Cy5 antibody. In parallel, the same batch of cells and exosomes analyzed by flow cytometry were subjected to confocal microscopy imaging for the study of the binding pattern of antibodies. In the case of cells, nuclear DNA was stained with Hoechst dye (a blue-fluorescent dye, emission wavelength 490 nm) before labeling with antibodies. Further experimental details and incubations are described in §3.6.4 (Supp. Data).

3.3.5 Immunomagnetic separation, double-tagging reverse transcription PCR of GAPDH transcripts and electrochemical genosensing

The procedure was evaluated on cells and exosomes derived from MCF7 breast cancer cell line as a model. Briefly, it consists of: i) Immunomagnetic separation of the cells/exosomes, ii) double-tagging reverse transcription PCR of GAPDH transcripts and iii) electrochemical genosensing. After the optimization, the approach was used for the evaluation of exosomes in undiluted human serum from breast cancer individuals.

This approach sequentially combines three different types of magnetic separations, as depicted in Figure 3.1. Firstly, the method involves the cells or exosome preconcentration based on the specific separation with magnetic particles modified with antiCDX antibody (being CDX either CD81 or CD326; Fig. 3.1, panel A1). Then, they were lysed and, the released messenger RNAs (Fig. 3.1, panel A2) were captured by polydT-MPs based on the poly(A) tail followed by reverse transcription to obtain cDNA (Fig. 3.1, panel B1). After that, the cDNA was amplified by double-tagging PCR on the magnetic beads (Fig. 3.1, panel B2), using a double-tagging set of primers specific for GAPDH. During PCR, the cDNA is not only amplified but also labeled at the same time with biotin/digoxigenin (BIO/DIG) tags. Finally, the electrochemical magneto-genosensing was performed on streptavidin-magnetic particles as a support, based on the BIO tag through biotin-streptavidin interaction. The DIG tag was used for labeling with antiDIG-HRP conjugate. The electrochemical readout of the double-tagged amplicons was based on peroxidase (HRP) enzyme as electrochemical reporter and performed on m-GEC electrodes, as previously reported[18] (Fig. 3.1, panel C). The experimental details are described in the next sections, and further detailed in §3.6.5 (Supp. Data).

A. Immunomagnetic separation of the cells and exosomes

100 µL of cells or exosomes (at different concentration ranging from 50 to 5.000 cells mL^{-1}, or 10^4 to 10^6 exosomes μL^{-1}) were incubated with $1 \cdot 10^6$ antiCDX-MPs (being CDX either CD81 or CD326) for 30 min at 25 °C while shaking, followed by washing with Tris 1x buffer containing 0.5% BSA. The content of the preconcentrated cells or exosomes on antiCDX-MPs was released by resuspending them on 1 mL of Lysis/Binding buffer, and disrupted using a syringe.

B. Double-tagging RT-PCR on magnetic beads

The mRNA extraction and purification on polydT-MPs based on the polyA tail of the transcripts was performed, followed by reverse transcription on polydT-MPs (Fig. 3.1, panel B1). The lysate was incubated with 15 µL of polydT-MPs (75 µg, equivalent to $7.5 \cdot 10^7$ MPs) for 15 min under gentle shaking at 25 ºC, washed three times and stored on ice. In order to obtain the cDNA, the retrotranscription (RT) was carried out on poly(dT)-MPs with Moloney Murine Leukemia Virus (M-MLV) reverse transcriptase. The RNA-poly(dT)-MPs were incubated with 10 nmol of dNTPs mix for 5 min at 65 ºC and cooled on ice for 1 min. After that, a mix containing 200 nmol of DTT, 40 U of RNaseOUT inhibitor and 1x First Strand Buffer was added and incubated at 37 ºC for 2 min. Finally, 200 U of M-MLV reverse transcriptase were added and incubated for 50 min at 37 ºC,

and 15 min at 70 ºC for inactivating the reaction. The cDNA was stored at -21ºC until use.

The double-tagging polymerase chain reaction (PCR) was performed in 15 µL of reaction mixture containing the cDNA (Fig. 3.1, panel B2). Each reaction mixture contained 7.5 pmol of each primer (DIG-Fw and BIO-Rev), 3.75 nmol of each dNTPs and 3U of Taq polymerase. The reaction was carried out in a buffer with 7.5 mmol L^{-1} Tris buffer (pH 9.0), 5.0 mmol L^{-1} KCl, 2.0 mmol L^{-1} $(NH_4)_2SO_4$ and 0.2 mmol L^{-1} $MgCl_2$ as a cofactor of the enzyme. The reaction mixture was exposed to an initial step at 95 °C for 3 min followed by 32 cycles of 95 °C for 30 s, 61 °C for 30 s, 72 °C for 30 s, and a last step of 7 min at 72 °C. Negative controls for both the RT and PCR were performed as above except adding mRNA or cDNA, respectively.

The performance of the double-tagging RT-PCR amplification was checked with 2 % agarose gel electrophoresis in TAE buffer containing 1×GelRed dye. The DNA bands were visualized by UV transillumination. A single DNA band was obtained in all samples sized around 371 bp. To confirm that GAPDH was amplified, all bands were cut from the gel and purified with GeneJET kit and DNA sequencing was performed.

3.3.6 RNA integrity analysis and DNA sequencing

For the integrity analysis, the RNA from breast cancer cells and exosomes was extracted using the Total Exosome RNA and protein isolation kit (Thermo Fisher Scientific, ref. 4478545), and analyzed with Agilent RNA 6000 Nano Kit (ref. 5067-1511, Agilent) by Genomics Bioinformatics Service (Institute of Biotechnology and Biomedicine, UAB, ES). The DNA sequences of the PCR amplicons were obtained with ABI Prism 3130XL Genetic Analyzer by the same GBS and were analyzed using Chromas v 2.6.6 (Technelysium Pty Ltd, Brisbane, QLD, AU) and Clustal Omega[21] software to check the chromatograms and the alignment of both sequences.

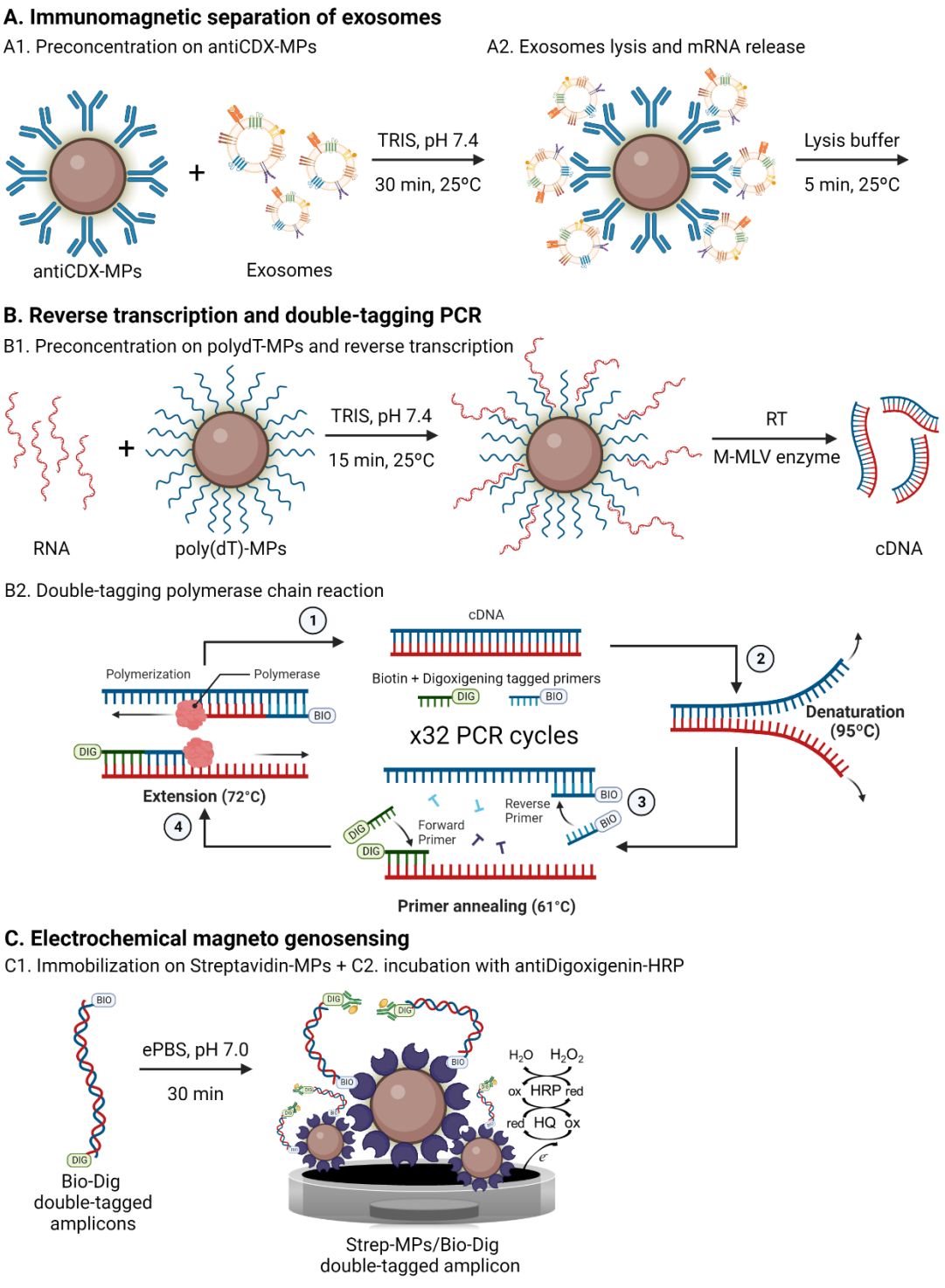

Figure 3.1. Schematic representation for the detection of GAPDH expression by immunomagnetic separation of exosomes (panel A1) and lysis (panel A2); mRNA extraction with poly(dT)-MPs and reverse transcription (panel B1), and double-tagging PCR (panel B2); and electrochemical magneto genosensing with amperometric readout (panel C). Created with BioRender.com.

3.3.7 Electrochemical magneto-genosensing

Briefly, after the double-tagging RT-PCR, the BIO-tag was used for the immobilization of the amplicons on streptavidin-magnetic particles through the high affinity biotin-streptavidin interaction, while the DIG tag allowed the labeling by the antiDIG-HRP, in one 15-min step. The procedure comprised, as described in Fig. 3.1, panel C: (a) the immobilization and preconcentration of the tagged amplicons on 7×10^7 strep-MPs and (b) the incubation with the electrochemical reporters in one step for 15 min at RT, with 10 µL (130 mU) of antiDIG-HRP. Two washing steps with 500 µL of Tris 1x buffer for 2 min at RT were performed. After incubation or washing step, a magnetic separator was positioned under the tubes until pellet formation on the tube side wall, followed by supernatant separation; (c) magnetic actuation on the m-GEC; and (d) amperometric readout using applying a potential of -100 mV (vs. $Ag/AgCl_{sat.}$), under enzyme saturation conditions in ePBS buffer, upon the addition of hydroquinone and hydrogen peroxide. All experimental steps are described in detail in §3.6.5 (Supp. Data). The steady-state cathodic amperometric current (I_{cat}, in µA) was used for the electrochemical signal plotted in all the figures. Different parameters of the electrochemical genosensing, such as the washing step time, the incubation time with the electrochemical reporter, the concentration of strep-MPs and the electrochemical reporter, and finally the procedure in one or two steps for the electrochemical genosensing were previously optimized by our group[18].

3.3.8 Electrochemical magneto-genosensing of transcripts from exosomes of breast cancer patients

Blood samples from healthy donors (n = 10, 5 men and 5 women, mean age 30/ SD=5) and breast cancer donors (n = 10, stage IV, all women, mean age 50/SD=6) were obtained from the Hospital del Mar (Barcelona, ES). The work was carried out in accordance with the principles of voluntariness and confidentiality.

In this instance, the IMS of the exosomes from 1 mL undiluted human serum (healthy and breast cancer patients) was directly performed on magnetic particles modified with the epithelial biomarker CD326 (antiCD326-MPs). The IMS involved the following steps: i) IMS of the exosomes with antiCD326-MPs (containing 2×10^6 MPs per tube), and 1.0 mL of human serum, were simultaneously incubated for 30 min with gentle shaking at 25°C, followed by washing with Tris 1x buffer containing 0.5% BSA. Then, the exosome-coated antiC326-MPs were resuspended with 100 µL of Tris 1x buffer, stored on ice and immediately used for RNA extraction. All further steps were performed as described in Experimental section, including double-tagging reverse

transcription PCR of GAPDH transcripts and electrochemical genosensing. The complete assays protocols, as well as the preparation of the human serum from blood, are provided in §3.6.7.

3.3.9 Statistical analysis

The statistical analyses and calculations were performed using GraphPad Prism 8 (San Diego, CA, US) while plots were represented using Origin Pro 2017 (Northampton, MA, US).

3.3.10 Safety considerations

All works were performed in a biosafety cabinet, and all material decontaminated by autoclaving or disinfected before discarding in accordance with U.S. Department of Health and Human Services guidelines for level 2 laboratory Biosafety.[22]

3.4 Results and discussion

3.4.1 Characterization of the exosomes derived from MCF7 breast cancer cell line

An estimation of the size diameter distribution and concentration of purified exosomes derived from MCF7 breast cancer cell line was performed by nanoparticle tracking analysis (NTA). Figure 3.2, panel A, shows that the size diameter distribution of exosomes ranges from 30 up to 210 nm, which is represented by exosomes with 90, 120, 150 and 195 nm in diameter, in accordance with the expected size range for exosomes[23] . Further information of size diameter distribution was obtained by Cryo-TEM. Micrographs of exosomes sample shows well-shape exosomal vesicles with closed circular lipid bilayers (Fig. 3.2, panel B) with around 110 nm in diameter. Cryo-TEM micrographs also reveal the presence of some exosome aggregates.

Confocal microscopy demonstrated qualitatively that the CD81 and CD326 membrane receptors are well-expressed in the MCF7 breast cancer cell line (Fig. 3.2, panel C(i)), as well as their expression on MCF7-derived exosomes covalently immobilized on magnetic particles (Fig. 3.2, panel C(ii)). The intense green color of the magnetic particles was due to autofluorescence around 580 nm [24]. Negligible nonspecific adsorption was observed (Fig. 3.2, panel C(ii), negative). The CD81 tetraspanin was also shown with strong labeling in exosomes, although a poor labelling pattern was achieved for CD326 biomarker.

Quantitative pattern of MCF7 cell line was also studied by flow cytometry analyzing the expression to CD81 and CD326, as shown in Figure 3.2, panel D. The

negative control which the signal appears onto the left side confirm that there a negligible (<0.1%) nonspecific reaction with the secondary antibody (antiMouse Cy5 secondary antibody) with the MCF7 cells (Fig. 3.2, panel D(i), blue histogram). As expected, the percentage marker expression to CD81 and CD326 biomarkers are high as >95% for MCF7 cells (Fig. 3.2, panel D(i), red and green histograms). The same CD81 and CD326 biomarkers on exosomes derived from MCF7 breast cancer cell line were also studied by flow cytometry. As expected, exosomes covalently immobilized on magnetic particles (exosomes-MPs) highly expressed CD81, but CD326 showed a low expression pattern with this model (<5%) (Fig. 3.2, panel D(ii), red and green histograms), according with the results obtained by confocal microscopy. Tetraspanins are the most frequently identified proteins in exosomes and are considered classical markers. Comparing the expression levels of cells and their derived exosomes, and according to many studies[25–27], cell-membrane biomarkers are not always identically expressed in the cells as well as in their derived exosomes. This data suggests that the exosomal molecular profile needs to be carefully assessed to achieve a better experimental approach design.

Regarding the genetic material in MCF7 cells and exosomes, it was characterized by RNA integrity analysis, obtaining significatively different patterns, as shown in §3.6.6 (Supp. Data).

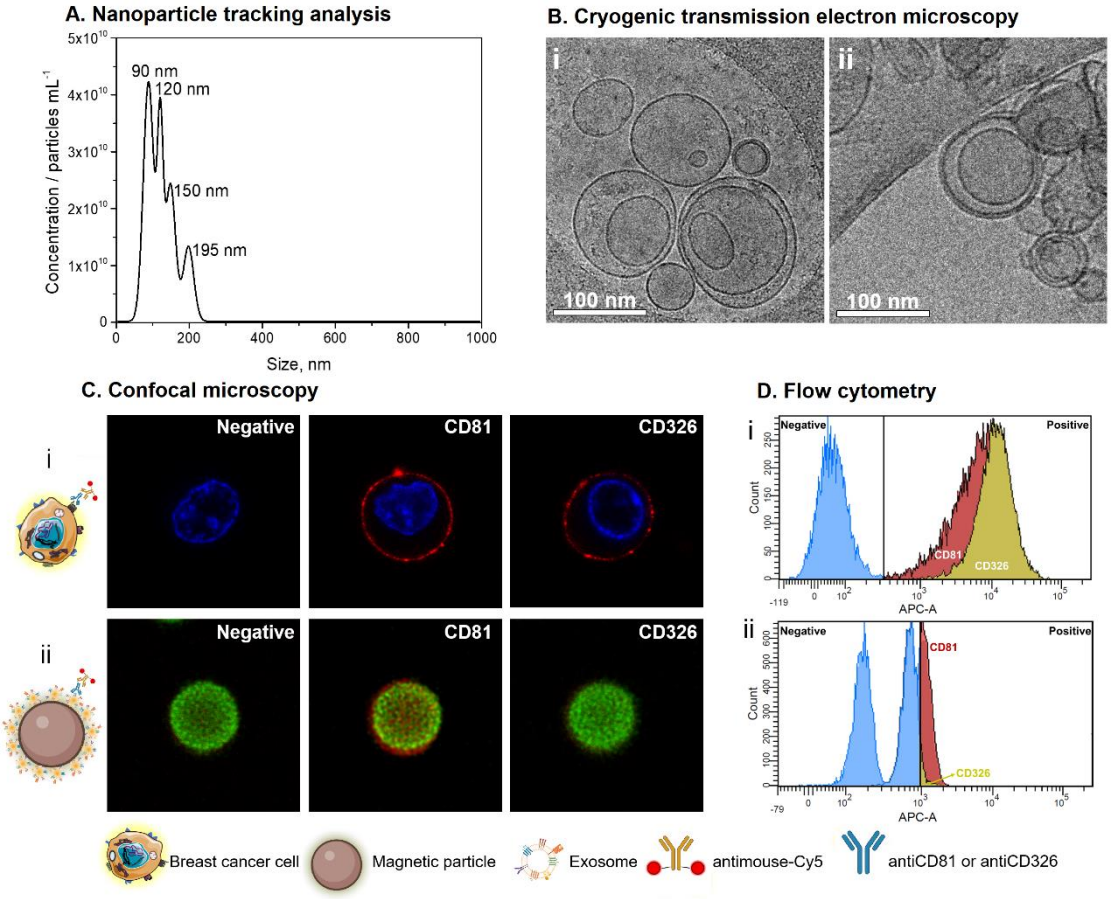

Figure 3.2. A) Characterization by NTA of purified exosomes derived from MCF7 breast cancer cell line. (B) Cryo-TEM images (i) and (ii) of purified exosomes at an acceleration voltage of 200 kV. (C) Confocal microscopy images and (D) flow cytometry study for (i) MCF7 breast cancer cell line and (ii) their exosomes covalently immobilized on MPs. For confocal microscopy, DNA appears in blue color, magnetic particles in green color, while the exosomal protein membrane in red color. For flow cytometry, the negative control onto the stained-blue regions on the left side and stained red or green dark regions on the right side for a positive relative expression of membrane protein markers.

3.4.2 Immunomagnetic separation, double-tagging reverse transcription PCR of GAPDH transcripts and electrochemical genosensing

Firstly, all steps from the proposed IMS/ double-tagging RT-PCR/ electrochemical genosensing detection method were tested and optimized with MCF7 cells and purified exosomes, as described in §3.6.5 (Supp. Data). The DNA sequences of the PCR amplicons were also obtained. The genome sequence for *Homo sapiens* mRNA GAPDH transcript was identified by using BLAST software[28]. Further details are provided in §3.6.6 and Figure 3.7 (Supp. Data).

The calibration plots for the detection of GAPDH transcripts from MCF7 cells and its derived exosomes are comparatively shown in Figure 3.3. Two different immunomagnetic separation (IMS) approaches were tested. Firstly, IMS of MCF7 cells by using antiCDX-MPs (where CDX being any of CD81 or CD326 biomarkers); followed

by the double-tagging RT-PCR and electrochemical genosensing. Thus, different concentrations of MCF7 cells ranging from 50 to 5,000 cells mL^{-1} were evaluated for the calibration plot. The electrochemical responses were fitted using nonlinear regression (four parameter logistic equation, GraphPad prism software) (Fig. 3.3, panel A). The limit of detection (LOD) of 45 cells mL^{-1} (r^2 = 0.996) and 67 cells mL^{-1} (r^2 = 0.998) was reached for cells immunocaptured by using CD81 and CD326 biomarkers, respectively. Although the strategy was able to clearly detect cells by GAPDH transcript amplification, improved analytical simplification, this LOD values are not suitable for application in breast cancer diagnosis, since the clinical CTC count assay approved by the U.S Food and Drug Administration (FDA), must be smaller than 5 cells per 7.5 mL^{-1} [7]. At this point, considering the performance of the proposed genosensor, the study was further focused on cancer-related exosomes. These extracellular vesicles are considered as new biomarker for the detection of cancer in early-stages, since it is related to cell-to-cell communication and increased in cancer cells.[11,29]

The IMS of exosomes (ranged from 100 to 4.0 x 10^4 exosomes μL^{-1}) derived from MCF7 cell line was performed on antiCD81-MPs and/or antiCD326-MPs followed by the double-tagging RT-PCR for the specific GAPDH transcripts on poly(dT)-MPs, and subsequent electrochemical genosensing. The electrochemical responses were fitted using nonlinear regression (four parameter logistic equation, GraphPad prism software) (Fig. 3.3, panel B). The LOD of 415 exosomes μL^{-1} (r^2 = 0.991) and 1225 exosomes μL^{-1} (r^2 = 0.98) were reached using CD81 and CD326 biomarkers, respectively. IMS of exosomes improve analytical simplification, avoiding ultracentrifugation or other separation steps and have the advantage of a specific capture of exosomes by epithelial breast cancer biomarker, which is currently used in most of the CTCs-enrichment methods such as CellSearch[7]. Since the number of exosomes in biological fluids ranges from 1×10^1 to 3×10^7 exosomes μL^{-1} [30], the LOD for double-tagging RT-PCR based on GAPDH transcripts coupled with electrochemical genosensing was feasible and reliable to detect and quantify cancer-related exosomes. In this approach, the exosomes are specifically isolated and preconcentrated by IMS, while the double-tagging RT-PCR are used as strategy to amplify the signal and thus to improve the LOD by and order of 2. For this reason, a common and ubiquitous transcript based on GAPDH was selected to achieve this goal. The LOD is improved by a factor of 2 (from 1 x 10^5 to 4 x 10^2 exosomes μL^{-1})[31,32] by including the double-tagging RT-PCR, in which the both the target and signal amplification is achieved[33] , instead of using a second labelled antibody in a sandwich immunosensing format[27,31] or the intrinsic enzyme activity in exosomes[32]. The main

shortcoming is that in this approach, the unique source of specific is provided by the antibody on the MPs during the IMS.

The LOD obtained in this work was better in analytical performance than fluorescence[34], electrochemical[35] and Surface-enhanced Raman scattering[36] devices, and comparable to other reported approaches, such as rolling circle amplification[37] and microfluidic graphene oxide-based[30] detection.

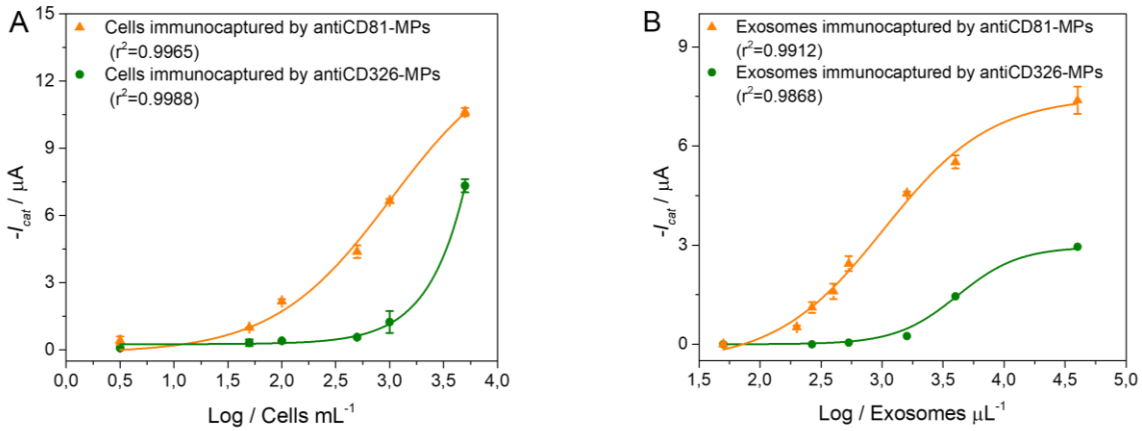

Figure 3.3. Electrochemical genosensing of GAPDH transcripts from (A) MCF7 cells ranging from 50 to 5,000 cells mL^{-1} and (B) their exosomes ranging from 100 to 4.0 x 10^4 exosomes µL^{-1}, according to NTA counting. In all cases, the cells and exosomes were lysed preconcentrated by IMS using antiCD81-MPs and antiCD326-MPs, followed by double-tagging RT-PCR on poly(dT)-MPs. The error bars show the standard deviation for n = 3.

3.4.3 Electrochemical magneto-genosensing of transcripts from exosomes of breast cancer patients

The performance of the double-tagging RT-PCR on magnetic beads and electrochemical genosensing was evaluated in serum-derived exosomes from healthy and breast cancer patients. The procedure and the results are depicted in Figure 3.4. All experimental parameters are described in §3.6.7 (Supp. Data).

Firstly, the GAPDH expression was evaluated in purified exosomes (without preconcentration on MPs) derived from healthy controls and breast cancer patients (Fig. 3.4, panel A), normalized per micrograms of exosomes (BCA protein assay results are detailed in §3.6.7). In this approach, the specific IMS and as such, the positive selection of CD326 exosomes (Fig. 3.4, panel B) was replaced by a not specific physical isolation (ultracentrifugation at 100,000 x *g*). In this case, the approach is based on amplification and detection through non-specific GAPDH biomarker. Then, the double-tagging RT-PCR for the specific GAPDH transcripts on poly(dT)-MPs was performed using 0.33 µg

per assay of serum-derived exosomes from both groups of samples, followed by subsequent electrochemical genosensing detection. The results of this analysis are shown in Figure 3.4, panel A. The results suggested that breast cancer patients overexpress GAPDH in total exosomes (6.7-fold, $p < 0.05$) and can be well discriminated from healthy individuals.

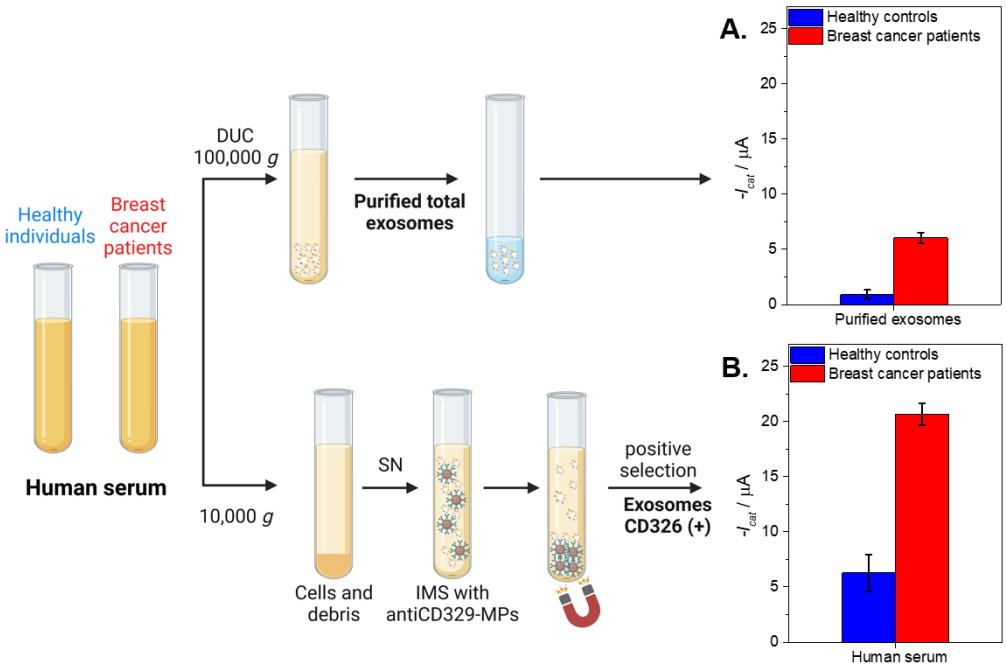

Figure 3.4. Panel A. Electrochemical genosensing of CD326+ exosomes from 1 mL of cell-free undiluted human serum (centrifuged at 10,000 x g) based on immunomagnetic separation with antiCD326-MP and further GAPDH transcripts detection. The whole procedure is also shown in Figure 3.1. Panel B shows the control of the purified total exosome population obtained by ultracentrifugation (100,000 x g) normalized according to protein content (0.33 µg per assay). In all cases, serum-derived exosomes from healthy controls (n = 10, pooled) and breast cancer (n = 10, pooled) patients were processed. The error bars show the standard deviation for n = 3.

Next, in order to achieve the analytical simplification, IMS of exosomes directly from undiluted human serum by using antiCD326-MPs was performed, followed by RNA extraction and PCR on poly(dT)-MPs of primer specific for GAPDH transcript labeled with DIG/BIO tags, and subsequent electrochemical genosensing. In this case, the approach is based on specific capture of exosomes by CD326 epithelial cancer-related biomarker, and further detection through non-specific GAPDH mRNA biomarker. The electrochemical genosensor is performed in 1 mL of undiluted human serum only pretreated by a short centrifugation pulse at 10,000 x *g* (to eliminate any remaining cells or particulate debris), followed by IMS with antiCD326-MP and electrochemical magneto-genosensing, as depicted in Figure 3.1. The results are presented in Figure 3.4, panel B. Notably, a significative overexpression (3.3-fold, $p<0.05$) of GAPDH on the

immunocaptured CD326 positive exosomes in breast cancer samples when compared with serum-derived exosomes from healthy individuals.

The signal obtained from the CD326-positive exosomes from healthy individuals is probably due to some cancer-related biomarkers may also exist on surface of the non-tumorigenic cells-derived exosomes[38] Thus, it is expected that exosomes-derived from healthy individuals also contain some bound cancer-related biomarkers in exosomes, but at increased levels in cancer-related exosomes from various carcinomas[39]. Magnetic particles used for exosome separation avoid the amplification of free mRNA that can be present in the serum samples. As mentioned in previous publications.[40], the expression of GAPDH may vary in several situations given that it is a multifunctional protein involved in more than 10 functions in mammalian cells. Although GAPDH has been considered as a housekeeping gene in several studies for gene expression normalization, its expression can vary in diseases in which the metabolic state of the cells is altered.[40]

To the best of the authors' knowledge, this is the first study that reports an overexpression of GAPDH gene on serum-derived exosomes from breast cancer patients. This is in accordance with the highly expressed GAPDH in breast cancer cells[41]. In fact, studies demonstrated that many cancer cells exhibit increased aerobic glycolysis, generating ATP and metabolic intermediates for cancer cell proliferation[42,43]. At this point, GAPDH is a key glycolytic enzyme and responsible for the dysregulation of glycolysis in cancer[44], and found overexpressed in human lung[45], prostate[46], renal[47], breast[41], pancreatic[48] and colorectal carcinoma[49], when compared to the normal tissues.

3.5 Conclusions

Breast cancer early diagnosis by standard techniques remains a difficult task due to the low specificity, availability, and high cost, added to the lack of breast cancer symptoms in the early stage and the small size of the primary tumor. The study of novel biomarkers including exosomes are currently under intense investigation. Here, a double-tagging RT-PCR on magnetic beads and electrochemical genosensing demonstrated a high sensitivity and specificity for GAPDH gene expression based on specific epithelial CD326 cancer-related exosomes, being able to detect the transcripts produced by as low as 1225 exosomes μL^{-1}. Also, the same analytical approach was able to detect MCF7 cells, as a model of circulating tumor cells, with an LOD of 67 cells mL^{-1}. Nevertheless, this LOD was not suitable for application in breast cancer diagnosis, since the clinical CTC count assay approved by the U.S Food and Drug Administration (FDA), must be smaller than 5 cells per 7.5 mL^{-1} of sample.

Although further studies should be done, our data clearly suggest the GAPDH expression in total exosomes from human serum from healthy and breast cancer individuals, revealed that GAPDH gene is overexpressed by 6.7-fold ($p < 0.05$) in breast cancer individuals, when compared to the healthy controls. Also, CD326 (+) exosomes specifically immunocaptured expressed the GAPDH gene as high as 3.3-fold ($p < 0.05$), when compared to the healthy controls. On the other hand, the serums were pooled in order to diminish the interindividual differences, but it should be done in individual samples to confirm the value of GAPDH as a biomarker in breast cancer at different metastatic stages.

To the best of the author's knowledge, this is the first study that report an overexpression of GAPDH gene on serum-derived exosomes from breast cancer patients. At this point, the GAPDH gene extends its concept, being no longer considered only a housekeeping gene used as a simple control for RNA, becoming a marker of cancer in clinical diagnostic. Although, the electrochemical genosensor presented in this work this approach was not enough sensible to be applied on the detection of CTCs, it can be potentially relevant in the early diagnosis for many diseases based on the specificity provided by epithelial cancer-related biomarker. In fact, the electrochemical genosensor for the quantification of exosome biomarkers has been shown to be highly specific, reproducible, and open potential for portability. In conclusion, this work shows a promising, specific and sensitive strategy to be implemented at primary health care in low-resource settings based on a minimally invasive liquid biopsy.

3.6 Supplementary data

3.6.1 Experimental

Chemicals and biochemicals

Magnetic particles (MPs) tosylactivated (Dynabeads M450 Tosylactivated, ref. 14013), MPs modified with EpCAM (also known as CD326) antibody (Dynabeads Epithelial Enrich, ref. 16102), MPs modified with poly(dt) (polydT-MPs, Dynabeads Oligo(dT), ref. 61002), MPs modified with streptavidin (strep-MPs, Dynabeads MyOne Streptavidin T1, ref. 65601) and mouse monoclonal antibody antiCD81 (ref. 10630D) were purchased from Thermo Fisher Scientific (MC, US). Mouse monoclonal antibody antiEpCAM (ref. ab7504) and Cy®5 fluorophore dye (anti-mouse, ref. ab97037) were purchased from Abcam (Cambridge, GB). Antidigoxigenin-horseradish peroxidase Fab fragments (antiDIG-HRP, Ref. 11207733910) was purchased from Roche Diagnostics (Basel, CH).

Taq DNA polymerase (ref. 18038067), M-MLV reverse transcriptase (ref. 28025013) and RNaseOUT Recombinant ribonuclease Inhibitor (ref. 10777019), Total exosome RNA and protein isolation kit (ref. 4478545), DTT Solution 0.1M (ref. Y00147), FS Buffer 5x (ref. Y02321) and GeneJET Gel Extraction and DNA Cleanup Micro Kit (ref. K0831) were purchased from Thermo Fisher Scientific. Standard reaction buffer 10x with $MgCl_2$ (ref. 20.034-4182) was purchased from Biotools (Madrid, ES). Deoxynucleotide Mix 10mM (ref. D7295) was purchased from Sigma-Aldrich. The primers for the double-tagging PCR were selected for the specific amplification of GAPDH (glyceraldehyde 3-phosphate dehydrogenase) and were purchased from Sigma-Aldrich. The sequence for the digoxigenin-modified forward primer (DIG-Fw) was 5'-[DIG] CTTCTTTTGCGTCGCCAG; while the sequence for the biotin-modified reverse primer (BIO-Rev) was 5'-[BIO] AGCCCCSGCCTTCTCCA. All solutions were prepared with ultrapure MilliQ water (Millipore® System, resistivity 18.2 MΩ·cm) and solutions used in RNA preparation were RNase-free by treatment with 0.1% DEPC.

Buffers and solutions

Diethyl pyrocarbonate (DEPC, ref. D5758), ethylenediaminetetraacetic acid (EDTA, ref. E9884), glycine (ref. 410225), hydroquinone (ref. H9003), hydrogen peroxide (ref. 1072090500), lithium chloride (ref. 746460), lithium dodecyl sulfate (LiDS, ref. L9761), tris(hydroxymethyl)aminomethane (TRIS, ref. 252859), Tween 20 (ref. P9416) were purchased from Sigma-Aldrich (Merck KGaA, DE). DL-Dithiothreitol (DTT, ref. 46819) was purchased from Fluka (Thermo Fisher Scientific). All buffer solutions used

in RNA extraction were prepared with 0.1% diethylpyrocarbonate (DEPC) treated with Ultrapure water (Millipore® System, resistivity 18.2 MΩ cm) to prevent RNA degradation.

The composition of the solutions was:

- Tris 1x buffer: 0.1 mol L^{-1} TRIS-HCl, 0.15 mol L^{-1} NaCl, pH 7.4.
- Tris blocking buffer: 2% w/v BSA, 0.1% w/v Tween 20, 5 mmol L^{-1} EDTA, 0.1 mol L^{-1} TRIS-HCl, 0.15 mol L^{-1} NaCl, pH 7.4.
- ePBS buffer: 0.1 mol L^{-1} Na_2HPO_4, 0.1 mol L^{-1} KCl, pH 7.0.

For the RNA extraction with polydT-MPs, the solutions were:

- RNase-free water: 0.1% v/v DEPC.
- Binding Buffer: 20 mmol L^{-1} TRIS-HCl, pH 7.5, 1.0 mol L^{-1} LiCl, 2 mmol L^{-1} EDTA.
- Lysis/Binding buffer: 100 mmol L^{-1} Tris-HCl, 500 mmol L^{-1} LiCl, 10 mmol L^{-1} EDTA, 1% LiDS, 5 mmol L^{-1} DTT.
- Washing buffer A: 10 mmol L^{-1} TRIS-HCl, pH 7.5, 0.15 mol L^{-1} LiCl, 1 mmol L^{-1} EDTA, 0.1% LiDS.
- Washing buffer B: 10 mmol L^{-1} TRIS-HCl, pH 7.5, 0.15 mol L^{-1}, LiCl, 1 mmol L^{-1} EDTA.

3.6.2 Cell culturing, exosome isolation and purification from MCF7 cell line

MCF7 breast cancer cell line (ATCC, ref. HTB-22) was used. Expansion of cell population was carried out from 1,000,000 cells in T-175 flask containing 32 mL of Dulbecco's Modified Eagle Medium (DMEM, ref. 31966-047, Thermo Fisher Scientific), supplemented with 10% exosome-depleted fetal bovine serum (FBS, ref. 12007C, Sigma-Aldrich), 100 U mL^{-1} penicillin-streptomycin (ref. 15140122, Thermo Fisher Scientific). The temperature was maintained at 37°C in humidified, concentrated CO_2 (5%) atmosphere. Once cells reached approximately 95% confluence on T-175 flask, the culture medium was removed and stored at -21ºC until to exosome isolation.

Exosomes were purified according to *Théry et al.*[20] with minor changes. The supernatant of the cell culture from MCF7 breast cancer cell line, or from human serum was subjected to differential centrifugation as follow: 300 x *g* for 10 minutes (removal of residual cells), 2,000 x *g* for 10 minutes and 10,000 x *g* for 30 minutes (removal of cellular

debris). Then, a Beckman Coulter Optima L-80XP Ultracentrifuge at 100,000 x *g* for 60 minutes with a 70Ti rotor to pellet exosomes. After that, the supernatant was carefully removed, and crude exosome-containing pellets were resuspended in 1 mL of Tris 1x buffer (pH 7.4, 0.22 µm sterile-filtered) and pooled. A second round of same ultracentrifugation setting was carried out, and the resulting exosome pellet resuspended in 500 µL (per 100 mL of supernatant) of Tris 1x buffer (pH 7.4, 0.22 µm sterile-filtered), and storage at -80°C. All centrifugation steps performed at a temperature of 4°C.

The exosomal protein content was determined by using Pierce BCA Protein Assay Kit (ref. 23227, Thermo Fisher Scientific), following the manufacturer protocol, using bovine serum albumin (BSA) standards in Tris 1x buffer. The spectrophotometric measurements were done at 562 nm.

3.6.3 Immobilization of exosomes and antibodies on magnetic particles

Dynabeads M450 tosylactivated superparamagnetic particles (MPs, 4.5 µm in diameter) has a core of iron oxide salt encapsulated by a polystyrene polymer, which has a polyurethane external layer with the p-toluenesulfonate group[50]. It is a good leaving group, which allows an S_N2 reaction to occur in the presence of a nucleophile[51,52]. A nucleophilic reaction by an antibody, protein, peptide, or glycoprotein removes and replaces the sulfonyl ester groups from the polyurethane layer.

Two different approaches were used, as depicted in Figure 3.5. The first one involves the direct covalent immobilization of exosomes on magnetic particles (Fig. 3.5, panel A). The second approach is based on the covalent immobilization of the antibodies for a further immunomagnetic separation (IMS) of exosomes (Fig. 3.5, panel B).

Immobilization of exosomes on magnetic particles

The immobilization of exosomes on Dynabeads M450 tosylactivated superparamagnetic particles (MPs) (Fig. 3.5, panel A) were performed as follows: 3.5 x 10^{10} exosomes were added to 40 µL (1.6 x 10^7 MPs) Dynabeads M450 tosylactivated. The reaction kinetics are increased by adding 0.1 mol L^{-1} borate buffer, pH 8.5, in order to ensure the nucleophilic reaction by the amine group. The incubation step was performed overnight with gentle shaking at 4ºC. After that, 0.5 mol L^{-1} glycine solution was added to ensure the blocking of the any remaining tosylactivated groups, by an incubation for 2 h at 25ºC. After that, the exosomes-modified magnetic particles (exosomes-MP) were resuspended in 160 µL of Tris 1x buffer in order to achieve 1 x 10^6 MPs per 10 µL. The exosomes-MP were maintained at 4ºC until use and remain stable on MPs up to two months.

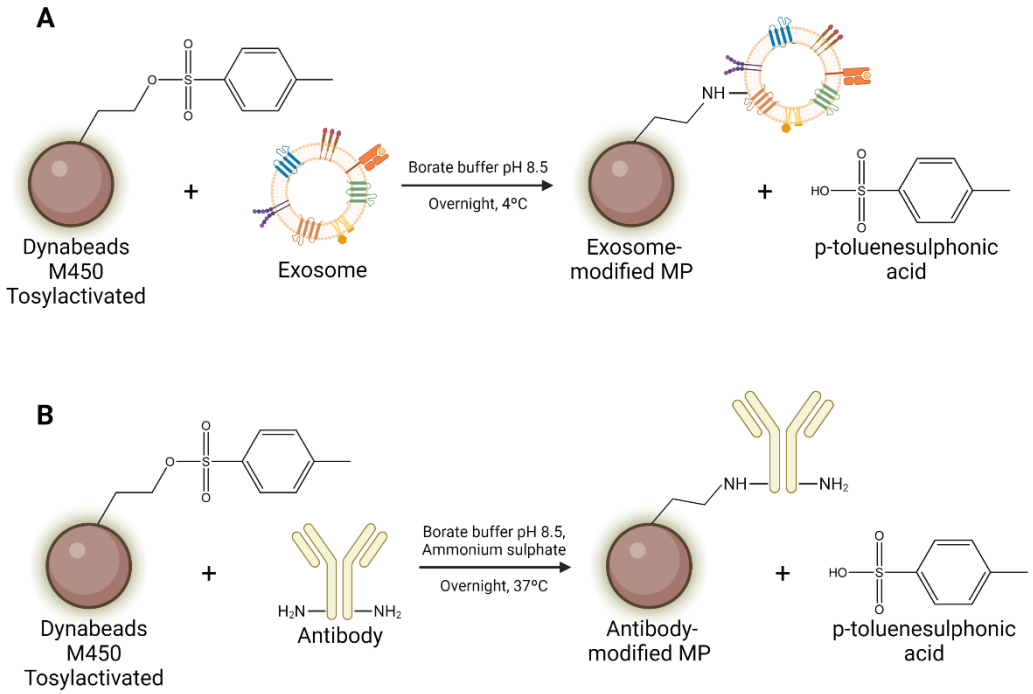

Figure 3.5. Covalent immobilization of (A) exosome or (B) antibody on Dynabeads® M450 tosylactivated. Created with BioRender.com.

Immobilization of antibodies on magnetic particles

The CD81 antibody (15 µg mL^{-1}, as previously optimized[27]) was added to 55 µL (2.2 x 10^7 MPs) Dynabeads M450 tosylactivated (Fig. 3.5, panel B). The reaction kinetics are increased by adding 0.1 mol L^{-1} borate buffer pH 8.5 and 3 mol L^{-1} ammonium sulphate in borate buffer. The incubation step was performed overnight (18-20h) with gentle shaking at 37ºC. After that, a blocking step with 0.5 mol L^{-1} glycine solution was performed for 2 h to ensure the blocking of the any remaining tosylactivated groups. After that, the antibody-modified magnetic particles (herein, antiCDX-MPs, where antiCDX = antiCD81) were resuspended in 220 µL (10 µL per assay to give 1 x 10^6 particles per assay) of Tris 1x buffer.

It is important to highlight that in this procedure it was no possible to achieve the immobilization of antiCD326 antibody on MPs. Therefore, commercially modified particles with EpCAM were used. EpCAM corresponds to CD326 (Cluster of Differentiation nomenclature), so in this work, antiCD326-MPs are equally referred to commercial antiEpCAM-MPs.

3.6.4 Characterization of the exosomes derived from MCF7 breast cancer cell line

Characterization of exosomes by nanoparticle tracking analysis and cryogenic transmission electron microscopy

The size distribution and concentration of exosomes were measured by nanoparticle tracking analysis (NTA) using the NanoSight LM10-HS system with a tuned 405 nm laser (NanoSight Ltd., GB). The purified exosomes were diluted in sterile-filtered TRIS buffer (50- to 100-fold). Nanosight NTA Software analyzed raw data videos by triplicate during 60 s with 50 frames s^{-1} and the temperature of the laser unit set at 24.8ºC. For the cryogenic transmission electron microscopy (Cryo-TEM), the exosomes (2.0 x 10^9) were directly laid on Formvar-Carbon EM grids and frozen in ethanol. TEM images were collected by a Jeol JEM 2011 (JEOL USA Inc., US) transmission electron microscope at an accelerating voltage of 200 kV. Exosomes were maintained at -182°C during the whole process.

Characterization of exosomes by bead-based flow cytometry and confocal microscopy

The analysis of the molecular biomarkers expressed in MCF7 cell line was firstly carried out by flow cytometry. The presence of the CD81 and CD326 biomarkers was investigated. The indirect labeling of 2 x 10^5 cells was performed by incubation of 100 µL (5 µg mL^{-1}) of the antibodies antiCD81 and antiCD326, for 30 min with gentle shaking at 25ºC. After that, three washing steps with Tris 1x buffer containing 0.5% BSA were performed. Afterwards, 100 µL (2 µg mL^{-1}) of antimouse-Cy5 antibody (far-red fluorescent dye, excitation 647 nm, emission 665 nm) was incubated for 30 min in the darkness with gentle shaking at 25 ºC. The labeled cells were resuspended in 200 µL of Tris 1x containing 0.5% BSA. The same procedure of labeling was performed in the case of the exosomes derived from MCF7 breast cancer cell line, but in this approach, and due to their size and resolution of the technique, the exosomes were firstly immobilized on the surface of MPs, as described on To achieve that, 3.5 x 10^{10} exosomes were covalently immobilized on 1.6 x 10^7 MPs, as described in §3.6.3, followed by the indirect labeling as described above, with antiCD81 or antiCD326.

The same batch of cells and exosomes analyzed by flow cytometry were subjected for confocal microscopy imaging for the study of the binding pattern of antibodies. In the case of cells, the cellular DNA was stained previously (before labeling

with antibodies) with Hoechst dye (blue fluorescent dye, excitation 350 nm, emission 490 nm).

3.6.5 Immunomagnetic separation, double-tagging reverse transcription PCR of GAPDH transcripts and electrochemical genosensing

Immunomagnetic separation of the cells and exosomes

The IMS of the cells exosomes was performed by antiCDX-MPs (being CDX any of CD81 or CD326 biomarkers) (containing 1×10^6 MPs per tube), and 100 µL either of MCF-7 cells (concentration ranging from 50 to 5.000 cells mL^{-1}) or exosomes (concentration ranging from 10^4 to 10^6 exosomes μL^{-1}), which were simultaneously incubated for 30 min with gentle shaking at 25°C, followed by three washing steps with Tris 1x buffer containing 0.5% BSA. The coated antiCDX-MPs were resuspended in 1.0 mL of Lysis/Binding buffer. Then, they were disrupted by pipetting up and down a couple of times to ensure a complete lysis. In order to ensure sample homogenization, the lysate was passed through a 21-gauge needle using a 2.0 mL syringe. Then, the lysate and antiCDX-MPs were separated by using a magnet plate separator, an antiCDX-MPs pellet on the bottom tube is formed, and the lysate is transferred to another tube.

Double-tagging RT-PCR on magnetic beads

The lysate of the cells or exosomes was incubated with 15 µL of poly(dT)-MPs (7 x 10^7 MPs) for 15 min under gentle shaking at 25ºC. Finally, the mRNA-coated MPs were washed with 500 µL of washing buffer A, followed by washing with 500 µL of washing buffer B, and finally resuspended with 100 µL of DEPC-treated water. The suspension of RNA-poly(dT)-MPs was stored on ice and immediately used.

The RNA reverse transcription (RT) was carried out on poly(dT)-MPs with Moloney Murine Leukemia Virus (M-MLV) reverse transcriptase. The RNA-poly(dT)-MPs was placed in a magnet tube separator, allowing to discard the supernatant (DEPC-treated water) from the RNA-poly(dT)-MPs that remain pelleted at the bottom of the tube for subsequent RT. The poly(dT)-MPs were incubated with 10 nmol of dNTPs mix for 5 min at 65 ºC and cooled on ice for 1 min. After that, a mix containing 200 nmol of DTT, 40 U of RNaseOUT inhibitor and 1x First Strand Buffer was added and incubated at 37 ºC for 2 min. Finally, 200 U of M-MLV reverse transcriptase were added and incubated for 50 min at 37 ºC, and 15 min at 70 ºC for inactivating the reaction. The cDNA was stored at -21ºC until use.

The double-tagging polymerase chain reaction (PCR) was performed in 15 µL of reaction mixture containing the cDNA as sample in order to obtain the GAPDH amplicons doubly labelled with biotin and digoxigenin. Each reaction mixture contained 7.5 pmol of each primer (DIG-Fw and BIO-Rev), 3.75 nmol of each deoxynucleotide triphosphate (dNTPs) and 3U of Taq polymerase. The reaction was carried out in a buffer with 7.5 mmol L^{-1} Tris buffer (pH 9.0), 5.0 mmol L^{-1} KCl, 2.0 mmol L^{-1} $(NH_4)_2SO_4$ and 0.2 mmol L^{-1} $MgCl_2$ as a cofactor of the enzyme. The reaction mixture was exposed to an initial step at 95 °C for 3 min followed by 32 cycles of 95 °C for 30 s, 61 °C for 30 s, 72 °C for 30 s, and a last step of 7 min at 72 °C.

Multiple negative samples for the RT and PCR, which contained all reagents except mRNA or cDNA were tested. The performance of the double-tagging PCR was analyzed with agarose gel electrophoresis followed by DNA sequencing analysis. The agarose gel electrophoresis was done with 2% agarose gel in TAE buffer containing 1×GelRed dye and a molecular weight marker of DNA fragments ranged from 100 to 1000 base pair (bp), that was used as size amplicon control. The DNA bands were visualized by UV transillumination, expecting a single DNA band at 371 bp in all samples. DNA bands obtained with samples of MCF-7 cells and exosomes were purified with GeneJET kit and analyzed, as described in §3.6.6 (Supp. Data).

Optimization of RT-PCR amplification cycles

As aforementioned, the detection of exosomes is a challenging task due to the low concentration in biological samples. Moreover, an intrinsic characteristic of the exosomes is the low RNA content compared to cells[53]. In order to increase the sensitivity of the approach, the double-tagging RT-PCR was optimized towards the number of cycles required for GAPDH transcript detection in exosomes. The cellular GAPDH transcript detection was used for comparison purposes. The double-tagging RT-PCR was performed with 28, 32, 36 and 40 cycles.

The double-tagged amplicons were submitted in parallel to gel electrophoresis and measured by electrochemical magneto genosensing. Negative controls were performed with all reagents, omitting the RNA (from cells and/or exosomes). Figure 3.6, panel A shows the gel electrophoresis for cellular and exosomal GAPDH amplicons. While the GAPDH amplicons from MCF7 cells were observed in all PCR cycles tested, the amplicons for exosomes are only evidenced after 36 cycles. Then, the GAPDH amplicons from exosomes were subjected to electrochemical genosensing. As expected, the electrochemical genosensing revealed that in the exosomes the GAPDH transcript was also amplified in all PCR cycles tested (Fig. 3.6, panel B). However, the signal-to-

noise ratio for the detection of the GAPDH amplicons is affected substantially by the increase in the PCR cycles (Fig. 3.6, panel B inset). Probably, this is due to a larger number of dimers formed as the PCR cycles increases, and the best signal-to-noise ratio was obtained with 32 cycles of PCR, as shown in the inset of the Figure 3.6, panel B. This result highlights the high sensitivity of the double-tagging RT-PCR coupled to the electrochemical detection.

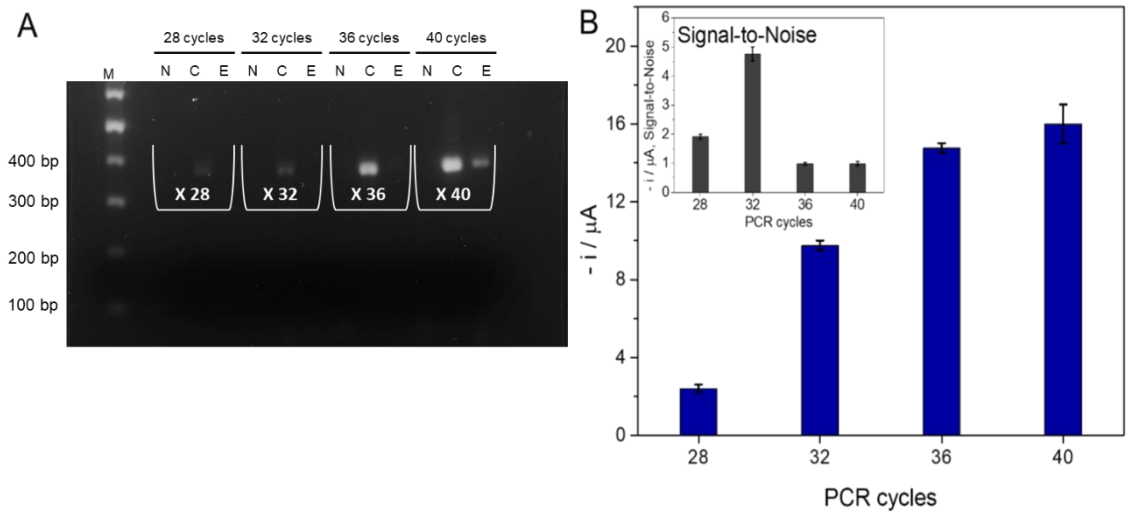

Figure 3.6. Evaluation of the number of cycles in the multiplex double-tagging PCR for GAPDH transcript detection from MCF7 cells and their exosomes, detecting by gel electrophoresis (panel A) and electrochemical genosensing (panel B). Panel A shows the gel electrophoresis with identified lanes for negative (N), cells (C) and exosomes (E) in the respective PCR cycles. Lane M corresponds to 100 bp DNA size marker. The correspondent signals for the multiplex electrochemical genosensing are shown in panel B: inset shows the signal-to-noise current. The error bars show the standard deviation for n = 3.

Electrochemical magneto-genosensing

The procedure for the detection of the BIO-DIG double-tagged PCR product is based on the immobilization on streptavidin-modified magnetic particles and its electrochemical detection with specific antibody for digoxigenin modified with HRP. The magneto-actuated electrochemical genosensing (Fig. 3.1, panel C) was performed in tubes and involved the following steps. (i) Immobilization of the amplicons on Strep-MPs. For that, 30 µL of the amplicons diluted 25-fold in Tris 1x buffer were incubated with 7 x 10^7 Strep-MPs during 5 min at 25 ºC. (ii) Labeling with electrochemical reporter. Incubation with 10 µL (130 mU) of antiDIG-HRP in Tris blocking buffer, during 30 min at 25 ºC, followed by three washing steps.

For the electrochemical readout, the strep-MPs coated with the amplicons were separated by using a magnet tube separator, a MPs pellet on the bottom tube is formed, followed by remove of the supernatant. Following, MPs pellet is resuspended in ePBS

buffer and a magneto-actuated graphite-epoxy composite (m-GEC) electrode is inserted into tube for remove the MPs pellet onto m-GEC surface, which is transferred into an electrochemical cell and measured by means of amperometry at -100 mV *vs.* $Ag/AgCl/KCl_{(sat.)}$ by using hydroquinone mediator. For that, a standard one compartment three-electrode electrochemical cell is filling with 19.8 mL of ePBS, 100 µL of 400 mmol L^{-1} hydroquinone (HQ) as electrochemical mediator, and 100 µL of 400 mmol L^{-1} H_2O_2 as substrate. A reproducible steady-current was obtained after 60 s. The cathodic current generated by monitoring benzoquinone species directly related with the amount of captured exosomes. The m-GEC surface cleaning procedure was carried out for every experiment by electrochemical treatment by applying a potential of +3 V for 5 s in 0.5 mol L^{-1} H_2SO_4 supporting electrolyte.

3.6.6 RNA integrity analysis and DNA sequencing

A comparative integrity study of RNA from MCF7 breast cancer and purified exosomes was performed. To achieve that, the RNA obtained by lysis of cells and exosomes were processed by classical RNA extraction and purification procedure followed by integrity analysis. The Total Exosome RNA and protein isolation kit were used to obtain RNA from MCF-7 cells (1×10^6 cells) and purified exosomes (1×10^{10} exosomes), following the manufacturer protocol. The samples were analyzed with Agilent RNA 6000 Nano Kit (ref. 5067-1511) from Agilent Technologies (CA, US) by Genomics Bioinformatics Service (Institute of Biotechnology and Biomedicine, UAB, ES) to characterize and quantify the RNA content.

Figure 3.7 shows the results of the RNA integrity analysis. Firstly, the quality of the extracted RNA was assessed by the Bioanalyzer RNA integrity numbers (RIN; 1 = totally degraded, 10 = intact). The cellular 18S and 28S ribosomal RNA (rRNA) are the most dominant peaks, and the RIN value was estimated to be 8.0 consistent with a good RNA quality (Fig. 3.7, panel A). In addition to the rRNA, one broadband (~100 to ~450 nucleotides) for cellular messenger RNA (mRNA) also is displayed. Unfortunately, rRNA nor mRNA peaks were not observed for RNA extracted from exosomes (Fig. 3.7, panel B). Since the algorithm is based on the ribosomal RNA, previous studies demonstrated that exosomes contain little or no rRNA[54,55] and mRNA[56], RIN values are only valid for cellular RNA quality assessments. It is important to highlight that RNA yield can differ substantially between different RNA isolation methods, which may be related to the low sensitivity of the extraction method.[57]

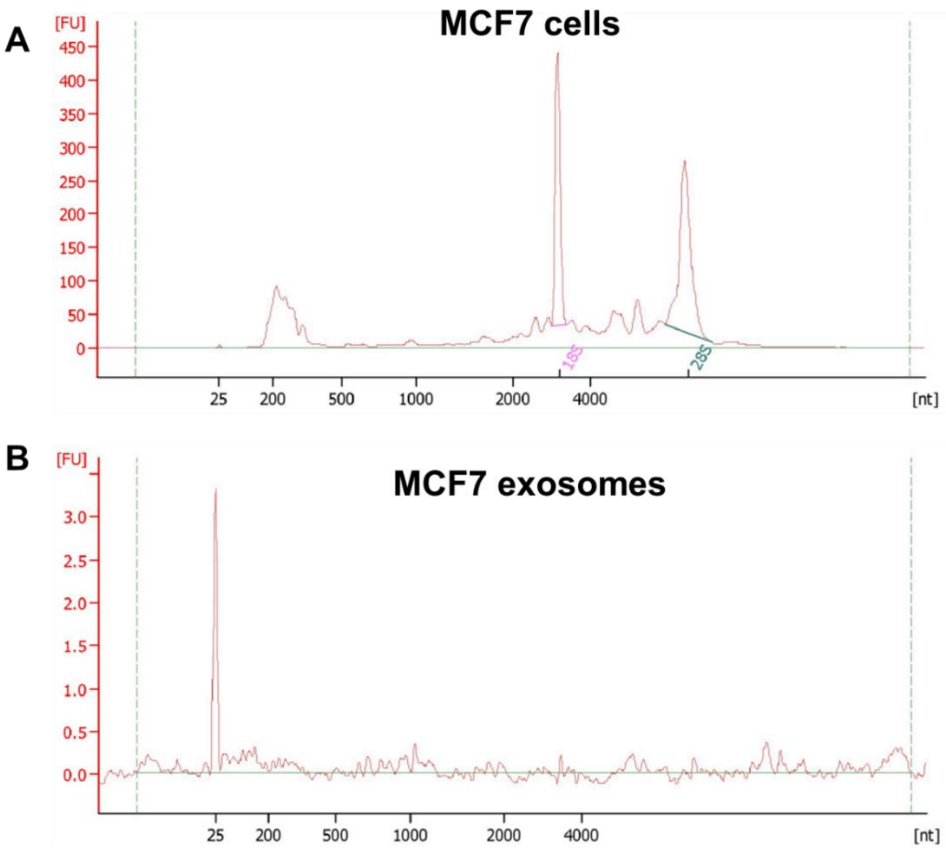

Figure 3.7. RNA integrity analysis of MCF-7 cells and exosomes samples. Panel A, the sample from MCF-7 cells shows rRNA 18s and 28s bands appear in a ratio 1.2, with a high RNA integrity number (RIN = 8.0). Panel B, the sample from exosomes does not show any rRNA band, the RNA concentration was below the bioanalyzer sensitivity.

Regarding the DNA sequencing analysis, an ABI Prism 3130XL Genetic Analyzer was used, with BigDye Terminator v3.1 Cycle Sequencing Kit (ref. 4336919, Thermo Fisher Scientific), provided by Genomics Bioinformatics Service (Institute of Biotechnology and Biomedicine, UAB, ES). The results were analyzed using Chromas v 2.6.6 (Technelysium Pty Ltd, Brisbane, QLD, AU) and Clustal Omega[21] software, to check the chromatograms and the alignment of both sequences. Then, the amplified sequence was identified using BLAST software [28]. As expected, the DNA sequencing revealed the entire specific GAPDH sequence in both cells and exosomes, with no other enriched fragments. This result demonstrated that both RNA extraction and reverse transcription can be performed on poly(dT)-MPs. Nonetheless, the use of poly(dT)-MPs and the magnetic actuation simplifies the analytical procedure, when compared to the classical procedure for RNA extraction, avoiding the use of separation columns and further centrifugation steps.

This procedure was able to identify the following sequence, that contains the forward primer sequence highlighted in blue color and the reverse primer sequence in red color.

Homo sapiens glyceraldehyde-3-phosphate dehydrogenase (GAPDH), transcript variant 1, mRNA. NCBI Reference Sequence: NM_002046.7.

GCTCTCTGCTCCTCCTGTTCGACAGTCAGCCGCAT**CTTCTTTTGCGTCGCCAG**CCGAGCCACATCGCTCAGACACCATGGGGAAGGTGAAGGTCGGAGTCAACGGATTTGGTCGTATTGGGCGCCTGGTCACCAGGGCTGCTTTTAACTCTGGTAAAGTGGATATTGTTGCCATCAATGACCCCTTCATTGACCTCAACTACATGGTTTACATGTTCCAATATGATTCCACCCATGGCAAATTCCATGGCACCGTCAAGGCTGAGAACGGGAAGCTTGTCATCAATGGAAATCCCATCACCATCTTCCAGGAGCGAGATCCCTCCAAAATCAAGTGGGGCGATGCTGGCGCTGAGTACGTCGTGGAGTCCACTGGCGTCTTCACCACCA**TGGAGAAGGCTGGGGCT**CATTTGCAGGGGGGAGCCAAAAGGGTCATCATCTCTGCCCCCTCTGCTGATGCCCCCATGTTCGTCATGGGTGTGAACCATGAGAAGTATGACAACAGCCTCAAGATCATCAGCAATGCCTCCTGCACCACCAACTGCTTAGCACCCCTGGCCAAGGTCATCCATGACAACTTTGGTATCGTGGAAGGACTCATGACCACAGTCCATGCCATCACTGCCACCCAGAAGACTGTGGATGGCCCCTCCGGGAAACTGTGGCGTGATGGCCGCGGGGCTCTCCAGAACATCATCCCTGCCTCTACTGGCGCTGCCAAGGCTGTGGGCAAGGTCATCCCTGAGCTGAACGGGAAGCTCACTGGCATGGCCTTCCGTGTCCCCACTGCCAACGTGTCAGTGGTGGACCTGACCTGCCGTCTAGAAAAACCTGCCAAATATGATGACATCAAGAAGGTGGTGAAGCAGGCGTCGGAGGGCCCCCTCAAGGGCATCCTGGGCTACACTGAGCACCAGGTGGTCTCCTCTGACTTCAACAGCGACACCCACTCCTCCACCTTTGACGCTGGGGCTGGCATTGCCCTCAACGACCACTTTGTCAAGCTCATTTCCTGGTATGACAACGAATTTGGCTACAGCAACAGGGTGGTGGACCTCATGGCCCACATGGCCTCCAAGGAGTAAGACCCCTGGACCACCAGCCCCAGCAAGAGCACAAGAGGAAGAGAGAGACCCTCACTGCTGGGGAGTCCCTGCCACACTCAGTCCCCCACCACACTGAATCTCCCCTCCTCACAGTTGCCATGTAGACCCCTTGAAGAGGGGAGGGGCCTAGGGAGCCGCACCTTGTCATGTACCATCAATAAAGTACCCTGTGCTCAACCA

3.6.7 Electrochemical magneto-genosensing of transcripts from exosomes of breast cancer patients

Human serum isolation

The human serum samples (healthy and breast cancer patients) were separated from the blood cells using a sterile empty tube without any anticoagulant, leave the tube

in a standing position for about 20-30 minutes for blood to be clotted. After that, centrifugation at 1500 x *g* (20 ºC) for 10 minutes was carried out for removal of residual cells and cellular debris. Following, the human serum (supernatant on top) was carefully removed, freeze at -80 ºC to preserve for further assays.

Detection of GAPDH transcripts from purified exosomes without preconcentration on MPs

This approach (Fig. 3.4, panel A) is based on amplification and detection through non-specific GAPDH biomarker. Firstly, exosomes were isolated from 1.0 mL of human serum from healthy (n = 10, pooled) and breast cancer (n = 10, pooled) patients by ultracentrifugation and resuspended in Tris 1x buffer, as described in §3.6.2 (Supp. Data). Then, the exosomes samples from healthy and breast cancer patients were analyzed with the BCA protein assay kit, and their protein concentrations were estimated to be 235 μg mL^{-1} and 335 μg mL^{-1}, respectively. To normalize the results according to the protein content, 0.33 μg of exosomes from healthy and breast cancer patients were subjected to RNA extraction based on poly(dT)-MPs, followed by double-tagging PCR, and subsequent electrochemical genosensing, as described above.

Immunomagnetic separation of the exosomes from undiluted human serum

Our detection approach was to isolate and detect exosomes from undiluted human serum (healthy and breast cancer patients) directly by immunomagnetic separation (IMS) based on antiCD326-MPs (Fig. 3.4, panel B). In this case, samples of undiluted human serum from healthy (n=10, pooled) and breast cancer patients (n=10, pooled) were centrifuged at 10,000 x *g* to eliminate possible cell debris remaining in the serum. The IMS of the exosomes was performed with antiCD326-MPs (containing 1 × 10^6 MPs per tube), and 1.0 mL of undiluted human serum, incubated for 30 min with gentle shaking at 25 °C, followed by three washing steps with Tris 1x buffer containing 0.5% BSA. Then, the exosomes-coated antiC326-MPs were resuspended with 100 μL of Tris 1x buffer, stored on ice and immediately used for RNA extraction. The exosomes-coated antiCD326-MPs were resuspended in 1.0 mL of Lysis/Binding buffer. The exosomes were disrupted by pipetting up and down a couple of times to ensure a complete lysis. In order to ensure sample homogenization, the lysate was passed through a 21-gauge needle using a 2.0 mL syringe. Then, the lysate and antiCD326-MPs were separated by using a magnet plate separator, an antiCD326-MPs pellet on the bottom tube is formed, followed by lysate separation, and transferred by another tube.

Double-tagging RT-PCR on magnetic beads

After that, the lysate was incubated with 15 µL of poly(dT)-MPs (75 µg MPs) for 15 min under gentle shaking at 25 ºC. Finally, the mRNA-coated MPs were washed with 500 µL of washing buffer A, followed by washing with 500 µL of washing buffer B, and finally resuspended with 100 µL of DEPC-treated water. The suspension of RNA-poly(dT)-MPs was stored on ice and immediately used for reverse transcription reaction, as for the case of the exosomes derived from MCF7 cells.

The double-tagging polymerase chain reaction (PCR) was also performed as above for the case of the exosomes derived from cell culturing.

Electrochemical magneto-genosensing

The procedure for the detection of the BIO-DIG double-tagged PCR product was also performed as above for the case of the exosomes derived from cell culturing.

3.7 Acknowledgements

A. Pallarès Rusiñol and S. Lima de Moura equally contributed to this work. C. Garcia Martín is gratefully acknowledged for her contribution. Also, ICTS “NANBIOSIS” NTA analysis service of *Institut de Ciència dels Materials de Barcelona* and Service of Microscopy of *Universitat Autònoma de Barcelona* are gratefully acknowledged.

3.8 References

(1) Sung, H.; Ferlay, J.; Siegel, R. L.; Laversanne, M.; Soerjomataram, I.; Jemal, A.; Bray, F. Global Cancer Statistics 2020: GLOBOCAN Estimates of Incidence and Mortality Worldwide for 36 Cancers in 185 Countries. *CA. Cancer J. Clin.* **2021**, *71* (3), 209–249. https://doi.org/10.3322/caac.21660.

(2) Weissleder, R.; Pittet, M. J. Imaging in the Era of Molecular Oncology. *Nature* **2008**, *452* (7187), 580–589. https://doi.org/10.1038/nature06917.

(3) Unger-Saldaña, K. Challenges to the Early Diagnosis and Treatment of Breast Cancer in Developing Countries. *World J. Clin. Oncol.* **2014**, *5* (3), 465–477. https://doi.org/10.5306/wjco.v5.i3.465.

(4) Japp, N. C.; Souchek, J. J.; Sasson, A. R.; Hollingsworth, M. A.; Batra, S. K.; Junker, W. M. Tumor Biomarker In-Solution Quantification, Standard Production, and Multiplex Detection. *J. Immunol. Res.* **2021**, *2021*. https://doi.org/10.1155/2021/9942605.

(5) Poudineh, M.; Sargent, E. H.; Pantel, K.; Kelley, S. O. Profiling Circulating Tumour Cells and Other Biomarkers of Invasive Cancers. *Nature Biomedical Engineering*. Nature Publishing Group February 6, 2018, pp 72–84. https://doi.org/10.1038/s41551-018-0190-5.

(6) Miller, M. C.; Doyle, G. V; Terstappen, L. W. M. M. Significance of Circulating Tumor Cells Detected by the CellSearch System in Patients with Metastatic Breast Colorectal and Prostate Cancer. *J. Oncol.* **2010**, *2010*. https://doi.org/10.1155/2010/617421.

(7) Allard, W. J. Tumor Cells Circulate in the Peripheral Blood of All Major Carcinomas but Not in Healthy Subjects or Patients With Nonmalignant Diseases. *Clin. Cancer Res.* **2004**, *10* (20), 6897–6904. https://doi.org/10.1158/1078-0432.CCR-04-0378.

(8) de Wit, S.; Manicone, M.; Rossi, E.; et al. EpCAMhigh and EpCAMlow Circulating Tumor Cells in Metastatic Prostate and Breast Cancer Patients. *Oncotarget* **2018**, *9* (86). https://doi.org/10.18632/oncotarget.26298.

(9) Ross, B. A. A.; Cooper, B. W.; Lazarus, H. M.; et al. Detection and Viability of Tumor Cells in Peripheral Blood Stem Cell Collections from Breast Cancer Patients Using Immunocytochemical and Clonogenic Assay Techniques. *Blood* **1993**, *82* (9), 2605–2610.

(10) Johnstone, R. M.; Adam, M.; Hammond, J. R.; Orr, L.; Turbide, C. Vesicle Formation during Reticulocyte Maturation. Association of Plasma Membrane Activities with Released Vesicles (Exosomes). *J. Biol. Chem.* **1987**, *262* (19), 9412–9420.

(11) Mathieu, M.; Martin-Jaular, L.; Lavieu, G.; Théry, C. Specificities of Secretion and Uptake of Exosomes and Other Extracellular Vesicles for Cell-to-Cell Communication. *Nat. Cell Biol.* **2019**, *21* (1), 9–17. https://doi.org/10.1038/s41556-018-0250-9.

(12) Harding, C.; Heuser, J.; Stahl, P. Endocytosis and Intracellular Processing of Transferrin and Colloidal Gold-Transferrin in Rat Reticulocytes: Demonstration of a Pathway for Receptor Shedding. *Eur. J. Cell Biol.* **1984**, *35* (2), 256–263.

(13) Samanta, S.; Rajasingh, S.; Drosos, N.; Zhou, Z.; Dawn, B.; Rajasingh, J. Exosomes: New Molecular Targets of Diseases. *Acta Pharmacol. Sin.* **2018**, *39* (4), 501–513. https://doi.org/10.1038/aps.2017.162.

(14) Davidson, S. M.; Riquelme, J. A.; Zheng, Y.; Vicencio, J. M.; Lavandero, S.; Yellon, D. M. Endothelial Cells Release Cardioprotective Exosomes That May Contribute to Ischaemic Preconditioning. *Sci. Rep.* **2018**, *8* (1), 15885. https://doi.org/10.1038/s41598-018-34357-z.

(15) Pividori, M. I.; Merkoçi, A.; Barbé, J.; Alegret, S. PCR-Genosensor Rapid Test for Detecting Salmonella. *Electroanalysis* **2003**, *15* (2324), 1815–1823. https://doi.org/10.1002/elan.200302764.

(16) Lermo, A.; Zacco, E.; Barak, J.; Delwiche, M.; Campoy, S.; Barbé, J.; Alegret, S.; Pividori, M. I. Towards Q-PCR of Pathogenic Bacteria with Improved Electrochemical Double-Tagged Genosensing Detection. *Biosens. Bioelectron.* **2008**, *23* (12), 1805–1811. https://doi.org/10.1016/j.bios.2008.02.020.

(17) Liébana, S.; Lermo, A.; Campoy, S.; Barbé, J.; Alegret, S.; Pividori, M. I. Magneto Immunoseparation of Pathogenic Bacteria and Electrochemical Magneto Genosensing of the Double-Tagged Amplicon. *Anal. Chem.* **2009**, *81* (14), 5812–5820. https://doi.org/10.1021/ac9007539.

(18) Carinelli, S.; Xufré, C.; Martí, M.; Pividori, M. I. Interferon Gamma Transcript Detection on T Cells Based on Magnetic Actuation and Multiplex Double-Tagging Electrochemical Genosensing. *Biosens. Bioelectron.* **2018**, *117*, 183–190. https://doi.org/10.1016/j.bios.2018.05.030.

(19) Ben Aissa, A.; Jara, J. J.; Sebastián, R. M.; Vallribera, A.; Campoy, S.; Pividori, M. I. Comparing Nucleic Acid Lateral Flow and Electrochemical Genosensing for the Simultaneous Detection of Foodborne Pathogens. *Biosens. Bioelectron.* **2017**, *88*, 265–272. https://doi.org/10.1016/j.bios.2016.08.046.

(20) Théry, C.; Amigorena, S.; Raposo, G.; Clayton, A. Isolation and Characterization of Exosomes from Cell Culture Supernatants and Biological Fluids. *Curr. Protoc. Cell Biol.* **2006**, *30* (1), 3.22.1-3.22.29. https://doi.org/10.1002/0471143030.cb0322s30.

(21) Chojnacki, S.; Cowley, A.; Lee, J.; Foix, A.; Lopez, R. Programmatic Access to Bioinformatics Tools from EMBL-EBI Update: 2017. *Nucleic Acids Res.* **2017**, *45* (W1), W550–W553. https://doi.org/10.1093/nar/gkx273.

(22) CDC. *Biosafety in Microbiological and Biomedical Laboratories (BMBL)*, 6th ed.; CDC, 2020.

(23) Chernyshev, V. S.; Rachamadugu, R.; Tseng, Y. H.; Belnap, D. M.; Jia, Y.; Branch, K. J.; Butterfield, A. E.; Pease, L. F.; Bernard, P. S.; Skliar, M. Size and Shape Characterization of Hydrated and Desiccated Exosomes. *Anal. Bioanal. Chem.* **2015**, *407* (12), 3285–3301. https://doi.org/10.1007/s00216-015-8535-3.

(24) Agrawal, A.; Sathe, T.; Nie, S. Single-Bead Immunoassays Using Magnetic Microparticles and Spectral-Shifting Quantum Dots. *J. Agric. Food Chem.* **2007**, *55* (10), 3778–3782. https://doi.org/10.1021/jf0635006.

(25) Rupp, A.-K.; Rupp, C.; Keller, S.; Brase, J. C.; Ehehalt, R.; Fogel, M.; Moldenhauer, G.; Marmé, F.; Sültmann, H.; Altevogt, P. Loss of EpCAM Expression in Breast Cancer Derived Serum Exosomes: Role of Proteolytic Cleavage. *Gynecol. Oncol.* **2011**, *122*, 437–446. https://doi.org/10.1016/j.ygyno.2011.04.035.

(26) Stoeck, A.; Keller, S.; Riedle, S.; Sanderson, M. P.; Runz, S.; Le Naour, F.; Gutwein, P.; Ludwig, A.; Rubinstein, E.; Altevogt, P. A Role for Exosomes in the Constitutive and Stimulus-Induced Ectodomain Cleavage of L1 and CD44. *Biochem. J.* **2006**, *393*, 609–618. https://doi.org/10.1042/BJ20051013.

(27) Moura, S. L.; Martín, C. G.; Martí, M.; Pividori, M. I. Multiplex Detection and Characterization of Breast Cancer Exosomes by Magneto-Actuated Immunoassay. *Talanta* **2020**, *211*, 120657. https://doi.org/https://doi.org/10.1016/j.talanta.2019.120657.

(28) Agarwala, R.; Barrett, T.; Beck, J.; et al. Database Resources of the National Center for Biotechnology Information. *Nucleic Acids Res.* **2018**, *46* (D1), D8–D13. https://doi.org/10.1093/nar/gkx1095.

(29) Théry, C.; Witwer, K. W.; Aikawa, E.; et al. Minimal Information for Studies of Extracellular Vesicles 2018 (MISEV2018): A Position Statement of the International Society for Extracellular Vesicles and Update of the MISEV2014 Guidelines. *J. Extracell. Vesicles* **2018**, *7* (1). https://doi.org/10.1080/20013078.2018.1535750.

(30) Zhang, P.; He, M.; Zeng, Y. Ultrasensitive Microfluidic Analysis of Circulating Exosomes Using a Nanostructured Graphene Oxide/Polydopamine Coating. *Lab Chip* **2016**, *16* (16), 3033–3042. https://doi.org/10.1039/c6lc00279j.

(31) Moura, S. L.; Martín, C. G.; Martí, M.; Pividori, M. I. Electrochemical Immunosensing of Nanovesicles as Biomarkers for Breast Cancer. *Biosens. Bioelectron.* **2020**, *150*, 111882. https://doi.org/https://doi.org/10.1016/j.bios.2019.111882.

(32) Moura, S. L.; Pallarès-Rusiñol, A.; Sappia, L.; Martí, M.; Pividori, M. I. The Activity of Alkaline Phosphatase in Breast Cancer Exosomes Simplifies the Biosensing Design. *Biosens. Bioelectron.* **2022**, *198*, 113826. https://doi.org/10.1016/j.bios.2021.113826.

(33) Lermo, A.; Campoy, S.; Barbé, J.; Hernández, S.; Alegret, S.; Pividori, M. I. In Situ DNA Amplification with Magnetic Primers for the Electrochemical Detection of Food Pathogens. *Biosens. Bioelectron.* **2007**, *22* (9–10), 2010–2017. https://doi.org/10.1016/j.bios.2006.08.048.

(34) Zhao, Z.; Yang, Y.; Zeng, Y.; He, M. A Microfluidic ExoSearch Chip for Multiplexed Exosome Detection towards Blood-Based Ovarian Cancer Diagnosis. *Lab Chip* **2016**, *16* (3), 489–496. https://doi.org/10.1039/C5LC01117E.

(35) Zhou, Q.; Rahimian, A.; Son, K.; Shin, D. S.; Patel, T.; Revzin, A. Development of an Aptasensor for Electrochemical Detection of Exosomes. *Methods* **2016**, *97*, 88–93. https://doi.org/10.1016/j.ymeth.2015.10.012.

(36) Zong, S.; Wang, L.; Chen, C.; Lu, J.; Zhu, D.; Zhang, Y.; Wang, Z.; Cui, Y. Facile Detection of Tumor-Derived Exosomes Using Magnetic Nanobeads and SERS Nanoprobes. *Anal. Methods* **2016**, *8*, 5001–5008. https://doi.org/10.1039/C6AY00406G.

(37) Huang, L.; Wang, D.-B.; Singh, N.; Yang, F.; Gu, N.; Zhang, X.-E. A Dual-Signal Amplification Platform for Sensitive Fluorescence Biosensing of Leukemia-Derived Exosomes. *Nanoscale* **2018**, *10* (43), 20289–20295. https://doi.org/10.1039/C8NR07720G.

(38) Schmelzer, E.; Reid, L. M. EpCAM Expression in Normal, Non-Pathological Tissues. *Front. Biosci.* **2008**, *13* (8), 3096–3100. https://doi.org/10.2741/2911.

(39) Tamkovich, S. N.; Yunusova, N. V.; Somov, A. K.; Afanas'ev, S. G.; Kakurina, G. V.; Kolegova, E. S.; Tugutova, E. A.; Laktionov, P. P.; Kondakova, I. V. Comparative Subpopulation Analysis of Plasma Exosomes from Cancer Patients. *Biochem. (Moscow), Suppl. Ser. B Biomed. Chem.* **2018**, *12* (2), 151–155. https://doi.org/10.1134/S1990750818020130.

(40) Sirover, M. A. On the Functional Diversity of Glyceraldehyde-3-Phosphate

Dehydrogenase: Biochemical Mechanisms and Regulatory Control. *Biochim. Biophys. Acta - Gen. Subj.* **2011**, *1810* (8), 741–751. https://doi.org/10.1016/j.bbagen.2011.05.010.

(41) Révillion, F.; Pawlowski, V.; Hornez, L.; Peyrat, J.-P. Glyceraldehyde-3-Phosphate Dehydrogenase Gene Expression in Human Breast Cancer. *Eur. J. Cancer* **2000**, *36* (8), 1038–1042. https://doi.org/10.1016/S0959-8049(00)00051-4.

(42) Fernandez-de-Cossio-Diaz, J.; Vazquez, A. Limits of Aerobic Metabolism in Cancer Cells. *Sci. Rep.* **2017**, *7* (1), 13488. https://doi.org/10.1038/s41598-017-14071-y.

(43) Jiang, B. Aerobic Glycolysis and High Level of Lactate in Cancer Metabolism and Microenvironment. *Genes Dis.* **2017**, *4* (1), 25–27. https://doi.org/10.1016/J.GENDIS.2017.02.003.

(44) Krasnov, G. S.; Dmitriev, A. A.; Snezhkina, A. V; Kudryavtseva, A. V. Deregulation of Glycolysis in Cancer: Glyceraldehyde-3-Phosphate Dehydrogenase as a Therapeutic Target. *Expert Opin. Ther. Targets* **2013**, *17* (6), 681–693. https://doi.org/10.1517/14728222.2013.775253.

(45) Tokunaga, K.; Nakamura, Y.; Sakata, K.; Fujimori, K.; Ohkubo, M.; Sawada, K.; Sakiyama, S. Enhanced Expression of a Glyceraldehyde-3-Phosphate Dehydrogenase Gene in Human Lung Cancers. *Cancer Res.* **1987**, *47* (21), 5616–5619.

(46) Rondinelli, R.; Epner, D.; Tricoli, J. Increased Glyceraldehyde-3-Phosphate Dehydrogenase Gene Expression in Late Pathological Stage Human Prostate Cancer. *Prostate Cancer Prostatic Dis.* **1997**, *1* (2), 66–72. https://doi.org/10.1038/sj.pcan.4500208.

(47) Vilà, M. R.; Nicolás, A.; Morote, J.; de Torres, I.; Meseguer, A. Increased Glyceraldehyde-3-Phosphate Dehydrogenase Expression in Renal Cell Carcinoma Identified by RNA-Based, Arbitrarily Primed Polymerase Chain Reaction. *Cancer* **2004**, *89* (1), 152–164. https://doi.org/10.1002/1097-0142(20000701)89:1<152::aid-cncr20>3.0.co;2-t.

(48) Mikuriya, K.; Kuramitsu, Y.; Ryozawa, S.; Fujimoto, M.; Mori, S.; Oka, M.; Hamano, K.; Okita, K.; Sakaida, I.; Nakamura, K. Expression of Glycolytic Enzymes Is Increased in Pancreatic Cancerous Tissues as Evidenced by Proteomic Profiling by Two-Dimensional Electrophoresis and Liquid Chromatography-Mass Spectrometry/Mass Spectrometry. *Int. J. Oncol.* **2007**, *30* (4), 849–855. https://doi.org/10.3892/ijo.30.4.849.

(49) Tang, Z.; Yuan, S.; Hu, Y.; Zhang, H.; Wu, W.; Zeng, Z.; Yang, J.; Yun, J.; Xu, R.; Huang, P. Over-Expression of GAPDH in Human Colorectal Carcinoma as a Preferred Target of 3-Bromopyruvate Propyl Ester. *J. Bioenerg. Biomembr.* **2012**, *44* (1), 117–125. https://doi.org/10.1007/s10863-012-9420-9.

(50) Xu, J.; Mahajan, K.; Xue, W.; Winter, J. O.; Zborowski, M.; Chalmers, J. J. Simultaneous, Single Particle, Magnetization and Size Measurements of Micron Sized, Magnetic Particles. *J. Magn. Magn. Mater.* **2012**, *324* (24), 4189–4199. https://doi.org/10.1016/j.jmmm.2012.07.039.

(51) Hoogenboom, R.; Fijten, M. W. M.; Kickelbick, G.; Schubert, U. S. Synthesis and Crystal Structures of Multifunctional Tosylates as Basis for Star-Shaped Poly(2-Ethyl-2-Oxazoline)S. *Beilstein J. Org. Chem.* **2010**, *6*, 773–783. https://doi.org/10.3762/bjoc.6.96.

(52) Cahiez, G.; Lefèvre, N.; Poizat, M.; Moyeux, A. A User-Friendly Procedure for the Preparation of Secondary Alkyl Chlorides. *Synthesis (Stuttg).* **2012**, *45* (02), 231–236. https://doi.org/10.1055/s-0032-1317927.

(53) Chevillet, J. R.; Kang, Q.; Ruf, I. K.; Briggs, H. A.; Vojtech, L. N.; Hughes, S. M.; Cheng, H. H.; Arroyo, J. D.; Meredith, E. K.; Gallichotte, E. N.; Pogosova-Agadjanyan, E. L.; Morrissey, C.; Stirewalt, D. L.; Hladik, F.; Yu, E. Y.; Higano, C. S.; Tewari, M. Quantitative and Stoichiometric Analysis of the MicroRNA Content of Exosomes. *Proc. Natl. Acad. Sci. U. S. A.* **2014**, *111* (41), 14888–14893. https://doi.org/10.1073/pnas.1408301111.

(54) Eldh, M.; Ekström, K.; Valadi, H.; Sjöstrand, M.; Olsson, B.; Jernås, M.; Lötvall, J. Exosomes Communicate Protective Messages during Oxidative Stress; Possible Role of Exosomal Shuttle RNA. *PLoS One* **2010**, *5* (12), e15353. https://doi.org/10.1371/journal.pone.0015353.

(55) Lässer, C.; Seyed Alikhani, V.; Ekström, K.; Eldh, M.; Torregrosa Paredes, P.; Bossios, A.; Sjöstrand, M.; Gabrielsson, S.; Lötvall, J.; Valadi, H. Human Saliva, Plasma and Breast Milk

Exosomes Contain RNA: Uptake by Macrophages. *J. Transl. Med.* **2011**, *9* (1), 9. https://doi.org/10.1186/1479-5876-9-9.

(56) Yuan, T.; Huang, X.; Woodcock, M.; Du, M.; Dittmar, R.; Wang, Y.; Tsai, S.; Kohli, M.; Boardman, L.; Patel, T.; Wang, L. Plasma Extracellular RNA Profiles in Healthy and Cancer Patients. *Sci. Rep.* **2016**, *6* (1), 19413. https://doi.org/10.1038/srep19413.

(57) Eldh, M.; Lötvall, J.; Malmhäll, C.; Ekström, K. Importance of RNA Isolation Methods for Analysis of Exosomal RNA: Evaluation of Different Methods. *Mol. Immunol.* **2012**, *50* (4), 278–286. https://doi.org/10.1016/j.molimm.2012.02.001.

Chapter 4. Vertical Flow Assay for breast cancer derived exosomes

4. Vertical Flow Assay for breast cancer derived exosomes

4.1 Abstract

The design of a Vertical Flow Assay (VFA) for the visual detection of exosomes derived from metastatic breast cancer cell lines (SKBR3 and MDA-MB-231) is presented. The VFA relies on the detection of membrane proteins on the exosomes (CD9, CD3, CD81 and EGFR1) in an ELISA-like format by using antiCDx and a secondary antibody labelled with alkaline phosphatase (ALP). In this paper-based approach is explored for the first time the visual readout achieved by the activity of the ALP enzyme upon the reaction of NBT/BCIP substrate to obtain the indigo dye insoluble product, which precipitates in the paper substrate. The design, materials, and construction of the VFA are optimized for the ALP labelling in terms of pore size, type of membrane and blocking agents. In all instances, the signal provided by the alkaline phosphatase (ALP) is directly addressed by visual readout, and further quantified by a smartphone and an image analysis software. Promising results are obtained for the potential use of paper-based VFA for the rapid (15 min) with an estimated limit of detection of $6 \cdot 10^7$ exosomes μL^{-1} and cost-effective analysis of cancer derived exosomes, avoiding the use of nanoparticles-based signal generating systems in a simpler format.

Keywords: Exosomes, alkaline phosphatase, breast cancer, liquid biopsy, Vertical Flow Assay, paper-based RDTs.

4.2 Introduction

The characterization of exosomes and other extracellular vesicles (EVs) is a challenging task due to their nanometric sizes that makes them out of the sensitivity range to most cell-oriented analysis platforms. Most of the techniques require extensive pre-treatment protocols, as well as the use of expensive equipment and skilled personnel. Despite this, portable devices have been reported, mainly based on electrochemical readout.[1–3] Still, there is a lack of RDTs (Rapid Diagnostic Test) following REASSURED criteria[4] for the detection and characterization of those nano-sized vesicles with simple and cost-effective assays.

Accordingly, the development of paper-based platforms for exosomes could provide interesting analytical features. Lateral Flow Assay (LFA) and Vertical Flow Assay (VFA) are based on the reaction of the analyte with a signal generating system which provides a naked-eye readout, integrated on a cellulose membrane and in a simple-to-use approach.[5] Nevertheless, those methodologies are not ideal when dealing with low analyte concentrations. As they rely on signals for naked-eye detection, often paper-based tests do not contain any readout amplification steps, as instrumental detection techniques. The use of nanomaterials, as gold nanoparticles or fluorescent beads, are usually implemented for enhancing the visual signals and improving the LODs.[5,6] Besides, the use of reader instruments enhance analytical capabilities, enabling to obtain quantitative analytical information which, in some instances, show similar LODs than biosensing device.[7] There are commercially available LFA readers, as iPeak (IUL Instruments, Barcelona, ES), ESEQuant Flex (Dialunox, Stokach, DE), just to mention a few. Even more interesting, nowadays the camera of almost any smartphone could be used for the optical readout. Many examples have been published with LFA strips, as for the detection of five mycotoxins in cereal samples using gold nanoparticles or fluorescent beads[8], or for the detection of prostate-specific antigens using quantum-dots fluorescent signals.[9] Also in the case of VFA, this reading strategy was used. For example, in the detection of multiple allergen detection[10], or for the detection of mycobacteria based on double-tagging PCR.[11]

In the case of exosomes, the detection of exosomes by LFA presents some intrinsic issues related with capillarity and active exosome movement through the hydrophilic membrane because of their bilipidic membrane.[12] Moreover the heterogeneity of EV in the samples can be a handicap for the uniform mobility of the front line. This fact clearly makes more difficult the application of lateral flow methods for the analysis of EVs.

Still, some attempts were reported. Mainly, they are based on LFA targeting membrane proteins of exosomes, usually ubiquitous markers as tetraspanin receptors CD9, CD63 and CD81[13–18] and showing LODs of around 10^7 EVs μL^{-1}. As a shortcoming of this approach, the device is not a fully integrated LFA strip. In order to prevent non-specific adsorption, the approach is based on a non-traditional LFA format in which the signal generating system is not stored in an integrated strip but preincubated with the exosomes aside from the strip, in a tube, in which the strip is then dipped in.

In this study, the mobility issues of EVs in paper-based platforms are prevented by the design of a different approach in which we take advantage of the hydrophobic

interaction between EVs and nitrocellulose membranes. It is based on Vertical Flow Assay, an alternative paper-based format, inspired on a classic dot blot immunoassay.[19] In VFA, also named flow-through assay, the direction of the liquid flow is perpendicular to the membranes and not parallel as in LFA.[20] The liquid flows through the different paper membrane layers of the system and provides even more rapid flow than LFA, as in this case capillarity forces are helped by gravity. This fact clearly reduces the assay time. VFA traditionally uses biologically-modified gold nanoparticles as signal generating system.[10,20–23] For example, in our research group, we have explored a VFA for the detection of mycobacteria.[11] That assay was based on the detection of double-tagged PCR amplicons and used streptavidin-modified gold nanoparticles to generate a visual signal, that was further quantitatively analyzed using an smartphone camera.[11] On the other hand, , enzymatic signal-generating systems are also suitable, being a competitive advantage over LFA.[21] In this study, the optical readout is based on alkaline phosphatases (ALP, EC 3.1.3.1). These enzymes catalyze the hydrolysis of phosphate monoesters in alkaline conditions, into inorganic phosphate and its corresponding alcohol.[24] The main advantage of ALP as a readout system in VFA relies on the fact that the enzymatic activity can be easily coupled with a myriad of substrates which, upon reaction, provide insoluble products which are stabilized on a paper substrate due to the vertical flow. As a shortcoming, the turnover number of ALP is low compared to other common enzymatic labels, reducing the sensitivity of the approach. The kinetics of the reaction of ALP with its substrate have a rate-limiting step in the hydrolysis of the covalent bond between the phosphate group and its corresponding alcohol. One the other hand, other reporters as horseradish peroxidase enzyme, catalyze a redox reaction, consequently with much faster kinetics.

In this study, the design, construction, and experimental parameters of VFA for the determination of exosomes derived from breast cancer cell lines using ALP as enzymatic label are described. An ELISA-like VFA format is proposed as a semiquantitative test for the determination of membrane proteins in exosomes, using a smartphone for the reading of the visual signals. Besides, the intrinsic ALP activity of the exosomes is also studied and compared with the gold-standard microplate assay.

4.3 Experimental

4.3.1 Instrumentation

Nanoparticle tracking analysis (NTA) was performed using the NanoSight LM10-HS system with a tuned 405 nm laser (NanoSight Ltd, Malvern, GB). Spectrophotometric measurements were performed on a Tecan Infinite m200 PRO (Tecan Group Ltd,

Männeford, CH) microplate reader controlled by Magellan v7.0 software. Flow cytometry was performed using Cytoflex LX (Beckman Coulter Inc, Indianapolis, IN, US), and analyzed with integrated software Cytexpert and FlowJo analysis software (FlowJo LLC, BD, NJ, US). Besides, for the visual signal quantification, pictures from the VFA cartridges were taken with a 12 megapixels smartphone camera at a distance of 23 cm, using a LED illumination support with 1100 Lm intensity, and a color temperature of 6000-6500 K. The pictures were treated and analyzed using the gel analysis tool from Fiji ImageJ software. [25]

The cartridges for the vertical flow assay devices (RVF, VF-1-01) were purchased from MedMira (Halifax, CA). Different membranes were tested in the VFA cartridges, following the design shown in Figure 4.1. Further experimental details and product references can be found in Table 4.2 (Supp. data). Figure 4.1, panel A shows the different components of the VFA cartridge. All details of VFA construction and materials are provided in §4.6.1 (Supp. data).

4.3.2 Chemicals and biochemicals

Calf intestine alkaline phosphatase enzyme (ALP, ref. 10713023001) was purchased from Roche Diagnostics (Merck kGaA, Darmstad, GE). The substrates for ALP used were para-nitrophenyl phosphate (pNPP, ref. 34045) and NBT/BCIP (1-Step NBT/BCIP Substrate Solution, ref. 34042) from Thermo Fisher Scientific (MA, US). Magnetic particles (MPs) tosylactivated (Dynabeads™ M450 Tosylactivated, ref. 14013) were purchased from Thermo Fisher Scientific (MC, US). The mouse monoclonal antibodies against tetraspanins, antiCD9 (ref. 10626D), antiCD63 (ref. 10628D), antiCD81 (ref. 10630D), and goat polyclonal antiMouse ALP conjugate (ref. 31320) was purchased from Thermo Fisher Scientific. The mouse monoclonal antibody against specific EGFR1 (Epithelial growth factor receptor, type 1) protein (ref. ab30) was purchased from Abcam (Cambridge, GB). For the cell culture, Dulbecco's Modified Eagle's Glutamax (DMEM, ref. 31966-021) and Dulbecco's Modified Eagle's/Ham's F-12 Nutrient (DMEM/F12, ref. 31331-028) mediums, and fetal bovine serum (FBS, ref. 26140079) were purchased from Gibco (Thermo Fisher Scientific). All other reagents were in analytical reagent grade. For the protein quantification, Pierce BCA Protein Assay kit (ref. 23227) was purchased from Thermo Fisher Scientific. The composition of all buffers and solutions is described in §4.6.1 (Supp. data).

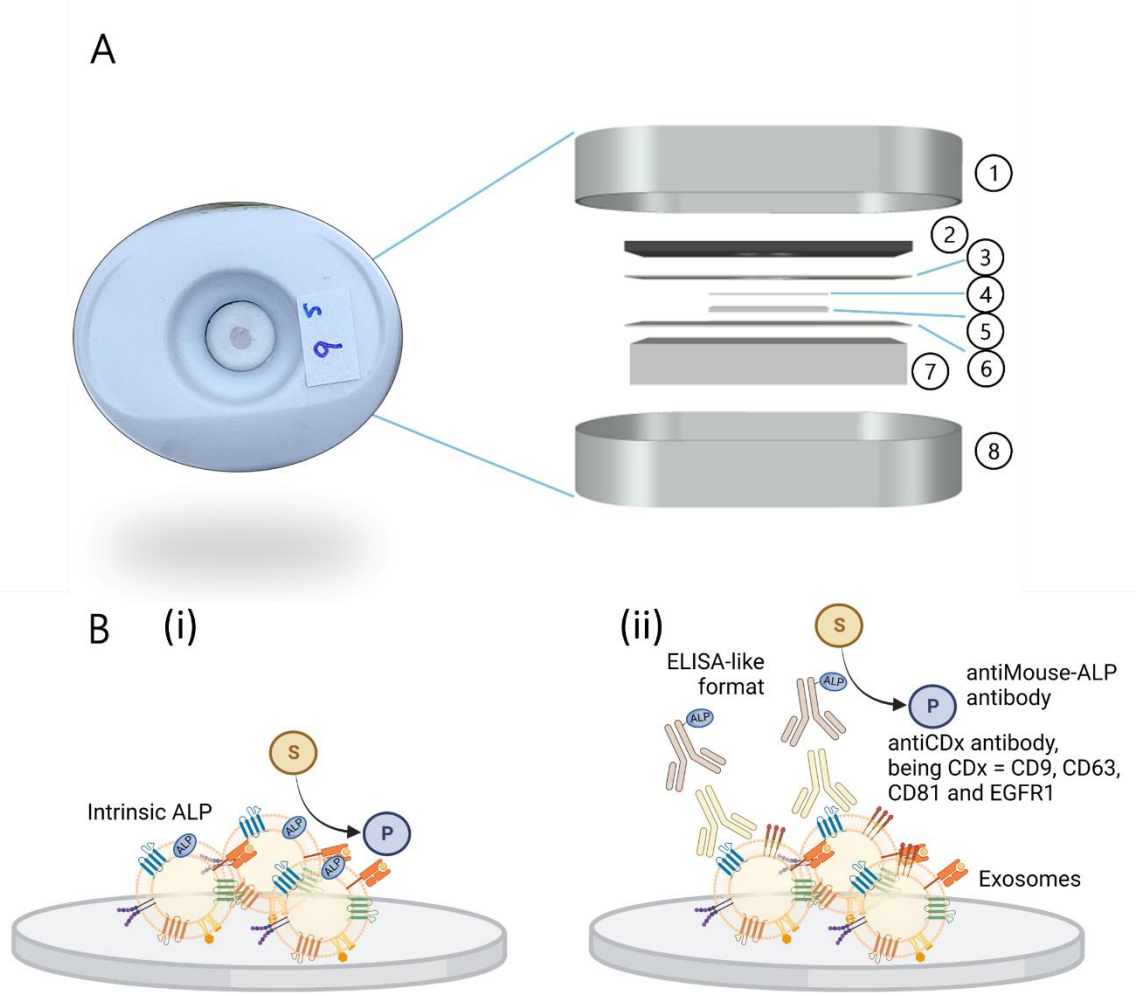

Figure 4.1. Panel A shows a schematic representation of the components for a VFA cartridge including the cover (1) and the support (8) and of the plastic MedMira cassette. Also (2) corresponds to a plastic support of the commercial device. Several membranes are attached to this plastic support using double-sided tape (3), as a nitrocellulose membrane (4), a medium weight cotton linter pad (5), plus a filter paper (6). Finally, an absorption cotton linter thick pad (7) was placed below the plastic support. Panel B shows the details of the two VFA approaches. (i) VFA for the determination of the intrinsic ALP activity of exosomes. (ii) ELISA-like VFA format relying on the detection of membrane proteins on the exosomes (CD9, CD3, CD81 and EGFR1) by using antiCDx and a secondary antibody labelled with ALP. Created with BioRender.com.

4.3.3 Cell culturing, exosome isolation and purification

Breast cancer cell lines SKBR3 (ATCC, ref. HTB-30) and MDA-MB-231 (ATCC, ref. HTB-26), and human fetal osteoblasts cell line (hFOB 1.19, ATCC ref. CRL-11372) were grown as described in §4.6.2 (Supp. data). Exosomes were purified from cell culture supernatant by differential ultracentrifugation as previously reported by our research group with minor changes.[2] Exosomes were resuspended in 10 mmol L^{-1} tris buffer solution (pH 7.4, 0.22 µm sterile-filtered) and stored at –21 °C. All exosomes purification steps are provided in §4.6.2 (Supp. data).

4.3.4 Characterization of exosomes by nanoparticle tracking analysis, cryogenic transmission electron microscopy and BCA protein assay

The size distribution and concentration of particles were estimated by NTA. The purified exosomes were diluted in filtered PBS buffer solution, between 500 and 10,000-fold depending on the sample initial concentration. Nanosight NTA software analyzed raw data videos by triplicate during 60 s with 25 frames/s. Cryogenic TEM images were collected by a Jeol JEM 2011 (JEOL USA Inc, US) transmission electron microscope at an accelerating voltage of 200 kV. Exosomes were maintained at -182 °C with liquid ethane during the whole process. The total protein concentration of the exosomes was estimated using the Bicinchoninic acid protein assay (BCA), following the manufacturer instructions, using bovine serum albumin (BSA) standards in tris buffer solution. The spectrophotometric measurement was done at 562 nm using a Tecan Infinite m200 PRO microplate reader.

4.3.5 Spectrophotometric determination of the ALP activity in exosomes

The gold-standard colorimetric assay for ALP activity in the exosomes samples was based on the monitoring of reaction rate (micromoles hydrolysed per minute, µmol min^{-1}) of p-nitrophenol phosphate (pNPP) substrate in DEA buffer, into p-nitrophenol (pNP). Absorbance data was converted into the rate of substrate hydrolysed, or enzyme activity (U L^{-1}), and further normalized to obtain specific activity (normalized by NTA particle concentration, or BCA total protein concentration). The protocol in detail of the spectrophotometric assay and activity calculation are described in §4.6.3.

4.3.6 Characterization of exosomes by flow cytometry

Flow cytometry was used to estimate the presence of membrane protein markers of interest in the surface of exosomes derived from SKBR3 and MDA-MB-231 breast cancer cell lines. Specifically, the presence of tetraspanin receptors CD9, CD63 and CD81, and epithelial specific EGFR1 receptor were evaluated. The flow cytometry assay is based on the immobilization of exosomes on the surface of magnetic particles, to increase its size within the resolution of the flow cytometer. To achieve that, 3.5 x 10^{10} EVs were covalently immobilized on 1.6 x 10^{7} MPs, as detailed described in §4.6.4 (Supp. data), followed by the indirect labelling with antiCDX (mouse) and antiMouse Cy5 secondary antibody (being CDX either CD9, CD63, CD81 or EGFR1 biomarkers).

4.3.7 Optimization of VFA design

The construction of VFA was carefully optimized, including all membranes and materials to improve the flow rate, enhance the sensitivity of the assay and reduce non-

specific background signals. As model analytes for optimization experiments, ALP enzyme and exosomes derived from SKBR3 cell line were used. To optimize the immobilization of exosomes on the VFA, different nitrocellulose membranes were tested, including unbacked nitrocellulose membranes for LFA of increasing capillarity flow rate (AE98, AE99, AE100), and cellulose nitrate membranes (NC membranes) of 0.1, 0.2 and 0.45 µm pore sizes. Besides, Protran BA85 (0. 45 µm pore size) membrane was also tested as standard blotting nitrocellulose membrane. Table 4.2 provides all details from the materials tested. As model analytes for the readout optimization, 500 mU mL^{-1} dilutions of ALP were used. To optimize the blocking of nitrocellulose membranes, different protein and non-protein agents were tested. Specifically, the blocking solution was the following: skimmed milk (2% w/v solution in tris buffer), casein (2% w/v solution in tris buffer), bovine serum albumin (2% and 5% w/v solution in tris buffer), glycine (0.5 mol L^{-1} in tris buffer) and poly-ethylene glycol (2% w/v in tris buffer). As model analytes, different dilutions of ALP conjugate of 500 mU mL^{-1}, 166 mU mL^{-1}, and 55 mU mL^{-1} were used. Besides, other experimental parameters were tested as immobilization time, the cellulose membrane used as sample pad, and the addition of a non-absorbent separation layer. The optimization experiments were performed following the standard protocol detailed in §4.6.5 and 4.6.6 (Supp. data) for testing of all nitrocellulose membranes and blocking solutions.

4.3.8 Vertical Flow Assay for the determination of membrane biomarkers in exosomes

The determination of the surface proteins of the EVs was done on a VFA nitrocellulose membrane in an ELISA-like format with indirect labelling, as shown in Figure 4.1, panel B (ii). In this assay, mouse monoclonal antibodies against markers of interest (tetraspanins CD9, CD63 and CD81, and epithelial specific EGFR1) were used to react with the immobilized exosomes. As secondary antibody, an antimouse-ALP conjugate antibody was used. The readout of the signals was done with NBT/BCIP substrate.

Briefly, the determination of surface markers on exosomes using VFA starts with the immobilization of 2 µL of the sample containing the exosomes on the nitrocellulose membrane by air drying at 4ºC for 1 h. The blocking of the membrane was done by adding 200 µL of BSA 2% (w/v) and air drying for 2 h at 37ºC. After blocking, washing was performed with 200 µL of tris buffer. Then, the indirect labelling was performed in one-step, by adding 100 µL of antibody solution mix and incubating for 1 h at 37 ºC. The solution mix contains the primary (0.5 µg mL^{-1}) and secondary (30 ng mL^{-1}) antibodies.

After labelling, the washing was performed with 300 µL of tris buffer. Finally, the readout was achieved by adding 10 µL of NBT/BCIP substrate. The substrate combines nitro-blue tetrazolium chloride (NBT) and 5-bromo-4-chloro-3'-indolyphosphate p-toluidine (BCIP). After just 15 minutes reaction, the membranes were washed again with 100 µL of tris buffer. The phosphate of BCIP is hydrolyzed by ALP, producing an intermediate that dimerizes to indigo dye upon oxidation with NBT, which is reduced to NBT-formazan. Both reaction products create an intense blue-purple precipitate on the surface of the VFA, which can be easily visualized with the naked eye. Besides the visual detection, the analytical performance of the assay was determined by imaging the colored dots using a smartphone camera under white LED light. The protocol of the assay is detailed described in §4.6.5 (Supp. data).

The working range of this assay was estimated by creating a calibration curve with exosomes derived from SKBR3 and MDA-MB-231, detected by antiCD81, as universal exosome marker, and antimouse-ALP conjugate. The range of concentrations comprise from 0 to $3 \cdot 10^8$ particles μL^{-1} according to NTA count.

To assess the specificity of the assay, different antibodies were tested with exosomes derived from SKBR3 and MDA-MB-231. antiCDx Mouse monoclonal antibodies specific against tetraspanins (CD9, CD63 and CD81), and epithelial specific biomarker EGFR1 were used. Beside the negative controls, other control were tested to determine the signal of the intrinsic ALP activity from the exosomes[1,26], performed as the positive test but avoiding the adding of the primary and secondary antibody.

The statistical analyses were performed using GraphPad Prism 8 (CA, US). The value $p < 0.05$ was considered significant.

4.3.9 Vertical Flow Assay for the determination of ALP activity in exosomes

To determine the intrinsic activity of ALP in exosomes by VFA, as shown in Figure 4.1, panel B (i), 2 µL of sample were immobilized on the nitrocellulose membrane by air drying in the fridge (4ºC) for 1 hour. Then, the remaining active sites of the nitrocellulose were blocked by adding 200 µL of BSA 2% (w/v) and air drying for 2h at 37ºC. The membrane was washed with 400 µL of Tris buffer. Then, 10 µL of NBT/BCIP substrate was added and the reaction was carried out for 2h at 37ºC. Finally, the nitrocellulose membrane was washed with 100 µL of Tris buffer and imaged using a smartphone camera under white LED light. The detailed protocol of the assay can be found in §4.6.6.

In this case, exosomes derived from SKBR3 and MDA-MB-231 were analyzed. Also, an ALP overexpressing exosomes sample from human fetal osteoblast (hFOB) cell

line were also analyzed. A calibration curve was created for each cell line, with dilutions ranging from 0 particles μL^{-1} to $7 \cdot 10^8$ particles μL^{-1}, according by NTA measurements. The dilutions used for the quantification in the microplate pNPP assay (§4.3.5) and in VFA cartridges were prepared from the same exosome samples, using 2, 4, 8 and 20-fold dilution factors. It should be noted that exosomes derived from SKBR3 were further diluted 8-fold to normalize its particle concentration according to NTA count.

The statistical analyses were performed using GraphPad Prism 8 (CA, US). The value $p < 0.05$ was considered significant.

4.3.10 Safety considerations

All works were performed in a Biosafety cabinet, and all material was decontaminated by autoclaving or disinfected before discarding following U.S. Department of Health and Human Services guidelines for level 2 laboratory Biosafety.[27]

4.4 Results and discussion

4.4.1 Characterization of exosomes by nanoparticle tracking analysis and cryogenic transmission electron microscopy

The NTA analysis of exosomes derived from SKBR3, MDA-MB-231 and hFOB cell lines revealed a similar size distribution. Figure 4.2 summarizes the results for the three cell lines derived exosomes. The size distribution histogram of SKBR3 exosomes shows only a peak at 115 nm. In the case of MDA-MB-231 exosomes, two peaks at 115 and 145 nm, and a smaller peak at 285 nm corresponding to small aggregates (Fig. 4.2, panel B). In the case of hFOB, NTA reveals a clear peak at 135 nm, and two smaller ones at 195 and 315 nm (Fig. 4.2, panel C). The exosomes were further imaged by Cryo-TEM, confirming the presence of individual and small aggregates of vesicles in the range between 50 and 400 nm, as shown in Figure 4.2.

Beside the size distribution, the particle and protein concentration were estimated by NTA and BCA protein assay, respectively. Exosomes derived from SKBR3 showed higher concentration (2.69 / SD 0.19 x 10^{12} particles mL^{-1} and 1.038 mg mL^{-1} total protein) than MDA-MB-231 (3.24 / SD 0.04 x 10^{11} particles mL^{-1} and 0.324 mg mL^{-1} total protein) and hFOB (3.47 / SD 0.04 x 10^{11} particles mL^{-1} and 0.310 mg mL^{-1} total protein). Table 4.1 summarizes the results.

Table 4.1. Particle concentration and total protein concentration of EVs samples

Sample	Particle concentration (particles mL^{-1})	Protein concentration (mg mL^{-1})
SKBR3	2.69 / SD 0.19 $\cdot 10^{12}$	1.038
MDA-MB-231	3.24 / SD 0.04 $\cdot 10^{11}$	0.324
hFOB	3.47 / SD 0.04 $\cdot 10^{11}$	0.310

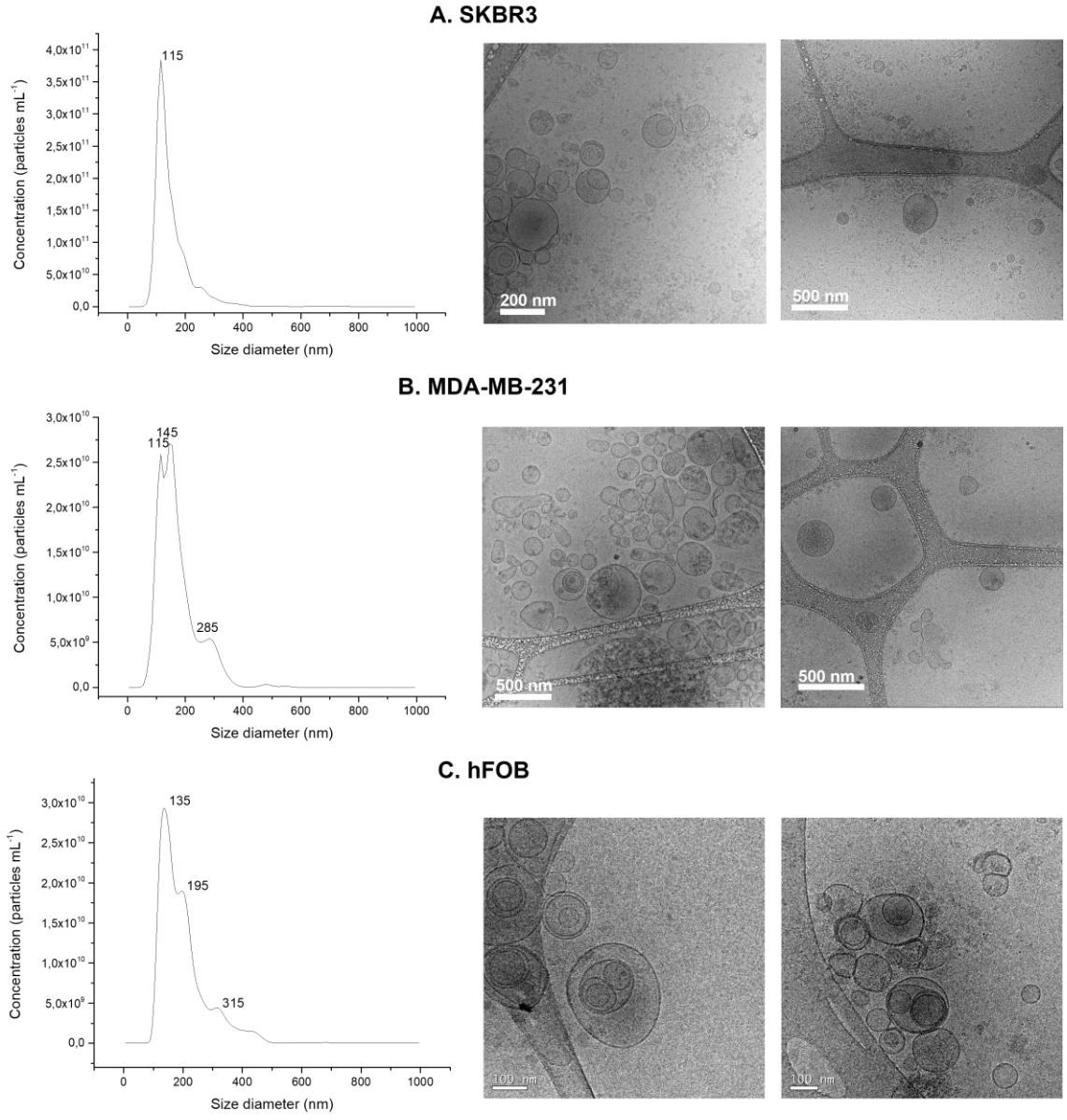

Figure 4.2. Characterization by NTA and Cryo-TEM micrographs of purified EVs samples from SKBR3 (panel A), MDA-MB-231 (panel B) breast cancer cell lines, and from hFOB (panel C) osteoblasts cell line. The NTA has been performed in the ICTS "NANBIOSIS" NTA analysis service of Institut de Ciència dels Materials de Barcelona. The Cryo-TEM images were obtained in the Service of Microscopy at Universitat Autònoma de Barcelona.

4.4.2 Characterization of exosomes by flow cytometry

The flow cytometry assay was performed staining the exosomes immobilized on magnetic particles, as previously described by our research group[1–3]. Figure 4.3 shows the histograms obtained from the bead-based flow cytometry assay of exosomes derived from SKBR3 and MDA-MB-231 as well as the percentage of positivity. As expected, tetraspanins CD9, CD63 and CD81, considered as general biomarkers of exosomes, were identified in both samples. Regarding the specific epithelial marker EGFR1, it was also confirmed in both samples, with 13% in SKBR3 exosomes and 37% in MDA-MB-231 exosomes. Dot blots of the flow cytometry results are shown in Figure 4.9 (Supp data) as well as a heat map representation of the positivity percentage.

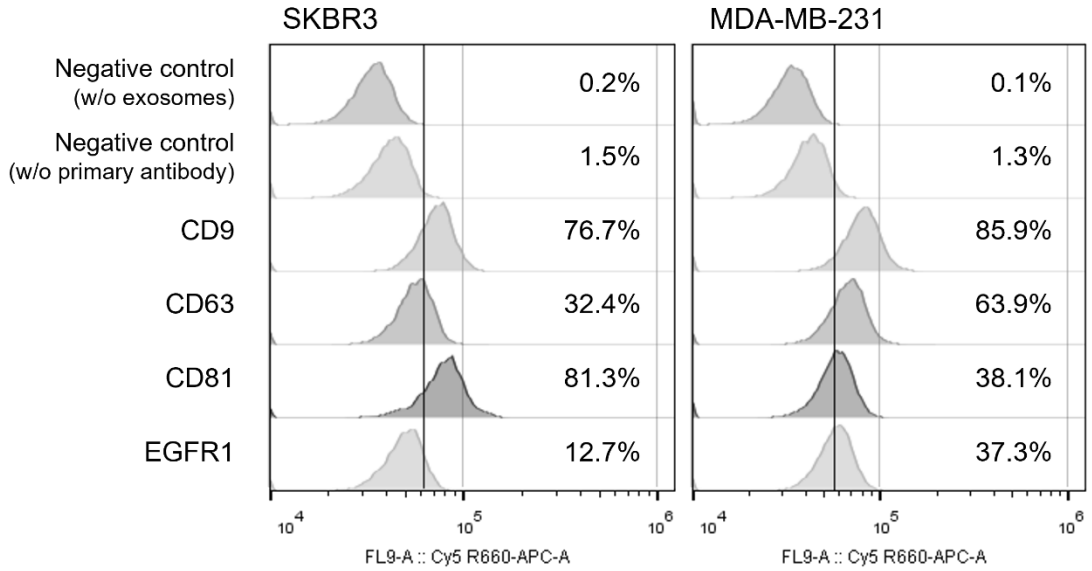

Figure 4.3. Histograms plots of the bead-based flow cytometry assay. Left panel corresponds to SKBR3 exosomes-modified MPs, and right panel, to MDA-MB-231 exosomes-modified MPs.

4.4.3 Optimization of VFA design

The most relevant experimental parameters related with the VFA construction and protocol were optimized in terms of the analytical performance based on the visual readout, including the optimization of the nitrocellulose membrane material, the pore size and blocking step.

Three different pore size for the nitrocellulose membrane were tested, ranging from 0.1 to 0.45 µm, using ALP adsorbed on the membrane at an activity of 1 mU (500 mU mL^{-1}). Figure 4.4, panel A, shows the images of three replicates of VFA cartridges, further analyzed, and quantified with ImageJ. No significant differences were observed with naked eye between the cellulose nitrate membranes tested, but the quantification

revealed that 0.2 µm showed an increased signal. Accordingly, further experiments were performed with this pore size.

The optimization of the type of membranes (including nitrocellulose, Protran BA85 and unbacked membranes AE98, AE99 and AE100) are described in Figure 4.4, panel B, in the ELISA-like formats described in Figure 4.1, panel B (ii) (based on antiCD81 mouse primary antibody an antimouse ALP-labelled secondary antibody) in exosomes derived from SKBR3 cell line. In all cases, the corresponding negative control (processed without exosomes) was included. It is important to select the membrane with lower background signals, as the labelling comes from the incubation with labelled antibodies, not from the deposited analyte. Figure 4.4, panel C, shows the images for the VFA cartridges, revealing clear differences between the membranes tested and the negative control in all cases. Particularly, unbacked membranes AE98, AE99 and AE100 showed less colored and more diffuse signals in all instances. On the other hand, Protran BA85 and NC 0.2 membranes show clear visual positive areas, with evident differences between negative (without exosomes) and positive samples. According to the results, in all cases nitrocellulose membranes 0.2 µm pore size were selected in further experiments.

Besides, the blocking agent for the nitrocellulose membranes was also optimized using different buffers, as shown in Figure 4.4, panel C. Casein and skimmed milk clearly reduce the appearance of colored signal in the membrane. In the case of glycine blocking solution, it provides clear purple signals at the test dot, although yellowish background also appears. Regarding BSA and PEG blocking solutions, both provide optimal blocking of the background and high intensity purple signals. According to ImageJ quantification, BSA 2% (w/v) solution was finally selected for further experiments.

4.4.4 Vertical Flow Assay for the determination of membrane biomarkers in exosomes

A calibration plot of the ELISA-like format was performed using an antiCD81 monoclonal antibody against the biomarker and a secondary ALP labelled antibodies. The results are shown in in Figure 4.5, panel A, for SKBR3 and MDA-MB-231 derived exosomes. The VFA assay signal are detectable at concentrations higher than 10^7 particles μL^{-1} with the proposed protocol using antiCD81 antibody. Specifically, the limits of detection estimated for the SKBR3 derived exosomes is $6.00 \cdot 10^7$ particles μL^{-1} while for MDA-MB-231 being $5.96 \cdot 10^7$ particles μL^{-1}. This LOD is calculated at 15 min reaction time, but it can be improved in those cases in which the number of exosomes is limited, by increasing the reaction time.

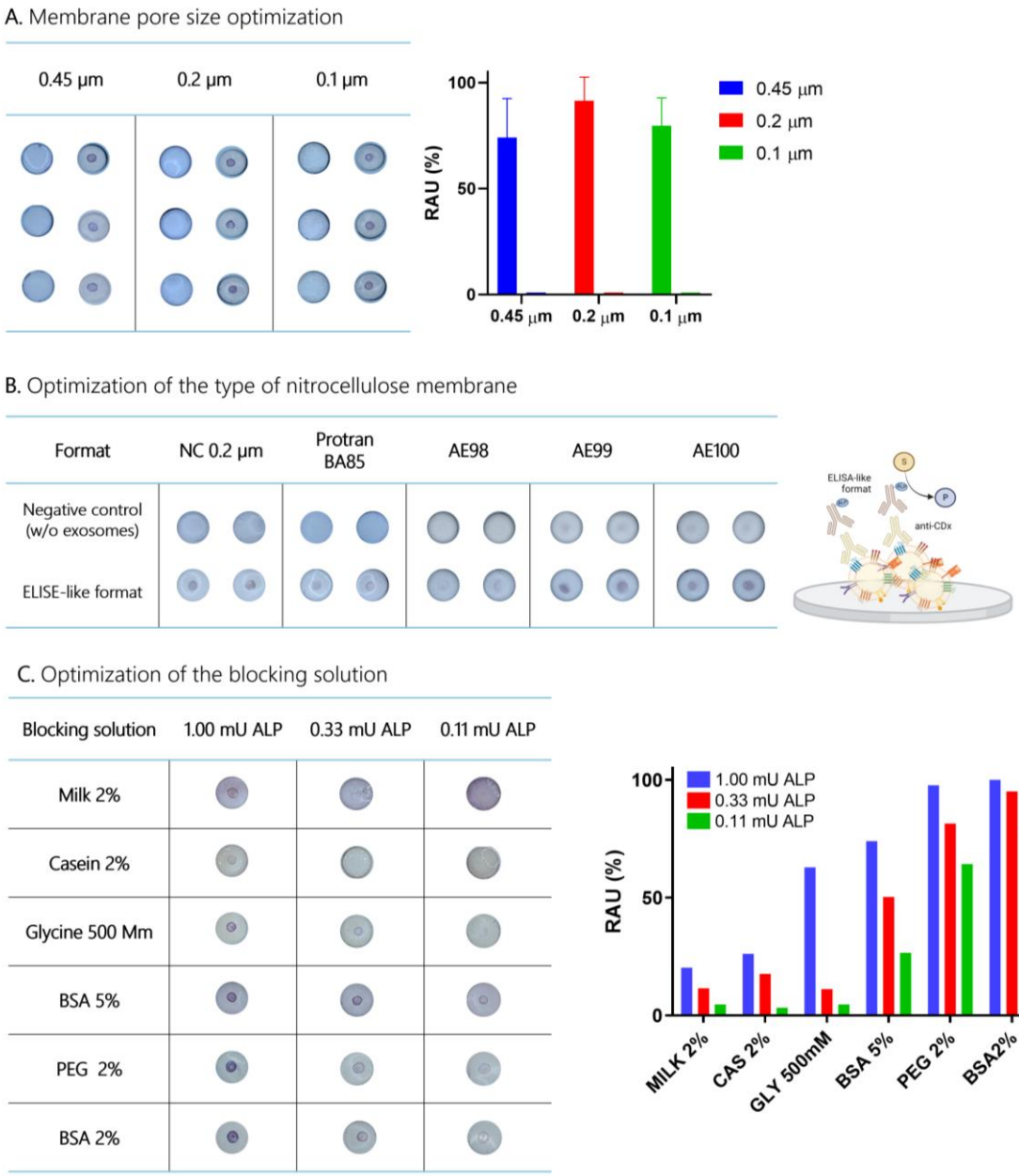

Figure 4.4. Panel A. Optimization of the pore size of nitrocellulose membrane. The images show the VFA cartridges of nitrocellulose membranes at different pore size (0.45, 0.2 and 0.1 µm) performed with 1 mU ALP. The bar plot shows the Image J colorimetric quantification of the visual signals, in relative area units, normalized by the maximum signal (n=3). Panel B. Optimization of the type of nitrocellulose membrane. The images show the VFA cartridges with different nitrocellulose membranes for the ELISA-like format. Panel C. Blocking solution optimization. The images of the VFA cartridges with ALP at 1 mU, 0.33 mU, and 0.11 mU of ALP. Different blocking agent solutions in tris buffer were tested. The plot with the ImageJ colorimetric quantification of the visual signals, in relative area units, normalized by the maximum signal is also shown. The negative controls are included in all cases.

The specificity of the assay was confirmed by reaction with a panel of antibodies against tetraspanins and EGFR1 biomarkers. Figure 4.5, panel B, shows the VFA cartridges with 2 µL of immobilized exosomes of SKBR3 and MDA-MB-231, labelled with CD9, CD63, CD81 and antiEGFR1, and the corresponding negative controls, and a

control showing the intrinsic activity of the exosomes, as detailed in §4.3.9. Compared with that negative control of intrinsic ALP activity, the labelling with ALP conjugated secondary antibodies clearly enhances the reaction rate as higher amounts of enzyme are ready to react with the substrate on the surface of the VFA, producing higher signals.

Higher intensities in all VFA cartridges reacting with primary and secondary antibodies are shown, with different intensities proportional to the presence of the biomarker in the surface of the exosomes. The colorimetric quantification with ImageJ (§4.6.5, Supp. data) confirms the naked-eye interpretation, showing a 2 to 5-fold increase in the peak areas, compared to negative controls. From that data, a heat map of the signals was then calculated for the semi-quantitative analysis of the different protein markers. The area signals were normalized respect to antiCD63 signals, which showed similar profile in both exosome samples. Then, relative expression ratios were calculated for the different protein markers, as shown in the heat map. In the case of SKBR3 exosomes, the three tetraspanins have similar expression, with relative ratios of 1.07 and 1.11 for CD9 and CD81, respectively. In the case of EGFR1 is expressed only a 0.41 as the CD63 biomarker. For the MDA-MB-231 exosomes, CD9 has a similar expression with a relative ratio of 0.92; while CD81 account for a 0.61 as the CD63. Regarding EGFR1, this marker is expressed a 0.64 ratio as the CD63. These results are similar to those obtained with the bead-based flow cytometry study, showing a good agreement in the protein expression patterns of both methods.

A. Calibration plot SKBR3 and MDA-MB-231 exosomes

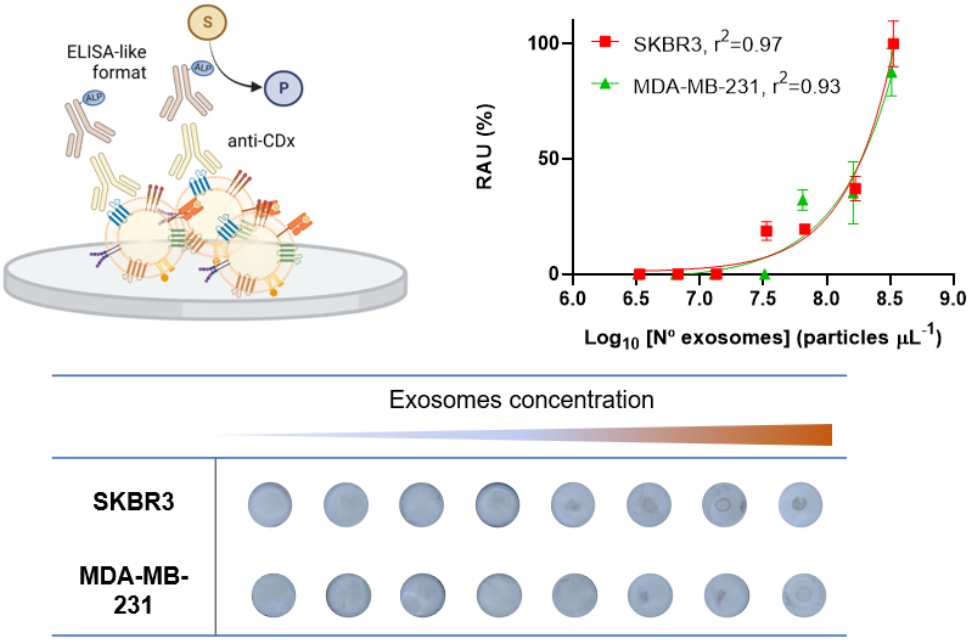

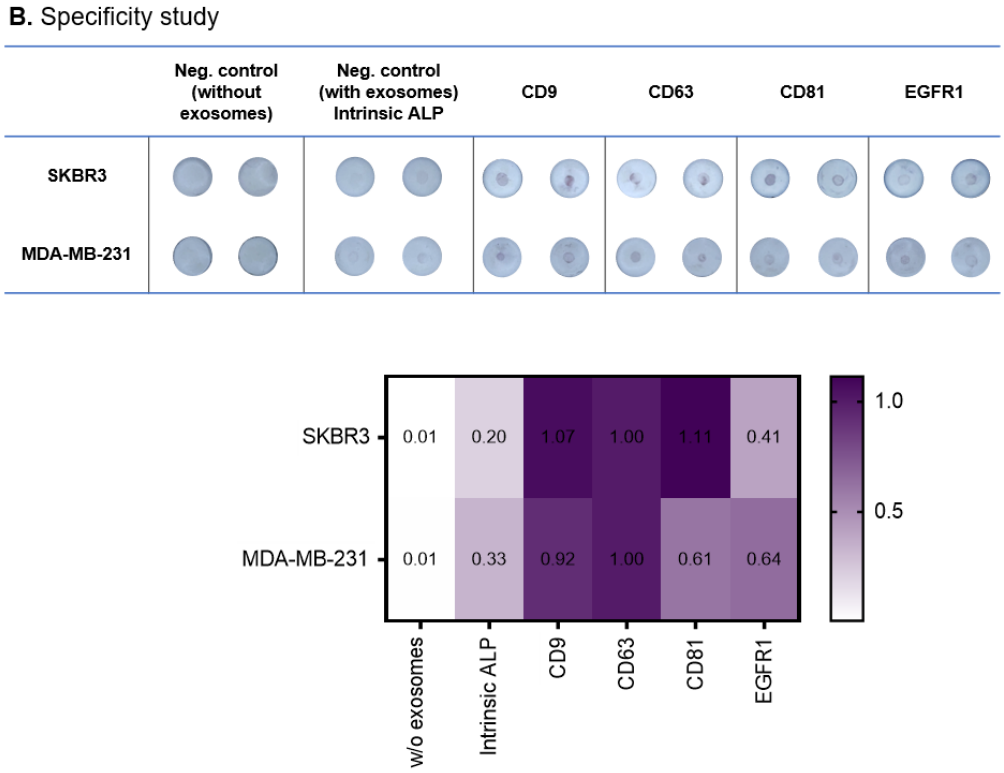

Figure 4.5. ELISA-like VFA format determination of surface protein markers. Panel A shows calibration plots with exosomes derived from SKBR3 and MDA-MB-231 using CD81 as primary antibody, general markers for exosomes. Panel B shows pictures of the cartridges obtained with a panel of antibodies against markers of interest (CD9, CD3, CD81 and EGFR1) using exosomes derived from SKBR3 and MDA-MB-231, plus a heat map of the colorimetric signals.

4.4.5 Intrinsic ALP activity determination in exosomes

Considering that in some instances the exosomes can provide an intrinsic ALP activity, as previously reported by our research group [1,26,28], an VFA format was designed and tested for its determination. Specifically, a calibration curve was created for exosomes derived from SKBR3, MDA-MB-231 and hFOB cell lines. Pictures from the VFA cartridges are shown in Figure 4.6, panel A. Clearly, the VFA can obtain directly proportional signals of the intrinsic ALP enzyme from the exosomes samples. An intense purple precipitated is obtained after the reaction with the immobilized exosomes, while the nitrocellulose background show no significant colored signals. In order to obtain higher sensitivities, the reaction was carried out for 2 hours, otherwise the signal from diluted samples would not be visible. Note that after 30 minutes of reaction, the signals from the stock samples were clearly visible but the dilutions were still uncolored.

From the results shown in Figure 4.6, it can be concluded that the intrinsic activity of ALP in exosomes derived from hFOB and SKBR3 is 4-fold higher than in MDA-MB-231 exosomes. These results agree with the conventional microplate pNPP assay for ALP determination, as presented in §4.6.3 (Supp. data). In detail, exosomes derived

from hFOB show an ALP specific activity of 152.9 mU mg^{-1}, while SKBR3 exosomes being 128.0 mU mg^{-1} and MDA-MB-231 exosomes, only being 25.4 mU mg^{-1}.

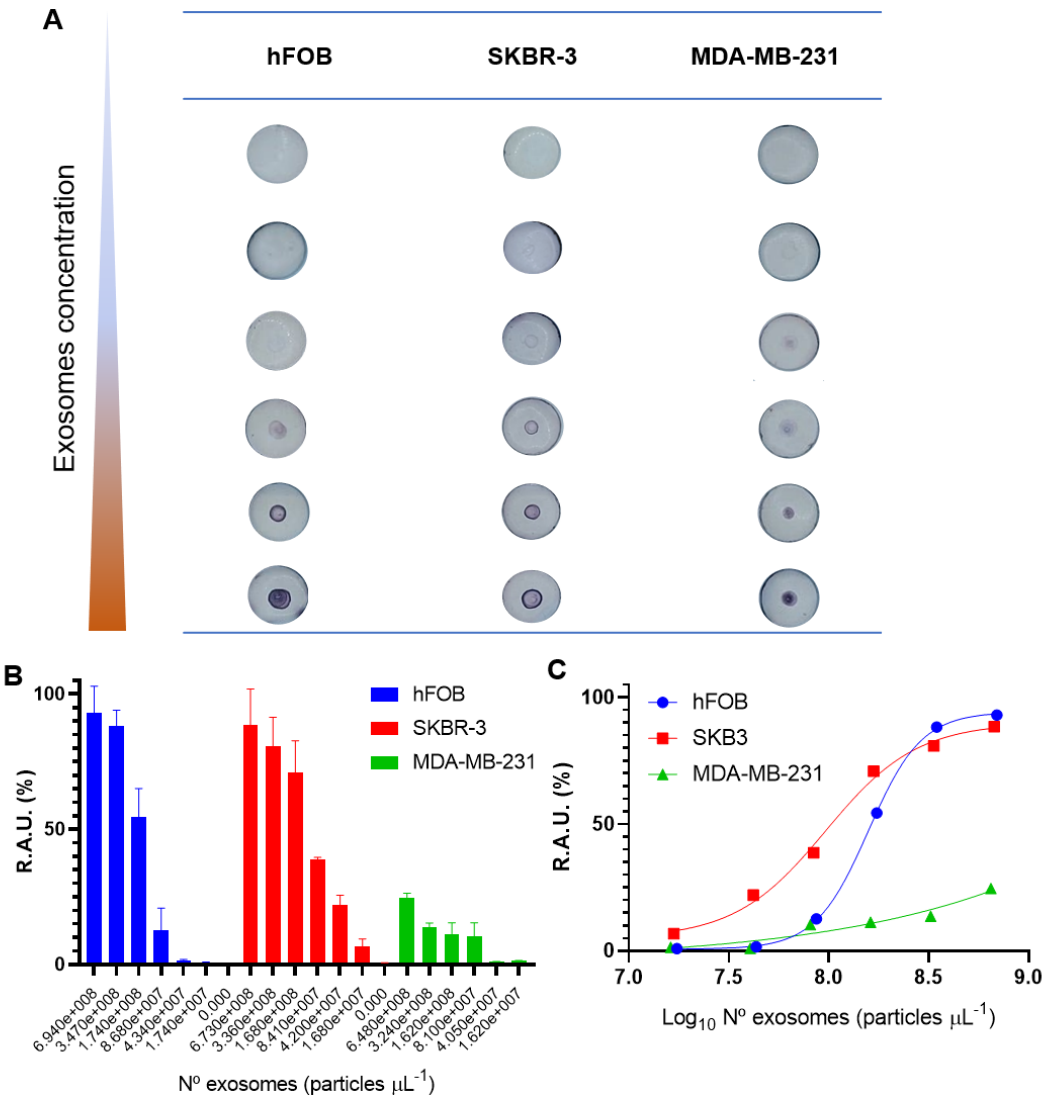

Figure 4.6. VFA determination of the intrinsic activity of ALP in exosomes derived from SKBR3, MDA-MB-231 and hFOB. Panel A shows pictures of the VFA cartridges membranes with dilutions of the exosomes. Panel B shows a bar plot of the Image J colorimetric quantification of the visual signals, in relative area units, normalized by the maximum signal (n=2). Panel C shows the non-linear regression (four parameters logistic equation) calibration curves obtained from the ImageJ quantification signals. r^2=0.98 (hFOB); 0.96 (SKBR3); 0.87 (MDA-MB-231). n=2.

Regarding the LOD of the proposed VFA assay for the determination of intrinsic ALP activity, it can be estimated to be approximately $1 \cdot 10^7$ particles μL^{-1} with 2 hours reaction time. Calculated with the NTA-normalized specific ALP activity of the exosomes samples from the pNPP assay (§4.6.3, Supp. data), the LOD corresponds to 2 µU of ALP, approximately. Therefore, the proposed VFA assay, only immobilizing 2 µL of sample, is limited to samples with ALP activity higher than 1 mU mL^{-1} to be detected.

4.5 Conclusions

In this work, we explored for the first time a paper-based VFA for the detection of exosomes, relying on ALP enzyme for the readout. To the best of authors knowledge, this novel approach is the first paper-based VFA for the analysis of exosomes based on ALP as enzymatic reporter. The insoluble product from the reaction of NBT/BCIP substrate with ALP enzyme is suitable for the detection on nitrocellulose membranes. The main advantage of ALP as a readout system in VFA relies on the fact that the enzymatic activity can be easily coupled with a myriad of substrates which, upon reaction, provide insoluble products which are stabilized on a paper substrate due to the vertical flow. As a shortcoming, the turnover number of ALP is low compared to other common enzymatic labels, reducing the sensitivity of the approach.

In this study, two VFA formats were designed and tested. Firstly, an ELISA-like VFA approach based on ALP labelling was designed, aimed for the semi-quantitative determination of surface markers on breast cancer cells derived exosomes. The assay provides an expression profile from biomarkers of interest on the surface of the exosomes, which agree with those obtained with the gold standard flow cytometry assay as reference molecular characterization method. In detail, the expressions levels obtained by both methods agree on SKBR3 derived exosomes (CD81 > CD9 > CD63 > EGFR1) and on MDA-MDB-231 derived exosomes (CD9 ≥ CD63 > CD81 > EGFR1). These results highlight the potentiality of VFA as a novel cost-effective RDT for exosomes characterization. Besides, the combination of VFA and ImageJ colorimetric quantification enabled the determination of the colored signal from ALP activity on the nitrocellulose membranes. An estimated limit of detection of $6 \cdot 10^7$ particles μL^{-1} using antiCD81 as primary antibody was found using SKBR3 and MDA-MB-231 derived exosomes as model samples, in 15 min reaction time. And secondly, a VFA format for the determination of the intrinsic ALP activity of the exosomes is also presented. The results shown in VFA cartridges agree with the gold-standard microplate assay for ALP determination with pNPP substrate. In this case, the reaction time had to be extended until 2 hours for increasing the sensitivity of the assay, as the intrinsic ALP is limited in the exosomes. An estimated LOD of $1 \cdot 10^7$ particles μL^{-1} was found, corresponding to 2 µU of ALP enzyme (or 1 mU mL^{-1}), calculated with the NTA-normalized specific ALP activity of the exosomes samples.

Finally, as the main drawback of VFA, the sensitivity of the assays is limited. This issue might be solved by increasing sample amount and concentration of the reagents, but also, because its reaction rate remains linear, by simply allowing a reaction to

proceed for a longer period of time. The substrate must be available for the enzyme to react on the nitrocellulose, so washing steps should be avoided until imaging. Unfortunately, the increase of reaction times often leads to higher background signal resulting in low signal-to-noise ratios. Besides, other colorimetric ALP substrates could be tested in VFA, looking for increased colored signals.

Our future perspectives also include to improve the design of the VFA with the deposition of multiple samples, in which two or three replicate spots could be measured at the same time. Also, the testing of the proposed VFA formats with other types of samples as biofluids. The study prove that the exosomes are retained directly over the membrane, while the smaller and soluble molecules can pass through the membrane of 0.2 µm. This result pointed out the potential application of VFA to exosomes samples in complex biological matrices (*e.g.*, serum, plasma, urine) with minimal pretreatments.

4.6 Supplementary data

4.6.1 Experimental

Construction of vertical flow assay cartridges

The Vertical Flow Assay cartridges were constructed as shown in Figure 4.7, adapted from RVF cartridges from Medmira. All details and references of all VFA materials tested are provided in Table 4.2. The plastic cassettes (panel 1 and 8) and plastic supports (panel 2, sized 28 x 20 x 1 mm, plus Ø 9 mm central hole) were reused from the commercial devices. On the plastic support, a double-sided tape (panel 3) of the same dimensions was sticked. Then, the following membranes were sticked in order: i) a nitrocellulose membrane (panel 4, square or round pieces with Ø > 11 mm), a medium weight cotton linter pad (panel 5, square pieces sized 12 x 12 mm), plus a filter paper (panel 6, pieces sized 28 x 20 mm). Then, an absorbent pad (panel 7, pieces sized 28 x 20 mm) was putted below the membrane's unit.

In the case of ELISA-like format, described in §4.3.8, an additional non-absorbent separation membrane (square pieces sized 11 x 11 mm) between nitrocellulose (panel 4) and cotton linter pad (panel 5) was used. This fiber glass layer helped to reduce the background signals when using ALP-modified secondary antibodies.

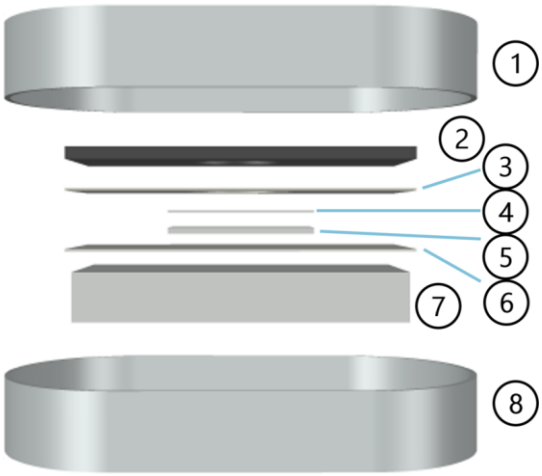

Figure 4.7. Schematic representation of the components for a VFA cartridge including the cover (1) and the support (8) of the MedMira cassette. Also (2) corresponds to a plastic support of the commercial cassette. Several membranes are attached to this plastic support using double-sided tape (3), as a nitrocellulose membrane (4), a medium weight cotton linter pad (5), plus a filter paper (6). Finally, an absorption cotton linter thick pad (7) was placed below the plastic support.

Table 4.2. Summary of the vertical flow assay materials, including cassettes and membranes used in this work

Material	Name	Supplier
Cassettes and plastic support	VFA cassettes	Ref. RVF VF-1-01, MedMira (Halifax, CA)
Double-sided tape	Double-sided tape	Ref. Medical Tape 1567, 3M (Saint Paul, MN, US)
Nitrocellulose membrane	NC – 0.2 µm pore size	Ref. 7182-001, Cytiva (München, GE)
	NC – 0.1 µm pore size	Ref. 7181-002, Cytiva
	NC – 0.45 µm pore size	Ref. 7184-001, Cytiva
	AE98	Ref. 10549916, Cytiva
	AE99	Ref. 10548081, Cytiva
	AE100	Ref. 10547017, Cytiva
	Protran BA85	Ref. 10402506, Cytiva
Separation membrane	VF2	Ref. 8145-2250, Cytiva
Medium weight pad	SP	Ref. CFSP203000, Merck-Millipore (Darmstadt, HE, GE)
	CF4	Ref. 8114-6621, Cytiva
Filter paper	Filter paper	(Local supplier) Density 64 g m^2
Absorption thick pad	CF7	Ref. 8117-2250, Cytiva

Buffers and solutions

All buffer and solutions were prepared with analytical reagent grade salts and ultrapure MilliQ water (Millipore® System, resistivity 18.2 MΩ·cm). Tris(hydroxymethyl)aminomethane (tris, ref. 252859), sodium phosphate dibasic (ref. 71636), potassium phosphate dibasic (ref. 795496), sodium chloride (ref. S3014), potassium chloride (ref. P3911), bovine serum albumin (ref. A4503), casein (ref. C7088), glycine (ref. 50046), and poly-ethylene glycol (ref. 8.07485) were purchased from Sigma-Aldrich (Merck KGaA, DE). Skimmed milk was purchased from local supplier (Nestlé Sveltesse).

The composition of the solutions was:

- Tris 1x buffer: 0.1 mol L^{-1} Tris-HCl, 0.15 mol L^{-1} NaCl, pH 7.4.
- PBS 1x buffer: 10 mmol L^{-1} Na_2HPO_4, 137 mmol L^{-1} NaCl, 2.7 mmol L^{-1} KCl, 1.8 mmol L^{-1} K_2HPO_4.
- PBS - 0.5% BSA buffer: 2% w/v BSA in PBS 1x buffer.
-

Specifically, the composition of blocking solutions tested for the VFA was:

- Skimmed milk 2%: 2% w/v of skimmed milk in Tris 1x buffer.
- Casein 2%: 2 % w/v of casein in Tris 1x buffer.
- Bovine serum albumin 2% and 5 %: 2% w/v, or 5% w/v, of BSA in Tris 1x buffer.
- Glycine 0.5M: 0.5 mol L^{-1} of glycine in Tris 1x buffer.
- Poly-ethylene glycol 2%: 2% w/v of PEG in Tris 1x buffer.

4.6.2 Cell culturing, exosome isolation and purification

The cell lines used were breast cancer cell lines SKBR3 (ATCC, ref. HTB-30) and MDA-MB-231 (ATCC, ref. HTB-26), and human fetal osteoblastic (hFOB) cell line (hFOB 1.19, ATCC ref. CRL-11372). Expansion of cell population was carried out from $5 \cdot 10^6$ cells in T-175 flask containing 35 mL of Dulbecco's Modified Eagle's medium for SKBR3 and MDA-MB-231 cell lines, and DMEM/Ham's F-12 Nutrient medium for hFOB. The media were supplemented with 10% exosome-depleted fetal bovine serum (FBS) and 100 U mL^{-1} penicillin-streptomycin. The temperature was maintained at 37 °C in a humidified, concentrated CO_2 (5%) atmosphere. Once cells reached approximately 95% confluence on the T-175 flask, the culture supernatant was removed and stored at –21 ºC until to exosome isolation.

Exosomes were purified according to what previously reported by our research group.[2] The supernatant from the SKBR3, MDA-MB-231 and hFOB cell lines were

subjected to differential centrifugation as follows: 300 x *g* for 5 minutes (removal of residual cells), 2,000 x *g* for 15 minutes and 10,000 x *g* for 30 minutes (removal of cellular debris, large and medium-sized EVs). Then, ultracentrifugation at 100,000 x *g* for 60 minutes was performed using a Beckman Coulter Optima L-80XP, either with a 70Ti or 50.2Ti rotor to pellet exosomes and other small EVs. After that, the supernatant was carefully removed, and crude exosome-containing pellets were resuspended in 1 mL of Tris 1x buffer (pH 7.4, 0.22 µm sterile-filtered) and pooled. The second round of the same ultracentrifugation setting was carried out, and the resulting exosome pellet resuspended in 500 µL (per each 100 mL of supernatant) of Tris 1x buffer (pH 7.4, 0.22 µm sterile-filtered) and storage at –21 °C. All centrifugation steps were performed at a temperature of 4 °C.

4.6.3 Spectrophotometric determination of the ALP activity in exosomes

The gold-standard colorimetric method for the determination of ALP activity is based on pNPP substrate hydrolysis in alkaline conditions. It was performed with exosomes in solution samples in 96-well microtiter plates. The procedure was performed following three steps: i) Serial dilutions of exosomes samples derived from SKBR3, MDA-MB-231 and hFOB cell lines were prepared in Tris 1x buffer (dilution factors: 1/1, 1/2, 1/4, 1/8, 1/20). Besides, sample derived from SKBR3 cell line was firstly diluted 1/8 to normalized NTA particle concentration, before serial dilutions. ii) Reaction with pNPP substrate was performed by incubating 2µL of each dilution were incubated with 198 µL of 10 mmol L^{-1} pNPP in DEA buffer, containing 6.0 mmol L^{-1} $MgCl_2$, cofactor of the ALP enzyme. The reaction was performed at 37ºC. iii) Optical readout was performed by monitoring the absorbance at 405 nm at 30 min, 1h, 2h and 4h using a Tecan Infinite m200 PRO microplate reader.

The activity of ALP enzymes on exosomes was calculated using the following Equation 1. The absorbance rate was transformed to rate of micromoles hydrolyzed per minute (µmol min^{-1}) of pNPP substrate. This ALP activity (U mL^{-1}) was them normalized by NTA particle concentration (U per nº of particles) and BCA protein concentration (U per mg of protein) to calculate the specific enzymatic activity.

Equation 1:

$$Enzymatic\ activity = \frac{\Delta Abs}{min} \cdot \frac{DF}{\varepsilon \cdot b} \cdot \frac{TV}{SV} = \frac{\mu mol}{\min \cdot mL} = \frac{U}{mL}$$

Being ΔAbs min^{-1} the slope of the reaction progression, DF is the dilution factor applied to each sample, ε the molar absorption coefficient equal of p-nitrophenol (18.5

mL µmol^{-1} cm^{-1}) at 405 nm in DEA buffer at 25ºC, b is the light length path in the microplate (0.565 cm), TV is the total volume and SV is the sample volume used in the assay.

Figure 4.8 shows the 405 nm absorbance of exosomes samples from SKBR3, MDA-MB-231 and hFOB cell lines at 4 hours reaction time. Table 4.3 shows the specific ALP activities of the exosomes samples. According to the specific activity normalized by BCA protein concentration, hFOB exosomes had the highest specific activity, as expected. Their activity is similar to SKBR3 exosomes, and 6-fold increase of MDA-MB-231 exosomes. Between breast cancer derived exosomes, SKBR3 has 5-fold increased activity than MDA-MB-231. Focusing on NTA normalized specific activity results, the comparison between samples shows comparable results for hFOB and MDA-MB-231. On the other hand, SKBR3 shows a different behavior, which might be caused by the presence of protein aggregates in the sample, leading to an overestimation of particle concentration by NTA analysis.

Table 4.3. ALP specific activities of exosomes samples from hFOB, SKBR3 and MDA-MDA-231 cell lines.

Sample	Specific ALP activity (mU mg^{-1})	Specific ALP activity (mU (10^9particles)$^{-1}$)
SKBR3	128.0	0.049
MDA-MB-231	25.4	0.025
hFOB	152.9	0.137

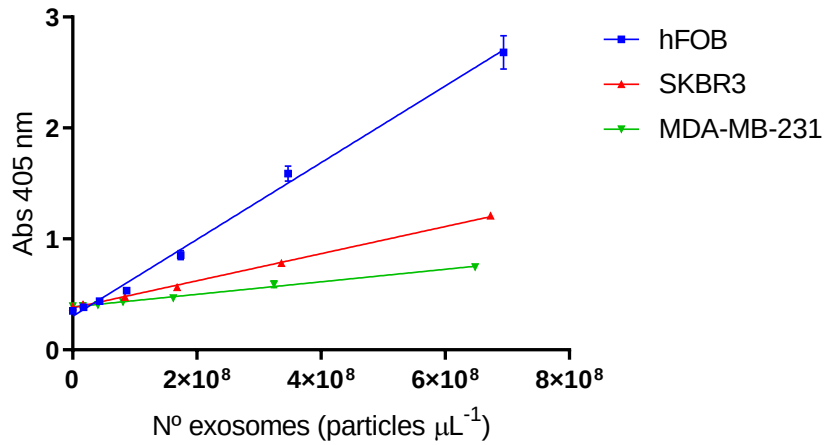

Figure 4.8. Calibration curves of the spectrophotometric ALP determination based on pNPP hydrolysis of exosomes samples from SKBR3, MDA-MB-231 and hFOB cell lines at 4 hours reaction time. n=3.

4.6.4 Characterization of exosomes by bead-based flow cytometry assay

Flow cytometry was used to estimate the presence of membrane protein markers of interest in the surface of exosomes derived from SKBR3 and MDA-MB-231 breast

cancer cell lines. Specifically, the presence of tetraspanin receptors CD9, CD63 and CD81, and epithelial specific EGFR1 receptor were evaluated. The flow cytometry assay is based on the immobilization of exosomes on the surface of magnetic particles, to increase its size within the resolution of the flow cytometer.

The immobilization of exosomes on Dynabeads M450 tosylactivated superparamagnetic particles (MPs) were performed as follows: 3.5 x 10^{10} exosomes were added to 40 µL of MPs, equivalent to 1.6 x 10^{7} particles. The reaction was carried out in 0.1 mol L^{-1} borate buffer pH 8.5, in order to ensure the nucleophilic reaction by the amine group. The incubation step was performed overnight with gentle shaking at 4 ºC. After that, 0.5 mol L^{-1} glycine solution was added to ensure the blocking of the any remaining tosylactivated groups, by an incubation for 4 h at 25 ºC. After that, the exosomes-modified magnetic particles (exosomes-MP) were resuspended in 160 µL of 10 mmol L^{-1} PBS buffer to dilute the MPs suspension at 1 x 10^{5} MPs per µL. The exosomes-MP were maintained at 4 ºC until use.

The presence of the CD9, CD63, CD81 and EGFR1 biomarkers was investigated. The indirect labelling of 5 x 10^{5} exosome-modified MPs was performed by incubation of 100 µL (5 µg mL^{-1}) of the primary antibodies (*i.e.,* antiCD9, antiCD63, antiCD81, and antiEGFR1), for 60 min with gentle shaking at 4ºC. After that, three washing steps with PBS buffer containing 0.5% BSA were performed. Afterwards, 100 µL (2 µg mL^{-1}) of antimouse-Cy5 secondary antibody were incubated for 30 min in the darkness with gentle shaking at 4ºC. Again, three washing steps with PBS buffer containing 0.5% BSA were performed. The labelled MPs were resuspended in 1000 µL of PBS buffer.

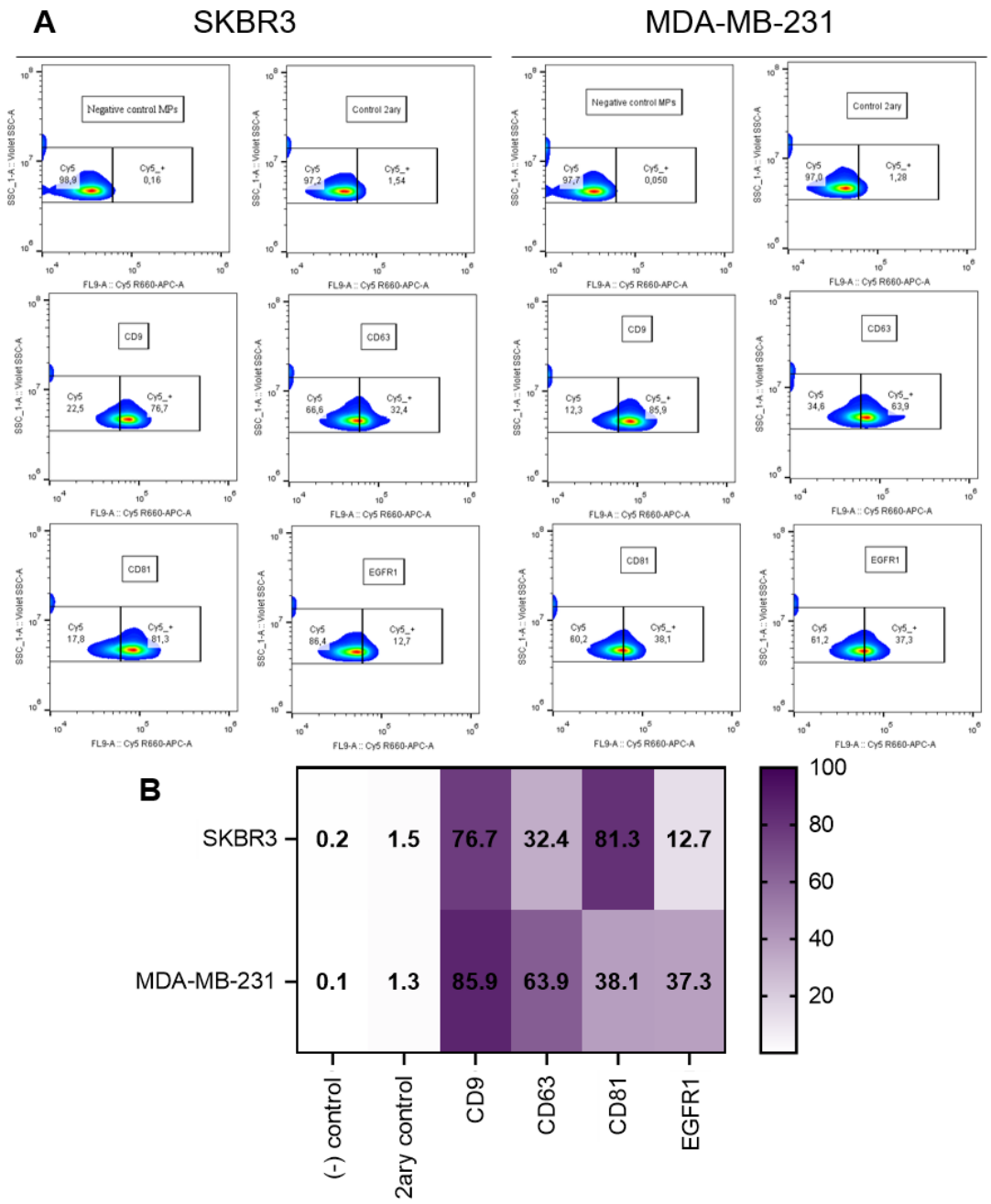

Figure 4.9. Dot blot (panel A) and heat map (panel B) of bead-based flow cytometry analysis of protein surface markers on exosomes derived from SKBR3 and MDA-MB-231.

Figure 4.9, panel A, show dot blot plots of the bead-based flow cytometry measurements of SKBR3 and MDA-MB-231 exosomes-modified MPs. As insets in each plot, the positivity percentage of the sample is shown. In Figure 4.9, panel B, a heat map representation of the positivity percentage is shown.

4.6.5 Standard protocol for ELISA-like experiments using VFA

For the ELISA-like determination of surface markers, ALP labelled antibodies were used as enzymatic reporters. It is important to note that in this case, a non-

absorbent fiber glass membrane was added under the VFA nitrocellulose membrane, as detailed in §4.6.1. This additional layer helps to reduce the background signal coming from the unbounded ALP labelled antibodies that flow though the nitrocellulose. The following protocol was used for the experiments:

1. Immobilization: 2 µL of sample were dropped at the center of the VFA nitrocellulose membrane, using a micropipette without touching the surface of the membrane. The VFA were air dried for 1h in the fridge (4ºC).
2. Blocking: 200 µL of BSA 2% (w/v) in Tris buffer were added and incubated for 2h at 37ºC in the oven.
3. Incubation: a primary antibody (0.5 µg mL^{-1} in Tris buffer) plus an ALP labelled secondary antibody (30 ng mL^{-1} in Tris buffer) were incubated for 2h at 37 ºC. This allows a 1-step incubation of the antibodies in the VFA.
4. Washing: 200 µL of Tris buffer.
5. Incubation: 100 µL of the antibodies' solution were added and incubated for 1h at 37ºC.
6. Washing: 300 µL of Tris buffer.
7. Revealing: 10 µL of NBT/BCIP were added and incubated for 15 minutes at room temperature.
8. Washing: 100 µL of Tris buffer
9. Imaging with a smartphone camera.

4.6.6 Standard protocol for the determination of intrinsic ALP activity using VFA

For the determination of intrinsic activity of ALP on samples immobilized on the VFA, standard VFA were constructed as detailed in §4.6.1. The following protocol was used for the experiments.

1. Immobilization: 2 µL of sample (*i.e.*, being purified ALP enzyme for optimization experiments, or exosomes samples for intrinsic ALP determination) were dropped at the center of the VFA nitrocellulose membrane, using a micropipette without touching the surface of the membrane. The VFA were air dried for 1h in the fridge (4ºC).
2. Blocking: 200 µL of BSA 2% (w/v) in Tris buffer were added and incubated for 2h at 37ºC in the oven.
3. Washing: 400 µL of Tris buffer.
4. Revealing: 10 µL of NBT/BCIP were added and incubated for 2h reaction time at 37ºC in the oven.

5. Washing: 100 µL of Tris buffer.
6. Imaging with a smartphone camera.

4.6.7 ImageJ colorimetric signal quantification

The imaging of VFA cartridges was performed under controlled illumination to avoid interferences in the signal quantification. All the cartridges from the same sample in an experiment were imaged at the same time. The illumination conditions were controlled by using a portable photographic studio with LED white lights of 1100 Lm and a color temperature of 6000–6500 K. The images were taken at a distance of 21 cm with a smartphone. The rear camera was used, with a resolution of 12 megapixels. Autofocus was enabled, the zoom set up at 2x, and the flashlight was turned off during the data acquisition procedure.

For the colorimetric quantification, the images were processed with Image J software, Fiji version. All images were transformed to 8-bit. Then, the test dots were outlined using a circular selection tool, and the area under each peak was then numerically integrated using the ImageJ gel analysis toolbox. Finally, the values were processed using GraphPad v8.0 analysis software.

4.7 Acknowledgements

J. Marfà, M. Bernuz, Z. Gholami and O. Tomàs Badell are gratefully acknowledged for their contributions. Also, ICTS “NANBIOSIS” NTA analysis service of *Institut de Ciència dels Materials de Barcelona* and Service of Microscopy of *Universitat Autònoma de Barcelona* are gratefully acknowledged.

4.8 References

(1) Moura, S. L.; Pallarès-Rusiñol, A.; Sappia, L.; Martí, M.; Pividori, M. I. The Activity of Alkaline Phosphatase in Breast Cancer Exosomes Simplifies the Biosensing Design. *Biosens. Bioelectron.* **2022**, *198*, 113826. https://doi.org/10.1016/j.bios.2021.113826.

(2) Moura, S. L.; Martín, C. G.; Martí, M.; Pividori, M. I. Multiplex Detection and Characterization of Breast Cancer Exosomes by Magneto-Actuated Immunoassay. *Talanta* **2020**, *211*, 120657. https://doi.org/https://doi.org/10.1016/j.talanta.2019.120657.

(3) Moura, S. L.; Martín, C. G.; Martí, M.; Pividori, M. I. Electrochemical Immunosensing of Nanovesicles as Biomarkers for Breast Cancer. *Biosens. Bioelectron.* **2020**, *150*, 111882. https://doi.org/https://doi.org/10.1016/j.bios.2019.111882.

(4) Land, K. J.; Boeras, D. I.; Chen, X. S.; Ramsay, A. R.; Peeling, R. W. REASSURED Diagnostics to Inform Disease Control Strategies, Strengthen Health Systems and Improve Patient Outcomes. *Nat. Microbiol.* **2019**, *4* (1), 46–54. https://doi.org/10.1038/S41564-018-0295-3.

(5) Huang, Y.; Xu, T.; Wang, W.; Wen, Y.; Li, K.; Qian, L.; Zhang, X.; Liu, G. Lateral Flow Biosensors Based on the Use of Micro- and Nanomaterials: A Review on Recent Developments. *Microchim. Acta* **2020**, *187* (1). https://doi.org/10.1007/s00604-019-3822-x.

(6) Martín-Gracia, B.; Martín-Barreiro, A.; Cuestas-Ayllón, C.; Grazú, V.; Line, A.; Llorente, A.; De La Fuente, J. M.; Moros, M. Nanoparticle-Based Biosensors for Detection of Extracellular Vesicles in Liquid Biopsies. *J. Mater. Chem. B* **2020**, *8* (31), 6710–6738. https://doi.org/10.1039/d0tb00861c.

(7) Ben Aissa, A.; Jara, J. J.; Sebastián, R. M.; Vallribera, A.; Campoy, S.; Pividori, M. I. Comparing Nucleic Acid Lateral Flow and Electrochemical Genosensing for the Simultaneous Detection of Foodborne Pathogens. *Biosens. Bioelectron.* **2017**, *88*, 265–272. https://doi.org/10.1016/j.bios.2016.08.046.

(8) Liu, Z.; Hua, Q.; Wang, J.; Liang, Z.; Li, J.; Wu, J.; Shen, X.; Lei, H.; Li, X. A Smartphone-Based Dual Detection Mode Device Integrated with Two Lateral Flow Immunoassays for Multiplex Mycotoxins in Cereals. *Biosens. Bioelectron.* **2020**, *158*, 112178. https://doi.org/10.1016/j.bios.2020.112178.

(9) Bock, S.; Kim, H. M.; Kim, J.; An, J.; Choi, Y. S.; Pham, X. H.; Jo, A.; Ham, K. M.; Song, H.; Kim, J. W.; Hahm, E.; Rho, W. Y.; Lee, S. H.; Park, S. M.; Lee, S.; Jeong, D. H.; Lee, H. Y.; Jun, B. H. Lateral Flow Immunoassay with Quantum-Dot-Embedded Silica Nanoparticles for Prostate-Specific Antigen Detection. *Nanomaterials* **2022**, *12* (1). https://doi.org/10.3390/nano12010033.

(10) Ross, G. M. S.; Salentijn, G. I.; Nielen, M. W. F. A Critical Comparison between Flow-through and Lateral Flow Immunoassay Formats for Visual and Smartphone-Based Multiplex Allergen Detection. *Biosensors* **2019**, *9* (4). https://doi.org/10.3390/bios9040143.

(11) Ben Aissa, A.; Araújo, B.; Julián, E.; Zanoni, M. V. B.; Pividori, M. I. Immunomagnetic Separation Improves the Detection of Mycobacteria by Paper-Based Lateral and Vertical Flow Immunochromatographic Assays. *Sensors* **2021**, *21* (18). https://doi.org/10.3390/s21185992.

(12) Gurung, S.; Perocheau, D.; Touramanidou, L.; Baruteau, J. The Exosome Journey: From Biogenesis to Uptake and Intracellular Signalling. *Cell Commun. Signal.* **2021**, *19* (1), 1–19. https://doi.org/10.1186/s12964-021-00730-1.

(13) Oliveira-Rodríguez, M.; Serrano-Pertierra, E.; García, A. C.; Martín, S. L.; Mo, M. Y.; Cernuda-Morollón, E.; Blanco-López, M. C. Point-of-Care Detection of Extracellular Vesicles: Sensitivity Optimization and Multiple-Target Detection. *Biosens. Bioelectron.* **2017**, *87*, 38–45. https://doi.org/10.1016/j.bios.2016.08.001.

(14) Moyano, A.; Serrano-Pertierra, E.; Duque, J. M.; Ramos, V.; Teruel-Barandiarán, E.; Fernández-Sánchez, M. T.; Salvador, M.; Martínez-García, J. C.; Sánchez, L.; García-Flórez, L.; Rivas, M.; Blanco-López, M. D. C. Magnetic Lateral Flow Immunoassay for Small Extracellular Vesicles Quantification: Application to Colorectal Cancer Biomarker Detection. *Sensors* **2021**, *21* (11). https://doi.org/10.3390/s21113756.

(15) Yu, Q.; Zhao, Q.; Wang, S.; Zhao, S.; Zhang, S.; Yin, Y.; Dong, Y. Development of a Lateral Flow Aptamer Assay Strip for Facile Identification of Theranostic Exosomes Isolated from Human Lung Carcinoma Cells. *Anal. Biochem.* **2020**, *594*, 113591. https://doi.org/10.1016/j.ab.2020.113591.

(16) Dong, D.; Zhu, L.; Hu, J.; Pang, D. W.; Zhang, Z. L. Simple and Rapid Extracellular Vesicles Quantification via Membrane Biotinylation Strategy Coupled with Fluorescent Nanospheres-Based Lateral Flow Assay. *Talanta* **2019**, *200*, 408–414. https://doi.org/10.1016/j.talanta.2019.03.069.

(17) Oliveira-Rodríguez, M.; López-Cobo, S.; Reyburn, H. T.; Costa-García, A.; López-Martín, S.; Yáñez-Mó, M.; Cernuda-Morollón, E.; Paschen, A.; Valés-Gómez, M.; Blanco-López, M. C. Development of a Rapid Lateral Flow Immunoassay Test for Detection of Exosomes Previously Enriched from Cell Culture Medium and Body Fluids. *J. Extracell. Vesicles* **2016**, *5* (1), 5. https://doi.org/10.3402/jev.v5.31803.

(18) Serrano-Pertierra, E.; Oliveira-Rodríguez, M.; Rivas, M.; Oliva, P.; Villafani, J.; Navarro, A.; Blanco-López, M. C.; Cernuda-Morollón, E. Characterization of Plasma-Derived Extracellular Vesicles Isolated by Different Methods: A Comparison Study. *Bioengineering* **2019**, *6* (1). https://doi.org/10.3390/bioengineering6010008.

(19) Renart, J.; Behrens, M. M.; Fernández-Renart, M.; Martinez, J. L. Immunoblotting Techniques. In *Immunoassay*; Diamandis, E. P., Christopoulos, T. K., Eds.; Academic Press,

1996; pp 537–554. https://doi.org/10.1016/b978-012214730-2/50024-8.

(20) Oh, Y. K.; Joung, H. A.; Kim, S.; Kim, M. G. Vertical Flow Immunoassay (VFA) Biosensor for a Rapid One-Step Immunoassay. *Lab Chip* **2013**, *13* (5), 768–772. https://doi.org/10.1039/c2lc41016h.

(21) Moumita, M.; Shankar, K. M.; Abhiman, P. B.; Shamasundar, B. A. Development of a Sandwich Vertical Flow Immunogold Assay for Rapid Detection of Oxytetracycline Residue in Fish Tissues. *Food Chem.* **2019**, *270* (July 2018), 585–592. https://doi.org/10.1016/j.foodchem.2018.07.124.

(22) Shi, F.; Sun, Y.; Wu, Y.; Zhu, M.; Feng, D.; Zhang, R.; Peng, L.; Chen, C. A Novel, Rapid and Simple Method for Detecting Brucellosis Based on Rapid Vertical Flow Technology. *J. Appl. Microbiol.* **2020**, *128* (3), 794–802. https://doi.org/10.1111/jam.14519.

(23) Prajapati, A.; Verma, N.; Pandya, A. Highly Sensitive Vertical Flow Based Point-of-Care Immunokit for Rapid and Early Detection of Human CRP as a Cardiovascular Risk Factor. *Biomed. Microdevices* **2020**, *22* (2). https://doi.org/10.1007/s10544-020-00480-w.

(24) Tang, Z.; Chen, H.; He, H.; Ma, C. Assays for Alkaline Phosphatase Activity: Progress and Prospects. *TrAC Trends Anal. Chem.* **2019**, *113*, 32–43. https://doi.org/10.1016/J.TRAC.2019.01.019.

(25) Schindelin, J.; Arganda-Carrera, I.; Frise, E.; Verena, K.; Mark, L.; Tobias, P.; Stephan, P.; Curtis, R.; Stephan, S.; Benjamin, S.; Jean-Yves, T.; Daniel, J. W.; Volker, H.; Kevin, E.; Pavel, T.; Albert, C. Fiji - an Open Platform for Biological Image Analysis. *Nat. Methods* **2009**, *9* (7). https://doi.org/10.1038/nmeth.2019.Fiji.

(26) Sanchez, M. A.; Felice, B.; Sappia, L. D.; Lima Moura, S.; Martí, M.; Pividori, M. I. Osteoblastic Exosomes. A Non-Destructive Quantitative Approach of Alkaline Phosphatase to Assess Osteoconductive Nanomaterials. *Mater. Sci. Eng. C* **2020**, *115*, 110931. https://doi.org/10.1016/j.msec.2020.110931.

(27) CDC. *Biosafety in Microbiological and Biomedical Laboratories (BMBL)*, 6th ed.; CDC, 2020.

(28) Sappia, L.; Felice, B.; Sanchez, M. A. A.; Martí, M.; Madrid, R.; Pividori, M. I.; Pividori, I. Electrochemical Sensor for Alkaline Phosphatase as Biomarker for Clinical and in Vitro Applications. *Sensors Actuators B Chem.* **2019**, *281* (September 2018), 221–228. https://doi.org/10.1016/j.snb.2018.10.105.

Chapter 5. Aldehyde dehydrogenase detection in exosomes by nano-flow cytometry

5. Aldehyde dehydrogenase detection in exosomes by nano-flow cytometry

5.1 Abstract

The development of novel methods for the detection of the intrinsic enzymatic activity is of great interest for the design of rapid diagnostic tests (RDTs) for exosomes. In this direction, it is well known that aldehyde dehydrogenases (ALDH) enzymes are overexpressed in several cancers, but little is known about its expression in cancer-derived exosomes. Thus, the main objective of this chapter was to develop a novel method for the detection and assessment of ALDH activity in exosomes. To achieve this task, exosomes derived from breast cancer cell lines (SKBR3, MDA-MB-231 and MCF7 cell lines) were obtained from cell culture supernatant by differential ultracentrifugation. Different methods were used to characterize the vesicles and its molecular content, including the membrane protein markers of the exosomes, and their enzymatic activity. A novel method based on nano-flow cytometry was developed for the detection of ALDH directly inside the exosomes, based on fluorescent readout. It combines the labelling of the vesicles with protein-binding fluorescent dyes for its identification, and the reaction with a resorufin-based substrate. As this substrate is also used by other enzymes, a specific ALDH inhibitor were evaluated in the ALDH activity by the reduction of resorufin-based fluorescent readout. In summary, this study represents the first step towards the development of a new RDT targeting ALDH intrinsic activity of exosomes for breast cancer diagnostics.

Keywords: Exosomes, Aldehyde dehydrogenase, Breast cancer, Liquid biopsy, Nano-flow cytometry, Enzymatic biomarkers.

5.2 Introduction

Exosomes are nano-sized extracellular vesicles (30-200 nm) naturally released by most cell types[1]. These vesicles are related with the intercellular communication mechanisms, delivering biological cargos to other cells in a paracrine and endocrine way among the extracellular space.[2] The molecular content of exosomes consists of genetic material (various types of RNA and DNA) and transmembrane and cytosolic molecules (lipids and proteins, including enzymes), some of which are molecular markers of the parental cells.[3] The molecular characterization of exosomes and EVs is a challenging task for cell-oriented current technologies due to their small size. The majority of these techniques require extensive protocols and pre-treatments, the use of benchtop equipment and skilled personnel. There is a lack of rapid diagnostic test (RDTs) following REASSURED criteria[4] for the detection and characterization of those nano-sized vesicles with easy-to-use devices. Although some portable devices have been reported, mainly based on electrochemical readout[5–7], the molecular cargo of exosomes is still not fully characterized[2]. Their small size makes exosomes challenging analytes for most conventional cell-oriented analysis methods, due to electronic noise, voltage adjustment and sheath purification Accordingly, and to solve this issue, novel strategies have been developed , in order to artificially increase the size of the particles by binding to magnetic particles, as bead-based flow cytometry[8]. Some commercial kits are also based on this approach, including MACSPlex Exosome Kit (Miltenyi Biotec, Bergisch Gladbach, DE). Besides, new technologies available in the market have great potentiality. Of particular interest for exosomes characterization is high-resolution flow cytometry or nano-flow cytometry.[9–11] These emerging cytometric technologies increase their resolution up to vesicles of 100 nm of diameter[10,11], in the range of individual exosomes.

One of the most promising strategies for developing new RDTs for the detection of exosomes is based on targeting their intrinsic enzymatic content. This approach simplifies the analytical procedure by avoiding the use of labelled reporters as specific antibodies used in the immunoassays as ELISA. As previously mentioned, the use of ALP enzyme was the labelling method to detect exosomes derived from hFOB osteoblasts[12]. Based on those evidences, an electrochemical immunosensor with magnetic actuation was developed also with hFOB exosomes.[13] The intrinsic activity of ALP was known to be overexpressed in breast cancer[14] and the immunosensor was able to discriminate between exosomes from serum of breast cancer patients and healthy donors.[13] Another potential enzymatic biomarker for cancer diseases are aldehyde dehydrogenases (ALDH, EC 1.2.1.3), and particularly ALDH1A3 isoform[15]. The relationship of these oxidoreductases with cancer diseases has been previously

described for colorectal[16], glioblastoma[17–19], prostate[20], or breast[21–23] cancer disease. The overexpression of ALDHs has been related with poor prognosis of the disesase[17,19,22] and treatment resistance[16,24,25]. Although their presence has not been described in exosomes, ALDHs are potential candidates to be used of diagnostic biomarkers for cancer diseases.

In this chapter, the development of a novel method based on nano-flow cytometry for the analysis of ALDH intrinsic enzymatic activity of exosomes derived from breast cancer cells lines is rationally studied. Firstly, the ALDH content of breast cancer cells was evaluated by intracellular staining, and further detected by flow cytometry, while its activity was determined by fluorometric kinetic assays. Then, exosomes derived from SKBR3, MDA-MB-231 and MCF7 breast cancer cell lines were isolated and purified by differential ultracentrifugation from cell culture supernatants. To verify the integrity of the purified exosomes, they were by nanoparticle tracking analysis, cryogenic transmission electron microscopy and bead-based flow cytometry. The ALDH activity in exosomes was evaluated by nano-flow cytometry. The method developed in this study involves the use of: (i) fluorescent reporters for the detection of the vesicles; (ii) fluorescent ALDH substrates able to cross exosome membrane and to react with the enzyme inside the nano-sized vesicles. For the analysis of the enzymatic activity, the ALDH substrate, resorufin propionate, was used as it produces a fluorescent product when hydrolyzed by the enzyme. Because resorufin propionate is also suitable for esterase enzymes, a specific ALDHs inhibitor was also used to indirectly determine the presence of ALDH in cancer-derived exosomes.

5.3 Experimental

5.3.1 Instrumentation

Nanoparticle tracking analysis (NTA) was performed using the NanoSight LM10-HS system with a tuned 405 nm laser (NanoSight Ltd, Malvern, GB). Cryogenic transmission electron microscopy images were acquired by a Jeol JEM 2011 (JEOL USA Inc, US). Spectrophotometric measurements were performed on a Tecan Infinite m200 PRO (Tecan Group Ltd, Männeford, CH) microplate reader controlled by Magellan v7.0 software. Conventional and nano-Flow cytometry measurements were performed using a Cytoflex LX (Beckman Coulter Inc, Indianapolis, IN, US) and analyzed with the integrated software Cytexpert and FlowJo analysis software (FlowJo LLC, BD, NJ, US).

5.3.2 Chemicals and biochemicals

Tosylactivated magnetic particles (MPs) (Dynabeads M450 Tosylactivated, ref. 14013), FITC-labelled mouse monoclonal antibodies against tetraspanins, antiCD9 (ref. MA119557), antiCD63 (ref. MA119602), antiCD81 (ref. A15753), as well as mouse monoclonal antiVinculin (ref.MA5-11690) and PE-labelled goat anti-Rabbit secondary antibody (antirabbit-PE, ref. P2771MP) were purchased from Thermo Fisher Scientific (Waltham, MA, US). Rabbit polyclonal antibody against ALDH1A3 (ref. GTX110784) was purchased from Genetex (Irvine, CA, US). Cy5-labelled goat anti-Mouse (antimouse-Cy5, ref. ab97037) was purchased from Abcam (Cambridge, GB). For exosome membrane staining, Cell Trace CFSE green kit (ref. C34554) and Cell Trace Violet kit (ref.C34557) were purchased from Thermo Fisher Scientific. For the ELISA quantification, HRP-conjugated antiCD63 antibody (ref. NBP2-42225H) was purchased from Novus Biologicals (Bio-Techne R&D Systems SLU, Madrid, ES), and Pierce TMB substrate kit (ref. 23227) was purchased from Thermo Fisher Scientific. For the protein quantification, Pierce BCA Protein Assay kit (ref. 23227) was purchased from Thermo Fisher Scientific. For cellular lysis and protein extraction, M-PER reagent (ref. 78501) was also purchased from Thermo Fisher Scientific. For the cell culture, Dulbecco's Modified Eagle's Glutamax (DMEM, ref. 31966-021) medium, and fetal bovine serum (FBS, ref. 26140079) were purchased from Gibco (Thermo Fisher Scientific). The composition of all buffers and solutions is described in §5.6.1 (Supp. Data).

For ALDH activity studies, hexanal (ref. 115606) was purchased from Sigma Aldrich, and nicotinamide adenine dinucleotide oxidized form (NAD^+, ref. BIB3014) and reduced form (NADH, ref. BIB3012) were purchased from Apollo Scientific (Bredbury, UK). Resorufin propionate (from now on, named as RP) and specific ALDHs inhibitor (ref. ABD0305), shown on Figure 5.1, were provided by Prof. Jaume Farrés research group and Advanced Biodesign (Saint-Priest, FR).

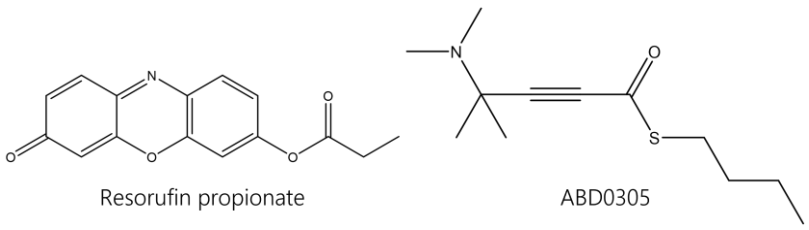

Figure 5.1. Structures of ALDH resorufin propionate substrate and ABD0305 inhibitor.

5.3.3 Cell culturing, exosome isolation and purification

Breast cancer cell lines SKBR3 (ATCC, ref. HTB-30), MDA-MB-231 (ATCC, ref. HTB-26) and MCF7 (ATCC, ref. HTB-22) were grown as described in §5.6.2 (Supp. Data). Exosomes were purified from cell culture supernatant by differential ultracentrifugation as previously reported by our research group with minor changes.[8] Exosomes were resuspended in 25 mmol L^{-1} HEPES buffer solution (pH 7.4, 0.22 µm sterile-filtered) and stored at –21 ºC. All exosomes purification steps are provided in §5.6.2 (Supp. Data).

5.3.4 Characterization of EVs by nanoparticle tracking analysis, cryogenic transmission electron microscopy and BCA protein assay

The size distribution and concentration of particles were estimated by NTA. The purified exosomes were diluted in filtered PBS buffer solution, between 100 and 500-fold depending on the sample initial concentration. NanoSight NTA software analyzed raw data videos by triplicate during 60 s with 25 frames/s. Cryogenic TEM images were collected by a Jeol JEM 2011 (JEOL USA Inc, US) transmission electron microscope at an accelerating voltage of 200 kV. Exosomes were maintained at -182 °C with liquid ethane during the whole process. The total protein concentration of the EVs was estimated using the Bicinchoninic acid protein assay (BCA), following the manufacturer instructions, using bovine serum albumin (BSA) standards in HEPES buffer solution. The spectrophotometric measurements were done at 562 nm.

5.3.5 Characterization of exosomes by bead-based flow cytometry assay

Conventional flow cytometer was used to estimate the presence of general protein markers of exosomes in the surface of EVs derived from SKBR3, MDA-MB-231 and MCF7 breast cancer cell lines. Specifically, the presence of tetraspanin receptors CD9, CD63 and CD81 was determined, following MISEV2018 guidelines[26], to confirm the presence of exosomes The bead-based flow cytometry relies on the immobilization of exosomes on the surface of magnetic particles, to increase its size within the resolution of the flow cytometer. To achieve that, exosomes were covalently immobilized on MPs, followed by the direct labelling with FITC-modified antiCDX mouse monoclonal antibodies (being CDX either CD9, CD63 or CD81 biomarkers). All experimental details described in §5.6.3 (Supp. Data).

5.3.6 Intracellular staining of ALDH in breast cancer cells

According to literature[25], ALDHs are localized in different cellular compartments, including nucleus, cytoplasm and endoplasmic reticulum, but their presence in cellular

membranes was not reported. To determine the presence of ALDH inside breast cancer cells, intracellular staining with flow cytometry detection was used. Fixation and permeabilization of cellular membranes were needed in order to allow the antibodies to react with cytosolic proteins. As primary antibody, a specific antibody against isoform ALDH1A3 from rabbit was used, further detected with an antirabbit-PE as secondary antibody. As intracellular control assay, an antibody against vinculin (cytoskeletal protein) from mouse was used, detected by an antimouse-Cy5. All experimental details of the assay are provided in §5.6.4 (Supp. Data).

5.3.7 Sandwich ELISA for the determination of ALDH

To determine the presence of ALDH1A3 on exosome membrane, exosomes derived from SKBR3 breast cancer cell line were subjected to sandwich ELISA. As a control for the exosome membrane staining, the antiCD81 antibody was added in the assay as general exosome membrane biomarker. Specific antibodies against ALDH1A3 and antiCD81 were used to capture the exosomes, further labelled by HRP-conjugated antiCD63 antibodies, and revealed with TMB and H_2O_2. The spectrophotometric measurements were done at 450 nm. All experimental details of the assay are provided in §5.6.5 (Supp. Data).

5.3.8 Fluorometric determination of ALDH activity

As standard quantification method for the ALDH activity in cells and exosomes, a fluorometric assay based on the oxidation of hexanal using NAD^+ as cofactor was used. The kinetic reaction was recorded by measuring the fluorescence emission from NADH reduced form (excitation wavelength 340 nm; emission wavelength 460 nm) produced during the reaction. Breast cancer cells and exosomes were lysed using M-PER reagent, following the protocol provided by the manufacturer, and extracts were quantified by BCA protein assay kit. All spectrophotometric measurements were done using black 96-well fluorescence microplates (ref. 237108) from Thermo Fisher Scientific, and a Tecan Infinite m200 PRO microplate reader. To find the linear range of the enzymatic reaction, different dilutions of cells extract, or exosomes were incubated, in HEPES reaction buffer, with 500 µmol L^{-1} of NAD^+, 5 µmol L^{-1} of NADH and 250 µmol L^{-1} of hexanal. In the case of cellular extract, the fluorescence of the reaction is recorded for 100 minutes, with measurements each 30 seconds, at 25 ºC. Meanwhile in the case of exosomes, more time (4 hours) and temperature (37 ºC) were applied to increase the reaction kinetics.

5.3.9 Nano-Flow cytometry studies of breast cancer exosomes

The nano-flow cytometry method for the analysis of exosomes combines different fluorescent labelling of the vesicles. All experimental details can be found in §5.6.6 (Supp. Data).

5.3.9.1 CFSE and Violet staining of exosomes

Firstly, exosomes derived from SKBR3, MDA-MB-231 and MCF7 breast cancer cell lines were labelled with cell tracking reagents. From the same commercial source, a range of different colors are available (*i.e.,* referred to CellTrace™ kits, Thermo Fisher Scientific), allowing to adjust the exosomes staining for each experiment with combination of fluorophores. In this study, CellTrace™ CSFE proliferation kit (excitation 488 nm, emission 525 nm, ref. C34554, Thermo Fisher Scientific) and CellTrace™ Violet proliferation kit (excitation 425 nm, emission 450 nm, ref. C34557, Thermo Fisher Scientific) were used for exosome staining (Fig. 5.2, panel A). Cell tracking reagents react covalently with proteins and due to their fluorescence emission they allow to separate the exosomes from background signals.[10,11] The incubation parameters (exosome concentration, temperature, and time) for exosome labelling with cell tracking reagents, as well as the instrumental parameters of the nano-cytometer (channels gain, threshold, and range) were optimized. The optimal exosome concentration ranges from 10^8 to 10^9 particles mL^{-1}, according to NTA measurements. The CFSE/Violet concentration was optimized to 20 µmol L^{-1}, with 2 hours of incubation at 37 ºC. After incubations, all samples were diluted to 1 mL with HEPES buffer and stored at 4 ºC until measurement by nano-flow cytometry. Regarding the instrumental parameters, the gain of B525-FITC channel was set to 1,000 units, while V450-Violet to 500 units. Thresholds were adjusted manually at 700 units in both channels.

5.3.9.2 Analysis of membrane markers on CFSE-labelled exosomes

For the detection of surface membrane proteins on exosomes, the Violet vesicles (from now, named as CellTrace Violet-labelled exosomes) were incubated with FITC-modified primary antibodies against tetraspanins CD9, CD63 and CD81 (Fig. 5.2, panel B). This assay allows to locate the exosomes (tetraspanin-containing vesicles) on the subpopulation of vesicles that were labelled with violet staining (protein-containing vesicles). The assay was done with 20 µL of exosomes (containing 8.60 x 10^7 particles, according to NTA counting) derived from SKBR3 breast cancer cell lines directly labelled with 5 µL of FITC-modified antiCDX mouse monoclonal antibodies (being CDX either CD9, CD63 or CD81 biomarkers) for 45 minutes at RT. In parallel, non-labelled control samples (not incubated with the cell tracking reagent) and without antibodies were

prepared with the same corresponding volumes of HEPES buffer. After incubations, all samples were diluted to 1 mL with HEPES buffer and stored at 4 ºC until measurement by nano-flow cytometry.

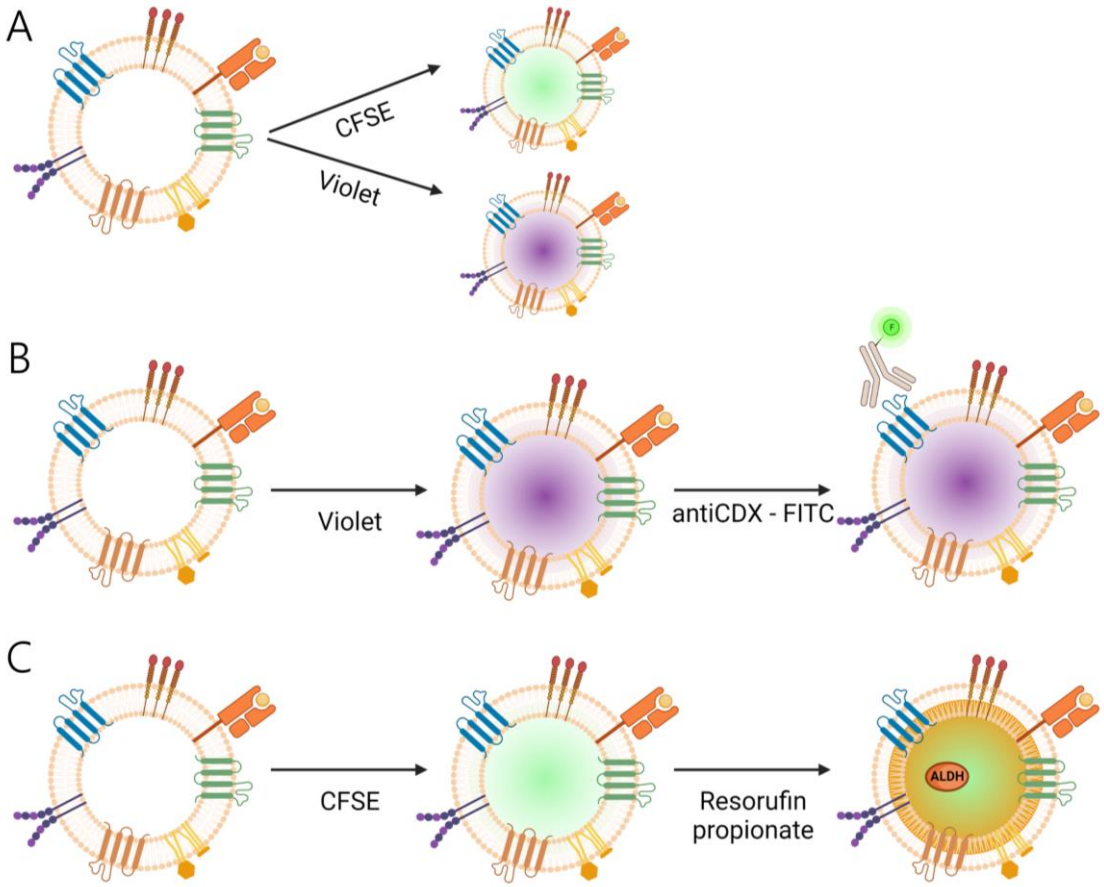

Figure 5.2. Scheme of the exosome staining methods studied. On Panel A, to identify the exosomes on nano-flow cytometry experiments, the vesicles were labelled with protein-binding fluorescent reporters as CFSE or Violet stainings. On Panel B, to determine the presence of membrane protein biomarkers, Violet-labelled exosomes were incubated with FITC-modified primary antibodies. On Panel C, to assess the intrinsic activity of ALDH enzymes inside the vesicles, CFSE-labelled exosomes were incubated with resorufin propionate substrate.

5.3.9.3 ALDH activity determination in breast cancer exosomes

To determine the ALDH activity on exosomes derived from SKBR3, MDA-MB-231 and MCF7 breast cancer cell lines were labelled with the CFSE vesicles (from now, named as CellTrace CFSE-labelled exosomes) and incubated with resorufin propionate substrate (Fig. 5.2, panel C). This small, hydrophobic, and non-ionic molecule is able to cross the exosomes lipidic bilayer membrane and react with the intraexosome ALDH enzyme to produce resorufin (excitation 525 nm, emission 585 nm) by its esterase ability. The concentration of the substrate was optimized at 25 µmol L^{-1} with 2 hours at 25 ºC incubation. Resorufin propionate substrate stock was dissolved in DMSO, and ABD0305 inhibitor, in ethanol. Therefore, and to not adversely affect the biological activity of the

exosomes, at least a 100-fold dilution in HEPES buffer from the stocks were used as working solutions. Besides ALDH, other esterase enzymes are also able to react with the substrate. Therefore, a specific ALDH inhibitor (ref. ABD0305) was used to indirectly determine the ALDH activity by inhibiting its contribution on the resorufin signal. The concentration of the inhibitor was optimized at 10 µmol L^{-1} with 2 hours at 37 ºC incubation, always prior to substrate incubation. The resorufin was detected with the Y610 detector, showing better results than Y585 detector. Additionally, to evaluate the effect of the storage temperature on the ALDH enzymatic activity, a comparative study was done with exosomes obtained from i) 5-days frozen (-21 ºC) or ii) freshly obtained (<12h) and non-frozen (4 ºC) cell culture supernatants.

5.3.10 Statistical analysis

The statistical analyses were performed using GraphPad Prism 8 (CA, US). All experiments were done at least by duplicate. In the flow cytometry experiments, at least 10,000 cells or vesicles were recorded per each sample.

5.3.11 Safety considerations

All works were performed in a Biosafety cabinet, and all material was decontaminated by autoclaving or disinfected before discarding following U.S. Department of Health and Human Services guidelines for level 2 laboratory Biosafety.[27]

5.4 Results and discussion

5.4.1 Characterization of EVs by nanoparticle tracking analysis, cryogenic transmission electron microscopy and BCA protein assay

The NTA analysis of exosomes samples derived from breast cancer cell lines SKBR3, MDA-MB-231 and MCF7 revealed clear peaks between 100 and 200 nm, as expected. SKBR3 exosomes size distribution only shows a peak at 125 nm (Fig. 5.3, panel A) of individual vesicles. On the other hand, MDA-MB-231 and MCF7 exosomes size distributions show similar histograms, with a major peak at 145 nm and 115 nm, respectively, corresponding to individual vesicles. MDA-MB-231 show two lower peaks at 215 and 325 nm, corresponding to small aggregates (Fig. 5.3, panel B). Meanwhile, MCF7 exosomes size distribution also shows aggregates, although at smaller diameters of 155 nm and 205 nm (Fig. 5.3, panel C). The exosomes from the three breast cancer cell lines were further analyzed by Cryo-TEM, confirming the presence of individual and small aggregates of vesicles in the range between 50 and 400 nm, as shown in Figure 5.3.

Table 5.1. NTA particle concentration and total protein concentration of EVs samples

Sample	Particle concentration (particles mL^{-1})	Protein concentration (mg mL^{-1})
SKBR3	4.30 / SD 0.05 $\cdot 10^{11}$	0.874
MDA-MB-231	5.65 / SD 0.22 $\cdot 10^{10}$	0.220
MCF7	1.64 / SD 0.08 $\cdot 10^{11}$	0.221

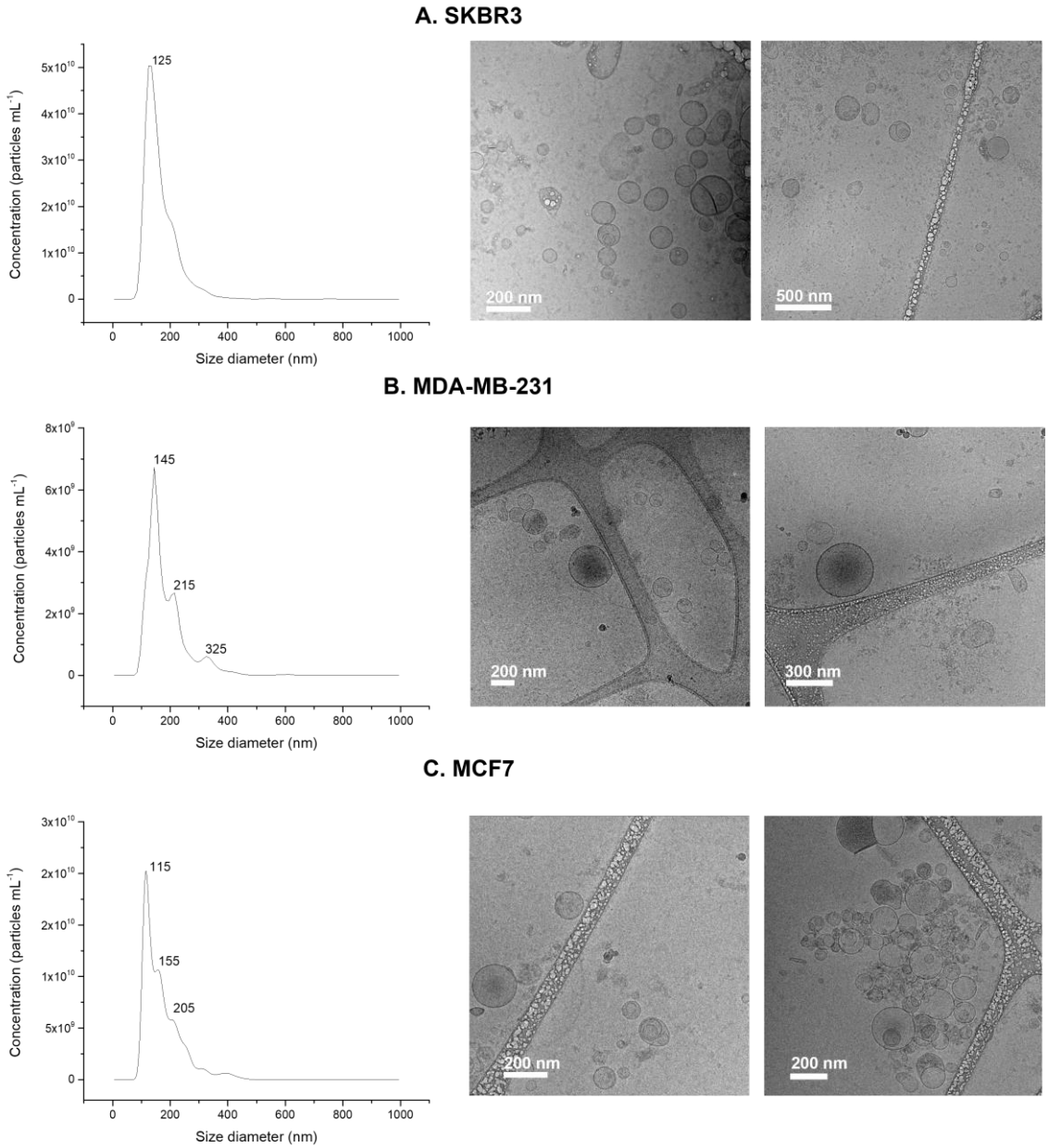

Figure 5.3. Characterization by NTA and Cryo-TEM micrographs of purified exosomes samples from SKBR3 (panel A), MDA-MB-231 (panel B) and MCF7 (panel C) breast cancer cell lines. The NTA characterization analyzed raw data videos by triplicate during 60 s with 25 frames per second and the temperature of the laser unit set at 24.8°C. Cryo-TEM images were obtained at an acceleration voltage of 200 kV.

Particle concentration of the samples used for this study was estimated by NTA, and total protein concentration was estimated by BCA protein assay, as shown in Table 5.1. Exosomes sample derived from SKBR3 is more concentrated (4.30 / SD 0.05 $\cdot 10^{11}$ particles mL^{-1} and 0.874 mg mL^{-1}) than the other two samples. In the case of MDA-MB-231, NTA showed a concentration approximately 8 times lower than SKBR3 (5.65 / SD 0.22 $\cdot 10^{10}$ particles mL^{-1}), being protein concentration only 4 times lower (0.220 mg mL^{-1}). On the other hand, in MCF7 exosome samples, both measurements agree, being approximately 4 times lower (1.64 / SD 0.08 $\cdot 10^{11}$ particles mL^{-1}, and 0.221 mg mL^{-1}). Although the NTA, is the gold-standard method for exosome counting, it cannot differentiate between vesicles and protein aggregates leading to overestimated results.

5.4.2 Characterization of exosomes by bead-based flow cytometry assay

The presence of tetraspanin markers on the surface of exosomes derived from SKBR3, MDA-MB-231 and MCF7 cell lines immobilized on MPs was determined by flow cytometry as shown in Figure 5.4. The presence of CD9, CD63 and CD81 as ubiquitous protein biomarkers was successfully identified in the three samples as shown in the histograms depicted in Figure 5.4. FITC-modified mouse monoclonal antiCDX (being CDX CD9, CD63 and CD81) antibodies were used. As a control of specific staining, anti-CDX antibodies were incubated with negative control MPs (protein-modified MPs, without exosomes). This control sample show less than 1 % of positivity for each of the three FITC-modified anti-tetraspanin antibodies (*i.e.,* 0.7 % CD9, 0.3 % CD63, and 1.0 % CD81).

The results from the bead-based assay showed positive signals in the three exosomes samples with the three markers investigated. Specifically, exosomes derived from SKBR3 show 100 % of positivity in CD9, 51 % in CD63, and 44 % in CD81 markers. Next, exosomes derived from MDA-MB-231 show 39 % of positivity in CD9, 64 % of CD63, and 38 % in CD81. And finally, exosomes derived from MCF7 show a 92 % of positivity in CD9, 67 % in CD63 and 48 % in CD81. The results confirm the presence of these biomarkers on the exosomes membranes.

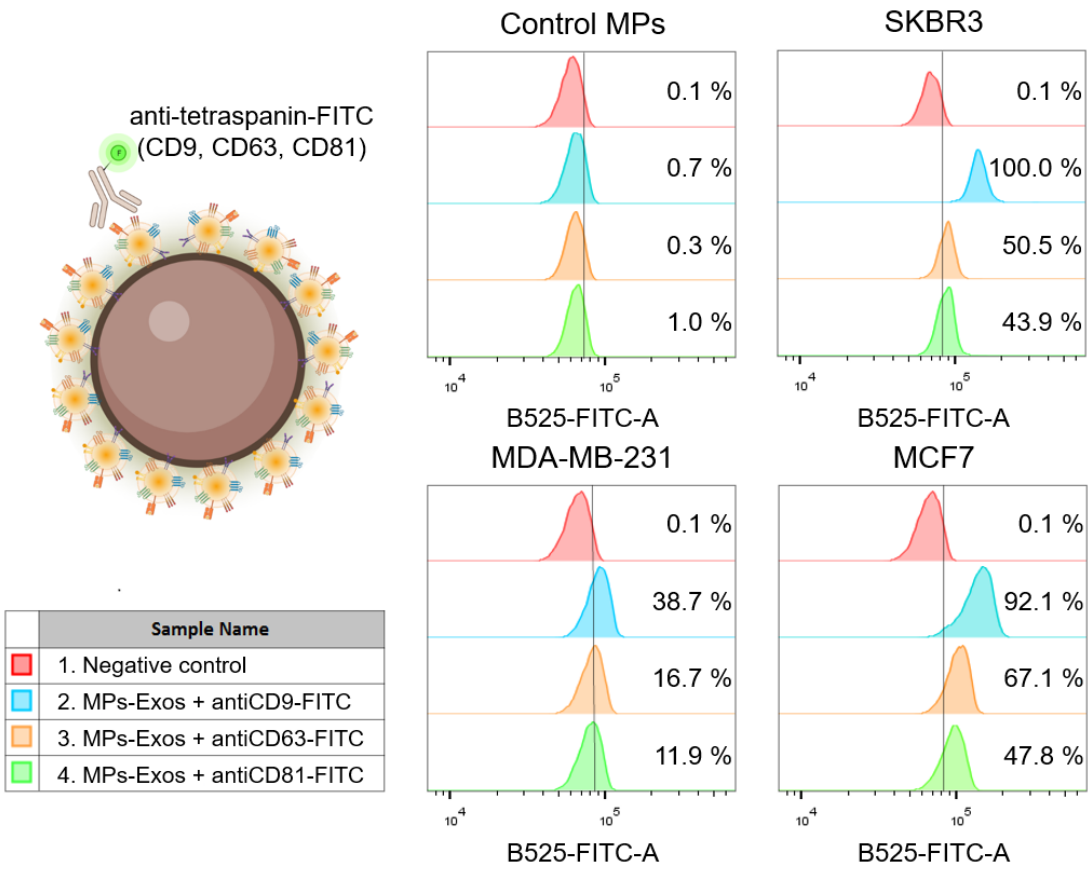

Figure 5.4. Bead-based flow cytometry assay for the characterization of protein surface markers in exosomes derived from breast cancer cell lines. Magnetic particles were covalently modified with exosomes derived from SKBR3, MDA-MB-231, and MCF7. Specific antibodies against tetraspanins CD9, CD63 and CD81, modified with FITC were used. As control sample, antibody modified magnetic particles, blocked with glycine, were used to verify the specificity of the immunoaffinity reaction.

5.4.3 Intracellular staining of ALDH in breast cancer cells

Before the evaluation of intraexosome ALDH enzymatic activity, it was studied the presence of ALDH enzyme in breast cancer cells from SKBR3, MDA-MB-231 and MCF7, by intracellular staining as reference method. Also, the comparison between the signals from different cell lines enabled to classify them according to the concentration of the enzyme. The isoform ALDH1A3 was reported as target for its overexpression in cancer disease, according to literature.[16,19,21]

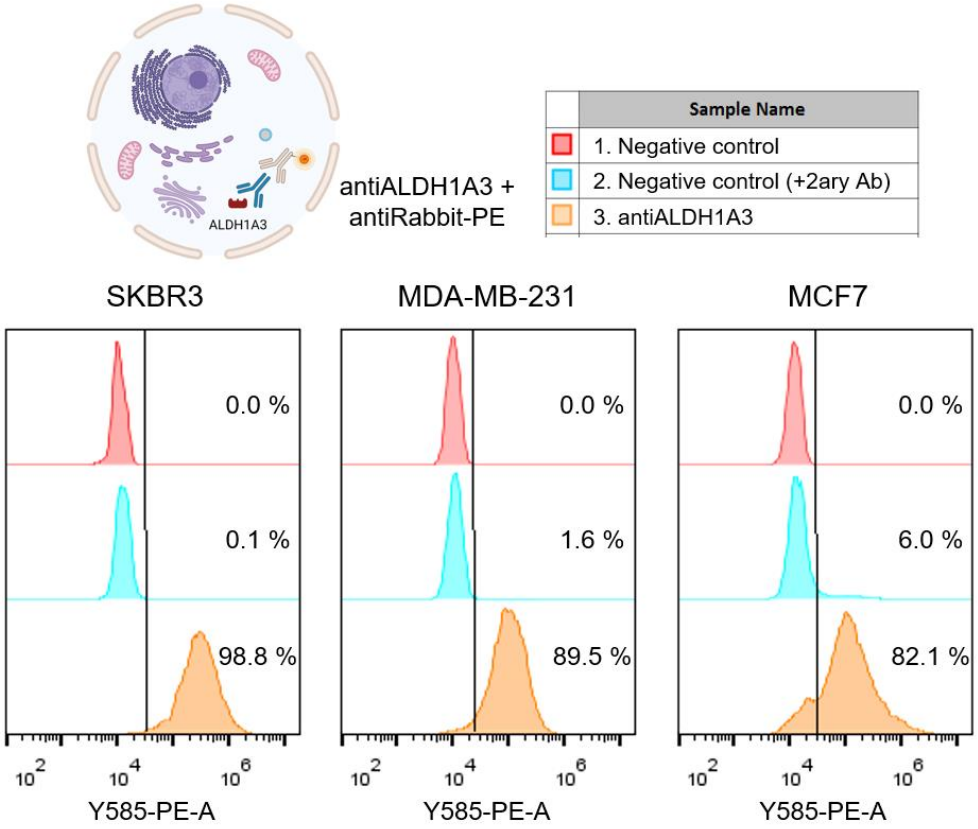

Figure 5.5. Histograms from intracellular staining of cells from SKBR3, MDA-MB-231 and MCF7 breast cancer cell lines with antiALDH1A3 antibodies, labelled with PE-modified antirabbit secondary antibodies. In red color, negative controls of the experiment, only cells; in blue color, control with cells only incubated with secondary antibodies; in orange color, cells with antiALDH1A3 antibodies plus labelled secondary antibodies.

Figure 5.5 shows histograms of the three breast cancer cell lines reacting with antiALDH1A3 antibodies, labelled with antiRabbit-PE secondary antibodies. Firstly, the permeabilization of the cells and their integrity was confirmed by reaction with antibodies against vinculin, showing more than 90 % of positivity in all cases (99.6 % in SKBR3 cells, 99.0 % in MDA-MB-231 cells, and 92.5 % in MCF7 cells), as depicted in §5.6.4 and Figure 5.10 (Supp. data). Then, the specificity of the secondary antibody labelling was evaluated by control samples without primary antibodies, showing 0.1 % of positivity in SKBR3 cells and 1.6 % in MDA-MB-231 cells. In the case of MCF7, although some unspecific labelling was detected (6.0 %), the whole cell population was shifted to positivity when labelled with anti-ALD1A3 antibody. In detail, SKBR3 cells show the highest percentage of ALDH1A3 positivity (98.8 %) among the cells tested, being MDA-MB-231 an 89.5 % and MCF7, an 82.1 %.

5.4.4 Sandwich ELISA for the determination of ALDH

To evaluate the presence and location of ALDH1A3 enzyme in the membranes of exosomes derived from SKBR3 cell line were investigated. As shown in §5.4.3 with intracellular staining and flow cytometry, SKBR3 cells show a high expression of ALDH1A3 in the cytosol. As a reference and standard method for determining protein markers, sandwich ELISA was used.

As expected, the sandwich ELISA using antiALDH1A3 as capture antibody did not show higher signals in the presence of SKBR3 exosomes, as shown in Figure 5.6. Meanwhile, a calibration curve was determined with the same exosomes samples captured by antiCD81 antibodies and detected by antiCD63-HRP, at the same experimental conditions. In conclusion, the results confirm that exosomes derived from SKBR3 cell line did not express ALDH1A3 in their membranes. Therefore, the exosomes show a similar ALDH compartmentalization as the cells, that locate the enzyme only in the intracellular space, in agreement previous studies[25] and also results from intracellular staining in §5.4.3.

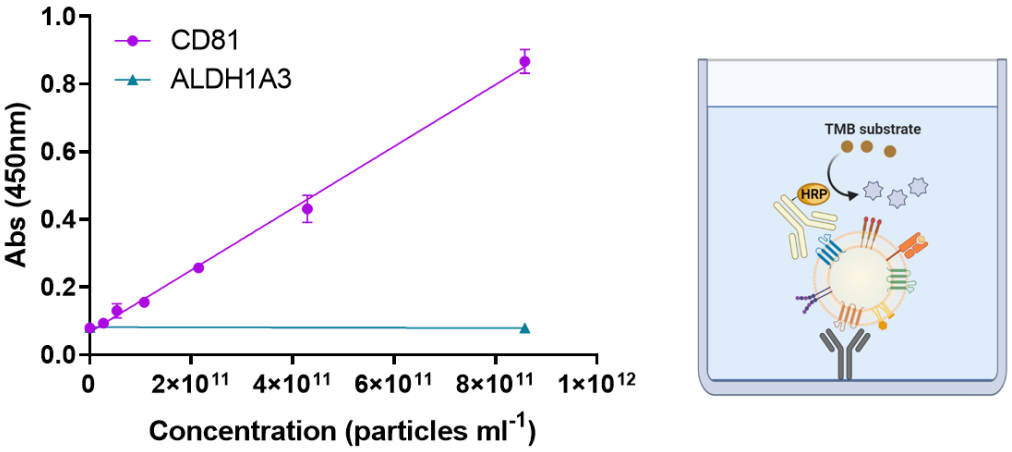

Figure 5.6. Sandwich ELISA determination of ALDH1A3 presence in the membranes of exosomes derived from SKBR3 breast cancer cell line. Antibodies against ALDH1A3 were used to capture the exosomes, further labelled by antiCD63-HRP as ubiquitous membranes protein marker. Besides, a calibration curve using antiCD81 was done, verifying exosomes integrity.

5.4.5 Fluorometric determination of ALDH activity

The fluorometric assay based on hexanal allowed to determine the specific activity of ALDHs in cellular extracts from breast cancer cell lines SKBR3, MDA-MB-231 and MCF7. The specific activity of the three cell lines was normalized per milligrams of total protein as shown in Table 5.2. As expected, and in agreement with the ALDH1A3

expression level, SKBR3 cells show higher ALDHs activity (0.433 U mg^{-1}) than MDA-MB-231 (0.391 U mg^{-1}) and MCF7 (0.353 U mg^{-1}).

Table 5.2. Specific activity data from cellular extract of breast cancer cells from SKBR3, MDA-MB-213 and MCF7 cell lines.

Sample – Cellular extract	Specific ALDH activity (U mg^{-1})	Protein concentration of cellular extracts (mg mL^{-1})
SKBR3	0.433	7.91
MDA-MB-231	0.391	3.95
MCF7	0.353	0.72

In the case of exosomes, this method was not sensitive enough to determine the specific activity of the samples from the three breast cancer cell lines. The recorded fluorescent signals from exosome samples were of similar intensity as the NADH internal standard background signal. Not conclusive results were obtained with the fluorometric assay based on hexanal oxidation and NADH fluorescence detection.

5.4.6 Nano-Flow cytometry studies of breast cancer exosomes

The improved resolution of nano-flow cytometry enabled the study of exosomes in solution without a previous immobilization on microparticles. Although this approach represents a clear advantage, as the reduction of non-specific reactions, the sensitivity of the assays might be compromised. The nanometric size of exosomes do not allow to separate the particles from instrumental noise by its size, using forward and side scattering detectors of the cytometer. The vesicles must be fluorescently stained to separate the particles from noise[11,28]. For example, cell tracking reagents as CFSE used for the analysis of cell proliferation by flow cytometry, are also suitable to label exosomes as they are bright enough to be detected as single vesicles or small aggregates. In this work, exosomes derived from SKBR3, MDA-MB-231 and MCF7 breast cancer cell lines were successfully detected by nano-flow cytometry using CellTrace CFSE and CellTrace Violet staining. Then, FITC-modified primary antibodies against tetraspanins were used to detect membrane proteins of SKBR3 exosomes, combined with Violet exosomes. Finally, resorufin propionate was used to detect the ALDH activity inside breast cancer exosomes.

5.4.6.1 CFSE and Violet staining of exosomes

The protocol for exosomes staining with the CellTrace™ kits was carefully studied and optimized. Different parameters were studied, including exosomes and reagent concentration, incubation time and temperature and instrumental parameters gain and

thresholds, as described in §5.6.6.1 (Supp. Data). The optimized conditions for CFSE staining of exosomes were 20 μmol L^{-1} of CFSE incubated for 2 hours at 37 ºC with gentle shaking, as shown in Figure 5.11 (Supp. Data). Regarding the Violet staining, the optimal conditions were found to be equal, 20 μmol L^{-1} of Violet incubated for 2 hours at 37 ºC with gentle shaking, as shown in Figure 5.15 (Supp. Data).

In parallel, the optimal exosomes concentration range able to be measured by nano-flow cytometry (in this work, using Cytoflex LX cytometer) was studied. Serial dilutions of CFSE-labelled SKBR3 exosomes were measured, as depicted in Figure 5.12 (Supp. Data). The optimal concentration was determined by the abort rate of the measurements, which must be lower than 8.0 % according to manufacturer technical recommendations. In our case, the optimal concentration of particles in the sample was found to be in the range of 10^7 particles mL^{-1}, calculated according to NTA particle counting. This fact was further confirmed by measuring CFSE-labelled exosomes from different cell lines, as shown in Figure 5.13 (Supp. Data), with concentrations between $1.09 \cdot 10^7$ particles mL^{-1} and $1.58 \cdot 10^8$ particles mL^{-1}. The concentration of particle successfully detected by nano-flow cytometry using CFSE staining was compared with the NTA particle counting, as shown in Figure 5.14 (Supp. Data), obtaining a variable ratio of labelled particles. Further experiments should be designed to provide an insightful view of this issue.

5.4.6.2 Analysis of membrane markers on CFSE-labelled exosomes

Next step was to verify the presence of exosomes as a labelled subpopulation of the vesicles by the detection of membrane tetraspanins considered the canonical markers for exosomes. To do that, exosomes derived from SKBR3 were stained with CellTrace violet reagent and afterwards they were labelled with FITC-modified primary antibodies against CD9, CD63 and CD81. In Figure 5.7, panel A, a dot plot representing the profile of the exosome sample is shown, using V450-Violet and Violet-SSC-A channels. The distribution of the dots allowed to identify two subgroups selected by the depicted gates in the dot plot graph. The FITC fluorescence of the violet-labelled vesicles, which was due to the labelled antibodies, was then analyzed using B525-FITC channel. As shown in Figure 5.7, panel B, vesicles selected by Gate 1 were enriched by tetraspanin-expressing vesicles compared to Gate 2, suggesting that Gate1 was selecting vesicles with features of exosomes that is high expression of the protein markers of exosomes. As expected from previous results (§5.4.2), CD9 was the most abundant tetraspanin, followed by CD63 and CD81, respectively. For following experiments, the exosomes subpopulation was selected according to ‘Gate 1’.

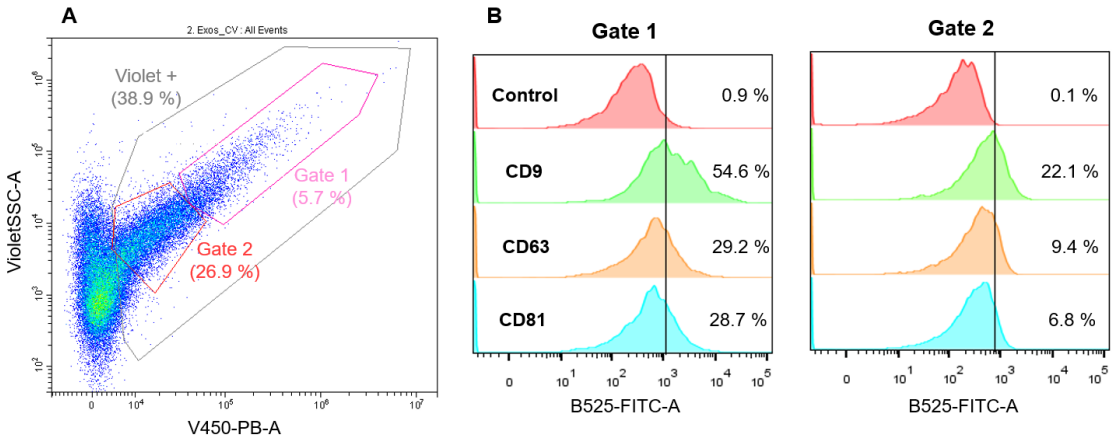

Figure 5.7. Analysis of the membrane protein markers of exosomes derived from SKBR3 breast cancer cell line. Panel A shows a dot plot representation of a measurement with the different gates: in grey, the total vesicles violet labelled; in pink, Gate 1 subpopulation; and in red, Gate 2 subpopulation. Panel B and C show the tetraspanin expression of both subpopulations, respectively, determined by B525-FITC-A fluorescent signals.

With the nano-flow cytometry, the dye labelling combined with the specific-antibody staining for the exosomes revealed the heterogeneity of the composition of the sample under study. The differences between extracellular vesicles could be related to the different biogenesis pathways that result in the expression of molecular patterns that allow them to be differentiated.

5.4.6.3 ALDH activity determination in breast cancer exosomes

Resorufin propionate is one of the ALDH substrates using esterase activity. It was chosen as a small and non-ionic substrate, potentially able to cross the exosomes lipidic bilayer and react with the material inside. The cleavage of the resorufin propionate do not require redox cofactors (as NAD^+/NADH) to occur, producing resorufin and propionate ion. Different experimental parameters were optimized for the detection of ALDH activity in exosomes. Parameters as concentration of ALDH substrate and inhibitor, temperature and incubation times were optimized, as described in §5.6.6.3 (Supp. Data). The established experimental values were 25 µmol L^{-1} of resorufin propionate for 2 hours at 25 ºC, while for ALDH inhibitor, 0.4 mmol L^{-1} for 2 hours at 37 ºC. The signal from resorufin was detected in Y610-RP channel.

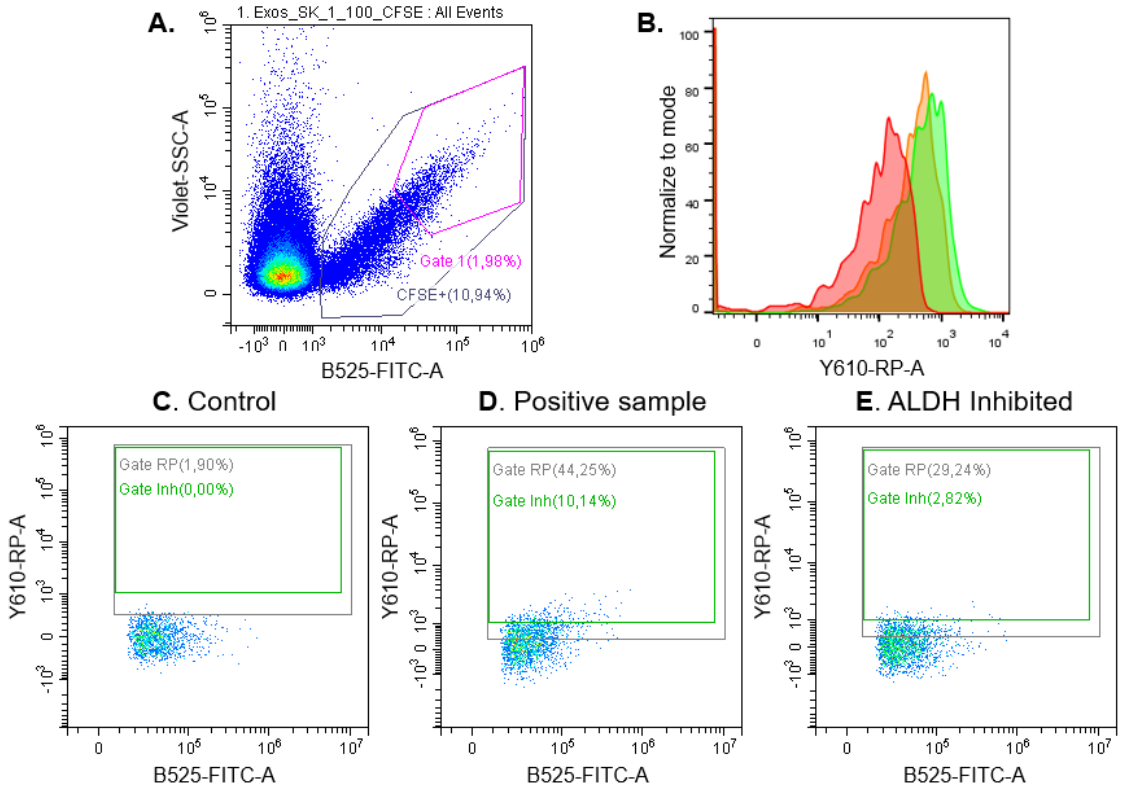

Sample	GeoMean (from 'Gate 1')	Gate RP (%)	Gate Inh (%)
Control	1.5	1.9	0.00
Positive sample	234.1	44.3	10.1
Inhibited	90.6	29.4	2.8

Figure 5.8. Analysis of the resorufin propionate reaction for ALDH activity detection on exosomes by nano-flow cytometry. On the Panel A, dot plot representation of CFSE-labelled SKBR3 exosomes as control sample, with total CFSE positive and Gate 1 subpopulations selected. Then, on Panels C, D and E, dot plot representation (on x axis, B525-FITC-A channel, on y axis Y610-RP-A channel) of the resorufin signals from the vesicles contained in Gate 1 from control sample (Panel C), an SKBR3 positive sample (Panel D) and an ALDH inhibited SKBR3 sample (Panel E). On Panel B, an histogram representation of the resorufin signals from the three SKBR3 samples. On the table, geometric mean of the Y610-RP signals, plus percentages of the vesicles contained in Gate RP (in grey) and Gate Inh (in green).

For this assay, the detection of ALDH activity was performed in CFSE-labelled exosomes derived from SKBR3, MDA-MB-231 and MCF7. Firstly, the 'Gate 1' exosomes subpopulation was identified in the dot plot with Violet-SSC-A and B252-FITC channels, as shown in Figure 5.8, panel A. Subsequently, the signal from the resorufin in the gate 1 for the three samples: (i) negative control, (ii) exosomes incubated with RP, and (iii) exosomes incubated with ALDH inhibitor and with RP, consecutively. In detail, to determine if part of the catalysis of the RP was due of the presence of intraexosome ALDH, the sample (iii) of exosomes was treated with the ABD0305 inhibitor prior incubation with the RP. The results are shown in Figure 5.8, panel B, as overlayed

histograms. The individual samples represented in a dot plot graph with B525-FITC (X-axis), and Y610-RP (Y-axis) channels were used for further analysis (Fig. 5.8, panels C, D and E). As can be observed in Figure 5.8, panel C, the exosomes labelled only with the CSFE staining (i) were plotted and used to define the RP positive staining, named as 'Gate RP' (grey square in the graphs). Figure 5.8, panel E, shows sample (iii) incubated with the specific ALDH inhibitor, followed by the RP, and was used to define the upper limit of the RP, named as 'Gate Inh' (green square in the graphs). Figure 5.8, panel D shows positive sample (ii) with a 44.3 % of positivity of the exosomes in 'Gate RP', with a geometric mean of 234.1 in the Y610-RP channel. As shown in Figure 5.8, panel E, the action of the inhibitor reduced to a 29.4 % the positive RP+ CFSE-labelled exosomes, with a geometric mean of 90.6. Therefore, using the geometric mean of the positive sample as an indirect measurement of the whole enzymatic activity (100 %), inhibition of the ALDH reduced it to a 38.7 %, suggesting that the presence of ALDH accounts for more than half (61.3 %) of the esterase activity inside the exosomes.

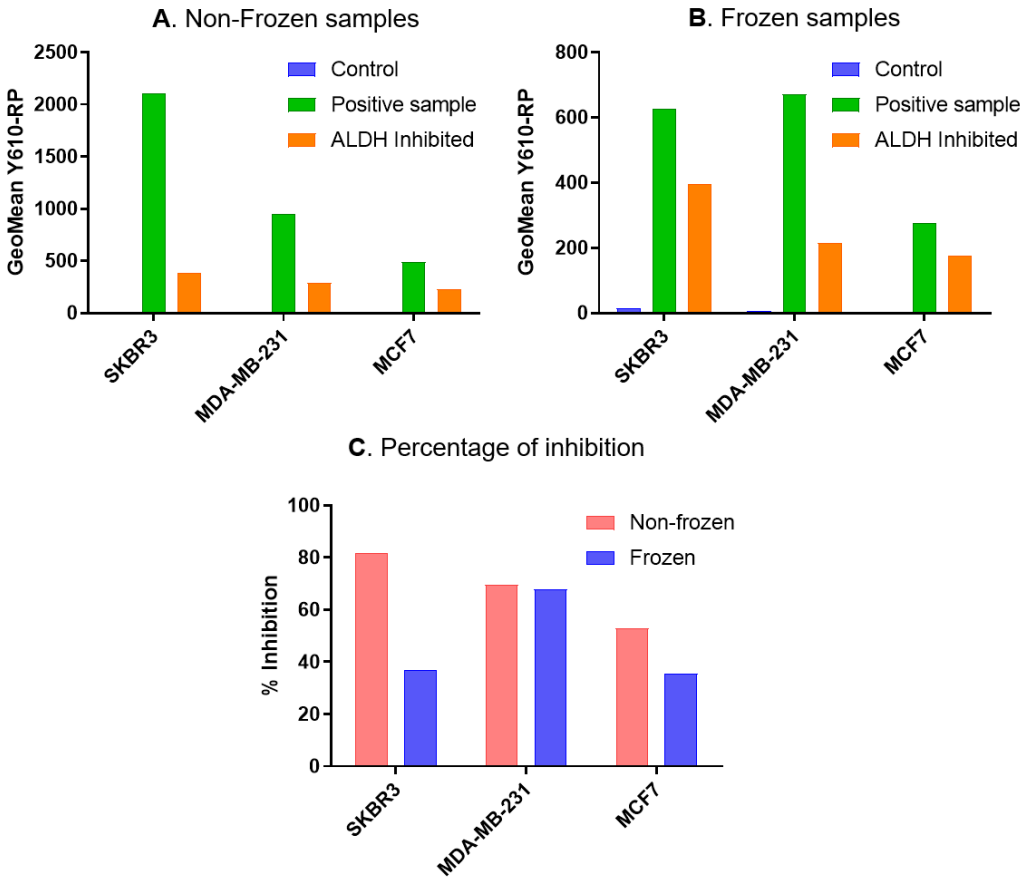

Figure 5.9 Effect of the storage temperature on the ALDH activity of the exosomes. On Panel A, bar graph representation geometric mean on Y610-RP-A channel of exosomes non-frozen samples from SKBR3, MDA-MB-231 and MCF7 breast cancer cell lines. On Panel B, bar graph from frozen samples from the three cell lines. Blue bars: control samples; green bars: positive samples; orange bars: inhibited samples. On Panel C, the percentage of inhibition is calculated for frozen and non-frozen samples by the normalized difference of positive versus inhibited samples.

Finally, and to assess whether the storage temperature of the samples might adversely affect the ALDH activity, frozen and non-frozen exosomes were analyzed. First, exosomes stored according to the standard procedures within our research group[8,13] in which cell culture supernatants are frozen at -21 ºC before ultracentrifugation, were compared with exosomes isolated from freshly obtained supernatants. Both exosome samples were isolated and purified according to §5.6.2. The obtention of non-frozen exosomes samples within the same day of supernatants was done in approximately four hours. The ALDH activity in the newly obtained exosomes derived from SKBR3, MDA-MB-231 and MCF7 breast cancer cell lines was determined using the same experimental and analysis protocol previously described.

As shown in Figure 5.9, in all samples the same tendencies can be observed. Firstly, the activity of ALDH in the exosomes was clearly diminished by sample freezing. And secondly, the inhibitor was more effective in non-frozen exosomes samples compared to frozen samples. Figure 5.9, panel A and B, shows bar graphs of the Y610 geometric mean of each sample from non-frozen and frozen samples, respectively. On Figure 5.9, panel C, the percentage of inhibition was calculated as an indirect measurement of ALDH activity. As previously explained, considering the whole enzymatic activity as 100 %, the decrease of the signal in inhibited samples is estimated as the percentage of ALDHs enzyme contribution. Regarding SKBR3 exosomes samples, ALDH contribution accounts for 81.8 % in non-frozen samples while decreases to 37.1 % in the frozen samples. In the case of MCF7, the same tendency is confirmed, with a 53.0 % of ALDH contribution in non-frozen samples, decreasing to 35.6 % in frozen samples. Finally, in MDA-MB-231 exosomes samples, the percentage remains stable between 69.6 % in non-frozen and 67.9 % in frozen samples. In the case of SKBR3 exosomes samples, those results were confirmed twice by replicating the experiments with new exosomes samples, confirming the adverse effect on ALDH activity by the freezing of the exosomes.

5.5 Conclusions

In summary, a novel method for the analysis of the aldehyde dehydrogenase enzymatic activity based on nano-flow cytometry was developed. Firstly, the intracellular staining of SKBR3, MDA-MB-231 and MCF7 breast cancer cells, and the fluorometric assays using hexanal as substrate, confirmed the presence of ALDH enzyme of the cytoplasmatic space of the cells. Regarding the exosomes, the advances in nano-flow cytometry have allowed the direct analysis of the exosomes to look for the expression of

interesting biomarkers as enzymes. In this study, it has been set up for the detection of intraexosome enzymatic activity. The key points of these assay are: (i) the labelling of the exosomes with dyes combined with specific antibodies and (ii) the use of fluorescent substrates capable to cross the exosome membrane to detect the presence of the enzyme by its biological function.

The set up was applied to detect the activity of ALDH as a biomarker overexpressed in several cancers. The use of resorufin propionate as substrate, which was able to permeabilize inside the nano-sized vesicles, allowed the measurement of esterase enzymatic activity by creating a fluorescent signal. Moreover, the use of an inhibitor specific for the ALDH, allowed to determine the contribution of the ALDH to the complete fluorescence signal obtained with the RP alone. However, the lack of specificity of resorufin propionate as ALDH substrate is not ideal. New suitable substrates should be tested in future experiments to try to obtain specific fluorescent signals for the enzymes of interest. If the new substrate requires the use of ionic cofactors such as NAD^+, the hydrophobicity of the membranes will prevent its internalization. Therefore, the exosomes should be lysed to release its internal cargo, and consequently, nano-flow cytometry method will not be able to detect the vesicles.

Nevertheless, the determination of ALDH activity by the nano-flow cytometry, was able to compare the inner enzymatic activity in exosomes derived from different cell lines. SKBR3 showed greater signals than MDA-MB-231 and MCF7, as expected from ALDH1A3 intracellular staining of the cells and fluorometric assay with the cellular extracts. As the standard exosomes isolation protocol includes the freezing of the samples after ultracentrifugation until their usage, it was possible that the storage temperature may affect the enzymatic activity of the exosomes cargo. To prove that, a comparison was done with frozen and non-frozen exosomes samples obtained from the same cell culture flasks. The results show great and conclusive differences in the resorufin signals in exosomes from the three different cell lines. The procedure to obtain and analyze non-frozen exosomes, from cell culture supernatants until nano-flow cytometry measurements within the same day, was laborious and time-consuming. From the results. it is clear that the activity of this enzyme is critically affected by any change in the quaternary structure, that may be altered by freezing. The recognition by an antibody instead of enzymatic activity demonstrated less dependence in the folding of the protein, which can be explain by the fact that the antibody might recognized contiguous epitopes of the protein. Nevertheless, the comparative experiment was repeated per duplicate confirming the results and the trends observed. On the other hand, this effect of the enzymatic activity by freezing was not observed for intrinsic

alkaline phosphatase activity in exosomes, previously studied by our research group. This fact highlights that the structure integrity of the enzymes should be carefully considered and studied in cases where the exosomes must be frozen for further studies

A triple labelling experiment was also performed for SKBR3 exosomes. The determination of the resorufin propionate signals coming from tetraspanin containing vesicles also Violet-labelled was tried with unsuccessful results. The fluorescent signals from FITC-modified antibodies might overlap the lower intensity signals from resorufin in the exosomes. New appropriate fluorophore combinations should be tried to overcome this incompatibility and improve the performance of the assays.

5.6 Supplementary Data

5.6.1 Materials and methods

Buffers and solutions

4-(2-hydroxyethyl)-1-piperazineethanesulfonic acid (HEPES, ref. 252859), DL-dithiothreitol (DTT, ref. D0632), sodium phosphate dibasic (ref. 71636), potassium phosphate dibasic (ref. 795496), sodium chloride (ref. S3014), potassium chloride (ref. P3911), magnesium chloride (ref. M8266), boric acid (ref. B6768), glycine (ref. 50046), and bovine serum albumin (BSA, ref. A4503) were purchased from Sigma-Aldrich (Merck KGaA, DE). Sodium carbonate (ref. 131648) was purchased from Panreac (ES). Skimmed milk was purchased from local supplier (Nestlé Sveltesse). All solutions were prepared with ultrapure MilliQ water (Millipore® System, resistivity 18.2 MΩ·cm).

The composition of the buffers and solutions was:

- HEPES buffer: 25 mmol L^{-1} HEPES, 25 mmol L^{-1} $MgCl_2$, pH 7.4.
- HEPES reaction buffer: 50 mmol L^{-1} HEPES, 50 mmol L^{-1} $MgCl_2$, 5mM DTT, pH 8.0.
- PBS 1x buffer: 10 mmol L^{-1} Na_2HPO_4, 137 mmol L^{-1} NaCl, 2.7 mmol L^{-1} KCl, 1.8 mmol L^{-1} K_2HPO_4, pH 7.4.
- PBS - 0.5 % BSA buffer: 0.5 % w/v BSA in PBS 1x buffer.
- Skimmed milk 3 % in PBS: 3 % w/v of skimmed milk in PBS 1x buffer.
- Carbonate/bicarbonate buffer: 100 mmol L^{-1} Na_2CO_3, pH 9.6.
- Boric acid buffer: 100 mmol L^{-1} H_3BO_3, pH 8.5.
- Glycine blocking solution: 500 mmol L^{-1} glycine in PBS 1x buffer.

5.6.2 Cell culturing, exosome isolation and purification

The cell lines used were breast cancer cell lines SKBR3 (ATCC, ref. HTB-30), MDA-MB-231 (ATCC, ref. HTB-26) and MCF7 (ATCC, ref. HTB-22). Expansion of cell population was carried out from 5 x 10^6 cells in T-175 flask containing 35 mL of Dulbecco's Modified Eagle's medium. The media were supplemented with 10 % exosome-depleted fetal bovine serum (FBS) and 100 U mL^{-1} penicillin-streptomycin. The temperature was maintained at 37 °C in a humidified, concentrated CO_2 (5 %) atmosphere. Once cells reached approximately 95 % confluence on the T-175 flask, the culture supernatant was removed and stored at –21 ºC until to exosome isolation.

Exosomes were purified according as previously reported by our research group.[8] The supernatant from the SKBR3, MDA-MB-231 and MCF7 cell lines were subjected to

differential centrifugation as follows: 2,000 x *g* for 15 minutes (removal of residual cells) and 10,000 x *g* for 30 minutes (removal of cellular debris, large and medium-sized EVs). Then, a Beckman Coulter Optima L-80XP ultracentrifuge at 100,000 x *g* for 60 minutes, either with a 70Ti or 50.2Ti rotor to pellet exosomes and other small EVs. After that, the supernatant was carefully removed, and crude exosome-containing pellets were resuspended in 1 mL of HEPES buffer (pH 7.4, 0.22 µm filtered and sterile) and pooled. The second round of the same ultracentrifugation setting was carried out, and the resulting exosome pellet resuspended in 250 µL (per each 100 mL of supernatant) of HEPES buffer (pH 7.4, 0.22 µm filtered and sterile) and stored at –21 °C. All centrifugation steps were performed at a temperature of 4 °C.

5.6.3 Characterization of exosomes by bead-based flow cytometry assay

Conventional flow cytometry was used to estimate the presence of general protein markers of exosomes in the membranes of the EVs derived from SKBR3, MDA-MB-231 and MCF7 breast cancer cell lines. The presence of tetraspanin receptors CD9, CD63 and CD81 was evaluated, following MISEV2018 guidelines[26], to confirm the presence of exosomes in the samples. The vesicles were immobilized on magnetic particles as solid support, following previously reported protocols.[8]

The immobilization of exosomes on Dynabeads M450 tosylactivated superparamagnetic particles (MPs) were performed as follows: 3.5 x 10^{10} exosomes were added to 40 µL of MPs, equivalent to 1.6 x 10^{7} particles. The reaction was carried out in 0.1 mol L^{-1} borate buffer pH 8.5, in order to ensure the nucleophilic reaction by the amine group. The incubation step was performed overnight with gentle shaking (~900 rpm) at 4 ºC. After that, 0.5 mol L^{-1} glycine solution was added to ensure the blocking of the any remaining tosylactivated groups, by an incubation for 2 h at room temperature. After that, the exosomes-modified magnetic particles (exosomes-MP) were resuspended in 160 µL of 10 mmol L^{-1} PBS buffer to dilute the MPs suspension at 1 x 10^{5} MPs per µL. The exosomes-MP were maintained at 4 ºC until use.

The presence of the CD9, CD63 and CD81 biomarkers was investigated using FITC-modified primary antibodies. The direct labeling of 5 x 10^{5} exosome-modified MPs was performed by incubation with 5 µL (5 µg mL^{-1}) of primary antibodies (*i.e.,* FITC-modified antiCD9, antiCD63 and antiCD81), for 30 min with gentle shaking at 4 ºC. After that, three washing steps with PBS buffer containing 0.5 % BSA were performed. The labeled MPs were resuspended in 500 µL of PBS 1x buffer and measured by flow cytometry.

5.6.4 Intracellular staining of ALDH in breast cancer cells

To evaluate the presence of ALDH enzyme in breast cancer cells from SKBR3, MDA-MB-231 and MCF7, an intracellular staining was performed as reference method.

Firstly, the fixation of 3 x 10^5 cells from culture was done by incubation with 200 µL of diluted formaldehyde 4 % in PBS for 10 minutes at room temperature. Then, the microplate was centrifuged (3 min at 800 x *g*), supernatant was discarded, and cells were incubated with 200 µL of PBS containing 2 % of FBS and 0.1 % of saponin, for 10 minutes at room temperature. Then, the supernatant was discarded after centrifugation, and cells were resuspended in FBS containing 0.3 % of saponin for permeabilization of cellular membranes. Then, fixed and permeabilized cells were incubated with 2.5 µg mL^{-1} (3 µL) of specific rabbit polyclonal antibodies against ALDH1A3 for 45 minutes at room temperature. At the same time, intracellular positive control samples were incubated at the same conditions with mouse monoclonal antibodies against vinculin, an ubiquitous cytoskeletal protein of mammalian cells.

Then, two washing steps were performed with PBS containing 2 % of FBS and 0.1 % of saponin, and the cells were resuspended in the same buffer containing 8 µg mL^{-1} (1 µL) of secondary antibodies antirabbit-PE and incubated for 30 minutes at room temperature. In the case of the control samples, they were incubated with antimouse-Cy5 at the same conditions. Finally, two washing steps were performed, and the cells were resuspended in 200 µL PBS 1x buffer and analyzed by flow cytometry.

As a positive control of the permeabilization of cellular membranes, and to confirm their integrity, breast cancer cells were analyzed with antibodies against vinculin. Figure 5.10 shows histograms of the samples, in all cases with more than 90 % of positivity. In detail, 99.6 % in SKBR3 cells, 99.0 % in MDA-MB-231 cells, and 92.5 % in MCF7 cells.

5.6.5 Sandwich ELISA for the determination of ALDH

Exosomes derived from SKBR3 breast cancer cell line were subjected to sandwich ELISA determination of ALDH1A3 presence on their membranes. Besides, the integrity of the vesicles and well-functioning of the ELISA method was evaluated by reacting with antiCD81 as general exosome membrane biomarker.

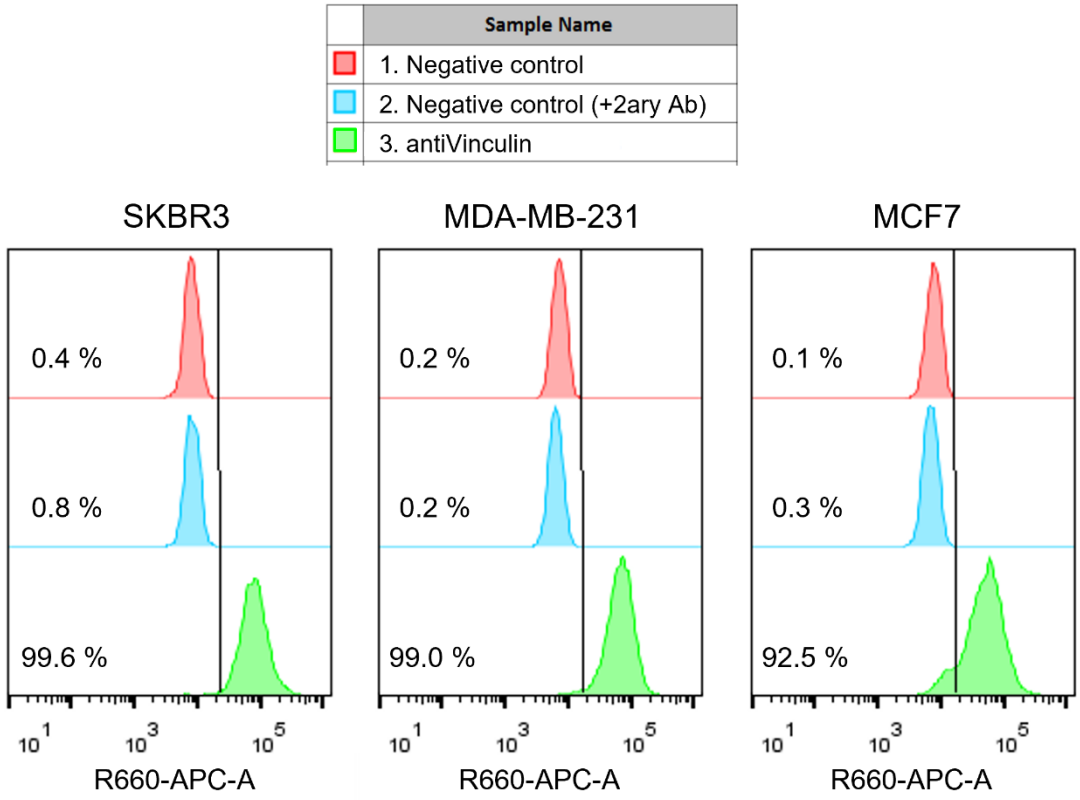

Figure 5.10. Histograms from intracellular staining of cells from SKBR3, MDA-MB-231 and MCF7 breast cancer cell lines with antiVinculin antibodies, labelled with Cy5-modified antimouse secondary antibodies. In red color, negative controls of the experiment, only cells; in blue color, control with cells only incubated with secondary antibodies; in green color, cells with antiVinculin antibodies plus labelled secondary antibodies.

Firstly, specific antibodies against ALDH1A3 (1:250 dilution factor, 0.4 µg mL^{-1}) and antiCD81 (1:250 dilution factor, 2 µg mL^{-1}) were diluted in carbonate/bicarbonate buffer and were incubated (100 µL per well) overnight at 4 ºC in Maxisorp polystyrene microplates. Then, the coating solution was removed, and remaining sites were blocked (skimmed milk 3 % in PBS) for 2 hours at room temperature and gentle shaking (550 rpm). Blocking solution was removed and plates were washed with PBS – 0.5 % BSA three times. Meanwhile, six different exosomes samples were prepared in PBS, with concentrations ranging from $3.42 \cdot 10^8$ to $1.07 \cdot 10^7$ particles mL^{-1}, according to NTA measurements. The samples were incubated by triplicates for 1 hour at room temperature and gentle shaking. Then, supernatants were carefully removed, and three washing steps were applied. To label the vesicles, HRP-conjugated antiCD63 (1:1000 dilution factor, 0.3 µg mL^{-1}) antibodies were incubated for 1 hour at room temperature and gentle shaking. Again, supernatants were carefully removed, and three washing steps were applied. Finally, TMB substrate solution (1:1 TMB and H_2O_2 from Pierce TMB substrate kit) was incubated for 30 minutes at room temperature. The reaction was

stopped by adding 2 mol L^{-1} sulfuric acid and the colored product was quantified spectrophotometrically at 450 nm.

5.6.6 Nano-Flow cytometry studies of breast cancer exosomes

5.6.6.1 CFSE and Violet staining of exosomes

For CFSE and Violet staining, exosomes derived from SKBR3 breast cancer cell line were used to optimize several experimental parameters, including the concentration, the temperature and time of incubation and some cytometer parameters such as threshold and gains. For the CFSE assay, exosomes were incubated with CFSE 20 µmol L^{-1} for 30 minutes, 1 hour and 2 hours at 37 ºC to study the incubation time, following previous studies.[11,28] Additionally, a sample with exosomes and CFSE 20 µmol L^{-1} was incubated for 2 hours at RT to study the incubation temperature. All tubes were diluted to 1 mL with HEPES buffer and measured by nano-flow cytometry. Regarding the instrumental parameters, different channel gains and thresholds were analyzed with exosomes samples. As shown in Figure 5.11, the best discriminated exosome population when comparing all the previously mentioned parameters was the sample incubated with CFSE for 2 hours at 37 ºC and a B525 (FITC) channel gain of 1,000 units (Fig 5.11, panel E).

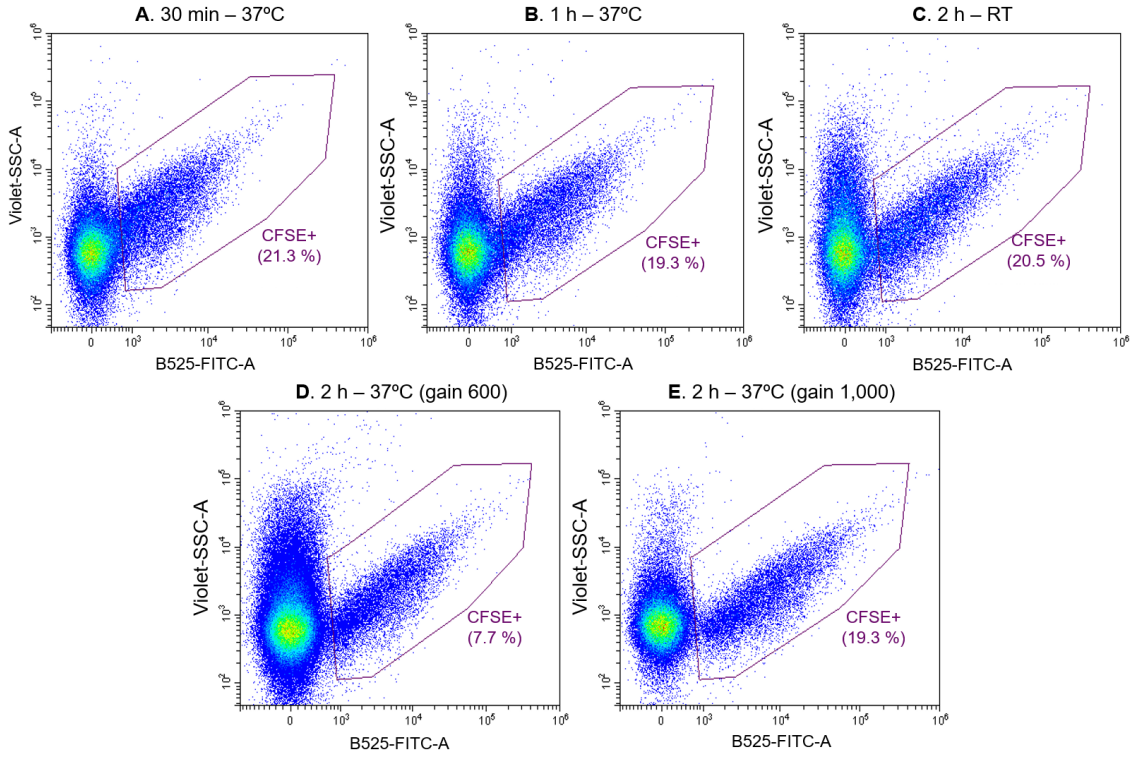

Figure 5.11. Optimization of the CFSE labelling of exosomes. Dot plot representations (on x axis: B525-FITC-A channel signal, on y axis Violet-SSC-A). Incubations with CFSE were performed at 37ºC for 30 minutes (Panel A), 1 hour (Panel B), 2 hours (Panel D and E). On Panel C, the incubation was done for 2 hours at room temperature. The gain of B525 channel was optimized to 1,000 units (Panel E).

In parallel, serial dilutions of SKBR3 exosomes incubated with 20 μmol L^{-1} of CFSE for 2 hours at 37 ºC were measured to test the exosomes concentration range suitable for nano-flow cytometric measurements. As shown in Figure 5.12, the concentration of the sample clearly affects the abort rate of the measurements, directly related with the quality of the results. Briefly, if two particles enter the laser beam too close together, and the instrument cannot detect them independently, the instrument will abort them both. Following Cytoflex LX manufacturer technical recommendations, an abort rate below 8.0 % is considered as good quality results in the case of nanoparticles samples. In our case, the best results were obtained with a 100-fold dilution of the exosomes sample, shown in Figure 5.12, panel C. The NTA count of SKBR3 exosomes sample allows to calculate the corresponding concentration of particles in the measured tube, which was $6.45 \cdot 10^7$ particles mL^{-1}.

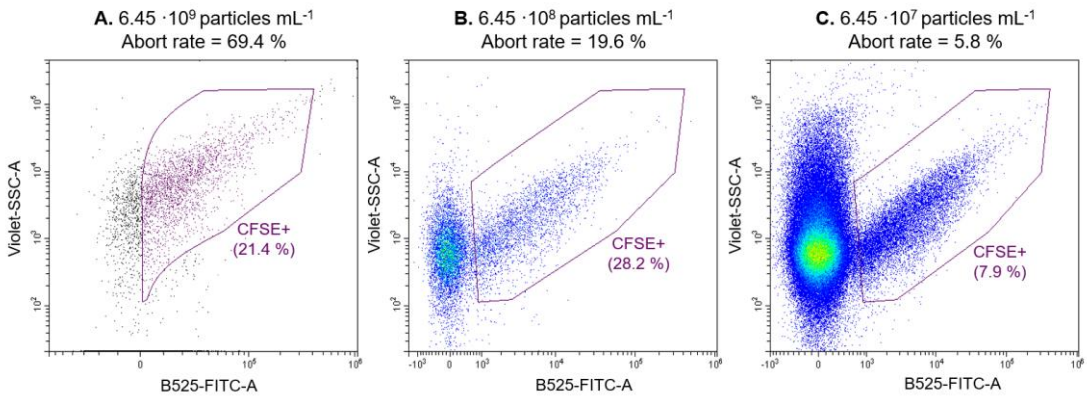

Figure 5.12. Optimization of exosomes concentration on nano-flow cytometry measurements. Dot plot representations (on x axis: B525-FITC-A channel signal, on y axis Violet-SSC-A). 10-fold serial dilutions of SKBR3 exosomes CFSE labelled. The concentrations were calculated according to NTA particle counting.

To further test the CFSE labelling protocol, as well as the exosomes concentration range suitable for the nano-flow cytometry measurements, exosomes derived from various cell lines[1] were measured, as shown in Figure 5.13. As can be observed, variable percentages of CFSE+ vesicles were obtained. This fact can is related with the exosomes concentration, as more diluted samples had to be recorded for longer times, therefore, increasing the noise signals measured. As previously explained, the acquisition settings of the cytometer were configured to measure a minimum of 10,000 particles in the CFSE+ gate.

[1] Exosomes derived from THP1, HOM2 and SHSY-5Y cell lines were kindly provided by M. Bernuz.

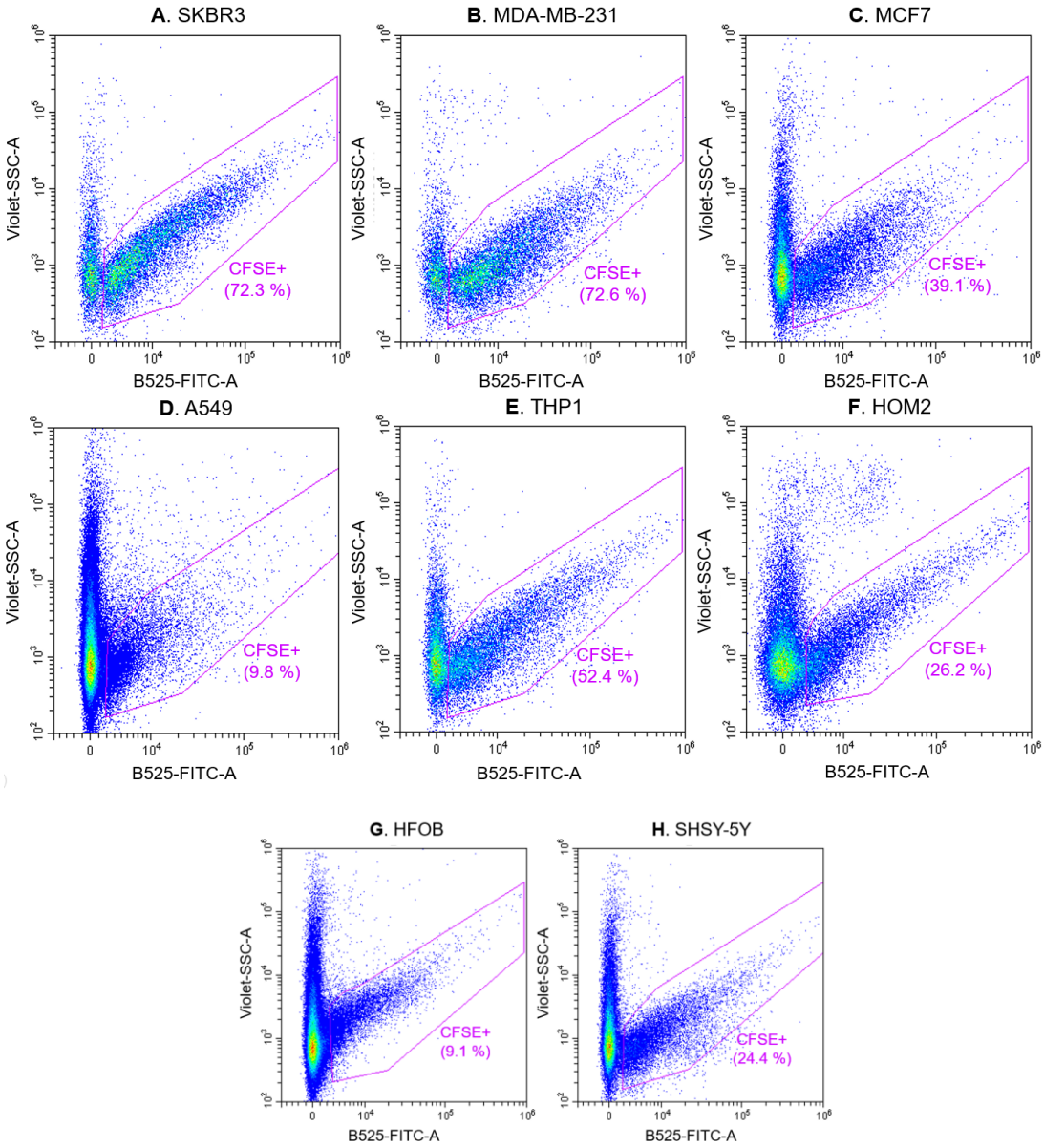

Figure 5.13. Nano-flow cytometry measurements of exosomes derived from cell culture supernatants. Dot plot representations (on x axis: B525-FITC-A channel signal, on y axis Violet-SSC-A). CFSE labelled exosomes derived from SKBR3 (Panel A), MDA-MB-231 (Panel B) and MCF7 (Panel C) breast cancer cell lines; from A549 (Panel D) lung cancer cell line; from THP1 (Panel E) monocytic cell line; from HOM2 (Panel F) lymphoblastoid cell line; from HFOB (Panel G) osteoblasts cell line; and SHSY-5Y (Panel H) neuroblastoma cell line.

A comparison was done between the particle counting by Nanoparticle tracking analysis and CFSE labelled particles in nano-flow cytometry (concentration of CFSE+ particles subpopulation), as shown in Figure 5.14 bar graph and table. It can be observed that there is not a consistent labelling ratio between the cell lines. The differences might be related to different methodological issues, as the overestimation of particle concentration due to vesicles and protein aggregates in NTA.

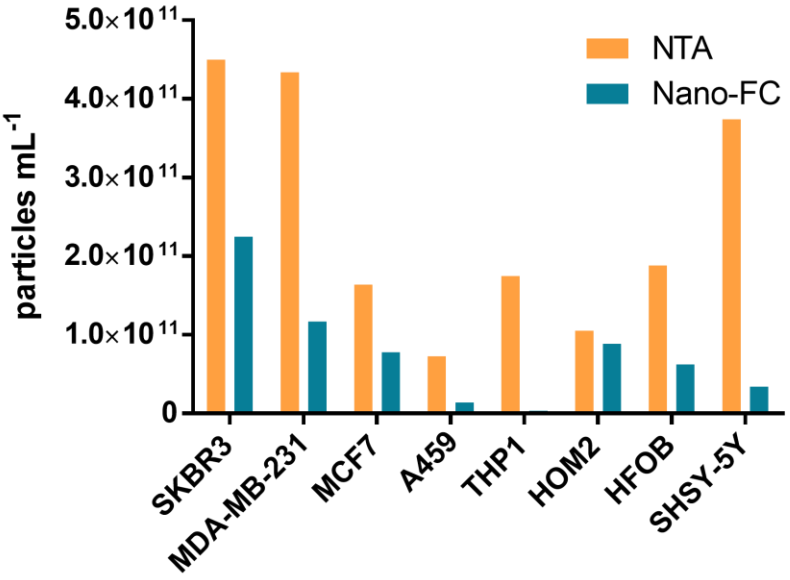

Exosomes cell line	NTA (particles mL^{-1})	Nano-FC (particles mL^{-1})	% Nano-FC vs. NTA
SKBR3	4.50e+11 / SD 3.13e+09	2,25E+11	50,0%
MDA-MB-231	4.34e+11 / SD 7.75e+09	1,17E+11	27,0%
MCF7	1.64e+11 / SD 7.55e+09	7,76E+10	47,3%
A459	7.25e+10 / SD 2.69e+09	1,39E+10	19,2%
THP1	1.75e+11 / SD 7.14e+09	3,64E+09	2,1%
HOM2	1.05e+11 / SD 3.87e+09	8,87E+10	84,5%
HFOB	1.88e+11 / SD 5.16e+09	6,24E+10	33%
SHSY-5Y	3.74e+11 / SD 1.68e+10	3,39E+10	9,1%

Figure 5.14. Comparison of NTA vs Nano-flow cytometry. Both bar graph and table show the particle concentration determined by each method of eight different cell lines: SKBR3, MDA-MB-231, and MCF7 breast cancer cell lines; A549 lung cell line, THP1 monocyte cell line, HOM2 lymphoid cell line, HFOB osteoblast cell lines, and SHSY-5Y neuroblastoma cell line. The ratio of particle concentration determined by nano-flow cytometry versus NTA.

In the case of Violet staining, exosomes derived from SKBR3 were incubated with CellTrace Violet at concentrations of 5 µmol L^{-1}, 10 µmol L^{-1} and 20 µmol L^{-1} for 1 hour and 2 hours at 37 ºC. With the knowledge of CFSE staining optimization results, all incubation were performed at 37 ºC. All tubes were diluted to 1 mL with HEPES buffer and measured by nano-flow cytometry. As can be seen in Figure 5.15 when all the previously mentioned parameters were compared, the incubation of the exosomes for 2 hours at 37 ºC in the presence of Violet staining at a concentration of 20 µmol L^{-1} was the best condition to discriminate the exosomes from the background noise, as determined for CFSE (47.5 %). The gain of the V450 (Violet) channel was optimized manually to 500 units (Fig 5.15).

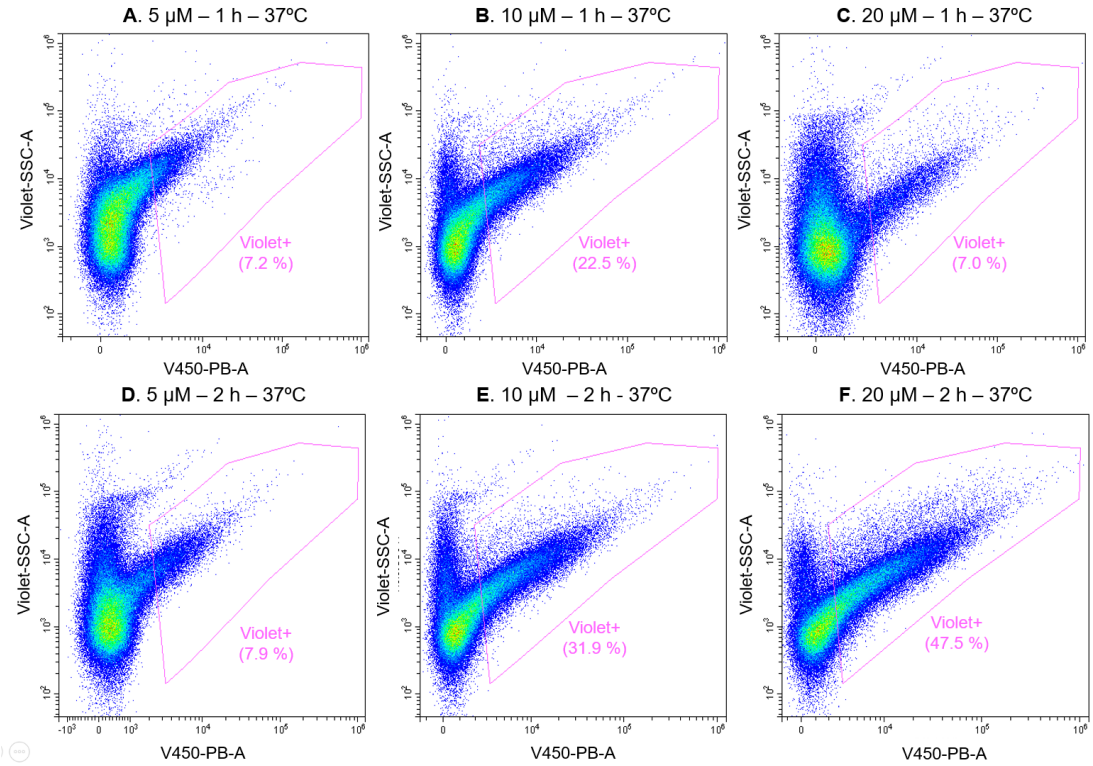

Figure 5.15. Optimization of the Violet labelling of exosomes. Dot plot representations (on x axis: V450-PB-A channel signal, on y axis Violet-SSC-A channel). Incubations with Violet at 5, 10 and 20 µmol L^{-1} staining were performed at 37 ºC for 1 hour (Panel A, B, C) and 2 hours (Panel D, E, F).

5.6.6.2 *Analysis of membrane markers on CFSE-labelled exosomes*

For exosome labelling with FITC-modified antibodies, 15 µL of exosomes from SKBR3 breast cancer cell line were incubated with 20 µmol L^{-1} of Violet staining for 2 hours at 37 ºC. Later, 5 µL of FITC-modified mouse monoclonal antibodies against tetraspanins (CD9, CD63 and CD81) were incubated for 45 minutes at RT. In all experiments, control tubes without the staining and the antibodies were included and manipulated following the same conditions. All tubes were diluted to 1 mL with HEPES buffer and measured by nano-flow cytometry.

5.6.6.3 *ALDH activity determination in breast cancer exosomes*

For ALDH activity assays, resorufin propionate substrate and ALDH specific inhibitor concentrations and incubation times were optimized. In all experiments, all samples were filled until 1 mL with HEPES buffer after incubations and measured by nano-flow cytometry.

Exosomes derived from SKBR3 breast cancer cell lines were incubated with 20 µmol L^{-1} CFSE for 2 hours at 25 ºC in the presence of different concentrations of the resorufin propionate substrate, ranging from 2.5 µmol L^{-1} to 50 µmol L^{-1}. As shown in Figure 5.16, the optimal concentration was considered 25 µmol L^{-1} because high intensity

signals were observed in Y610-RP channel. The 50 µmol L^{-1} concentration was discarted, considering the potential harmful effect of DMSO (used as diluent in the RP stock solution) to the exosomes.

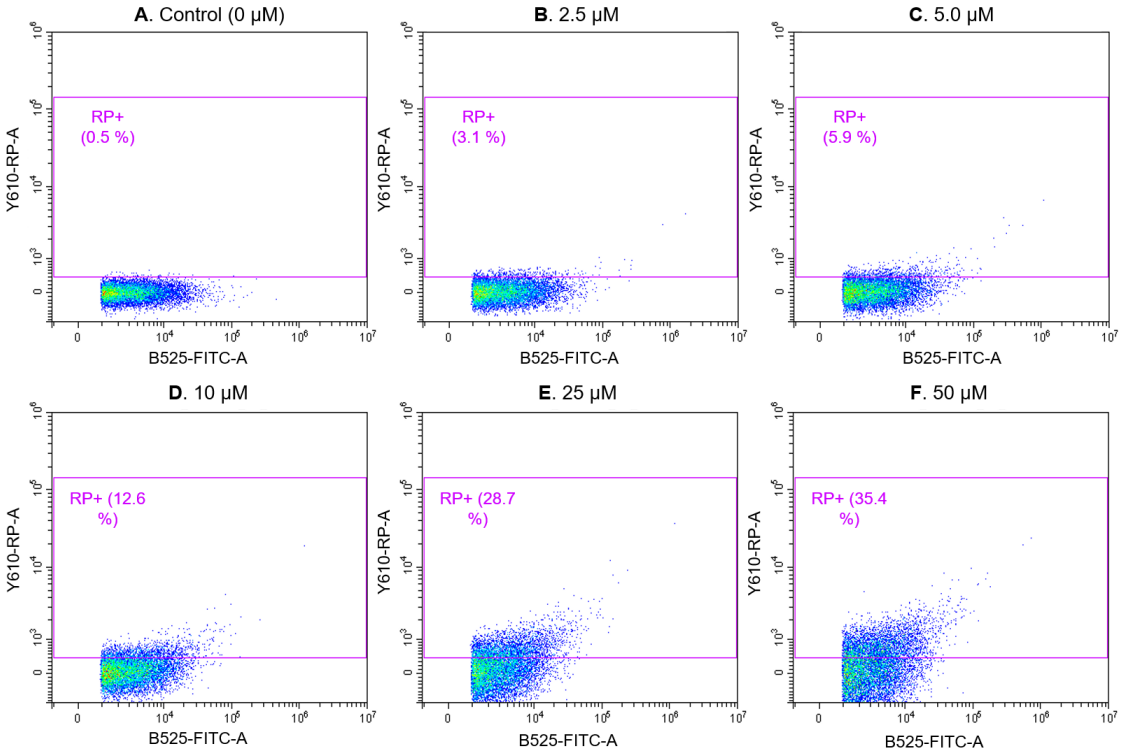

Figure 5.16. Optimization of resorufin propionate concentration. Dot plot representations (on x axis: B525-FITC-A channel signal, on y axis Y610-RP-A channel). Incubations with different concentrations of resorufin propionate, ranging from 2.5 µmol L^{-1} to 50 µmol L^{-1}, plus a negative control sample.

In parallel, the resorufin propionate incubation time was examined. CFSE-labelled SKBR3 exosomes were incubated with 25 µmol L^{-1} resorufin propionate substrate for different times (30 minutes, 1 hour and 2 hours) at 25 ºC (data not shown). The results showed that different incubation times do not increase significantly the resorufin fluorescent signals. Although, an incubation time of 2 hours was chosen to amplify the signal of the enzymatic reaction.

For the ALDH inhibitor assay, SKBR3 exosomes were incubated with CFSE staining and ABD0305 as ALDH specific inhibitor at concentrations of 0.4 mmol L^{-1} (100-fold dilution) and 4 mmol L^{-1} (10-fold dilution) for 1 hour and 2 hours at 37 ºC. Then, each sample was incubated with 25 µmol L^{-1} resorufin propionate for 2 hours. As can be observed in Figure 5.17, the 4 mmol L^{-1} dilution inhibits more the signal, although it might be also attributed to the effect of ethanol in the biological activity of exosomes. Therefore, in order to prevent unspecific inhibition a concentration of 0.4 mmol L^{-1} was used as working solution with 2 hours incubation time.

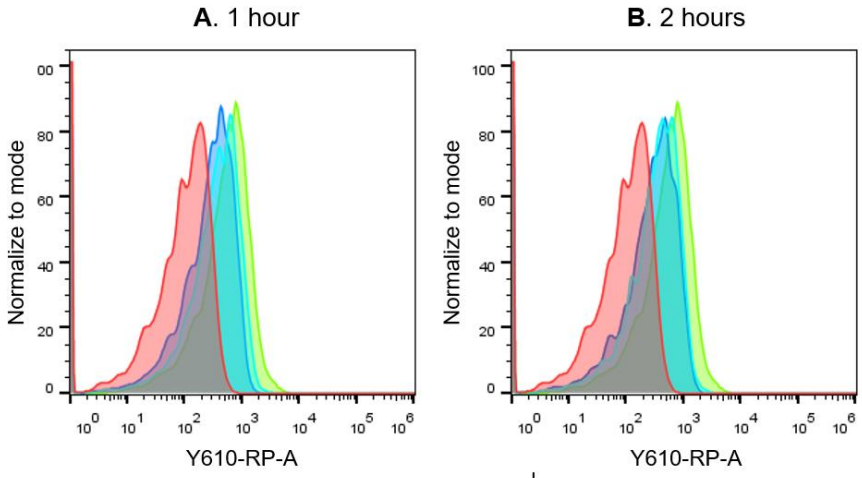

Sample		1 h Inhibitor incubation	2 h Inhibitor incubation
Control		9.57	
Positive sample		98.6	
0.4 mmol L^{-1}		35.1	36.5
4 mmol L^{-1}		21.0	20.5

Figure 5.17. Optimization of ALDH inhibitor incubation. Panel A and B, histogram representations (on x axis: Y610-RP-A channel signal, on y axis: normalized count to mode). On the table, geometric mean of the samples previously represented, with 1 hour inhibitor incubation (Panel A) and 2 hours (Panel B).

Finally, for the comparison of frozen exosomes (stored -21 ºC) with non-frozen exosomes (stored at +4 ºC), 15 µL of each exosomes sample (SKBR3, MDA-MB-231 and MCF7 cell lines) were incubated with 25 µmol L^{-1} of CFSE and 0.4 mmol L^{-1} ALDH inhibitor for 2 hours at 37 ºC. Then, the samples were incubated with 25 µmol L^{-1} of resorufin propionate substrate for 2 hours at 25 ºC. Tubes without CFSE, ALDH substrate and ALDH inhibitor were filled with the same correspondent volume with HEPES to have the same conditions.

5.7 Acknowledgments

M. Tuxans Serrano is gratefully acknowledged for her contributions. Also, Prof. Jaume Farrés and his research group members Dra. R. Pequerul, R. Jiménez and L. Costa are gratefully acknowledged for their contributions and financial support. M. Bernuz is acknowledged for providing exosomes samples. Also, ICTS “NANBIOSIS” NTA analysis service of *Institut de Ciència dels Materials de Barcelona* and Service of Microscopy of *Universitat Autònoma de Barcelona* are gratefully acknowledged.

5.8 References

(1) Johnstone, R. M.; Adam, M.; Hammond, J. R.; Orr, L.; Turbide, C. Vesicle Formation during Reticulocyte Maturation. Association of Plasma Membrane Activities with Released Vesicles (Exosomes). *J. Biol. Chem.* **1987**, *262* (19), 9412–9420.

(2) Gurung, S.; Perocheau, D.; Touramanidou, L.; Baruteau, J. The Exosome Journey: From Biogenesis to Uptake and Intracellular Signalling. *Cell Commun. Signal.* **2021**, *19* (1), 1–19. https://doi.org/10.1186/s12964-021-00730-1.

(3) Samanta, S.; Rajasingh, S.; Drosos, N.; Zhou, Z.; Dawn, B.; Rajasingh, J. Exosomes: New Molecular Targets of Diseases. *Acta Pharmacol. Sin.* **2018**, *39* (4), 501–513. https://doi.org/10.1038/aps.2017.162.

(4) Land, K. J.; Boeras, D. I.; Chen, X. S.; Ramsay, A. R.; Peeling, R. W. REASSURED Diagnostics to Inform Disease Control Strategies, Strengthen Health Systems and Improve Patient Outcomes. *Nat. Microbiol.* **2019**, *4* (1), 46–54. https://doi.org/10.1038/S41564-018-0295-3.

(5) Park, J.; Park, J. S.; Huang, C. H.; Jo, A.; Cook, K.; Wang, R.; Lin, H. Y.; Van Deun, J.; Li, H.; Min, J.; Wang, L.; Yoon, G.; Carter, B. S.; Balaj, L.; Choi, G. S.; Castro, C. M.; Weissleder, R.; Lee, H. An Integrated Magneto-Electrochemical Device for the Rapid Profiling of Tumour Extracellular Vesicles from Blood Plasma. *Nat. Biomed. Eng.* **2021**, *5* (7), 678–689. https://doi.org/10.1038/s41551-021-00752-7.

(6) Jeong, S.; Park, J.; Pathania, D.; Castro, C. M.; Weissleder, R.; Lee, H. Integrated Magneto-Electrochemical Sensor for Exosome Analysis. *ACS Nano* **2016**, *10* (2), 1802–1809. https://doi.org/10.1021/acsnano.5b07584.

(7) Zhou, Q.; Rahimian, A.; Son, K.; Shin, D. S.; Patel, T.; Revzin, A. Development of an Aptasensor for Electrochemical Detection of Exosomes. *Methods* **2016**, *97*, 88–93. https://doi.org/10.1016/j.ymeth.2015.10.012.

(8) Moura, S. L.; Martín, C. G.; Martí, M.; Pividori, M. I. Multiplex Detection and Characterization of Breast Cancer Exosomes by Magneto-Actuated Immunoassay. *Talanta* **2020**, *211*, 120657. https://doi.org/https://doi.org/10.1016/j.talanta.2019.120657.

(9) George, S. K.; Lauková, L.; Weiss, R.; Semak, V.; Fendl, B.; Weiss, V. U.; Steinberger, S.; Allmaier, G.; Tripisciano, C.; Weber, V. Comparative Analysis of Platelet-derived Extracellular Vesicles Using Flow Cytometry and Nanoparticle Tracking Analysis. *Int. J. Mol. Sci.* **2021**, *22* (8), 1–10. https://doi.org/10.3390/ijms22083839.

(10) Morales-Kastresana, A.; Telford, B.; Musich, T. A.; McKinnon, K.; Clayborne, C.; Braig, Z.; Rosner, A.; Demberg, T.; Watson, D. C.; Karpova, T. S.; Freeman, G. J.; Dekruyff, R. H.; Pavlakis, G. N.; Terabe, M.; Robert-Guroff, M.; Berzofsky, J. A.; Jones, J. C. Labeling Extracellular Vesicles for Nanoscale Flow Cytometry. *Sci. Rep.* **2017**, *7* (1), 1–10. https://doi.org/10.1038/s41598-017-01731-2.

(11) Ender, F.; Zamzow, P.; von Bubnoff, N.; Gieseler, F. Detection and Quantification of Extracellular Vesicles via FACS: Membrane Labeling Matters! *Int. J. Mol. Sci.* **2020**, *21* (1). https://doi.org/10.3390/ijms21010291.

(12) Sanchez, M. A.; Felice, B.; Sappia, L. D.; Lima Moura, S.; Martí, M.; Pividori, M. I. Osteoblastic Exosomes. A Non-Destructive Quantitative Approach of Alkaline Phosphatase to Assess Osteoconductive Nanomaterials. *Mater. Sci. Eng. C* **2020**, *115*, 110931. https://doi.org/10.1016/j.msec.2020.110931.

(13) Moura, S. L.; Pallarès-Rusiñol, A.; Sappia, L.; Martí, M.; Pividori, M. I. The Activity of Alkaline Phosphatase in Breast Cancer Exosomes Simplifies the Biosensing Design. *Biosens. Bioelectron.* **2022**, *198*, 113826. https://doi.org/10.1016/j.bios.2021.113826.

(14) Zulauf, N.; Brüggmann, D.; Groneberg, D.; Oremek, G. M. Expressiveness of Bone Markers in Breast Cancer with Bone Metastases. *Oncol.* **2019**, *97* (4), 236–244. https://doi.org/10.1159/000500675.

(15) Castellví, A.; Pequerul, R.; Barracco, V.; Juanhuix, J.; Parés, X.; Farrés, J. Structural and

Biochemical Evidence That ATP Inhibits the Cancer Biomarker Human Aldehyde Dehydrogenase 1A3. *Commun. Biol.* **2022**, *5* (1). https://doi.org/10.1038/s42003-022-03311-1.

(16) Durinikova, E.; Kozovska, Z.; Poturnajova, M.; Plava, J.; Cierna, Z.; Babelova, A.; Bohovic, R.; Schmidtova, S.; Tomas, M.; Kucerova, L.; Matuskova, M. ALDH1A3 Upregulation and Spontaneous Metastasis Formation Is Associated with Acquired Chemoresistance in Colorectal Cancer Cells. *BMC Cancer* **2018**, *18* (1), 1–15. https://doi.org/10.1186/s12885-018-4758-y.

(17) Li, G.; Li, Y.; Liu, X.; Wang, Z.; Zhang, C.; Wu, F.; Jiang, H.; Zhang, W.; Bao, Z.; Wang, Y.; Cai, J.; Zhao, L.; Kahlert, U. D.; Jiang, T.; Zhang, W. ALDH1A3 Induces Mesenchymal Differentiation and Serves as a Predictor for Survival in Glioblastoma. *Cell Death Dis.* **2018**, *9* (12), 1–11. https://doi.org/10.1038/s41419-018-1232-3.

(18) Wu, W.; Schecker, J.; Würstle, S.; Schneider, F.; Schönfelder, M.; Schlegel, J. Aldehyde Dehydrogenase 1A3 (ALDH1A3) Is Regulated by Autophagy in Human Glioblastoma Cells. *Cancer Lett.* **2018**, *417*, 112–123. https://doi.org/10.1016/j.canlet.2017.12.036.

(19) Ni, W.; Xia, Y.; Luo, L.; Wen, F.; Hu, D.; Bi, Y.; Qi, J. High Expression of ALDH1A3 Might Independently Influence Poor Progression-Free and Overall Survival in Patients with Glioma via Maintaining Glucose Uptake and Lactate Production. *Cell Biol. Int.* **2020**, *44* (2), 569–582. https://doi.org/10.1002/cbin.11257.

(20) Wang, S.; Zhou, X.; Liang, C.; Bao, M.; Tian, Y.; Zhu, J.; Zhang, T.; Yang, J.; Wang, Z. ALDH1A3 Serves as a Predictor for Castration Resistance in Prostate Cancer Patients. *BMC Cancer* **2020**, *20* (1), 1–8. https://doi.org/10.1186/s12885-020-06899-x.

(21) Marcato, P.; Dean, C. A.; Liu, R. Z.; Coyle, K. M.; Bydoun, M.; Wallace, M.; Clements, D.; Turner, C.; Mathenge, E. G.; Gujar, S. A.; Giacomantonio, C. A.; Mackey, J. R.; Godbout, R.; Lee, P. W. K. Aldehyde Dehydrogenase 1A3 Influences Breast Cancer Progression via Differential Retinoic Acid Signaling. *Mol. Oncol.* **2015**, *9* (1), 17–31. https://doi.org/10.1016/j.molonc.2014.07.010.

(22) Qiu, Y.; Pu, T.; Guo, P.; Wei, B.; Zhang, Z.; Zhang, H.; Zhong, X.; Zheng, H.; Chen, L.; Bu, H.; Ye, F. ALDH+/CD44+ Cells in Breast Cancer Are Associated with Worse Prognosis and Poor Clinical Outcome. *Exp. Mol. Pathol.* **2016**, *100* (1), 145–150. https://doi.org/10.1016/j.yexmp.2015.11.032.

(23) Liu, C.; Qiang, J.; Deng, Q.; Xia, J.; Deng, L.; Zhou, L.; Wang, D.; He, X.; Liu, Y.; Zhao, B.; Lv, J.; Yu, Z.; Lei, Q. Y.; Shao, Z. M.; Zhang, X. Y.; Zhang, L.; Liu, S. ALDH1A1 Activity in Tumor-Initiating Cells Remodels Myeloid-Derived Suppressor Cells to Promote Breast Cancer Progression. *Cancer Res.* **2021**, *81* (23), 5919–5934. https://doi.org/10.1158/0008-5472.CAN-21-1337.

(24) Dhar, D.; Antonucci, L.; Nakagawa, H.; Kim, J. Y.; Glitzner, E.; Caruso, S.; Shalapour, S.; Yang, L.; Valasek, M. A.; Lee, S.; Minnich, K.; Seki, E.; Tuckermann, J.; Sibilia, M.; Zucman-Rossi, J.; Karin, M. Liver Cancer Initiation Requires P53 Inhibition by CD44-Enhanced Growth Factor Signaling. *Cancer Cell* **2018**, *33* (6), 1061-1077.e6. https://doi.org/10.1016/j.ccell.2018.05.003.

(25) Zanoni, M.; Bravaccini, S.; Fabbri, F.; Arienti, C. Emerging Roles of Aldehyde Dehydrogenase Isoforms in Anti-Cancer Therapy Resistance. *Front. Med.* **2022**, *9*, 544. https://doi.org/10.3389/FMED.2022.795762/BIBTEX.

(26) Théry, C.; Witwer, K. W.; Aikawa, E.; et al. Minimal Information for Studies of Extracellular Vesicles 2018 (MISEV2018): A Position Statement of the International Society for Extracellular Vesicles and Update of the MISEV2014 Guidelines. *J. Extracell. Vesicles* **2018**, *7* (1). https://doi.org/10.1080/20013078.2018.1535750.

(27) CDC. *Biosafety in Microbiological and Biomedical Laboratories (BMBL)*, 6th ed.; CDC, 2020.

(28) Hoen, E. N. M. N. t.; van der Vlist, E. J.; Aalberts, M.; Mertens, H. C. H.; Bosch, B. J.; Bartelink, W.; Mastrobattista, E.; van Gaal, E. V. B.; Stoorvogel, W.; Arkesteijn, G. J. A.; Wauben, M. H. M. Quantitative and Qualitative Flow Cytometric Analysis of Nanosized Cell-Derived Membrane Vesicles. *Nanomedicine Nanotechnology, Biol. Med.* **2012**, *8* (5), 712–720. https://doi.org/10.1016/j.nano.2011.09.006.

Chapter 6. Final remarks

6. Final remarks

The development of novel rapid diagnostic tests based on exosomes is an arduous and challenging task. It involves the integration of multiple research fields, such as bioanalytical chemistry, cellular and molecular biology, biochemistry, and microscopy, among others. The potential applications of exosomes in medical devices fuel the research in this field, which grows continuously despite the challenges. As explained in previous chapters, the focus on exosomes as biomarkers responds the social need to develop rapid diagnostic tests for the early detection of different non-communicable conditions. Of course, the COVID-19 pandemic has triggered even more the RDTs research field with unprecedented interest and funding, but still there is a need to develop RDTs especially for non-communicable diseases as cancer. The availability of exosomes in many biological fluids represent an important advantage towards developing new tests with minimally invasive procedures such as liquid biopsies.

The molecular characterization of the biological cargo of extracellular vesicles is the cornerstone for understanding their biogenesis and function. In the case of exosomes, their nanometric sizes makes even more difficult to analyze them and require the use of high-resolution instrumentation. Characterization techniques for nanomaterials such as nanoparticle tracking analysis, tunable resistive pulse sensing or nano-flow cytometry could overcome some of the limitations of conventional techniques, although at high costs. Nevertheless, new technological improvements and experimental assays are needed to better assess their complex molecular cargo.

This doctoral dissertation aims to contribute to the exosomes research field, focusing on the development of novel platforms and rapid diagnostic tests for resource-scarce settings. In specific, RDTs targeting breast cancer as one of the most preeminent diseases.

As general remarks of all experimental chapters, exosomes derived from breast cancer cell lines SKBR3, MDA-MB-231 and MCF7 were cultured and isolated by differential ultracentrifugation as standard method. These exosomes were physically characterized by nanoparticle tracking analysis to determine their size distribution and particle concentration, as well as by cryogenic transmission electron microscopy to assess their morphology. Besides, the total protein content of the exosomes samples was determined by BCA protein assay as routine method. Bead-based flow-cytometry

assays were designed to characterize the surface protein markers of exosomes, focusing on ubiquitous exosomes protein markers such as tetraspanins CD9, CD63 and CD81.

The use of biologically-modified magnetic particles was also a key point of all experimental works in this dissertation. The immunomagnetic separation of exosomes, cells or mRNA molecules provide great advantages in terms of analytical performance, improving analyte purification and preconcentration, as well as rapid and simpler protocols. The functionalization of MPs with biological receptors (antibodies, proteins, nucleic acids, biomimetic materials) is done by easy handling protocols and provides wide versatility to IMS. In the case of exosomes, antibody-modified MPs are the most used tool for capturing the nanovesicles, even from biological matrices as serum or plasma. These exosome-coated MPs can be further used as solid support to characterize the nanovesicles with magneto-actuated optical or electrochemical assays. Also, MPs are a suitable solid support for exosomes analysis on cell-oriented instruments and techniques, as conventional flow cytometry and confocal microscopy.

On Chapter 3, an electrochemical magneto-genosensor was used to analyze the mRNA transcripts inside the exosomes. Double-tagging PCR targeting GAPDH sequence was used to create biotin-digoxigenin double-tagged amplicons, further captured on streptavidin-modified magnetic particles and labelled with anti-Digoxigenin labelled with HRP. This approach combines the specific isolation of the exosomes with the amplification of the transcripts to increase the signal of the final device and improve the LODs. The genosensor was tested and optimized using breast cancer cells and exosomes from MCF7 cell line. The cells and exosomes were firstly isolated by immunomagnetic separation with antiCD81-MPs, as general exosome protein marker, and with antiEpCAM-MPs, as epithelial specific marker. An impressive limit of detection of 1225 exosomes μL^{-1} was obtained with MCF7 exosomes specifically captured by epithelial EpCAM biomarker. The combination of magnetic capture and PCR amplification successfully increase the sensitivity of the assay. Later, the test was challenged to human serum samples from breast cancer patients and healthy individuals, obtaining promising results. The signals from exosomes immunocaptured by epithelial EpCAM biomarker of breast cancer patients serum was 3.3-fold compared to healthy individuals. As future perspectives, the biosensor should be tested with a higher number of specimens and from patients with different types of breast cancer, also at different disease stages. For the electrochemical detection, the integrated and miniaturized devices with screen-printed electrodes could substitute the manufactured magnetic graphite-epoxy composite electrodes.

On Chapter 4, Vertical Flow Assay was explored as a non-conventional paper-based platform for the semi-quantitative determination of surface protein markers on exosomes using alkaline phosphatase as enzymatic reporter. The reaction of ALP with NBT/BCIP substrate produces an intense blue/purple precipitate on the surface of the nitrocellulose membranes. The materials, construction, and reagents of VFA were carefully optimized to improve the performance of the assay. The intensity of the colored signals was quantified using a smartphone and ImageJ software, which enabled to quantify the signals. In specific, samples from SKBR3 and MDA-MB-231 breast cancer exosomes were analyzed. The limit of detection of the exosomes on VFA using antiCD81 and ALP conjugate secondary antibodies was approximately $6 \cdot 10^7$ particles μL^{-1}. The determination of surface markers on VFA allowed to obtain expression patterns of SKBR3 and MDA-MB-231 breast cancer exosomes. Those patterns showed good agreement with bead-based flow cytometry assays as reference molecular characterization method. Besides, the determination of the intrinsic ALP activity of the exosomes was also presented, showing good agreement with the gold-standard method. An estimated LOD of $1 \cdot 10^7$ particles μL^{-1} was found, corresponding to 2 µU of ALP enzyme (or 1 mU mL^{-1}) with 2 hours of reaction time. An important aspect to address in future studies was the construction of the VFA cartridges. The performance of the tests was critically dependent on the manufacturing and the correct placing of the membranes. Therefore, the construction of the VFA cartridges by automatized industrial procedures will enable to improve the performance and reproducibility of the tests.

On Chapter 5, the activity of ALDH as new enzymatic biomarker for cancer was investigated for the first time in exosomes by nano-flow cytometry in breast cancer exosomes. The presence of ALDH enzymes was confirmed in breast cancer cells from SKBR3, MDA-MB-231 and MCF7 by intracellular staining. Their activity was assessed by fluorometric kinetic assay using hexanal as substrate and monitoring NADH production. In the case of exosomes, the ALDH activity assay was done using resorufin propionate as suitable substrate for nano-flow cytometry. The detection of exosomes with this technique required the use of fluorescent stainings to identify the exosomes population. The suitability of resorufin propionate as ALDH substrate combined its ability to permeabilize inside the vesicles with its non-specificity for ALDH enzymes. This substrate reacts with ALDH using its esterase activity, and therefore, it can react with other esterase enzymes. For that reason, the ALDH content was indirectly determined using the decrease of the fluorescent signals when incubating with a specific ALDH inhibitor. This method allowed to determine the ALDH activity in exosomes from breast cancer, which showed great dependence on storage temperature of the samples.

Consequently, the potential of ALDH to be used as enzymatic reporters in rapid diagnostic test depends on the improvement of exosomes obtention and storage conditions, as well as to find new substrates specific for ALDH suitable for exosomes. Future studies will also focus on other targets of interest with increased ALDH activity, as exosomes derived from A549 lung cancer cell line, which showed very promising results in preliminary nano-flow cytometry experiments.

Finally, the focus on exosomes as targets in RDTs has opened new possibilities for our research group in the clinical diagnosis field. This new focus on exosomes takes advantage of the expertise of the group in bioanalytical chemistry and biosensing design and applies it to new targets of interest. The combination of magnetic particles with optical assays and electrochemical biosensors has proven to be also successful for exosomes analysis and detection. This doctoral dissertation continues the research path from the group on breast cancer diagnosis, presenting new applications of exosomes as biomarkers. Nevertheless, as previously mentioned, the potentiality of exosomes as circulating biomarkers is not only limited to cancer disease. Currently in our research group, exosomes are also being explored as circulating biomarkers of Alzheimer's disease, providing its ability to cross the blood-brain barrier. Their molecular cargo is being assessed with sequencing tools to find specific protein biomarkers of the disease in exosomes, enabling its specific detection and quantification in peripheral biofluids. Besides, the miRNA cargo of the exosomes is also being explored to be used as target in new biosensors. Finally, also in the group, new biomimetic materials specific for exosomes, as tailor-made peptides, are being explored for their use in RDTs.

Chapter 7. Scientific communications

7. Scientific communications

7.1 List of publications

The activity of alkaline phosphatase in breast cancer exosomes simplifies the biosensing design.

S.L. Moura, A. Pallarès-Rusiñol, L. Sappia, M. Martí, M.I. Pividori, Biosens. Bioelectron. 198 (2022) 113826. https://doi.org/10.1016/j.bios.2021.113826.

Comparative study of gold and carbon nanoparticles in nucleic acid lateral flow assay.

J.C. Porras, M. Bernuz, J. Marfa, A. Pallarès-Rusiñol, M. Martí, M.I. Pividori, Nanomaterials. 11 (2021) 1–11. https://doi.org/10.3390/nano11030741.

Advances in exosome analysis.

A. Pallarès-Rusiñol, M. Bernuz, S.L. Moura, C. Fernández-Senac, R. Rossi, M. Martí, and M. I. Pividori. Advances in Clinical Chemistry. **In press.**

Magnetic separation of cell secreted vesicles with tailored magnetic particles and downstream applications.

M. Bernuz, A. Pallarès-Rusiñol, R. Rossi, C. Fernández-Senac, M. Martí and M. I. Pividori, Cell Secreted Vesicles: Methods and Protocols. Springer Protocols. **In press.**

7.2 List of conferences and congresses

1. Authors: M. Mesas Gómez*, A. Pallarès Rusiñol*, S. Lima Moura, A. Ben Aissa, M.Martí Ripoll, M.I. Pividori Gurgo
   Title: "*Detection of Circulating Tumor Cells by Electrochemical magneto Immunosensing and Genosensing.*"
   Type of participation: Poster presentation
   Congress: *XXXVI Reunión Bienal de la Real Sociedad Española de Química*
   Place: Sitges, Spain.
   Date: 25 to 29 June 2017

2. Authors: A. Pallarès Rusiñol*, M. Mesas Gómez, S. Lima Moura, A. Ben Aissa, M.Martí Ripoll, M.I. Pividori Gurgo
   Title: "*Comparing electrochemical magneto immunosensing and genosensing for the detection of circulating tumor cells"*
   Type of participation: Oral presentation
   Congress: *XXII Transfrontier Meeting of Sensors and Biosensors*
   Place: Montpellier, France.

Date: 21 to 22 September 2017

3. Authors: A. Pallarès Rusiñol, M. Mesas Gómez, S. Lima Moura, M.Martí Ripoll, M.I. Pividori Gurgo*
   Title: "*Magneto-actuated rapid test for the detection of circulating tumor cells"*
   Type of participation: Poster presentation
   Congress: *12th International Conference on the Scientific and Clinical Applications of Magnetic Carriers*
   Place: Copenhaguen, Denmark.
   Date: 22 to 26 May 2018

4. Authors: A. Pallarès Rusiñol, M. Mesas Gómez, S. Lima Moura, M.Martí Ripoll, M.I. Pividori Gurgo*
   Title: "*Comparing Rapid Diagnostic Test for the detection of circulating tumor cells"*
   Type of participation: Poster presentation
   Congress: *XXIII Congreso de la Sociedad Iberoamericana de Electroquímica, SIBAE 2018*
   Place: Cusco, Perú.
   Date: 3 to 8 June 2018

5. Authors: A. Pallarès Rusiñol, M. Mesas Gómez, S. Lima Moura, M.Martí Ripoll*, M.I. Pividori Gurgo
   Title: "*Comparing Rapid Diagnostic Test for the detection of circulating tumor cells"*
   Type of participation: Poster presentation
   Congress: *Biosensors 2018. 28th Anniversary World Congress on Biosensors*
   Place: Miami, FL, United States of America.
   Date: 12 to 15 June 2018

6. Authors: A. Pallarès Rusiñol, M. Mesas Gómez, S. Lima Moura, M.Martí Ripoll*, M.I. Pividori Gurgo
   Title: "*Magneto-actuated rapid test for the detection of circulating tumor cells"*
   Type of participation: Poster presentation
   Congress: *ECI 2018. 5th European Congress of Immunology*
   Place: Amsterdam, The Netherlands.
   Date: 2 to 5 September 2018

7. Authors: A. Pallarès Rusiñol*, M. Mesas Gómez, S. Lima Moura, M.Martí Ripoll, M.I. Pividori Gurgo
   Title: "*Comparing rapid diagnostic test for the detection of circulating tumor cells"*
   Type of participation: Poster presentation
   Congress: *11th Ibero-American Congress on Sensors*
   Place: Barcelona, Spain.
   Date: 17 to 20 September 2018

8. Authors: S. Lima Moura*, A. Pallarès Rusiñol, M. Martì, M. I. Pividori
   Title: "*Electrochemical immunosensing and genosensing for the detection of exosomes in human serum"*
   Type of participation: Oral presentation
   Congress: *11th Ibero-American Congress on Sensors*
   Place: Barcelona, Spain.
   Date: 17 to 20 September 2018

9. Authors: L. Vidal*, A. Pallarès Rusiñol, J. Salabert, M. González, A. Vallribera, R. M. Sebastián, M.I. Pividori

Title: "*Biotinylated phosphorus dendrimers. Synthesis and application as test line in lateral flow assays"*
Type of participation: Poster presentation
Congress: *XXIII Transfrontier Meeting on Sensors and Biosensors*
Place: Barcelona, Spain.
Date: 20 to 21 September 2018

10. Authors: M. Alcaraz*, A. Pallarès Rusiñol, M. Martí, M.I. Pividori
Title: "*Lateral Flow Assay of Interferon Gamma transcript as a biomarker of intracellular infections"*
Type of participation: Poster presentation
Congress: *XXIII Transfrontier Meeting on Sensors and Biosensors*
Place: Barcelona, Spain.
Date: 20 to 21 September 2018

11. Authors: A. Pallarès Rusiñol, S. Lima Moura, M. Martí, M.I. Pividori*
Title: "*Electrochemical genosensor for the detection of exosomes derived from breast cancer patients"*
Type of participation: Poster presentation
Congress: *XXIV Transfrontier Meeting on Sensors and Biosensors*
Place: Perpignan, France.
Date: 26 to 27 September 2019

12. Authors: J. Casasayas Cos*, S. Lima Moura, L. Sappia, A. Pallarès Rusiñol, M. Martí Ripoll, M.I. Pividori Gurgo
Title: "C*omparative study of different approaches for the detection of osteoblast-derived exosomes"*
Type of participation: Poster presentation
Congress: *XXIV Transfrontier Meeting on Sensors and Biosensors*
Place: Perpignan, France.
Date: 26 to 27 September 2019

13. Authors: A. Pallarès-Rusiñol*, M. Martí, M.I. Pividori
Title: "Novel methods for the detection of exosomes as biomarkers of non-communicable diseases"
Type of participation: Oral and Poster presentation
Congress: *Xth Doctoral Workshop, Dept. of Chemistry, UAB.*
Place: Bellaterra, Spain.
Date: 26 to 28 May 2021

14. Authors: A. Pallarès-Rusiñol*, Z. Gholami, M. Martí, M.I. Pividori
Title: "Vertical flow assay for exosomes characterization based on their intrinsic enzyme activity"
Type of participation: Oral presentation
Congress: *1º Optobiosens. Congreso virtual de la Red Nacional de Sensores y Biosensores Ópticos*
Place: Online congress.
Date: 27 to 28 May 2021

15. Authors: A. Pallarès-Rusiñol*, Z. Gholami, M. Martí, M.I. Pividori
Title: "Vertical flow assay for exosomes characterization based on their intrinsic enzyme activity"
Type of participation: Oral presentation
Congress: *XXV Transfrontier Meeting on Sensors and Biosensors*
Place: Online congress.

Date: 30 September 2021

16. Authors: A. Pallarès-Rusiñol*, M. Martí, M.I. Pividori
    Title: “Vertical flow assay for exosomes characterization based on alkaline phosphatase detection”
    Type of participation: Oral presentation
    Congress: *7th International Congress on Bio-sensing Technology*
    Place: Sitges, Spain.
    Date: 22 to 25 May 2022

17. Authors: M.I. Pividori*, A. Pallarès-Rusiñol, M. Tuxans, M. Martí,
    Title: “Fluorescence-based approaches for cancer-derived exosomes”
    Type of participation: Oral presentation
    Congress: *21st International Symposium on Bioluminescence and Chemiluminescence & XIX International Symposium on Luminescence Spectrometry*
    Place: Gijón, Spain.
    Date: 31 May to 3 June 2022

7.3 Other merits

1. Best Poster Award, XXXVIth Biennial Meeting Spanish Royal Society of Chemistry. 2017, June 25th-29th, Sitges, Spain.
2. Best Poster and Flash Contribution, Xth Doctoral Workshop of the Department of Chemistry from *Universitat Autònoma de Barcelona.* 2021, May 26th – 28th, Bellaterra, Spain.